

# The Regulation of Dystroglycan in Skeletal Muscle

---

Leanne Lipscomb BSc (Hons)

Thesis submitted to the University of  
Sheffield for the degree of Doctor of  
Philosophy

Department of Biomedical Science  
University of Sheffield

September 2013

# Table of Contents

---

Contents	ii
List of Abbreviations	vi
List of Figures	vii
Acknowledgements	x
Abstract	xi
Chapter 1: Introduction.....	1
1.1 Skeletal Muscle .....	2
1.2 Muscular dystrophy .....	4
1.3 Duchenne muscular dystrophy .....	4
1.4 Dystrophin.....	5
1.5 The dystrophin-associated glycoprotein complex (DGC).....	8
1.5.1 The protective role of the DGC .....	8
1.5.2 DGC components .....	9
1.6 Dystroglycan.....	11
1.6.1 Dystroglycan gene.....	11
1.6.2 $\alpha$ -dystroglycan.....	13
1.6.3 $\beta$ -dystroglycan.....	14
1.7 Sarcoglycan complex and sarcospan.....	17
1.8 $\alpha$ -dystrobrevin, syntrophins and nNOS.....	18
1.9 Animal models of DMD .....	19
1.9.1 The <i>mdx</i> mouse .....	20
1.9.2 The GRMD dog .....	20
1.9.3 Zebrafish as a model for muscular dystrophy.....	21
1.10 Treatments for DMD .....	24
1.10.1 Current treatment.....	24
1.10.2 Potential treatments .....	24
1.11 Project aims.....	32
Chapter 2: Materials and Methods .....	34
2.1 Zebrafish Husbandry .....	35
2.1.1 Home Office Regulation .....	35
2.1.2 Maintenance of adult zebrafish .....	35
2.1.3 Zebrafish Strains.....	35

2.1.4 Embryo Collection .....	36
2.1.5 Zebrafish media and solutions .....	36
2.2 Detection of muscle phenotype by birefringence assay.....	37
2.3 Zebrafish Motility Assays .....	37
2.3.1 Hatching assay.....	37
2.3.2 Swirl assay .....	37
2.3.3 Viewpoint Zebrabox System .....	38
2.4 Preparation of embryos for microscopy .....	39
2.4.1 Solutions used .....	39
2.4.2 Fixation .....	39
2.4.3 Labelling F-actin .....	40
2.4.4 Whole-mount immunofluorescence.....	40
2.4.5 Mounting of embryos onto microscope slides .....	41
2.5 Confocal microscopy .....	41
2.6 Chemical treatment of embryos .....	42
2.6.1 Treatment with tricaine .....	42
2.6.2 Drug treatment .....	42
2.7 Cell culture .....	44
2.7.1 Growth of cell lines .....	44
2.7.2 Drug treatment of myoblasts.....	44
2.8 Protein Biochemistry techniques.....	45
2.8.1 Buffers and solutions .....	45
2.8.2 Preparation of lysates .....	45
2.8.3 SDS Polyacrylamide Gel Electrophoresis (SDS-PAGE).....	46
2.8.4 Western blotting .....	46
2.8.5 Antibody binding and detection .....	47
2.9 Computer aided data analysis.....	47
2.9.1 Quantification of western blot bands .....	47
2.9.2 Quantification of birefringence image intensity.....	48
2.9.3 Line scanning and Fourier transform .....	48
2.9.4 Data analysis .....	49
2.9.5 Statistical Analysis .....	49
2.10 Antibodies used.....	50
2.10.1 Primary Antibodies.....	50
2.10.2 HRP (horse radish peroxidase)-conjugated secondary antibodies used in western blotting.....	50

2.10.3 Fluorescently conjugated secondary antibodies used in immunofluorescence .....	51
Chapter 3: A Dystroglycan nonsense mutation elicits a muscular dystrophy phenotype in zebrafish .....	52
3.1 Introduction .....	53
3.1.1 Loss of dystroglycan function in muscular dystrophy.....	53
3.1.2 Loss of dystroglycan in zebrafish causes a muscular dystrophy phenotype .	55
3.1.3 Chapter aims and hypotheses.....	57
3.2 Results .....	57
3.2.2 <i>dag1</i> <sup>hu3072</sup> embryos have a muscular dystrophy phenotype .....	57
3.2.1 Dystroglycan expression in zebrafish.....	60
3.2.3 <i>dag1</i> <sup>hu3072</sup> embryos have a loss of dystrophin expression.....	64
3.2.4 <i>dag1</i> <sup>hu3072</sup> embryos show impaired motility.....	66
3.5 Discussion.....	76
3.5.1 Dystroglycan mutant zebrafish display a muscular dystrophy phenotpye ...	76
3.5.2 Loss of dystrophin localisation in <i>dag1</i> mutants.....	78
3.5.3 Zebrafish locomotion analysis .....	78
3.6 Concluding remarks.....	79
Chapter 4: Regulation of dystroglycan in a zebrafish model of Duchenne Muscular Dystrophy ( <i>sapje</i> ) .....	80
4.1 Introduction .....	81
4.1.1 Loss of dystroglycan in Duchenne muscular dystrophy.....	81
4.1.2 Dystroglycan phosphorylation .....	82
4.1.3 Degradation of dystroglycan in the absence of dystrophin.....	83
4.2 Aims and hypotheses .....	84
4.3 Results .....	85
4.3.1 <i>sapje</i> zebrafish have a dystrophic phenotype .....	85
4.3.2 Loss of dystroglycan in <i>sapje</i> mutants .....	93
4.3.3 Levels of phosphorylated dystroglycan are elevated in <i>sapje</i> .....	96
4.3.4 Manipulation of dystroglycan phosphorylation .....	100
4.3.5 Manipulation of proteasomal degradation .....	106
4.4 Discussion.....	108
4.4.1 The muscular dystrophy phenotype of <i>sapje</i> progresses over time .....	108
4.4.2 Age-dependent decrease in dystroglycan levels in <i>sapje</i> .....	109
4.4.3 Increased phosphorylation of dystroglycan in <i>sapje</i> .....	110
4.4.4 Manipulation of dystroglycan phosphorylation .....	112
4.4.5 Manipulation of proteasomal degradation .....	114

4.5 Concluding remarks.....	115
Chapter 5: Chemical treatment of a zebrafish model of Duchenne Muscular Dystrophy ( <i>sapje</i> ).....	116
5.1 Introduction .....	117
5.1.1 Altered dystroglycan expression in <i>sapje</i> .....	117
5.1.2 Usefulness of zebrafish in drug discovery.....	118
5.2 Aims and hypotheses .....	119
5.3 Results .....	119
5.3.1 Development of the assay .....	119
5.3.2 Positive control compound .....	122
5.3.3 Src kinase inhibitors .....	123
5.3.4 Inhibiting ubiquitination and proteasomal degradation .....	134
5.3.5 Compound treatment of <i>dag1</i> embryos does not prevent development of the dystrophic phenotype.....	150
5.3.6 Chemical treatment does not affect larval motility.....	154
5.3.7 Treatment of larvae after the onset of muscle damage.....	157
5.4 Discussion.....	164
5.4.1 Inhibiting Src kinase .....	166
5.4.2 Inhibiting ubiquitination and proteasomal degradation .....	168
5.5 Concluding remarks.....	173
Chapter 6: Discussion.....	175
6.1 Summary .....	176
6.2 Model of dystroglycan loss in dystrophic muscle .....	176
6.3 Use of proteasomal inhibitors <i>in vivo</i> .....	180
6.4 Src kinase inhibitors <i>in vivo</i> .....	181
6.5 Towards new therapies for DMD.....	183
6.5.1 Therapies tested in clinical trials.....	183
6.5.2 Alternative therapies for DMD.....	184
References.....	187

# List of Abbreviations

---

AAV	adeno-associated virus
AON	anti-sense oligonucleotide
BM	Basement membrane
BMD	Becker muscular dystrophy
cGMP	cyclic guanosine monophosphate
DGC	Dystrophin-associated glycoprotein complex
dH <sub>2</sub> O	Distilled water
DMD	Duchenne muscular dystrophy
dpf	Days post fertilisation
ECM	Extracellular matrix
ENU	N-ethyl-N-nitrosourea
ERK	extracellular-signal-related kinase
hpf	Hours post fertilisation
kDa	Kilodaltons
MAPK	Mitogen-activated protein kinase
Mb	Mega base pairs (1,000,000 bp)
MTJ	Myotendinous junction
NMJ	Neuromuscular junction
nNOS	neuronal nitric oxide synthase
NO	Nitric oxide
PDE	Phosphodiesterase
PDE	Phosphodiesterase
POMT1/ POMT2	Protein O-mannosyltransferase 1 and 2
PTZ	Pentylentetrazole
TM	Transmembrane

# List of Figures

---

- Figure 1.1 Skeletal myofibre structure
- Figure 1.2 Modular representation of dystrophin protein
- Figure 1.3 Schematic showing the organisation of DMD gene
- Figure 1.4 The dystrophin-associated glycoprotein complex (DGC)
- Figure 1.5 Processing of the dystroglycan propetide
- Figure 1.6 Suppression of stop codons by aminoglycosides
- 
- Figure 3.1 Schematic of *dag1*<sup>hu3072</sup> mutation
- Figure 3.2 Loss of birefringence in *dag1* at 3 and 5dpf
- Figure 3.3 Confocal images of 3 and 5dpf larvae stained with rhodamine phalloidin
- Figure 3.4 Loss of dystroglycan immunoreactivity in *dag1* embryos
- Figure 3.5 Localisation of dystroglycan to NMJs
- Figure 3.6 Dystrophin staining in *dag1* mutants
- Figure 3.7 *dag1* larvae show impaired motility
- Figure 3.8 Effect of plate size on Viewpoint ZebraBox movement analysis
- Figure 3.9 Viewpoint ZebraBox movement analysis of 3, 4 and 5dpf larvae
- Figure 3.10 Viewpoint tracking analysis of *dag1* and sibling larvae
- 
- Figure 4.1 Characterisation of *sapje* zebrafish
- Figure 4.2 Loss of birefringence in *sapje* at 3 and 5dpf
- Figure 4.3 *sapje* show defects in motility
- Figure 4.4 Viewpoint tracking analysis of *sapje* and sibling larvae
- Figure 4.5 Confocal images of 3, 4 and 5dpf larvae stained with DAPI, MANDAG2 and rhodamine phalloidin
- Figure 4.6  $\beta$ -dystroglycan levels in sibling and *sapje* larvae

- Figure 4.7 Confocal images of 3dpf larvae stained with 1709
- Figure 4.8 Levels of phosphorylated  $\beta$ -dystroglycan in *sapje* and sibling larvae
- Figure 4.9 Ratio of phosphorylated to non-phosphorylated  $\beta$ -dystroglycan in *sapje* and sibling larvae
- Figure 4.10 Phosphorylated  $\beta$ -dystroglycan in PP2 treated myoblasts
- Figure 4.11 Phosphorylated  $\beta$ -dystroglycan in Dasatinib treated myoblasts
- Figure 4.12 Phosphorylated  $\beta$ -dystroglycan in embryos treated with Dasatinib for 24 hours
- Figure 4.13 Phosphorylated  $\beta$ -dystroglycan in embryos treated with Dasatinib for 48 hours
- Figure 4.14  $\beta$ -dystroglycan in MG132 treated embryos
- 
- Figure 5.1 Schematic of assay
- Figure 5.2 Treatment of embryos with aminophylline
- Figure 5.3 Chemical structure of Dasatinib
- Figure 5.4 Effect of 48 hour Dasatinib treatment on *sapje* muscle phenotype
- Figure 5.5 Effect of 48 hour Dasatinib treatment on the severity of the *sapje* muscle phenotype
- Figure 5.6 Effect of 72 hour Dasatinib treatment on *sapje* muscle phenotype
- Figure 5.7 Effect of 72 hour Dasatinib treatment on the severity of the *sapje* muscle phenotype
- Figure 5.8 Effect of Dasatinib treatment on levels of phosphorylated and non-phosphorylated  $\beta$ -dystroglycan
- Figure 5.9 Chemical structure of Saracatinib
- Figure 5.10 Effect of 48 hour Saracatinib treatment on *sapje* muscle phenotype
- Figure 5.11 Effect of 48 hour Saracatinib treatment on the severity of the *sapje* muscle phenotype
- Figure 5.12 Chemical structure of PYR-41
- Figure 5.13 Effect of 48 hour PYR-41 treatment on *sapje* muscle phenotype

- Figure 5.14 Effect of 48 hour PYR-41 treatment on the severity of the *sapje* muscle phenotype
- Figure 5.15 Effect of 72 hour PYR-41 treatment on *sapje* muscle phenotype
- Figure 5.16 Effect of 72 hour PYR-41 treatment on the severity of the *sapje* muscle phenotype
- Figure 5.17 Effect of PYR-41 treatment on levels of phosphorylated and non-phosphorylated  $\beta$ -dystroglycan
- Figure 5.18 Chemical structure of MG132 and Velcade
- Figure 5.19 Effect of 48 hour MG132 treatment on *sapje* muscle phenotype
- Figure 5.20 Effect of 48 hour MG132 treatment on the severity of the *sapje* muscle phenotype
- Figure 5.21 Effect of MG132 treatment on levels of phosphorylated and non-phosphorylated  $\beta$ -dystroglycan
- Figure 5.22 Effect of 72 hour MG132 treatment on *sapje* muscle phenotype
- Figure 5.23 Effect of 48 hour Velcade treatment on *sapje* muscle phenotype
- Figure 5.24 Effect of 48 hour Velcade treatment on the severity of the *sapje* muscle phenotype
- Figure 5.25 Effect of 48 hour Dasatinib treatment on *dag1* muscle phenotype
- Figure 5.26 Effect of 48 hour PYR-41 treatment on *dag1* muscle phenotype
- Figure 5.27 Effect of 48 hour MG132 treatment on *dag1* muscle phenotype
- Figure 5.28 Effect of tricaine on WT zebrafish motility
- Figure 5.29 Effect of drug treatment on motility of WT larvae
- Figure 5.30 Intensity profile plots of wildtype and *sapje* birefringence images at 3dpf
- Figure 5.31 Line scans and Fourier transforms of 3dpf larvae
- Figure 5.32 Fourier analysis of 3 and 5dpf sibling and *sapje* fish
- Figure 5.33 Fourier analysis of Dasatinib treated embryos
- Figure 5.34 Viewpoint tracking analysis of Dasatinib treated embryos
- Figure 6.1 Model for loss of dystroglycan in DMD

# Acknowledgements

---

Firstly, I would like to thank my supervisor, Professor Steve Winder, for giving me the opportunity to work in his lab, and for the guidance and support he has provided during my time as his student. I appreciate the enthusiasm and commitment he has shown towards my work. I would also like to thank Dr Gaynor Miller for providing additional advice whenever needed.

To all members of both Steve's lab and Kathryn Ayscough's lab, past and present, thank you for making the last few years so enjoyable. You have been great lab mates, and I will miss our coffee breaks! Special thanks go to Chris Moore, Grinu Mathew and Rob Piggott for providing helpful discussions and advice.

Thank you to my co-supervisor Henry Roehl, and my advisors, Carl Smythe and Tim Chico, for their suggestions and support during my studies. I would like to thank Mikko Juusola for help with the world of data transformation and Matlab. Thanks also go to team fish, for looking after the zebrafish aquarium and providing help of a technical nature.

I would also like to thank the Muscular Dystrophy Campaign for funding my work, and for providing opportunities to talk about my research with supporters of the charity.

Last, but not least, I would like to thank my family and friends for their continued support during the last 4 years. A special thank you goes to Matt Regan for supporting me with patience, encouragement, love and chocolate!

# Abstract

---

Dystroglycan is central to the dystrophin-associated glycoprotein complex (DGC), which helps provide stability to muscle fibres. The absence of dystrophin in Duchenne muscular dystrophy results in the loss of this complex. The phosphorylation of  $\beta$ -dystroglycan is thought to play an important role in controlling the integrity of the DGC. This phosphorylation event has been shown to promote  $\beta$ -dystroglycan internalisation, possibly as a prerequisite to degradation. The work presented in this thesis aimed to use the zebrafish to investigate new therapeutic approaches to restore dystroglycan to the membrane and assess the extent to which muscle attachments can be strengthened in the dystrophin mutant zebrafish (*sapje*). As in mammals, the stability of the zebrafish DGC is dependent on dystrophin expression. As such,  $\beta$ -dystroglycan levels in *sapje* decreased in an age-dependent manner. Loss of dystrophin led to an initial elevation in phosphorylated  $\beta$ -dystroglycan levels. Treatment of *sapje* fish with proteasome and kinase inhibitors was able to prevent or slow the progression of dystrophy, in a dose-dependent manner. This was associated with a concomitant increase in dystroglycan and decrease in phosphorylated dystroglycan. This work provides insight into the molecular mechanisms that lead to the loss of dystroglycan from the membrane in dystrophic muscles, and may have therapeutic implications in the future.

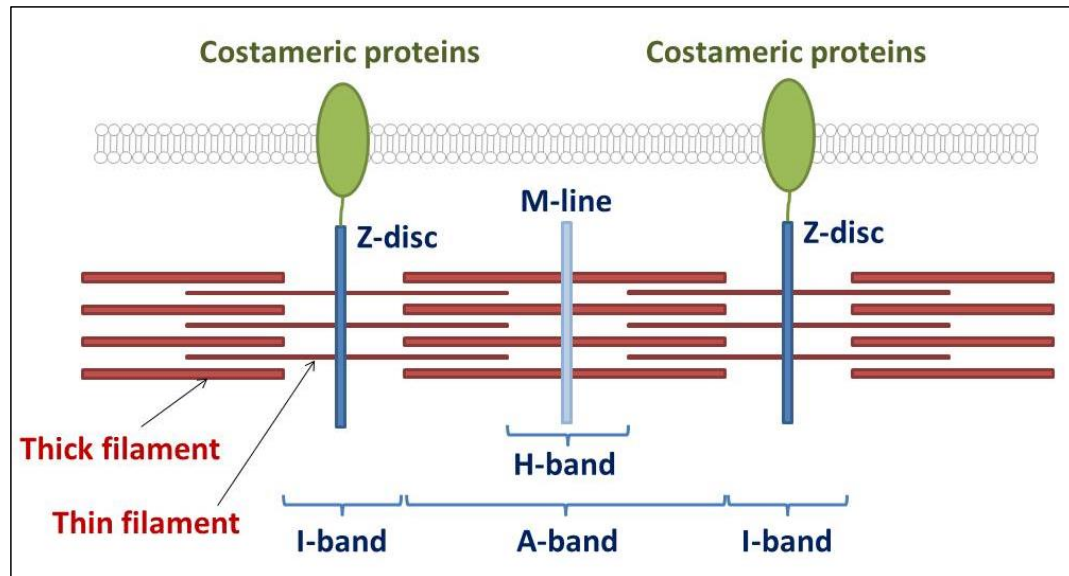
**Chapter 1: Introduction**

---

## 1.1 Skeletal Muscle

Skeletal muscle represents a significant component of vertebrate anatomy and has important roles in locomotion and energy metabolism. It is highly specialised to withstand the mechanical stresses caused by contraction, in order to maintain muscle cell integrity and force transmission.

Skeletal muscle is made up of long, multinucleated myofibres, which are formed by the fusion of myoblasts. Each myofibre is surrounded by the sarcolemma (plasma membrane) and an overlying basal lamina. Myofibres contain an ordered array of sarcomeres, the contractile units of striated muscle, which comprise myosin-containing thick filaments and actin-containing thin filaments. These myofilaments, together with additional structural and regulatory proteins, are arranged longitudinally as myofibrils. The contractile apparatus is linked to the sarcolemma by interactions with costameres, subsarcolemmal protein complexes (figure 1.1). These connections allow the transmission of contractile forces from sarcomeres across the sarcolemma to the extracellular matrix (ECM) and adjacent myofibres, allowing the synchronisation of muscle contraction and preventing sarcolemmal rupture. In addition to costameres, there are other sites of sarcolemmal attachment to the ECM including neuromuscular junctions (NMJs) and myotendinous junctions (MTJs).

**Figure 1.1: Skeletal myofibre structure**

The contractile apparatus is linked to the sarcolemma by interactions with costameres. Costameres are subsarcolemmal protein complexes that circumferentially align with the z-discs and physically couple sarcomeres with the sarcolemma. The costameric network comprises many proteins including DGC components, integrins,  $\alpha$ -actinin, vinculin and talin.

The importance of the basement membrane (BM), sarcolemma and cytoskeleton in skeletal muscle structure and function is highlighted by the vast number of muscle diseases caused by mutations in BM and cytoskeletal components, or the protein complexes linking them together. The two major protein complexes linking the cytoskeleton and basement membrane in adult skeletal muscle are the integrins and the dystrophin-associated glycoprotein complex (DGC), and these complexes are concentrated at costameres, NMJs and MTJs. A significant number of muscular dystrophies arise from mutations that affect the assembly of these complexes.

## 1.2 Muscular dystrophy

Muscular dystrophies are a heterogeneous group of genetic disorders characterised by progressive weakness and degeneration of skeletal muscle. Damage to muscle fibres activates satellite cells, located between the sarcolemma and basal lamina, to initiate muscle fibre regeneration. Myofibres of healthy muscle are roughly equal in diameter, with nuclei at the periphery. However, dystrophic muscle consists of fibres of varying sizes with centrally located nuclei, indicative of degeneration and regeneration. Continued muscle damage leads to the loss of regenerative capacity. Muscle is gradually replaced by fatty and fibrous tissue, leading to muscle wasting and weakness.

## 1.3 Duchenne muscular dystrophy

The most common form of muscular dystrophy is Duchenne muscular dystrophy (DMD), an X-linked disorder affecting 1 in 3500 boys (Emery, 1993). DMD was first described in the 19<sup>th</sup> century by Meryon (1852) and Duchenne (1868). Affected individuals show a progressive loss of muscle strength starting in early childhood, initially affecting proximal muscles, rapidly extending to distal muscles and eventually to most voluntary muscle groups (Emery, 1993). Continuous muscle wasting results in the loss of ambulation before the age of 12 and culminates in premature death in the 20s, usually due to respiratory or cardiac failure (Emery, 1993).

DMD results from mutations in the DMD gene (Koenig et al., 1987), which encodes the protein dystrophin (Hoffman et al., 1987). The DMD gene, localised to chromosome Xp21 (Davies et al., 1983), is the largest described in the human genome, spanning over

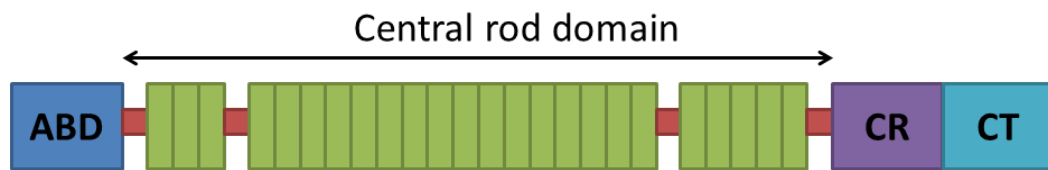
2.5Mb and comprising 79 exons (Coffey et al., 1992, Monaco et al., 1992, Roberts et al., 1993). The full length mRNA transcript is 14kb long and is predominantly expressed in muscle tissue, with lower levels in the brain (Chamberlain et al., 1988, Nudel et al., 1988). The protein product of the DMD gene was named dystrophin, since muscular dystrophy results from its absence (Hoffman et al., 1987).

Becker muscular dystrophy (BMD), a milder form of DMD, is also caused by mutations in the gene encoding dystrophin. In BMD, low levels of a truncated protein can be found, whereas DMD mutations result in the complete absence of functional dystrophin (Monaco et al., 1988, Koenig et al., 1989).

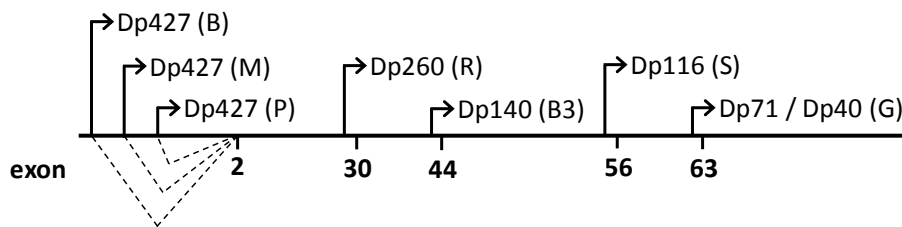
#### **1.4 Dystrophin**

Dystrophin is a 427kDa cytoskeletal linker protein found at the intracellular face of the sarcolemmal membrane. Dystrophin comprises 4 domains (Koenig et al., 1988): an N-terminal actin-binding domain, a long central rod domain consisting of 24 spectrin-like repeats interspersed with 4 hinge regions (Koenig and Kunkel, 1990), a cysteine rich domain and a C-terminal domain (figure 1.2). The cysteine rich domain consists of a WW domain (Bork and Sudol, 1994), 2 EF hands (Koenig et al., 1988) and a ZZ domain (Ponting et al., 1996). WW domains are protein interaction modules that are 30 amino acids in length. They contain 2 conserved tryptophan residues, which are involved in interactions with proline-rich binding motifs. EF hands are highly conserved motifs involved in the binding of  $\text{Ca}^{2+}$  and  $\text{Mg}^{2+}$  ions. ZZ domains, cysteine-rich zinc-finger domains, are modules thought to mediate protein-protein interactions.

Several promoters regulate the expression of full length and truncated isoforms of dystrophin (figure 1.3). The expression of 3 full length (427kDa) dystrophin isoforms, primarily found in brain, muscle and Purkinje neurons, is regulated by 3 independent promoters (Nudel et al., 1989, Klamut et al., 1990, Gorecki et al., 1992). These isoforms differ only by the 1<sup>st</sup> exon. In addition, the DMD gene also contains at least 4 internal promoters. These give rise to truncated protein products of 260, 140, 116, 71 and 40kDa, which are expressed in non-muscle tissues (Bar et al., 1990, Byers et al., 1993, Tinsley et al., 1993, D'Souza et al., 1995, Lidov et al., 1995). Defects in muscle dystrophin result in the most obvious phenotype (muscular dystrophy), although some DMD patients show other defects, such as cognitive impairment (Emery, 1993), which may be caused by deficiencies in other dystrophin isoforms.

**Figure 1.2 Modular representation of dystrophin protein**

Dystrophin is organised into 4 major domains: an N-terminal actin-binding domain, (ABD), a central rod domain consisting of 24 spectrin-like repeats (green) interspersed with 4 hinge regions (red), a cysteine rich domain (CR) and a C-terminal domain (CT).

**Figure 1.3 Schematic showing the organisation of DMD gene**

Promoters (depicted by arrows) in the 5' end of the gene drive the expression of 3 full length (427kDa) dystrophin isoforms in brain (B), muscle (M) and Purkinje neurons (P). Each transcript consists of unique first exons spliced to a common set of 78 exons. The 3 protein products are termed Dp427(B), Dp427(M) and Dp427(P), reflecting their primary location. The smaller isoforms are produced from 4 internal promoters (R: retina, B3: brain, S: Schwann cells, G: general). These promoters are located in the introns upstream of exons 30, 44, 56 and 63 as indicated above. These are expressed in the retina (R: Dp260), brain (B3: Dp140), Schwann cells (S:Dp116) or ubiquitously expressed (G:Dp71). Dp40 is produced by the alternative splicing of Dp71.

## **1.5 The dystrophin-associated glycoprotein complex (DGC)**

### **1.5.1 The protective role of the DGC**

In muscle, dystrophin plays an important structural role, forming part of a large complex at the sarcolemma termed the dystrophin-associated glycoprotein complex (DGC) (Ervasti et al., 1990). The DGC provides a stabilising mechanical link between the cytoskeleton of the myofibre and the surrounding ECM (Ervasti and Campbell, 1991, Ervasti and Campbell, 1993). This link is thought to protect the muscle from damage during repeated cycles of contraction and relaxation.

In the absence of dystrophin, there is a significant reduction in the entire DGC (Ohlendieck and Campbell, 1991, Ohlendieck et al., 1993). Therefore, the link between the cytoskeleton and ECM is compromised, making the sarcolemma more fragile and susceptible to mechanical injury, which results in muscle damage.

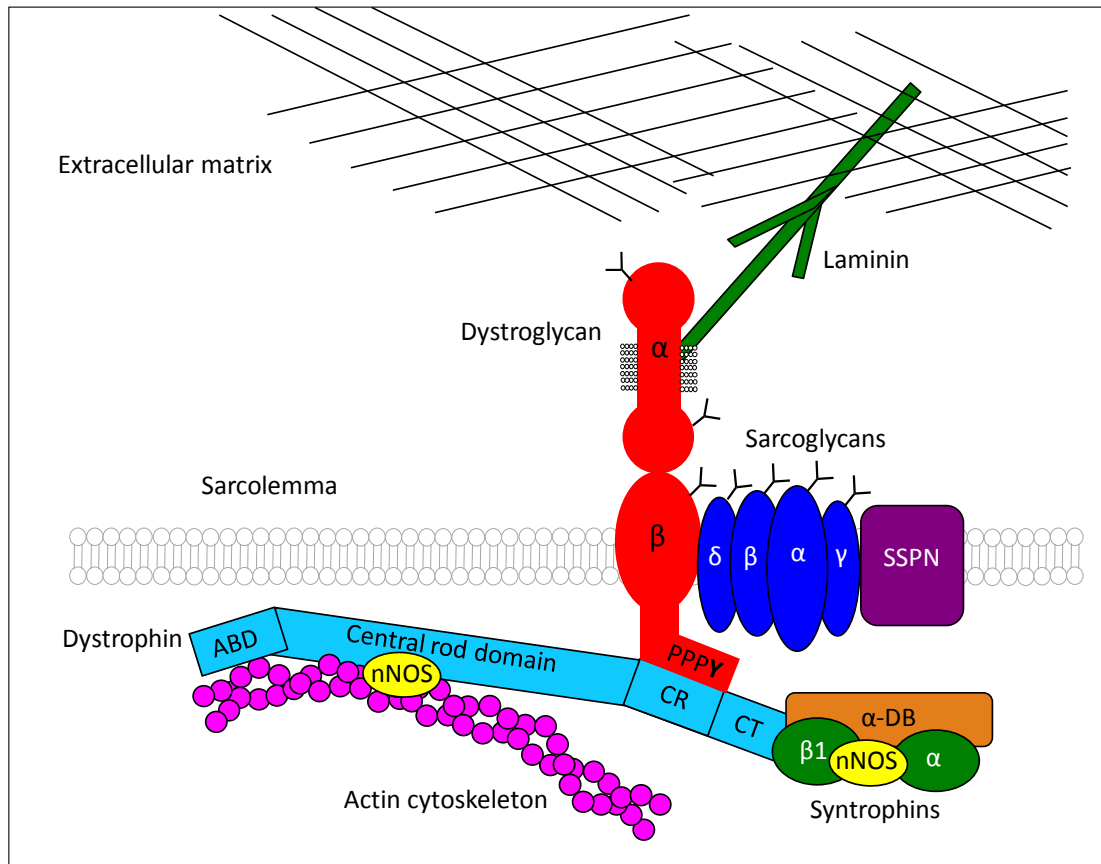
In addition to this mechanical role, the DGC may also act as a scaffold for signalling complexes. This is illustrated by its interactions with various signalling molecules, which are discussed further in subsequent sections. Thus, loss of complex components in muscular dystrophy may disrupt the signalling functions of the DGC as well as its protective role.

### 1.5.2 DGC components

In addition to dystrophin, the DGC consists of cytoplasmic ( $\alpha$ 1- and  $\beta$ 1-syntrophin,  $\alpha$ -dystrobrevin and nNOS), transmembrane ( $\beta$ -dystroglycan,  $\alpha$ -,  $\beta$ -,  $\gamma$ - and  $\delta$ -sarocglycan and sarcospan) and extracellular ( $\alpha$ -dystroglycan and laminin-2) proteins (figure 1.4). Many of these components have been implicated in various muscular dystrophies, highlighting the importance of the DGC in maintaining muscle integrity.

Dystrophin interacts with the DGC via its cysteine rich and C-terminal domains.  $\alpha$ -dystrobrevin and the syntrophins bind directly to each other and to the C-terminal region of dystrophin (Albrecht and Froehner, 2002).  $\beta$ -dystroglycan binds to the WW domain of dystrophin. This interaction is stabilised by one of two EF-hands located adjacent to the WW domain (Rentschler et al., 1999), and the ZZ domain (Ishikawa-Sakurai et al., 2004).

The cell adhesion protein dystroglycan is central to the DGC, interacting with the ECM via its  $\alpha$ -subunit and dystrophin via its  $\beta$ -subunit. Dystrophin completes the link between the cytoskeleton and ECM, by binding to actin, via its actin-binding sites in the N-terminal and rod domains (Rybakova et al., 1996, Rybakova and Ervasti, 1997, Amann et al., 1998).

**Figure 1.4: The dystrophin-associated glycoprotein complex (DGC)**

Representation of the key proteins in the DGC, which forms a link between the cytoskeleton and ECM. Dystroglycan (shown in red) is central to this complex. The PPPY motif in the C-terminal tail of  $\beta$ -dystroglycan binds to the WW domain within the cysteine rich domain of dystrophin. Phosphorylation of the tyrosine residue within this motif disrupts dystrophin binding.

(ABD – actin-binding domain; CR – cysteine rich domain; CT – C-terminal domain; SSPN – sarcospan;  $\alpha$ -DB –  $\alpha$ -dystrobrevin)

## 1.6 Dystroglycan

Dystroglycan expression is not muscle-specific and it has a variety of roles in other cell types. Given the important role of the DGC in preventing muscle damage, dystroglycan has been predominantly studied in the context of muscle and muscular dystrophies.

Until recently, no mutations in the dystroglycan gene had been identified in a human disease. This is thought to be due to the fundamental role of dystroglycan in mammalian development. Mouse dystroglycan knockouts are embryonic lethal due to the failure of the extra-embryonic Reichert's membrane to form (Williamson et al., 1997). Although mutations in dystroglycan itself are rare, mutations in enzymes involved in the post-translational modification of dystroglycan result in muscular dystrophy (see section 1.6.2).

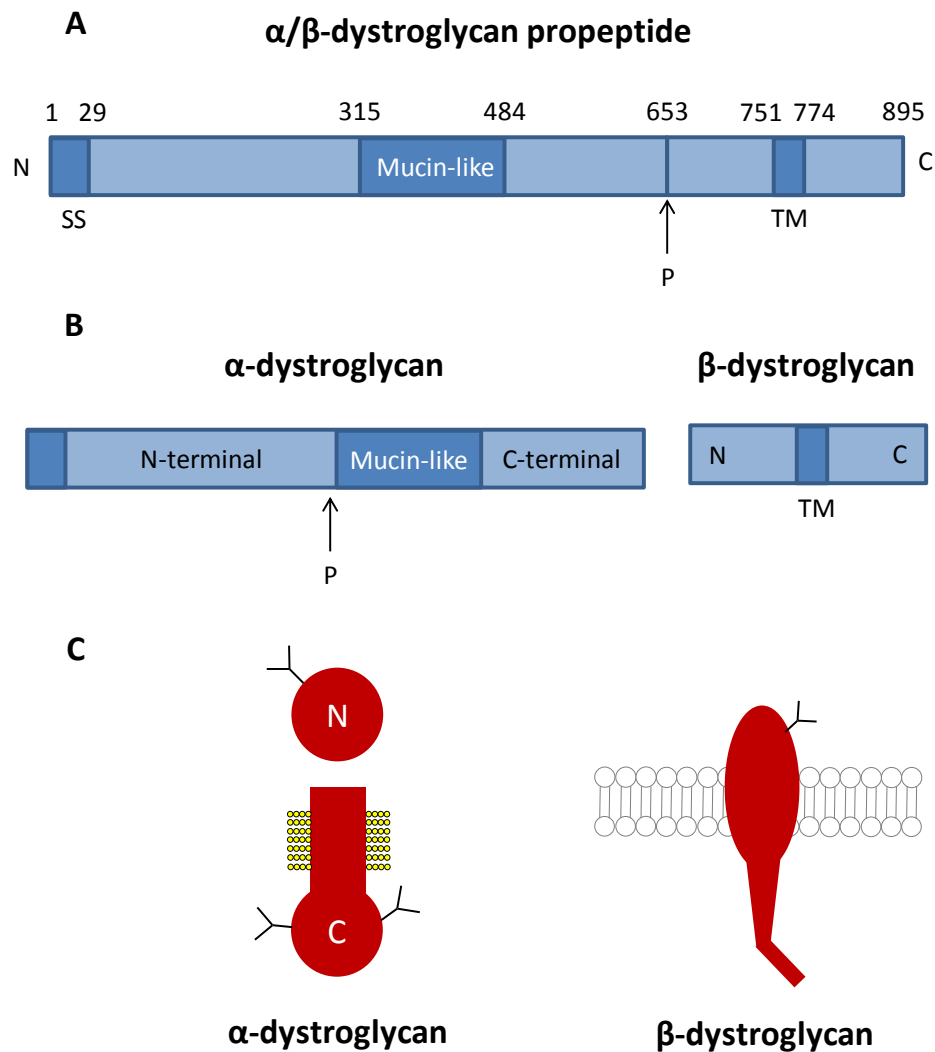
### 1.6.1 Dystroglycan gene

Dystroglycan was the first component of the DGC to be cloned (Ibraghimov-Beskrovnaya et al., 1992). The dystroglycan gene, *DAG1*, is located on human chromosome 3p21 and comprises 2 exons, separated by a large intron.

The dystroglycan gene encodes a propeptide that is post-translationally cleaved into  $\alpha$ - and  $\beta$ -subunits (Ibraghimov-Beskrovnaya et al., 1992, Holt et al., 2000) (figure 1.5).

These interact with each other non-covalently, forming a heterodimer within the DGC.

Figure 1.5: Processing of the dystroglycan propeptide



(A) The dystroglycan gene, *DAG1*, encodes a single 895 amino acid propeptide with a signal sequence (SS), a mucin-like region, and a transmembrane (TM) region. This propeptide is post-translationally cleaved (P) at residue 653, to yield  $\alpha$ - and  $\beta$ -dystroglycan shown in (B). The N-terminal domain of  $\alpha$ -dystroglycan is cleaved at residue 312 (Kanagawa et al 2004) to form the mature protein shown in (C). Carbohydrate side chains are shown schematically as circles for O-linked glycosylation and branches for N-linked glycosylation.  $\beta$ -dystroglycan is shown inserted in a lipid bilayer with its C-terminus on the intracellular side (C).

### 1.6.2 $\alpha$ -dystroglycan

The extracellular  $\alpha$ -dystroglycan comprises globular N- and C-terminal domains, connected by a central, heavily O-glycosylated, mucin-like domain (Ibraghimov-Beskrovnaya et al., 1992, Brancaccio et al., 1995) (figure 1.5). In addition to undergoing O-linked glycosylation,  $\alpha$ -dystroglycan contains 3 N-linked glycosylation sites. The sugar modifications are important for the interactions between dystroglycan and its various ECM ligands; although treatment with N-glycanases has no effect on the binding ability of dystroglycan, complete deglycosylation of  $\alpha$ -dystroglycan results in the loss of ligand binding (Ervasti and Campbell, 1993). This suggests that ligand interactions are mediated by the O-linked modifications of the mucin domain.

The extent of  $\alpha$ -dystroglycan glycosylation is dependent on tissue type, and is also developmentally regulated.  $\alpha$ -dystroglycan is predicted to be approximately 70kDa, but on an SDS-PAGE gel, mammalian skeletal muscle  $\alpha$ -dystroglycan has an apparent mass of approximately 156kDa (Ervasti and Campbell, 1991).

Reduced glycosylation of  $\alpha$ -dystroglycan, caused by mutations in genes encoding known or putative glycosyltransferases, is associated with a group of muscular dystrophies, known as the dystroglycanopathies (Muntoni et al., 2004, Godfrey et al., 2007a, Moore and Hewitt, 2009, Muntoni et al., 2011). These include Fukuyama congenital muscular dystrophy (FCMD) and muscle-eye-brain disease (MEB).  $\alpha$ -dystroglycan is present in these patients, but has a lower molecular mass, consistent with reduced glycosylation (Michele et al., 2002b). This hypoglycosylation of  $\alpha$ -

dystroglycan results in decreased binding to ECM ligands such as laminin (Michele et al., 2002b), thus disrupting the link between the DGC and the ECM.

Laminin binding is also affected by the only primary dystroglycan mutation that has been described so far in a human disease. A missense mutation within the N-terminal region of  $\alpha$ -dystroglycan was identified in this patient, who was diagnosed with limb girdle muscular dystrophy (LGMD) with severe cognitive impairment (Hara et al., 2011). This resulted in hypoglycosylation and reduced laminin binding activity of  $\alpha$ -dystroglycan in a mouse model harbouring the equivalent mutation. This further highlights the importance of a continuous link between the cytoskeleton and ECM.

### 1.6.3 $\beta$ -dystroglycan

$\beta$ -dystroglycan is also subject to N-linked glycosylation, producing a mature protein of approximately 43kDa. Glycosylation is necessary for the correct localisation of  $\alpha$ - and  $\beta$ -dystroglycan, but not for the proteolytic cleavage of the propeptide (Holt et al., 2000).

$\beta$ -dystroglycan consists of an extracellular domain, which interacts with the C-terminal of  $\alpha$ -dystroglycan independently of glycosylation (Di Stasio et al., 1999), a transmembrane domain, and a proline-rich cytoplasmic domain (figure 1.5). The cytoplasmic domain contains a PPXY motif, which binds to dystrophin through an interaction with its WW domain.

### 1.6.3.1 $\beta$ -dystroglycan interactions

In addition to dystrophin, the cytoplasmic tail of  $\beta$ -dystroglycan interacts with other cytoplasmic proteins. One such protein is utrophin, the autosomal homologue of dystrophin (Love et al., 1989). Utrophin binds dystroglycan via WW, EF and ZZ domains (Chung and Campanelli, 1999, Ishikawa-Sakurai et al., 2004), forming complexes analogous to the DGC (James et al., 1996). In adult muscle, these complexes are normally restricted to MTJs and NMJs (Khurana et al., 1991, Nguyen et al., 1991).  $\beta$ -dystroglycan also binds another cytolinker protein, plectin (Rezniczek et al., 2007). Both plectin (Rezniczek et al., 2007) and utrophin (Helliwell et al., 1992, Matsumura et al., 1992, Karpati et al., 1993b) are upregulated in dystrophin-deficient muscle, possibly as part of a compensatory mechanism.

Caveolin-3 has a WW-like domain, which is able to bind to the PPxY motif in  $\beta$ -dystroglycan (Sotgia et al., 2000). This interaction is able to disrupt the interaction between dystroglycan and dystrophin, thus may play a role in regulating dystrophin recruitment to the sarcolemma.

SH2 domain containing proteins, including c-Src, can bind to the PPxY motif in  $\beta$ -dystroglycan (Sotgia et al., 2001). Signalling molecules, including Grb2 (Yang et al., 1995) and components of the ERK/MAP kinase pathway (Spence et al., 2004), have also been shown to bind to the cytoplasmic tail of  $\beta$ -dystroglycan. This suggests that dystroglycan has a role in cell signalling, in addition to its function in maintaining a structural link between the cytoskeleton and ECM.

### 1.6.3.2 Phosphorylation of $\beta$ -dystroglycan

Phosphorylation of the tyrosine residue within the PPxY motif of  $\beta$ -dystroglycan (Y892 in humans, Y890 in mice) disrupts its interaction with dystrophin and utrophin (James et al., 2000, Ilsley et al., 2001). In the crystal structure of this interaction, Y892 is demonstrated to sit in a hydrophobic pocket of the WW domain, forming a hydrogen bond with a histidine residue from the WW domain (Huang et al., 2000). Addition of a phosphate group on the tyrosine would likely break this bond and make it too large to fit in the hydrophobic pocket.

Unlike dystrophin and utrophin interactions, phosphorylation of  $\beta$ -dystroglycan at the tyrosine residue of the PPxY motif does not affect the binding of  $\beta$ -dystroglycan and caveolin-3 (Sotgia et al., 2000). In addition, SH2 domain proteins are recruited in a phosphorylation-dependent manner (Sotgia et al., 2001). Therefore, tyrosine phosphorylation of  $\beta$ -dystroglycan may act as a regulatory switch, inhibiting the binding of dystrophin, whilst promoting the binding of caveolin-3 and SH2 domain proteins.

It is thought that phosphorylation of  $\beta$ -dystroglycan at the tyrosine residue in its PPxY motif is mediated by Src family kinases and that this modification plays a role in  $\beta$ -dystroglycan internalisation to an intracellular compartment (Sotgia et al., 2003, Miller et al., 2012). Consequently, this phosphorylation event may play an important role in controlling the localisation of dystroglycan and thus the integrity of the DGC.

### 1.7 Sarcoglycan complex and sarcospan

Sarcoglycans are N-glycosylated, transmembrane proteins that form a tetrameric complex as part of the DGC. 6 sarcoglycans ( $\alpha$ -,  $\beta$ -,  $\gamma$ -,  $\delta$ -,  $\epsilon$ - and  $\zeta$ -sarcoglycan) exist, but the predominant sarcoglycan complex in skeletal and cardiac muscle comprises  $\alpha$ -,  $\beta$ -,  $\gamma$ - and  $\delta$ -sarcoglycans (Chan et al., 1998, Holt and Campbell, 1998, Ozawa et al., 2005).

In addition to dystrophin deficiency causing sarcoglycan complex destabilisation, mutations in sarcoglycans themselves also cause muscular dystrophy. Limb-girdle muscular dystrophy (LGMD) types 2D, 2E, 2C and 2F arise from mutations in  $\alpha$ -,  $\beta$ -,  $\gamma$ - and  $\delta$ -sarcoglycans respectively (Laval and Bushby, 2004). Typically, mutations in one sarcoglycan result in the loss or reduction of the whole tetrameric complex (Vainzof et al., 1996).

The role of the sarcoglycan complex within the DGC has not been well defined, but it is thought to have both signalling and mechanical roles, providing additional support to the DGC and sarcolemma (Ozawa et al., 2005, Barton, 2006)

The sarcoglycan complex closely associates with the 4 transmembrane domain containing protein sarcospan, which is structurally related to the tetraspanin family (Crosbie et al., 1997, Crosbie et al., 1999, Crosbie et al., 2000). Tetraspanins play important roles in a wide range of cellular functions, such as adhesion and signalling, by clustering proteins at the membrane (Hemler, 2001). Thus, sarcospan may facilitate protein interactions at the DGC.

Complete or partial loss of the sarcoglycan complex results in the loss of sarcospan from the membrane, suggesting the stability of sarcospan is mediated by this complex (Crosbie et al., 1999, Crosbie et al., 2000). However, sarcospan-deficient mice do not show a dystrophic phenotype (Lebakken et al., 2000), suggesting muscle may be able to compensate for the absence of sarcospan. Indeed, loss of sarcospan results in an increase in  $\alpha 7\beta 1$  integrin expression (Marshall et al., 2012).  $\alpha 7\beta 1$  integrin is the main integrin complex found in muscle, and is also able to form connections between the cytoskeleton and ECM.

### **1.8 $\alpha$ -dystrobrevin, syntrophins and nNOS**

$\alpha$ -dystrobrevin is a cytoplasmic protein thought to play a signalling role within the DGC.  $\alpha$ -dystrobrevin deficient mice display a mild muscle disease phenotype, even though the assembly of the remaining DGC components at the sarcolemma is not affected (Grady et al., 1999). Neuronal nitric oxide synthase (nNOS), however, is displaced from the sarcolemma.

The sarcolemmal localisation of nNOS is essential for its function in regulating blood flow to meet the metabolic demands of contracting skeletal muscle. nNOS produces nitric oxide (NO) in response to muscle contractions. NO induces guanylyl cyclase to synthesise cyclic GMP (cGMP), which functions as a vasodilator, increasing the local blood flow to meet the increased energy demands.

nNOS is also displaced from the sarcolemma in the absence of dystrophin (Brenman et al., 1995) and this is thought to contribute to the dystrophic process (Thomas et al., 1998, Sander et al., 2000). Genetically increasing levels of nNOS is able to ameliorate the muscular dystrophy phenotype in dystrophin deficient *mdx* mice (Wehling et al., 2001). In addition, use of PDE5 inhibitors, which increase levels of cGMP, is able to reduce cardiomyopathy and improve diaphragm muscle pathology in the *mdx* mouse (Adamo et al., 2010, Percival et al., 2012).

Dystrophin and  $\alpha$ -dystrobrevin interact with  $\alpha$ 1- and  $\beta$ 1-syntrophin (Newey et al., 2000), which bind nNOS through PDZ domains (Brenman et al., 1996). Dystrophin can also directly recruit nNOS via spectrin-like repeat 17 (Lai et al., 2013), and this interaction may be essential for nNOS recruitment to the sarcolemma.

In addition to nNOS, the syntrophins are thought to be involved in localising several other proteins to the DGC, including signalling molecules, kinases and membrane channels (Gee et al., 1998, Schultz et al., 1998, Hasegawa et al., 1999, Neely et al., 2001, Oak et al., 2001). This further highlights a signalling role for the DGC.

### **1.9 Animal models of DMD**

Despite a wealth of research into DMD, no curative treatment exists. To further characterise the molecular mechanisms involved in the pathogenesis of DMD, and to develop treatments, several animal models have been utilised.

### 1.9.1 The *mdx* mouse

The most characterised model of DMD is the *mdx* mouse (Bulfield et al., 1984, Hoffman et al., 1987), but it has a mild phenotype compared with the human condition and lifespan is only slightly shortened (Chamberlain et al., 2007). The *mdx* mouse has a premature stop codon in exon 23 of the DMD gene, resulting in a lack of full length dystrophin (Sicinski et al., 1989). *mdx* muscle undergoes an initial period of degeneration, followed by successful regeneration (Dangain and Vrbova, 1984, Tanabe et al., 1986). Muscles are differentially affected, with the diaphragm showing the most severe pathology (Stedman et al., 1991). However, other, less affected muscles are more susceptible to contraction-induced injury (Dellorusso et al., 2001), and exercise can be used to speed up the disease progression (De Luca et al., 2003).

It is thought that the pathology in *mdx* mice may be moderated by a compensatory upregulation of utrophin. Double dystrophin and utrophin mutants (dKO mice) have a more severe phenotype which may be more comparable to DMD (Deconinck et al., 1997).

### 1.9.2 The GRMD dog

The golden retriever muscular dystrophy (GRMD) dog (Cooper et al., 1988) has a phenotype more closely related to the human disease than the *mdx* mouse, although the severity is often quite variable (Kornegay et al., 1988, Valentine et al., 1988).

Although dogs are not ideal animal models, and are large and expensive, this model can be used to test potential treatments identified in murine studies.

### **1.9.3 Zebrafish as a model for muscular dystrophy**

The zebrafish has emerged as a powerful tool for studying vertebrate development and disease due to its many advantages as a model organism. These include the rapid external development of optically transparent embryos, which are permeable to small molecules, and the ability to quickly generate large numbers of offspring. Zebrafish are genetically tractable, and many models of human diseases have been established, many of which closely resemble the condition (Lieschke and Currie, 2007).

Zebrafish offer many specific attributes that are particularly suited for the study of muscle diseases. Genes important for muscle development and the maintenance of muscle integrity are highly conserved between zebrafish and mammals. Orthologues of most human muscular dystrophy genes can be found in the zebrafish genome (Steffen et al., 2007), and dystrophic phenotypes arise where these genes are disrupted. In particular, components of the DGC are present in zebrafish (Chambers et al., 2003, Guyon et al., 2003), and disruptions in these genes affect muscle integrity (Parsons et al., 2002, Bassett et al., 2003, Guyon et al., 2005, Nixon et al., 2005, Hall et al., 2007, Gupta et al., 2011).

The zebrafish body is composed predominantly of skeletal muscle, which develops quickly and is fully differentiated by 48hpf (Kimmel et al., 1995). The somitic muscle

derives from segmented paraxial mesoderm. Slow-twitch muscle fibres differentiate first. These fibres originate from adaxial myoblasts, which migrate radially through the developing myotome to form a subcutaneous layer of mononucleated slow-twitch fibres (van Raamsdonk et al., 1978, Devoto et al., 1996). Fast-twitch muscle fibres, which make up most of the zebrafish trunk musculature, arise later from a separate pool of myoblasts, which fuse to form multinucleated fibres (Devoto et al., 1996, Henry and Amacher, 2004).

Trunk skeletal muscle is simply organised in the zebrafish embryo, with myotubes spanning each somite along the anterior-posterior axis. At the somite boundaries, the muscle fibres attach to the vertical myosepta, sheets of matrix separating adjacent somites that are equivalent to mammalian MTJs (Charvet et al., 2011). The notochord and horizontal myoseptum, which separates dorsal and ventral halves of the myotome, also serve as attachment sites for the muscle fibres. DGC components are concentrated at these muscle attachment points (Guyon et al., 2003).

In terms of evolution and anatomy, zebrafish are not as closely related to humans as mammalian models. Although zebrafish muscle shares many molecular and histological features with mammalian muscle, there are some obvious differences. For example, slow and fast muscle fibres are topographically separated in zebrafish, but are intermingled in mammals. In addition, unlike mammals, zebrafish musculature retains its somitic organisation throughout development.

Despite these limitations, the advantages of using zebrafish as a model system for muscular dystrophy outweigh the costs. For example, potential treatments can be analysed in fish on a much faster time scale than in mammals. Whilst it is not likely to replace other established models of muscular dystrophy such as the *mdx* mouse, the zebrafish can be an effective complement to mammalian models due to its useful attributes.

Simultaneous use of both fish and mouse models would be more efficient and cost-effective than using mammalian models alone. Although results from zebrafish studies cannot be directly translated into human therapy, they can be tested and refined in mammals. However, since zebrafish express many genes implicated in human muscular dystrophies, and mutations in these genes result in a dystrophic phenotype, this suggests that findings may be transferable to humans.

Many zebrafish models of muscular dystrophy exist, reviewed in (Berger et al., 2012, Lin, 2012). These fish have robust and readily recognisable phenotypes, which are visible early in development. These models of muscular dystrophies have facilitated many valuable insights into dystrophic pathologies.

The dystrophin-deficient zebrafish model of DMD, *sapje*, and a dystroglycan mutant have been utilised in this study, and are described in the relevant chapters.

## **1.10 Treatments for DMD**

### **1.10.1 Current treatment**

Currently, DMD patients are treated with the corticosteroids prednisone and deflazacort, although these drugs are associated with adverse side effects (Fenichel et al., 1991). These drugs improve muscle strength and slow the disease progression, though the mechanism of action is not entirely clear. It is thought these drugs may act to improve membrane stability (Jacobs et al., 1996), stimulate muscle repair (Anderson et al., 2000) and reduce inflammation (Kissel et al., 1991, Wehling-Henricks et al., 2004, Rhen and Cidlowski, 2005). Dose optimisation studies and the development of modified steroids may help to improve the balance between the benefits and unwanted effects associated with corticosteroids (Hoffman et al., 2012). However, side effects still remain a major limitation, especially when the drugs are used for long periods of time.

### **1.10.2 Potential treatments**

A number of different therapeutic approaches have been adopted with the aim of treating DMD, some of which are in clinical trials.

#### **1.10.2.1 Gene therapy**

Viral gene therapy can be used to directly replace the missing protein in a disease. However, in DMD, the large size of the dystrophin gene and the need to target all the affected muscles in the body represent limitations of this approach. Mini- and micro-

dystrophin genes, which can be cloned into AAV (adeno-associated virus) vectors, have been designed based on mildly affected BMD patient mutations. These have been used successfully in *mdx* mice (Wang et al., 2000).

A problem associated with introducing a previously absent protein is the risk of immune rejection. This is not seen in *mdx* mice, but gene therapy studies in dogs and humans have resulted in variable immunological responses (Wang et al., 2007, Mendell et al., 2010). If immune responses can be minimised, the need to target all affected muscles still remains a challenge. In addition, the truncated protein expressed may not be able to fulfil all the functions of dystrophin, for example the localisation of nNOS to the sarcolemma.

#### **1.10.2.2 Cell therapy**

The delivery of muscle precursor cells or stem cells into dystrophic muscles has been explored as a potential therapy for DMD. Despite the promising results achieved when healthy donor myoblasts were transplanted into *mdx* mice (Partridge et al., 1989), subsequent human trials have yielded poor results (Karpati et al., 1993a, Mendell et al., 1995). These disappointing results have been attributed to immune rejection, along with insufficient numbers and migration of transplanted cells.

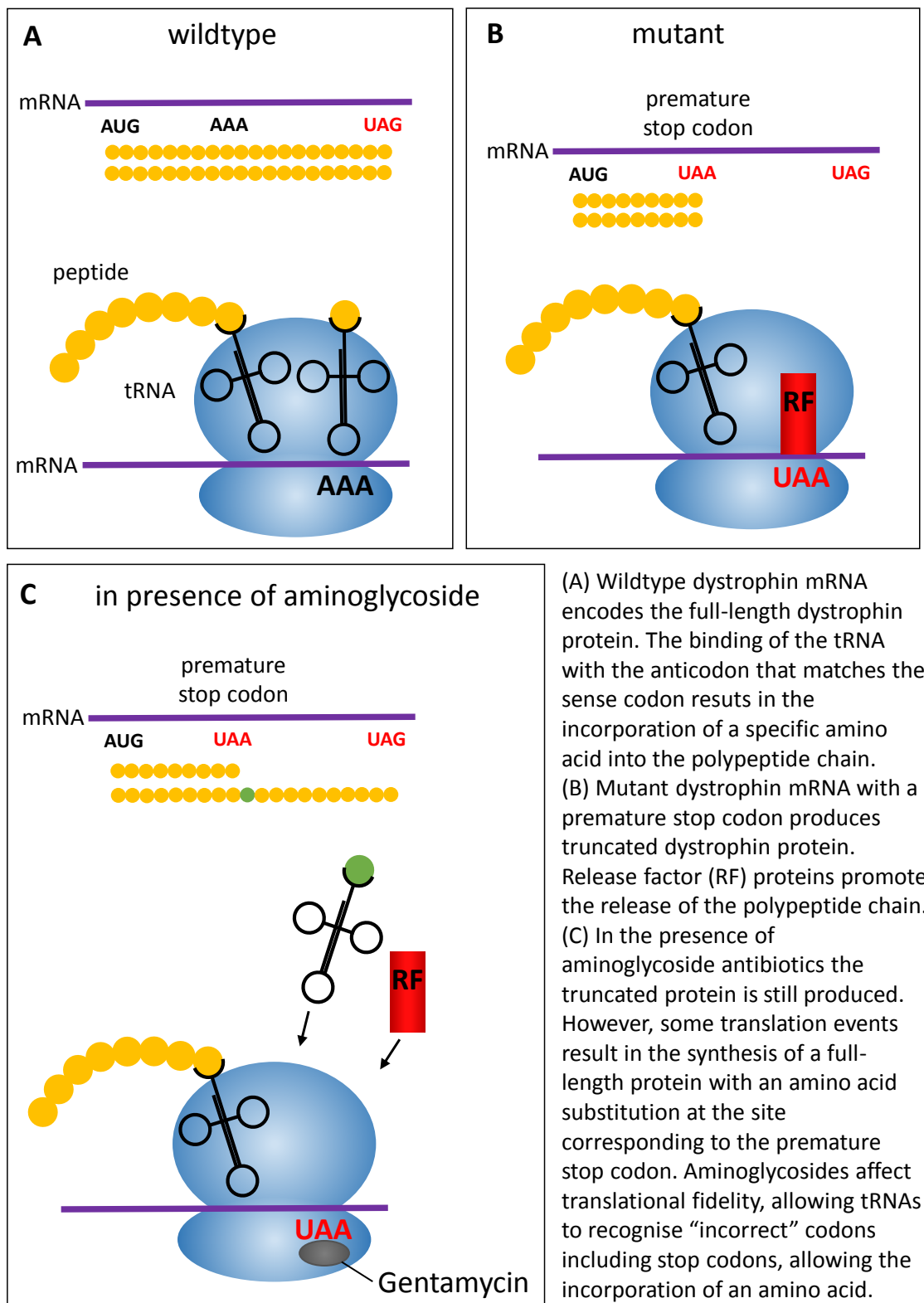
More recently, transplantation of mesoangioblasts resulted in the expression of dystrophin and an improvement in muscle function in GRMD dogs (Sampaolesi et al., 2006) and dKO mice (Berry et al., 2007). In contrast to myoblasts, mesoangioblasts are

able to migrate from the circulatory system, eliminating the need for intramuscular injections. Therefore, these cells may be able to migrate into inaccessible muscles such as the heart. However, the immune rejection of these cells may still be a problem. The potential of mesoangioblast therapy in humans is currently being explored in clinical trials (EudraCT no. 2011-000176- 33).

### **1.10.2.3 Premature stop codon read through**

Approximately 10-15% of DMD patients have nonsense mutations in dystrophin, which may be amenable to treatment with drugs that promote the read-through of premature stop codons, such as aminoglycosides.

Aminoglycoside antibiotics affect translational fidelity, resulting in the ability of transfer RNAs (tRNAs) to recognise incorrect codons (Davies et al., 1964). This allows the insertion of an alternative amino acid at the site of the premature stop codon (figure 1.6). Aminoglycosides bind to the decoding centre of ribosomal RNA (rRNA). This site normally facilitates accurate codon-anticodon pairing, however the conformational change induced by aminoglycoside binding decreases the accuracy of this pairing.

**Figure 1.6: Suppression of stop codons by aminoglycosides**

Aminoglycosides were able to restore protein translation in cell-based assays and in the *mdx* mouse (Barton-Davis et al., 1999), but the toxic effects and the need for regular intramuscular or intravenous administration limit the clinical use of these drugs.

PTC124 was developed as part of a cell-based screen for compounds that promote premature stop codon read through and can be delivered orally (Welch et al., 2007). Restoration of dystrophin expression and an improvement in muscle force was observed in *mdx* mice treated with PTC124 (Welch et al., 2007), but subsequent patient trials yielded disappointing results; although there was increase in dystrophin expression and an improvement in the six minute walk test (6MWT, a standardised measure of ambulation) in most patients treated with the drug, the results were not statistically significant (Finkel, 2010). Although the efficacy of PTC124 needs to be improved to achieve better clinical outcomes, this could be a promising therapy for a subset of DMD patients.

#### **1.10.2.4 Exon skipping**

As with premature stop codon read-through, exon skipping is also dependent on the individual mutation. However, it is estimated that 83% of mutations may be amenable to this type of gene correction (Aartsma-Rus et al., 2009).

This approach involves the design of anti-sense oligonucleotides (AONs), which hybridise with target mRNA sequences to alter RNA processing. Exclusion of mutation

containing exons restores the reading frame, resulting in the production of a truncated, partially functional dystrophin protein.

Exon skipping has been successful in *mdx* (Alter et al., 2006) and dKO mice (Goyenville et al., 2010), and has been taken into clinical trials. AONs targeting exon 51, which would be applicable to the largest proportion of DMD patients (approximately 13%), have been tested in clinical trials. Using intramuscular and systemic delivery routes, these AONs were able to restore dystrophin expression to varying degrees (van Deutekom et al., 2007, Kinali et al., 2009). Efficacy was limited by rapid clearance from the circulation and poor cellular uptake, but different chemical backbones could be used to enhance delivery to muscles (Betts et al., 2012).

Although progress in exon skipping is promising, several caveats remain. Since this therapy is mutation-specific, multiple AONs will need to be developed in order to treat different mutations. These may be regarded as different drugs by regulatory bodies, and each AON would have to progress through clinical trials separately. This would be expensive, time consuming and low frequency mutations may remain untreated. However, these problems could be overcome by the advent of multi-exon skipping (Yokota et al., 2012).

#### **1.10.2.5 Upregulation therapy**

Instead of replacing or repairing dystrophin expression, the expression of alternative proteins could be upregulated to compensate for dystrophin loss. This approach

circumvents any immunological problems associated with the introduction of dystrophin, and is not mutation-specific.

Overexpression of several genes has been successful in ameliorating the dystrophic phenotype in *mdx* mice. These include  $\alpha 7\beta 1$ -integrin (Burkin et al., 2001), nNOS (Wehling et al., 2001), cytotoxic T cell (CT) GalNAc transferase (Nguyen et al., 2002) and utrophin (Tinsley et al., 1996).

Studies using utrophin and CT GalNAc transferase resulted in an increase in dystroglycan expression at the sarcolemma of *mdx* mice. By forming complexes analogous to the DGC, utrophin is able to stabilise dystroglycan and other complex components to the sarcolemma, thus maintaining sarcolemmal integrity. CT GalNAc transferase is involved in the synthesis of the CT antigen, which was shown to glycosylate  $\alpha$ -dystroglycan in *mdx* mice overexpressing this enzyme. These transgenic *mdx* mice express increased levels of utrophin and complex components along the muscle fibre compared with their non-transgenic counterparts. Glycosylation of  $\alpha$ -dystroglycan with the CT antigen may promote the binding of extracellular ligands and stabilise its expression at the sarcolemma, where it can form complexes with utrophin. Therefore an increase in utrophin-associated glycoprotein complexes may be able to compensate for the loss of dystrophin.

#### **1.10.2.6 Utrophin upregulation as a therapy**

It may be possible to increase levels of utrophin pharmacologically using small, orally-bioavailable compounds. SMT C1100 was derived from a screen for transcriptional activators of utrophin. Despite promising results in the *mdx* mouse, plasma levels were not high enough in patient trials (Tinsley et al., 2011). New formulations may serve to improve the bioavailability of SMT C1100.

SMT C1100 or similar compounds could also be combined with other approaches that increase the levels of utrophin, dystroglycan and associated complex components, to further stabilise sarcolemmal integrity.

#### **1.10.2.7 Protease inhibitors**

Loss of dystrophin results in an intracellular environment that supports the activation of a variety of proteolytic systems. As such, the activities of several proteolytic pathways have been shown to be increased in dystrophic muscle (Kominami et al., 1987, Alderton and Steinhardt, 2000, Kumamoto et al., 2000, Nadarajah et al., 2011). The therapeutic potential of inhibiting pathways involving the proteasome, calpains, matrix metalloproteinases (MMPs) and lysosomal proteases have been investigated. Of these pathways, the proteasome system has probably received most attention in the literature.

Inhibition of the proteasome has been shown to improve the dystrophic pathology in dystrophin-deficient muscle (Bonuccelli et al., 2003, Assereto et al., 2006, Bonuccelli et

al., 2007, Gazzerro et al., 2010). Treatment of *mdx* mice and muscle explants from DMD patients with proteasome inhibitors is able to restore expression of dystroglycan and other DGC components at the sarcolemma. It is proposed that stabilising this complex to the membrane is able to improve muscle pathophysiology. However, simply overexpressing dystroglycan in *mdx* mice was not able to rescue the dystrophic phenotype (Hoyte et al., 2004). This may be explained by the failure to prevent the degradation or recycling of dystroglycan. Further evidence to support this hypothesis comes from work using a targeted gene knock-in mouse model (Miller et al., 2012). Substitution of a phenylalanine at tyrosine residue 890 in the C-terminal tail of  $\beta$ -dystroglycan prevented its phosphorylation and subsequent internalisation (see section 1.6.3.2). This resulted in the restoration of DGC components to the sarcolemma and an improvement in muscle function in *mdx* mice (Miller et al., 2012).

Preventing dystroglycan phosphorylation provides another therapeutic target for DMD. Numerous inhibitors of both tyrosine phosphorylation and proteasomal degradation have been developed and are approved for treatment of other diseases such as cancer by regulatory bodies such as the FDA. Therefore side effects have already been explored. Some of these drugs also have the advantage of an oral delivery route. These could potentially be adopted as DMD therapeutics.

### **1.11 Project aims**

This work aims to further investigate the potential of increasing dystroglycan function as a route for DMD therapy, using the zebrafish as a model. As discussed above, the

zebrafish provides a useful model for the evaluation of potential therapies, before translation to mammalian models and human trials.

The regulation of dystroglycan function in muscle will be investigated using dystroglycan (*dag1*) and dystrophin (*sapje*) mutant fish models. Characterisation of the effects of the *dag1* mutation on muscle structure and function will be carried out. *Sapje* fish will be used to investigate the protein expression levels and phosphorylation of dystroglycan in dystrophin-deficient muscle. Finally, the potential of chemically inhibiting dystroglycan degradation and phosphorylation as a therapy for DMD will be explored.

## **Chapter 2: Materials and Methods**

---

## **2.1 Zebrafish Husbandry**

### **2.1.1 Home Office Regulation**

All studies were performed in accordance with Home Office requirements for the use of animals in scientific research and regulated procedures were carried out under the UK Home Office project licence number 40/3134.

### **2.1.2 Maintenance of adult zebrafish**

Adult zebrafish are maintained in UK Home Office approved facilities in the Medical Research Council Centre for Developmental and Biomedical Genetics aquaria at the University of Sheffield. The aquaria follow a 14:10 hour light:dark cycle and are maintained according to standard protocols (Nüsslein-Volhard and Dahm, 2002).

### **2.1.3 Zebrafish Strains**

#### **2.1.3.1 Wildtype strains**

LWT (London Wildtype) embryos were used throughout for those experiments requiring wildtype embryos.

#### **2.1.3.2 Mutant strains**

Heterozygous dystrophin mutant (*sapje*<sup>ta222a</sup>) and dystroglycan mutant (*dag1*<sup>hu3072</sup>) zebrafish are kept as breeding stocks in the aquaria on a LWT background.

#### **2.1.4 Embryo Collection**

Embryos were obtained from the pair-wise mating of adult zebrafish (Nüsslein-Volhard and Dahm, 2002). Pairs of fish were placed into breeding trap tanks that prevent adult fish from ingesting embryos. These tanks consist of two plastic containers that fit tightly inside one another, the inner of which holds the fish and has a base that has been replaced by a grid. Embryos are able to pass through the grid and so are protected from the fish. The tanks also have a dividing wall to separate the male and female the night before embryo collection. The divider is removed the following morning and breeding is allowed to occur before collection of the resulting embryos.

Embryos were staged according to standard criteria (Kimmel et al., 1995) sorted into groups of approximately 50 and placed in Petri dishes (Sterilin) containing fresh E3 medium (see section 2.1.5.1). Embryos were incubated at 28.0°C up to a maximum of 5.2dpf, at which point they were destroyed using bleach.

#### **2.1.5 Zebrafish media and solutions**

All chemicals are from Sigma unless otherwise stated.

##### **2.1.5.1 E3 embryo medium**

E3 medium was composed of 5 mM NaCl, 0.17 mM KCl, 0.33 mM CaCl<sub>2</sub>, 0.33mM MgSO<sub>4</sub> and 0.0001% methylene blue diluted in distilled water (dH<sub>2</sub>O).

### **2.1.5.2 Tricaine (MS222)**

A 0.4% (w/v) stock solution was made by diluting 400mg of powdered MS222 in 97.9ml dH<sub>2</sub>O and 2.1ml of 1M Tris pH9. The pH was adjusted to 7 (Westerfield, 2000).

### **2.2 Detection of muscle phenotype by birefringence assay**

Larvae were anesthetized using a few drops of tricaine (MS222) and transferred to a glass dish. Larvae were viewed between two polarizing filters on a dissecting microscope (Leica MZ FLIII). The polarizing filters are rotated so that only light refracting through the striated muscle was visible. Images were acquired using a SPOT Idea™ USB camera (Diagnostic Instruments) and associated SPOT imaging software and exported in TIFF format.

### **2.3 Zebrafish Motility Assays**

#### **2.3.1 Hatching assay**

At 48, 50, 52 and 54hpf, embryos were divided into two groups depending on whether or not they had hatched from their chorions. At 3dpf, the muscle birefringence of the larvae was examined, and the percentage of sibling and mutant fish that had hatched at each time point was calculated.

#### **2.3.2 Swirl assay**

Larvae were divided into groups of approximately 20 for this assay. Petri dishes containing larvae in E3 media were swirled until larvae collected in the centre of the

dish (3cm diameter). When the swirling motion stopped, the number of larvae that swam out of the centre, and those left in the middle of the dish, were divided into separate dishes. The larvae were anaesthetised and muscle birefringence was examined. The percentage of sibling and mutant fish that had swam out of the centre was then calculated.

### **2.3.3 Viewpoint Zebrabox System**

Larvae were placed into individual wells of 24-well plates. After transfer to the wells, larvae were allowed to acclimatise for 10 minutes in the Zebrabox apparatus. The locomotion of each larva was then recorded and analysed in the Zebrabox recording apparatus, equipped with Videotrack software (both from Viewpoint, France).

The grid of the video-tracking software was aligned with the wells of the 24-well plate such that each fish was within one tracking area. The recording apparatus was used to capture movements within the predefined tracking areas. For tracking the larvae, the detection threshold was set at 15 (on a greyscale of 0–255), although this can be modified according to the contrast between the animal and the background. The length of the plate was used to set the scale in mm.

The Videotrack software automatically calculated the distance travelled and duration of movements within 3 predefined speed categories. The three speed categories were: Inactive movement (less than 2mm/s), slow movement (2- 10mm/s) and fast movement (more than 10mm/s).

A light cycle program of 30 seconds light, 2 minutes dark was used in order to induce movement of the larvae. This program was repeated 4 times for a total of 10 minutes recording time. Tracking data were exported into Excel.

## 2.4 Preparation of embryos for microscopy

### 2.4.1 Solutions used

Name	Components
PBS	137mM NaCl, 2.7mM KCl, 10mM Na <sub>2</sub> HPO <sub>4</sub> , 1.76mM KH <sub>2</sub> PO <sub>4</sub> (pH 7.4)
PBTX	PBS with 0.1% (v/v) Triton X-100
PBDT	PBS with 1% (w/v) BSA, 1% (v/v) DMSO and 1% (v/v) Triton X-100

### 2.4.2 Fixation

Unless otherwise stated, all washing steps were 5-10 minutes with gentle rocking, with embryos in 1.5 ml tubes.

Embryos were washed 2-3 times with PBS and then incubated with 4% paraformaldehyde in PBS for 2 hours at room temperature. Embryos were then washed 3 times with PBTX, once with 50% methanol in PBS and twice with methanol (Fisher), before being stored at -20°C in the final methanol wash.

Those embryos being stained with rhodamine phalloidin (section 2.4.3) were not washed with methanol and were stored at 4°C in PBS.

### 2.4.3 Labelling F-actin

Fixed embryos were incubated with PBTX for 1 ½ hours, followed by 1:20 rhodamine phalloidin (Molecular Probes, Invitrogen) in PBTX for 2 hours at room temperature.

Stained embryos were then washed 3 times with PBTX and stored at 4°C in Vectashield mounting medium with DAPI (Vector Labs).

### 2.4.4 Whole-mount immunofluorescence

Fixed embryos were rehydrated through a methanol/PBTX series (75, 50 and 25% methanol in PBTX) and then washed twice with PBTX. Embryos were washed with water for 5 minutes, acetone for 7 minutes (at -20°C) and then water again for 5 minutes. Embryos were then washed twice with PBDT for 30 minutes, before being incubated overnight at 4°C in PBDT containing the appropriate dilution of primary antibody (see table in section 2.10.1) Following primary antibody incubation, embryos were washed 3 times with PBDT for at least 30 minutes, before being incubated overnight with PBDT with the appropriate dilution of secondary antibody (see table in section 2.10.3). Following secondary antibody incubation, embryos were washed 3 times in PBDT before being stored at 4°C in Vectashield mounting medium with DAPI.

For those embryos co-stained with Alexa fluor 488 conjugated  $\alpha$ -bungarotoxin ( $\alpha$ -BTX) (Molecular Probes, Invitrogen), 1:20  $\alpha$ -BTX was added at the secondary antibody incubation stage.

### **2.4.5 Mounting of embryos onto microscope slides**

Glass microscopy slides (Fisher) were covered with 2 or 3 layers of insulating tape, and a chamber of approximately 5mm<sup>2</sup> excised from the centre using a scalpel. The head of the embryo was removed and the trunk placed onto the microscope slide in Vectashield mounting medium with DAPI. A glass coverslip (Scientific Laboratory Supplies, No. 0) was placed over the top. Pressure was applied to the coverslip to ensure the desired orientation and positioning of the sample. Slides were stored in the dark at 4°C until use.

### **2.5 Confocal microscopy**

Slides were examined using sequential scanning on an Olympus FV-1000 laser-scanning confocal system mounted on an Olympus BX61 upright microscope and driven by FV-10 ASW software (version 1.4). The FV-1000 confocal microscope system is fitted with a 40mW Argon ion gas laser emitting lines at 457, 476, 488 and 515nm, a 1mW He-Ne gas laser emitting light at 543nm, a 10mW He-Ne gas laser emitting light at 633nm, and a 30mW solid state diode laser emitting light at 405nm. Embryos were viewed using a 20X/0.75NA UPlanSApo lens, a 40X/1.00NA UPlanApo oil immersion lens or a 60X/1.42NA PlanApoN oil immersion lens. 40 or 60x objectives were used with Olympus immersion oil. Images were acquired using FV-10 ASW software (version 1.4) and exported in TIFF format. Images of each fluorescent channel and merged RGB images were exported. Images were processed using ImageJ crop and scale bar functions.

## 2.6 Chemical treatment of embryos

### 2.6.1 Treatment with tricaine

#### 2.6.1.1 Effect of larval movement on muscle birefringence

Dechorinated embryos were treated with 0.005% tricaine at 2.5dpf and incubated in the dark at 28°C. Images were acquired and processed as in section 2.2.

#### 2.6.1.2 Effect of larval sedation on Viewpoint tracking analysis

LWT larvae were treated with various concentrations of tricaine at 2.5dpf and incubated for 30 minutes. Viewpoint tracking analysis was carried out as described in section 2.3.3.

### 2.6.2 Drug treatment

#### 2.6.2.1 Compounds used

Compound	Source
Aminophylline	Sigma-Aldrich
Dasatinib (BMS-354825)	LC Laboratories
MG132	Calbiochem
PP2	Sigma-Aldrich
PYR-41	Sigma-Aldrich
Saracatinib (AZD0530)	LC Laboratories
Velcade (Bortezomib, PS-341)	LC Laboratories

Drugs were dissolved in DMSO and kept as stock solutions at -20°C.

### 2.6.2.2 Dechorionation of embryos

Embryos were dechorionated manually with fine forceps (Dumont #5), or chemically with pronase (0.1mg/ml in E3 for 40 minutes at 28°C, followed by several washes in E3).

### 2.6.2.3 Treatment of wildtype embryos

Dechorionated LWT (London wildtype) embryos were transferred into 6 well plates at 24hpf with the appropriate dilution of drug, or DMSO only, in E3 media. There were 50 embryos per well in a total volume of 5ml. The final concentration of DMSO was 1%. Embryos were treated continually for 24 or 48 hours at 28°C. Embryo lysates were prepared as described in section 2.8.2.2.

### 2.6.2.4 Treatment of *sapje*<sup>ta222a</sup> embryos

Dechorionated embryos from a heterozygous *sapje* cross were transferred into 6 well plates at 24hpf with the appropriate dilution of drug, or DMSO only, in E3 media. There were 50 embryos per well in a total volume of 5ml. The final concentration of DMSO was 1%. Embryos were treated continually for 48 or 72 hours at 28°C, before a birefringence assay was carried out to determine the percentage of fish affected by the muscle pathology (see section 2.2). The assay was carried out blinded. Embryo lysates were prepared as described in section 2.8.2.2.

For treatment after the onset of muscle damage, *sapje* larvae were identified at 3dpf. Larvae were treated in 6-well plates until 5dpf as above but with 10 fish per well.

## 2.7 Cell culture

### 2.7.1 Growth of cell lines

H-2K<sup>b</sup>-tsA58 mouse myoblasts cells (Morgan et al., 1994) were cultured in T75 tissue culture flasks (75cm<sup>2</sup>) (Greiner Bio-One) and maintained in DMEM (Dulbecco's modified Eagle medium) GlutaMAX™ with 4.5g/L glucose (Gibco). The medium was supplemented with 20% foetal calf serum, 2% chick embryo extract, 2% penicillin-streptomycin and 20 units/ml of mouse recombinant interferon- $\gamma$  (Peprotech).

Myoblasts were incubated at 33°C in a 10% CO<sub>2</sub> environment. Cells were passaged using 1% (v/v) trypsin-EDTA (Sigma), followed by centrifugation (11030 rotor, Sigma) at x80g for 3 minutes and resuspension in media. Myoblasts were kept at sub-confluent levels ( $\approx$ 50%) to prevent fusion into myotubes.

### 2.7.2 Drug treatment of myoblasts

Cells were plated into a 24-well plate and incubated overnight. The media were removed from the plates, and replaced with 500 $\mu$ l of media containing a specific concentration of drug diluted in DMSO, or DMSO only. The final concentration of DMSO was 0.1%. Cells were then incubated for 6 hours in the conditions described above. Drugs used are detailed in section 2.6.2.1.

## 2.8 Protein Biochemistry techniques

### 2.8.1 Buffers and solutions

Name	Components
RIPA buffer	50mM Tris.HCl (pH 7.5), 150mM NaCl, 1mM EGTA, 1mM EDTA, 1% (v/v) Triton-X, 0.5% (w/v) sodium deoxycholate, 0.1% SDS (w/v), 1mM azide supplemented with protease and phosphatase inhibitors (1mM sodium orthovanadate, 1mM PMSF , 10µM TPCK, 10µM leupeptin, 1µM pepstatin, 10µg/ml aprotinin, 10µg/ml benzamidine)
2X SDS Loading Buffer	100mM Tris.HCl (pH6.8), 0.85M β-mercaptoethanol, 4% (w/v) SDS, 0.2% (w/v) Bromophenol blue, 20% (v/v) Glycerol
SDS-PAGE Running Buffer	200mM glycine, 25mM Tris, 0.1% (w/v) SDS
Towbin Transfer Buffer	25mM Tris, 192mM glycine, 0.075% SDS, 20% Methanol
Tris buffered saline with Tween-20 (TBST)	50mM Tris. HCl (pH7.5), 150mM NaCl, 0.5% (v/v) Tween-20
ECL I	100mM Tris. HCl (pH 8.5), 1.25mM luminol, 0.2mM p-Coumaric acid,
ECL II	100mM Tris. HCl (pH 8.5), 0.02% (v/v)H <sub>2</sub> O <sub>2</sub>
Stripping Buffer	0.2M glycine, 0.1% (w/v) SDS, 1% (v/v) Tween-20. (pH 2.2)

### 2.8.2 Preparation of lysates

#### 2.8.2.1 H2K myoblasts

Cells were cultured in 24-well plates as described in section 2.7. The media were removed from the wells and the cells were washed in ice cold PBS (phosphate buffered saline) (see section 2.4.1). 20µl of ice-cold RIPA buffer containing phosphatase and protease inhibitors was added to each well, and the plate was incubated on ice for 15 min. Cells were harvested by scraping the cells from the wells using a pipette tip, followed by pipetting into a 1.5ml microcentrifuge tube. A sonicator (Soniprep 150) was used for a period of 10 seconds 3 times in order to shear genomic DNA. Samples were centrifuged to remove insoluble debris and mixed with an equal volume of 2x

SDS loading buffer. Lysates were then boiled for 5 minutes to denature the protein and either run on a gel, or stored at -20°C.

#### **2.8.2.2 Zebrafish embryos**

Zebrafish embryos (individual or pooled) were placed into microcentrifuge tubes with 20µl of ice-cold RIPA buffer per fish. Samples were homogenised by pipetting up and down or vortexing, and sonicating as described above. An equal volume of 2x SDS loading buffer was added, and lysates were boiled for 15 minutes. Samples were either stored at -20°C or centrifuged before running on a gel.

#### **2.8.3 SDS Polyacrylamide Gel Electrophoresis (SDS-PAGE)**

Any kD™ Mini-PROTEAN® TGX™ Precast gels (Bio-Rad) with 10 or 12 wells were placed into a Mini-PROTEAN® Tetra Cell electrophoresis tank. SDS running buffer was added up to the fill line. Protein samples (see section 2.8.2) were loaded onto the gel alongside a molecular weight marker (Thermo Scientific PageRuler Plus Prestained Protein Ladder), and run for approximately 1 hour at 150V. The gel containing the proteins separated by SDS-PAGE was then used for western blotting (section 2.8.4).

#### **2.8.4 Western blotting**

The Bio-Rad Mini Trans-Blot™ Electrophoretic Transfer Cell system was used to transfer the proteins from the SDS-PAGE gel to PVDF (polyvinylidene difluoride) membrane (GE Healthcare). Transfers were performed using the manufacturer's instructions. Towbin transfer buffer was used, and proteins were transferred at room temperature for 90 minutes at 400mA.

### **2.8.5 Antibody binding and detection**

Following protein transfer from the gel to the PDVF membrane, the membrane was placed in blocking solution for 1-2 hours on a rocker at room temperature. The blocking solution consisted of 5% (w/v) skimmed milk powder in TBST. The membrane was then incubated overnight at 4°C in the appropriate primary antibody at the recommended dilution (see table in section 2.10.1) in 5% skimmed milk powder in TBST. The membrane was washed 4 times with TBST at 15 minute intervals on a rocker at room temperature, before incubation with the appropriate HRP-conjugated secondary antibody (see table in section 2.10.2) for 1 hour at room temperature. The membrane was washed in TBST again at room temperature 3 times at 10 minute intervals. To obtain a signal, the membrane was developed by exposure to a mixture of ECL (enhanced chemiluminescence) reagents (1:1 ratio of each ECL reagent). Chemiluminescence signals were imaged on a Chemidoc™ XRS+ System (Biorad).

## **2.9 Computer aided data analysis**

### **2.9.1 Quantification of western blot bands**

Quantification was carried out in Image Lab™ software version 3.0 (Bio-Rad) with a rolling disk background subtraction (diameter 10mm). Volume measurements for each band were taken and the values were normalized against  $\alpha$ -tubulin signal and represented as a ratio of the average control signal for each antibody.

### 2.9.2 Quantification of birefringence image intensity

Images were acquired and exported in TIFF format as described in section 2.2, and converted to 8-bit greyscale using ImageJ software (NIH). The ImageJ threshold and wand tools were used to select the somitic muscle area. The average grey value of the pixels in the selected area was then measured. The mean value of wildtype sibling images was used to normalize values obtained from mutant images. Intensity values from mutant fish images were expressed as a percentage of average sibling intensity.

### 2.9.3 Line scanning and Fourier transform

Images were acquired as described in section 2.2, and converted to 8-bit greyscale using ImageJ software (NIH). The ImageJ straight line tool was used to draw a line along the dorsal myotome of the fish, from the start of the 3<sup>rd</sup> somite to the end 22<sup>nd</sup> somite. The “Plot Profile” tool was used to plot a graph of image intensity along the length of the fish and these data were exported into Microsoft Excel. This process was repeated for the ventral somites.

Excel files were imported into MATLAB (Mathworks) and processed using BIOSYST, program coding written by Mikko Juusola (Department of Biomedical Science, University of Sheffield). Line scans,  $L(i)$ , in which  $i$  represents gray-scale intensities over the length of the sample, were subjected to Fourier analysis using this program.

Sample interval was calculated by dividing the total distance of the line scan (in  $\mu\text{m}$ ) by the number of data points (approximately 800-1000). The interval was used to

calculate the sampling frequency using the following equation:

$$\text{Sampling frequency} = \frac{1000\mu\text{m}}{\text{Interval}}$$

The settings of the BIOSYST program were then changed to account for the sampling frequency. The “Analysis > Frequency Analysis > Set Parameters” command was used to set the window size to 200 data points. Line scans were divided into 50% overlapping stretches and windowed with a Blackman-Harris 4-term window, giving 5 to 7 200-point-long spectral samples. The spectral samples were averaged to improve the estimates of their power spectra,  $\langle |L(f)|^2 \rangle$ , where  $|\cdot|$  denotes the norm,  $f$  spatial frequency and  $\langle \rangle$  the average over the different stretches. The “Analysis > Frequency Analysis > Power Spectra” command was used to transform the line scan data to their averaged power spectra.

Power spectra files were exported from MATLAB into Origin 7 for the creation of graphs.

#### **2.9.4 Data analysis**

Data were processed using Microsoft Excel and then imported into GraphPad Prism software for the creation of graphs and statistical analysis.

#### **2.9.5 Statistical Analysis**

The D’Agostino-Pearson normality test was used to assess datasets for deviations from a normal Gaussian distribution, and Bartlett’s test was used to assess the equality of variances. If tests indicated that a dataset deviated from a Gaussian distribution, non-parametric methods were applied (e.g. Mann Whitney U-test). If the datasets followed

a normal distribution and had similar variances, parametric methods were applied (t-test or one-way ANOVA followed by multiple comparison post-tests). In all analyses, a threshold value of  $p < 0.05$  was considered statistically significant.

## 2.10 Antibodies used

### 2.10.1 Primary Antibodies

Name of Antibody	Epitope	Species	Dilution		Source/ Reference
			Western Blotting	Immuno-fluorescence	
MANDAG2	C-terminus of $\beta$ -dystroglycan (amino acids 881-895)	Mouse	1:100	1:100	(Pereboev et al., 2001)
1709	C-terminus of $\beta$ -dystroglycan (amino acids 881-895), with phosphorylated Y892	Rabbit	1:500	1:200	(Ilsley et al., 2001, Miller et al., 2012)
MANDRA1	C-terminus of dystrophin (amino acids 3667-3671)	Mouse	-	1:50	(Nguyen et al., 1992, Morris et al., 1998)
Anti- $\alpha$ -tubulin	$\alpha$ -tubulin	Mouse	1:3500	-	Sigma Aldrich

### 2.10.2 HRP (horse radish peroxidase)-conjugated secondary antibodies used in western blotting

Protein targeted against	Species raised in	Dilution
Anti-mouse IgG	Goat	1:5000
Anti-rabbit IgG	Goat	1:5000

All purchased from Sigma-Aldrich

**2.10.3 Fluorescently conjugated secondary antibodies used in immunofluorescence**

<b>Protein targeted against</b>	<b>Conjugate</b>	<b>Species raised in</b>	<b>Dilution</b>
Anti-mouse IgG	Alexa Fluor 488	Donkey	1:200
Anti-mouse IgG	Alexa Fluor 594	Goat	1:200
Anti-rabbit IgG	Alexa Fluor 488	Donkey	1:200

All purchased from Molecular Probes, Invitrogen

**Chapter 3: A Dystroglycan nonsense mutation elicits a muscular dystrophy phenotype in zebrafish**

---

### **3.1 Introduction**

#### **3.1.1 Loss of dystroglycan function in muscular dystrophy**

##### **3.1.1.1 Dystroglycan is a core component of the DGC**

Dystroglycan is central to the DGC, linking laminin in the ECM to actin in the cytoskeleton via the cytoskeletal linker dystrophin. The dystroglycan gene, *DAG1*, encodes a propeptide that is post-translationally cleaved into  $\alpha$ - and  $\beta$ -subunits (Ibraghimov-Beskrovnaya et al., 1992, Holt et al., 2000), which interact with each other non-covalently (Yoshida et al., 1994).  $\beta$ -dystroglycan is a transmembrane protein that interacts with dystrophin via its intracellular C-terminal domain, and  $\alpha$ -dystroglycan via its extracellular domain. The extracellular protein  $\alpha$ -dystroglycan is heavily glycosylated, and these modifications are important for the interactions between dystroglycan and its ECM ligands.

##### **3.1.1.2 Aberrant glycosylation of $\alpha$ -dystroglycan results in muscular dystrophy**

Hypoglycosylation of  $\alpha$ -dystroglycan results in decreased binding to laminin-2 (Michele et al., 2002a), disrupting the link between the DGC and the ECM. Reduced glycosylation of  $\alpha$ -dystroglycan, caused by mutations in genes encoding known or putative glycosyltransferases, is associated with a group of muscular dystrophies, known as the dystroglycanopathies (Godfrey et al., 2007b).

### 3.1.1.3 Mutations in dystroglycan are usually embryonic lethal in mammals

Although aberrations in dystroglycan processing cause muscular dystrophy, mutations in dystroglycan itself are rare due to its involvement in early embryogenesis. In fact, there has only been one dystroglycan mutation patient described to date (Hara et al., 2011). This rarity is possibly due to embryonic lethality; mouse dystroglycan knockouts are embryonic lethal due to the failure of the extra-embryonic Reichert's membrane to form (Williamson et al., 1997). The lethality of dystroglycan mutations in mammals has made the study of dystroglycan function in muscle somewhat challenging. Mice with a specific inactivation of the dystroglycan gene in skeletal muscle (MCK-DG null) were created, but these have a surprisingly mild phenotype (Cohn et al., 2002). Satellite cells in the MCK-DG null mice, which were not targeted by the muscle creatine kinase promoter used to create the conditional knockouts, were able to initiate expression of dystroglycan during muscle regeneration. The complete loss of dystroglycan in muscle was therefore not achieved. MORE-DG null mice, lacking dystroglycan in all embryonic tissues but not in extra-embryonic membranes, have a severe muscular dystrophy phenotype and eye and brain defects that resemble Walker-Warburg syndrome (Satz et al., 2008). However, these mice do not survive past the first month, with the majority dying within 48 hours of birth. Mouse models deficient in fukutin or POMT1, enzymes thought to be involved in dystroglycan glycosylation, are also embryonic lethal (Takeda et al., 2003, Willer et al., 2004).

Due to its rapid external development, the zebrafish circumvents the lethality of removing dystroglycan function that occurs in higher vertebrates. Therefore, the zebrafish represents an alternative model to study dystroglycanopathies, and the role of dystroglycan in muscle development and integrity.

### 3.1.2 Loss of dystroglycan in zebrafish causes a muscular dystrophy phenotype

#### 3.1.2.1 Dystroglycan morphant zebrafish

Removing the function of dystroglycan in zebrafish using antisense morpholino oligonucleotides (MO) produces a dystrophic phenotype (Parsons et al., 2002).

Injection of a dystroglycan MO results in the absence of dystrophin at the myosepta, loss of muscle integrity and cellular organisation, and necrosis of the muscle tissue.

#### 3.1.2.2 Dystroglycan mutant zebrafish

There are 2 zebrafish dystroglycan mutants, *patchytail* (Gupta et al., 2011) and *dag1<sup>hu3072</sup>* (Lin et al., 2011), both of which show a dystrophic phenotype.

Due to the transparency of zebrafish embryos, muscle integrity can be examined using muscle birefringence (Granato et al., 1996). The ordered array of muscle fibres in wildtype skeletal muscle results in the diffraction of polarised light. Thus under polarised light, the somitic muscle can be detected as bright areas in a dark background. Reduction in birefringence is indicative of muscle damage or disorganisation, as seen in the zebrafish dystroglycan mutants.

##### 3.1.2.2.1 patchytail

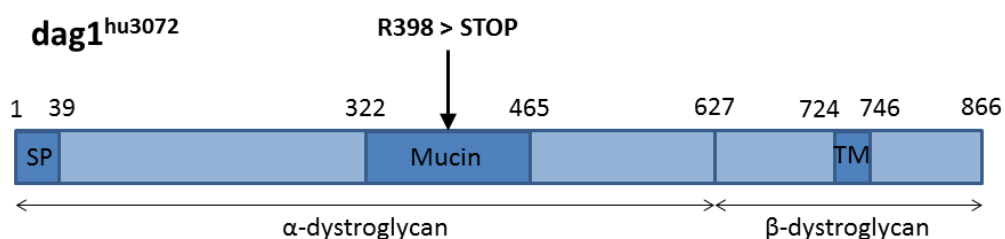
The *patchytail* mutant was identified from an ENU screen and is characterised by a dystrophic phenotype and impaired motility (Gupta et al., 2011). The mutation in *patchytail* is T1700A, which results in a missense change of valine to aspartic acid (V567>D) in the C-terminal domain of  $\alpha$ -dystroglycan. This domain of  $\alpha$ -dystroglycan is important for DGC assembly by interacting with the N-terminal domain of  $\beta$ -

dystroglycan. The *patchytail* mutation results in reduced levels of *dag1* mRNA transcripts as shown by RT-PCR, and a complete loss of both  $\alpha$ - and  $\beta$ -dystroglycan proteins according to western blot analysis. A mild dystrophic phenotype is exhibited in *patchytail* mutants at 3dpf, with loss of birefringence in posterior somites. The muscle degeneration progresses rapidly after 4dpf, with most somites exhibiting loss of birefringence by 7dpf. There is also impaired locomotion at 7dpf, with slower swimming speeds and a reduced touch-evoked escape response.

### 3.1.2.2.2 *dag1*<sup>hu3072</sup>

*dag1* was obtained from the Sanger Institute Zebrafish Mutation resource (Wienholds et al., 2003, Stemple, 2004). It is a TILLING mutant harbouring a C1568T change, which causes a premature termination of translation (R398> Stop) within the mucin domain of  $\alpha$ -dystroglycan (see figure3.1). *dag1* is a recessive allele and is maintained as a heterozygous stock.

**Figure 3.1: Schematic of *dag1*<sup>hu3072</sup> mutation**



A schematic drawing indicating the position of the mutation (R398 > STOP) within the mucin domain of dystroglycan in the *dag1*<sup>hu3072</sup> zebrafish (SP=signal peptide; TM=transmembrane domain). The protease site between  $\alpha$  and  $\beta$  dystroglycan is at residue 627.

### 3.1.3 Chapter aims and hypotheses

This chapter describes the further characterisation of *dag1*<sup>hu3072</sup> mutant fish in terms of muscle damage and motility.

Hypotheses:

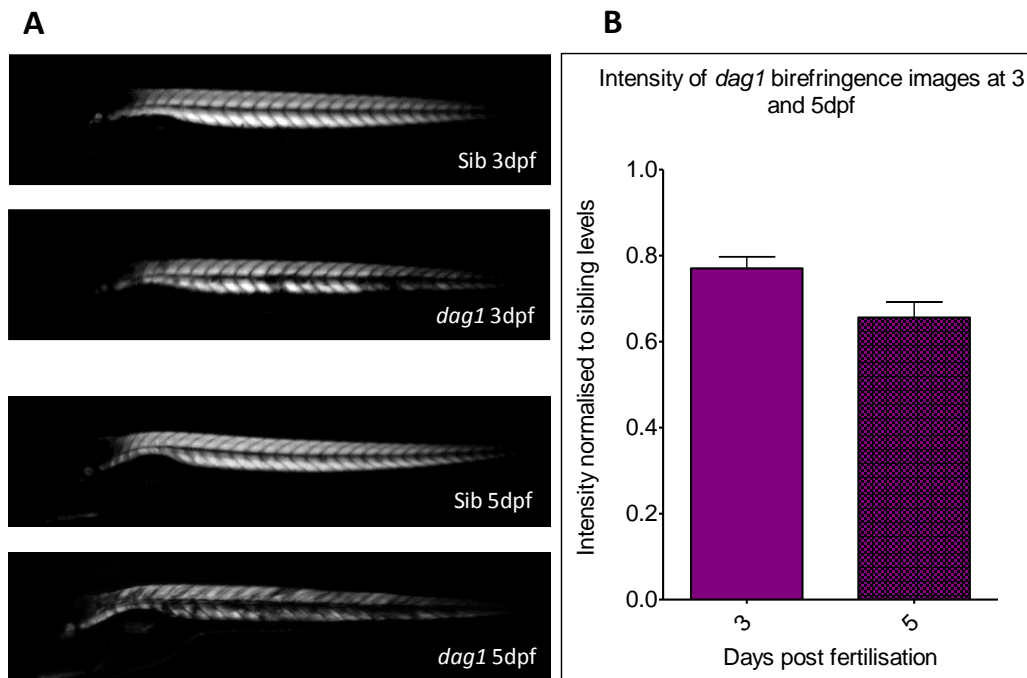
- The *dag1* mutation affects the stabilisation of the DGC and muscle integrity in zebrafish
- The *dag1* mutation affects zebrafish larval motility

## 3.2 Results

### 3.2.2 *dag1*<sup>hu3072</sup> embryos have a muscular dystrophy phenotype

A dystrophic phenotype can be observed in *dag1* larvae from 3dpf, while the skeletal muscle of siblings remains unaffected. This is shown by the loss of birefringence of the somitic muscles in *dag1* larvae (figure 3.2). Unlike the *patchytail* larvae, the muscle damage appears to be randomly distributed throughout the body, rather than only affecting posterior somites.

The dystrophic phenotype in *dag1* larvae progresses over time, with an increasing amount of muscle damage visible from 3 to 5dpf (figure 3.2). Birefringence intensity of sibling larvae was used as a benchmark to which all other values were normalised. At 3dpf, the intensity of birefringence in *dag1* fish is approximately 77% of sibling levels. The muscle birefringence decreases over time, and at 5dpf the intensity of the birefringence image is about 65% that of sibling larvae.

**Figure 3.2: Loss of birefringence in *dag1* at 3 and 5dpf****Birefringence of sibling and *dag1* muscle at 3 and 5dpf.**

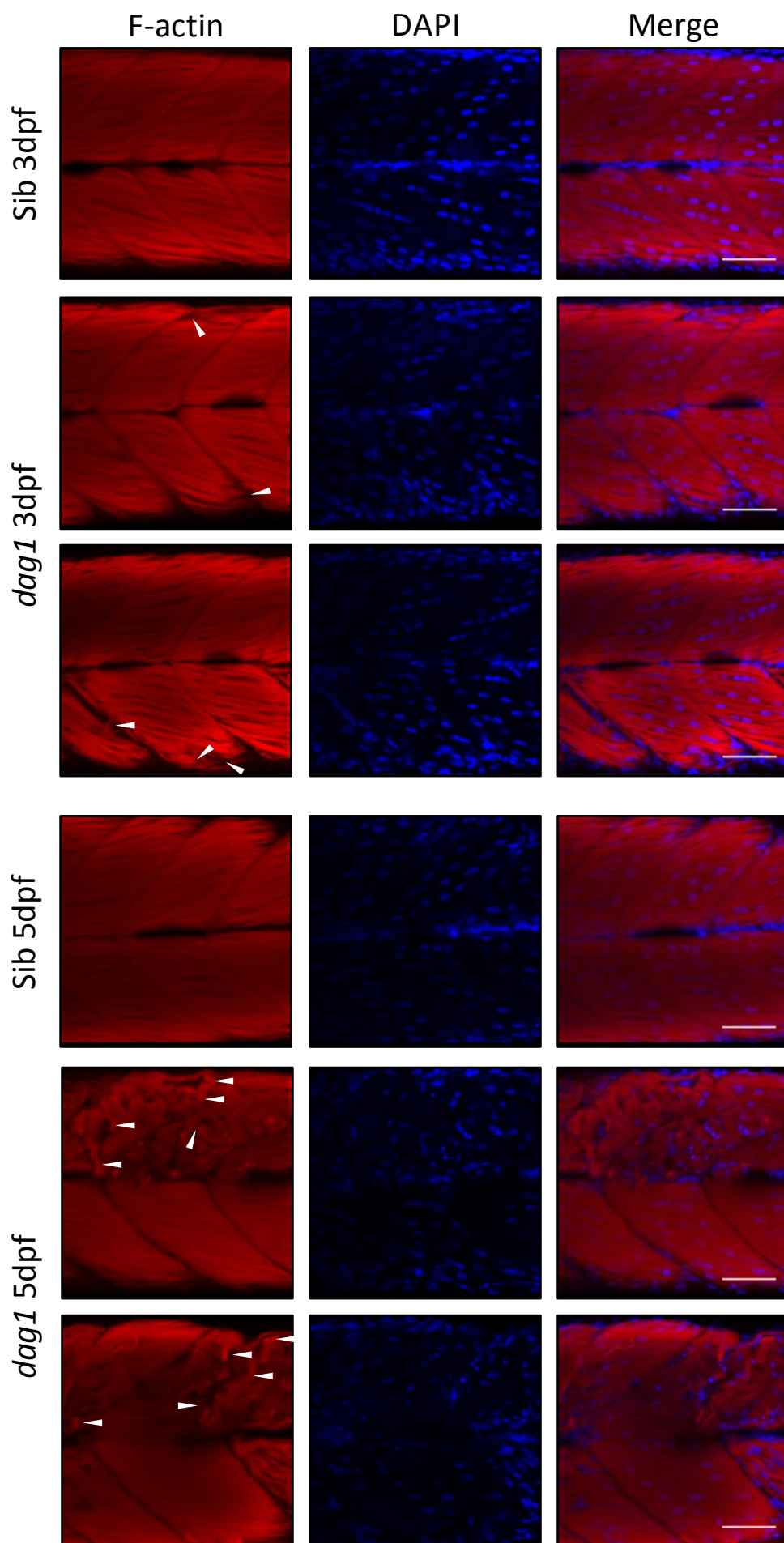
(A) Representative birefringence images at 3 and 5dpf. *dag1* mutants show a loss of birefringence compared to siblings (sib). The loss of birefringence progresses with age. (B) Quantification of *sapje* birefringence images. Each plot represents mean birefringence of 30 *sapje* larvae normalised against average sibling value and error bars represent SEM.

Myogenesis and myofibrillogenesis appear to be unaffected in *dag1* (Lin et al., 2011).

Labelling the F-actin of *dag1* larvae to visualise the muscle architecture suggests the cause of the dystrophic phenotype is due to detachment of muscle fibres from the vertical myosepta (figure 3.3). The severity of the phenotype increases with age, with more detachment and disorganisation of muscle fibres visible at 5dpf.

**Figure 3.3: Confocal images of 3 and 5dpf larvae stained with rhodamine phalloidin**

Rhodamine phalloidin staining shows the disrupted muscle structure in *dag1* somites (white arrow heads), compared with the neatly organised array of muscle fibres in sibling (sib) larvae (scale bars 50 $\mu$ m).

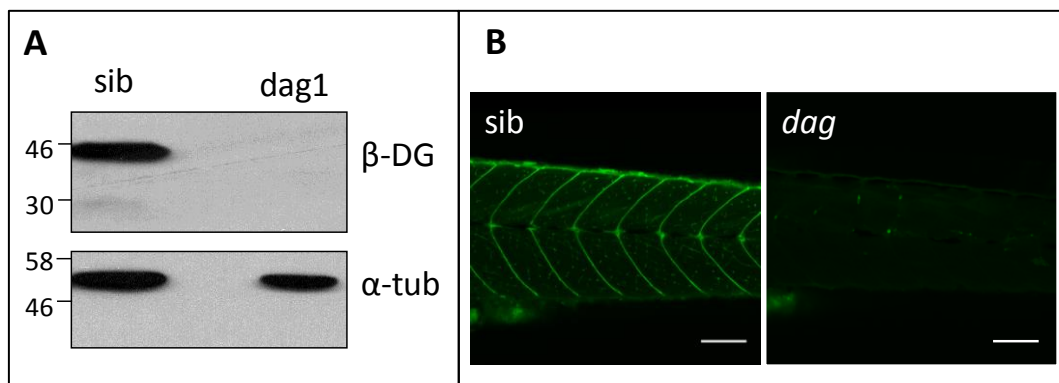


### 3.2.1 Dystroglycan expression in zebrafish

Excluding sarcospan, all DGC proteins are present in zebrafish and are concentrated at the myosepta (Parsons et al., 2002, Chambers et al., 2003, Guyon et al., 2003).

Western blot analysis of whole embryo lysates shows full length  $\beta$ -dystroglycan is expressed in wildtype, but not *dag1* embryos (figure 3.4). Whole mount immunohistochemistry was carried out on wildtype and *dag1* embryos to visualise the localisation of dystroglycan. Figure 3.4 shows dystroglycan expression at the myosepta of wildtype embryos and also shows punctate staining within the somites. The strong staining at the myosepta is lost in *dag1* embryos.

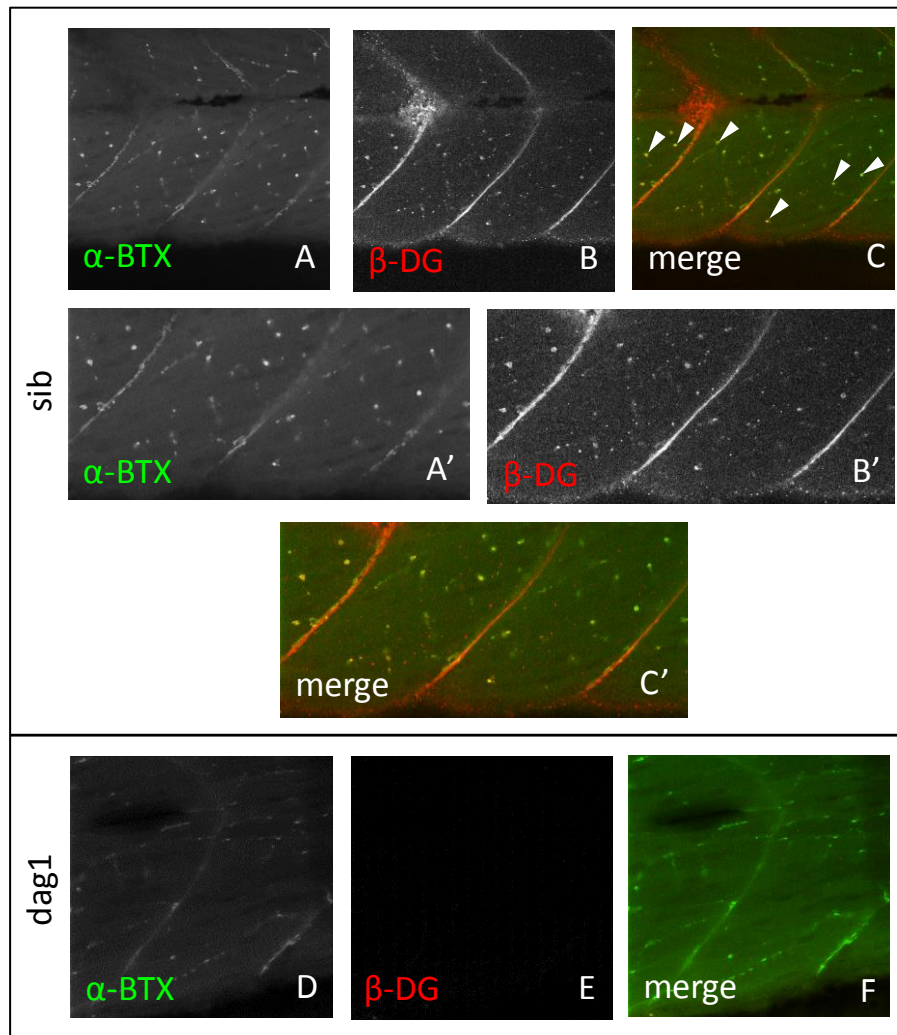
Loss of dystroglycan immunoreactivity was to be expected in the *dag1* embryos since the antibody used is targeted to the C-terminal tail of  $\beta$ -dystroglycan. The nonsense mutation in *dag1* is upstream of this epitope, so if any truncated dystroglycan was present, it would not contain this recognition sequence. There is some residual dystroglycan staining in *dag1* embryos; this could be explained by non-specific antibody binding to muscle detachments, skin and myosepta, which may be particularly sticky.

**Figure 3.4: Loss of dystroglycan immunoreactivity in *dag1* embryos**

(A) Western blot of embryo lysates probed with antibodies against  $\beta$ -dystroglycan (top panel) and  $\alpha$ -tubulin (bottom panel). (B) confocal images of 4dpf sibling (*sib*) and *dag1* larvae stained with MANDAG2 (antibody against  $\beta$ -dystroglycan).  $\beta$ -dystroglycan is localised to the vertical myosepta in siblings, and to structures within the somites, thought to be NMJs. This staining is lost in *dag1* larvae. Scale bar is 100 $\mu$ m.

In sibling embryos, dystroglycan co-localises with staining for postsynaptic acetylcholine receptors using Alexa Fluor-488 conjugated  $\alpha$ -bungarotoxin (figure 3.5), suggesting the staining seen within the somites is representative of neuromuscular junctions (NMJs). Dystroglycan staining at NMJs is lost in *dag1* fish. The dystroglycan deficient muscles of chimeric mice display a neuromuscular junction defect, characterised by fewer and fragmented nerve synapses (Cote et al., 1999). Postsynaptic receptor clusters were present in *dag1* mutants (figure 3.5), although extensive analysis of the number and size of clusters was not carried out. *patchytail* embryos show well developed postsynaptic receptor clusters, with no noticeable differences between those found in wildtype embryos. Together, these data suggest dystroglycan may not be required for zebrafish neuromuscular junction formation.

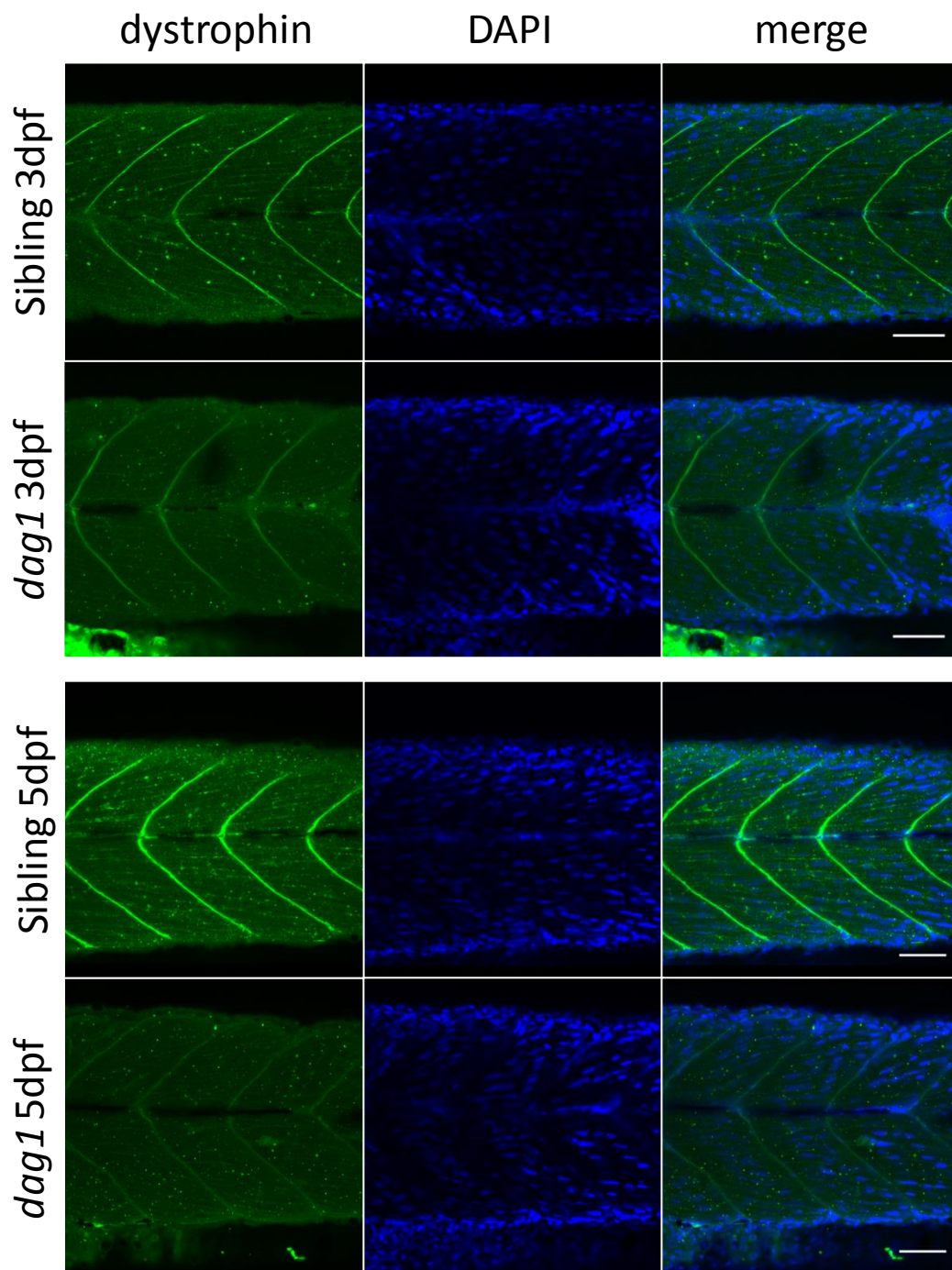
Figure 3.5: Localisation of dystroglycan to NMJs



Confocal images of 4dpf embryos stained with Alexa Fluor 488 conjugated  $\alpha$ -bungarotoxin ( $\alpha$ -BTX) and MANDAG2 (antibody against  $\beta$ -dystroglycan). In sibling (sib) embryos there is colocalisation between  $\alpha$ -BTX (A) and  $\beta$ -dystroglycan ( $\beta$ -DG) (B). In *dag1* embryos there is a loss of  $\beta$ -dystroglycan staining (E), but there appears to be acetylcholine receptor clustering (D & F).

### 3.2.3 *dag1*<sup>hu3072</sup> embryos have a loss of dystrophin expression

Members of the DGC are important for maintaining the stability of their interacting proteins. The effect of lack of dystroglycan on the stability of dystrophin was therefore investigated. Immunofluorescence staining for dystrophin showed expression at the myosepta of wildtype embryos. The expression of dystrophin in *dag1* embryos was seen to be reduced at 3 and 5dpf (figure3.6).

Figure 3.6: Dystrophin staining in *dag1* mutants

Confocal images of 3 and 5dpf larvae stained with MANDRA1 (antibody against dystrophin) and DAPI. In sibling embryos, dystrophin is localised to the vertical myosepta, to which muscle fibre attach. Dystrophin staining in muscle is not as strong in *dag1* mutants, especially at 5dpf. Scale bars are 50 $\mu$ m.

### **3.2.4 *dag1*<sup>hu3072</sup> embryos show impaired motility**

#### **3.2.4.1 Zebrafish locomotion behaviours**

Though locomotion and behaviour may be more commonly associated with juvenile and adult stages of zebrafish development, simple patterns of motility and behaviour can be observed during embryonic and early larval stages (Granato et al., 1996).

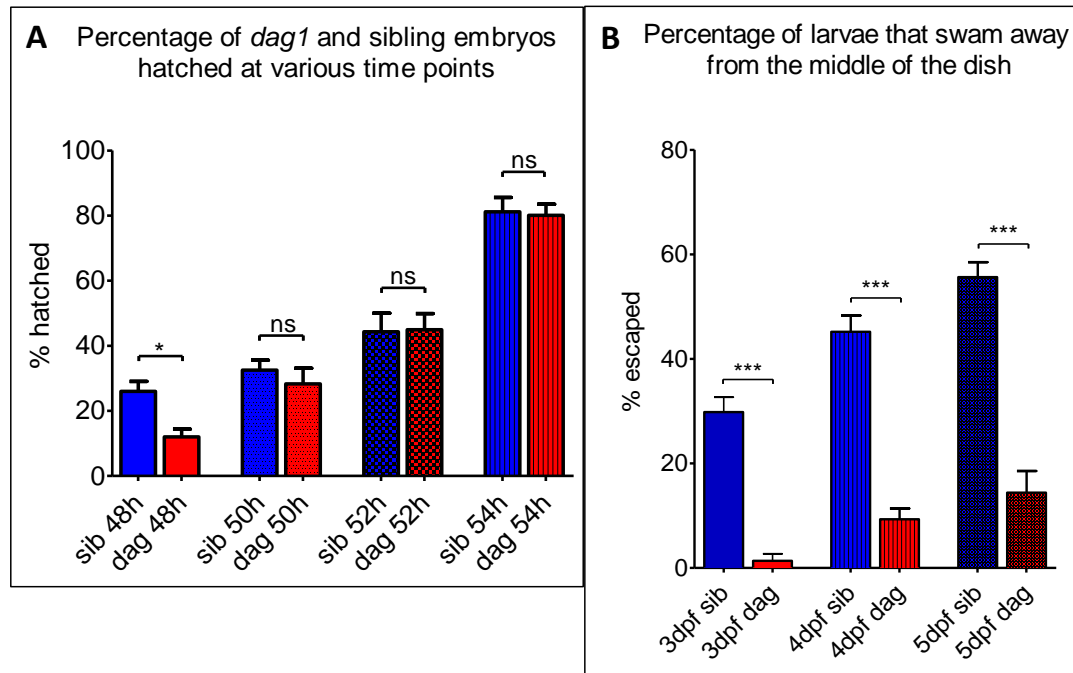
Zebrafish embryos are well suited to movement analysis as they perform well characterised behaviours from an early stage. The first spontaneous muscle contractions occur at 17hpf (Saint-Amant and Drapeau, 1998). These movements become stronger, more coordinated and occur more regularly as the embryo develops. As the embryo becomes close to hatching, it starts to change position within the chorion and displays slow, rhythmic movement of the pectoral fins. Hatching occurs between 48 and 60hpf, after which larvae move less often, but respond to tactile stimuli with an escape response (Granato et al., 1996). At 4-5dpf, the swim bladder inflates, and larvae are able to display more robust swimming behaviours.

#### **3.2.4.2 *dag1*<sup>hu3072</sup> embryo hatching is delayed compared with siblings**

In the developing zebrafish, hatching from the chorion results from a combination of processes. The release of enzymes from the hatching gland digests the chorion, weakening the membrane, and allowing the embryos to use muscular movement to release themselves from the chorion (Yamamoto et al., 1979). This hatching process normally occurs at around 48-60hpf (Granato et al., 1996).

Immotile zebrafish mutant embryos such as *frozen* and *sloth* are completely paralyzed and fail to hatch from their chorions (Granato et al., 1996). At 48hpf,  $12 \pm 2.39\%$  of *dag1*<sup>hu3072</sup> larvae have hatched, compared with  $26 \pm 3.05\%$  of sibling larvae (figure 3.7A). However, at later stages there is no significant difference between the percentage of *dag1* and sibling embryos that have hatched. There also seems to be a hatching delay in *patchytail* mutants, with only  $85 \pm 4\%$  of *patchytail* embryos hatched at 60hpf, compared with  $95 \pm 3\%$  of wildtype embryos (Gupta et al., 2011).

The delay in hatching observed in *dag1* mutant may suggest a mild muscle weakness during early development. However, this may also be explained by a disruption in hatching gland function. To establish whether defects in the hatching gland are responsible for the delay in hatching in *dag1* embryos, the morphology of the gland, and the levels of hatching enzymes could be examined in the mutant fish (Trivic et al., 2011).

**Figure 3.7 *dag1*<sup>hu3072</sup> embryos show impaired motility**

***dag1* zebrafish show defects in motility.** (A) The percentage of sibling (sib) and *dag1* embryos hatched from their chorions at 48, 50, 52 and 54hpf was calculated. Bars represent the mean data of 4 independent repeats, and error bars represent SEM. Each experiment included a total of at least 80 embryos. An unpaired t-test indicated a significant difference between the percentage of *dag1* embryos hatched at 48hpf compared with sibling embryos ( $t=3.619$ ,  $df=6$ ,  $p=0.011$ ). Unpaired t-tests indicated no significant differences between the percentage of sibling and *dag1* embryos hatched at subsequent time points. (B) An embryo swirl assay was carried out on sibling (sib) and *dag1* larvae at 3, 4 and 5dpf. A petri dish containing 20 larvae was swirled until larvae collected in the centre of the dish. The percentage of larvae that swam out of the centre (3cm diameter) of the petri dish was calculated. The bars represent the mean data of 3 independent repeats, and error bars represent SEM. Unpaired t-tests indicated significant differences between the percentage of sibling and *dag1* embryos that swam away from the middle of the dish at 3dpf ( $t=9.062$ ,  $df=4$ ,  $p=0.0008$ ), 4dpf ( $t=9.599$ ,  $df=4$ ,  $p=0.0007$ ) and 5dpf ( $t=8.179$ ,  $df=4$ ,  $p=0.0002$ ).

### 3.2.4.3 *dag1*<sup>hu3072</sup> larvae show defects in motility

*dag1*<sup>hu3072</sup> larvae show reduced motility in a swirl assay. When a petri dish of embryos is swirled around, the larvae collect in the middle of the dish. As this motion stops, wildtype larvae exhibit a swimming response away from the centre of the dish (Granato et al., 1996, Gupta et al., 2012). Significantly fewer *dag1*<sup>hu3072</sup> larvae escaped from the centre of the dish compared with sibling larvae at 3, 4 and 5dpf (figure 3.7B).

### 3.4.4.4 Measuring zebrafish locomotion using automated methods

Automated observation may be a more robust way of measuring zebrafish motility. Behaviours can be recorded more precisely, and a wide variety of parameters, including distance, speed and turning, can be measured with medium throughput. Zebrafish larval movement was analysed using the Viewpoint Zebrabox system and video tracking software (Emran et al., 2008).

When carrying out automated measurement of zebrafish movement, it is important to control conditions in order to get consistent results. Time of day can have an impact on zebrafish larval movement; they tend to be more active in the morning than later in the day (MacPhail et al., 2009). In addition, 5dpf larvae display a diurnal rhythm in locomotor activity, showing higher levels of activity during the day compared with at night (Prober et al., 2006). Density of raising may also influence motility; larvae raised in groups showed higher levels of activity compared with those raised individually (Zellner et al., 2011). Overcrowding of larvae may increase stress levels, which may in turn affect levels of motility. The size of the testing arena used in the assay is another factor affecting levels of motility; larvae in a 24-well plate showed elevated

locomotion compared with those in 48- and 96-well plates (Padilla et al., 2011).

Temperature can also affect locomotor activity (Burgess and Granato, 2008). Therefore it is important to keep these variables consistent between experiments in order to produce reproducible outcomes.

Larvae show characteristic locomotor responses to sudden changes in illumination.

(Burgess and Granato, 2007, Emran et al., 2008, MacPhail et al., 2009, Ali et al., 2012).

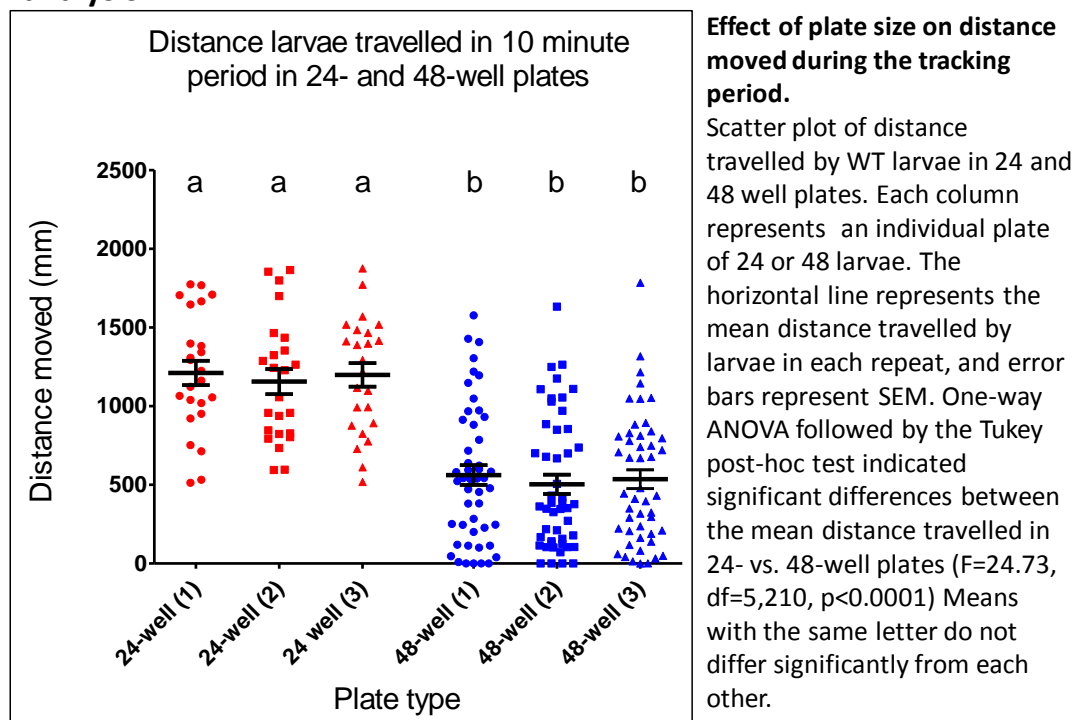
A startle response is elicited when lights are turned on, followed by a return to low baseline locomotion levels. The startle response is an unconditioned behaviour demonstrated by zebrafish from 4-5dpf, and is characterised by rapid acceleration in response to visual, touch or acoustic stimuli (Kimmel et al., 1974). When lights are turned off, there is an increase in locomotor activity, thought to facilitate navigation back to areas of illumination (Burgess and Granato, 2007). This behaviour, known as the visual-motor response, can be utilised to induce movement of zebrafish larvae in an automated assay format, in order to track and measure levels of motility in dystrophic mutants.

Before measuring the motility of *dag1* fish, wildtype larvae were used to validate the approach, in order to ensure consistent and reproducible results. 5dpf larvae were placed into individual wells of 48- or 24-well plates. After transfer to the wells, larvae were allowed to acclimatise for 10 minutes in the Zebrabox apparatus. This period of time has been shown to ensure low and stable levels of basal swimming activity (Ali et al., 2012). The locomotion of each larva was then recorded and analysed in the Zebrabox recording apparatus equipped with Videotrack software. A light cycle

program of 30 seconds light, 2 minutes dark was used in order to induce movement of the larvae. This program was repeated 4 times for a total of 10 minutes recording time.

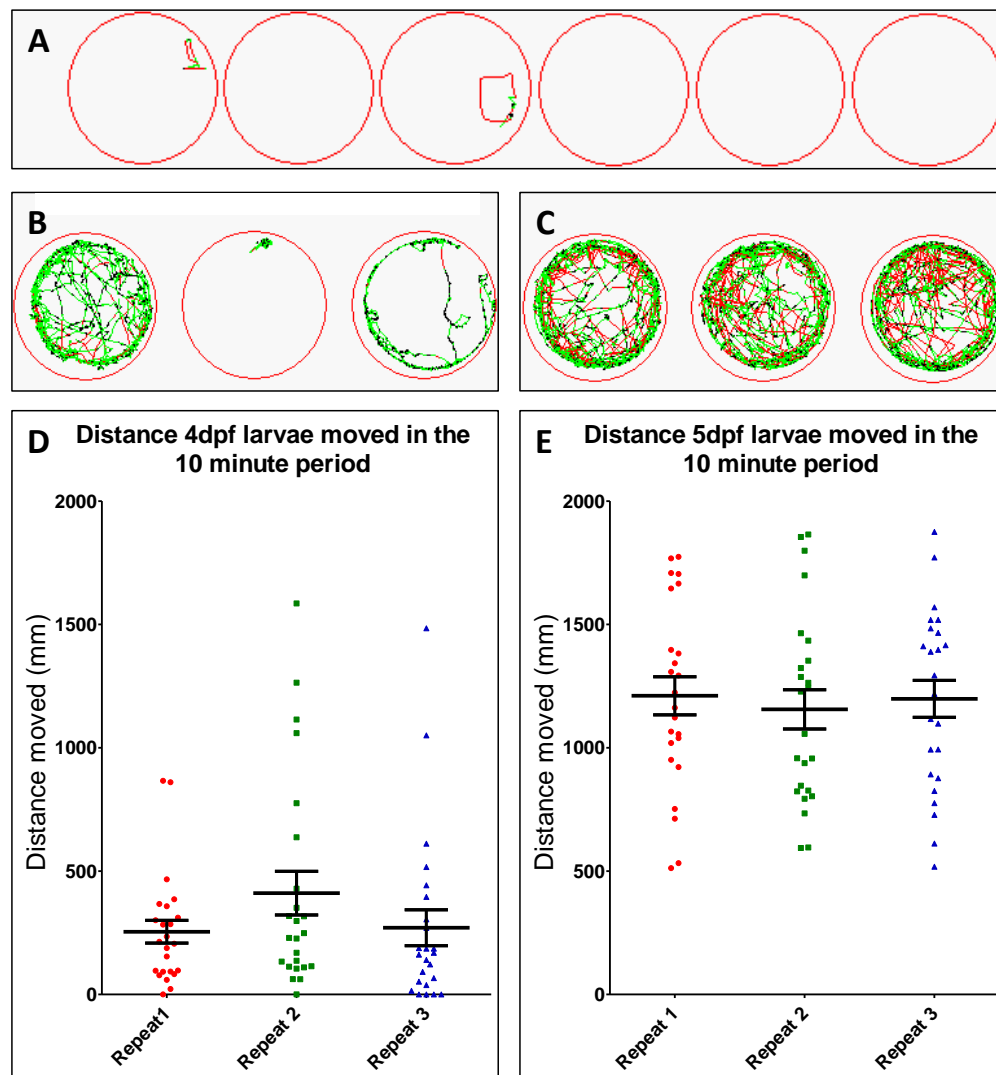
Carrying out the assay with a 24-well plate was found to give larger and less variable amounts of movement than with a 48-well plate. There was a significant effect of plate type on distance travelled in the 10 minute period, with larvae in the 24-well plate moving longer distances (figure 3.8). The smaller size of the wells in the 48-well plate could be limiting the locomotion of the larvae. The 24-well plate format was chosen for subsequent assays to promote consistent levels of motility between assays, and to ensure the movement of the larvae was not limited by the size of the well.

**Figure 3.8: Effect of plate size on Viewpoint Zebrafish movement analysis**



The motility assay was also carried out using 3 and 4dpf larvae. At 3dpf, spontaneous swimming is not very frequent but larvae elicit a response when given an external stimulus e.g. touch. When the viewpoint assay was carried out with 3dpf larvae, motility was very low, with most larvae not responding to the light flashes (see figure 3.9 for representative traces). At 4dpf, distances moved varied considerably, with some larvae moving large distances, but some not responding at all within the 10 minute period (figure 3.9). At 4dpf, the swim bladder inflates, but the timing of this varies, which could explain the variable responses; the larvae that didn't respond may not have fully inflated swim bladders. To ensure maximum response levels, future assays were carried out at 5dpf, although motility could potentially be quantified at earlier stages if the larvae were stimulated to move. This could be carried out using PTZ (pentylentetrazole), a convulsant agent that induces intense locomotor activity.

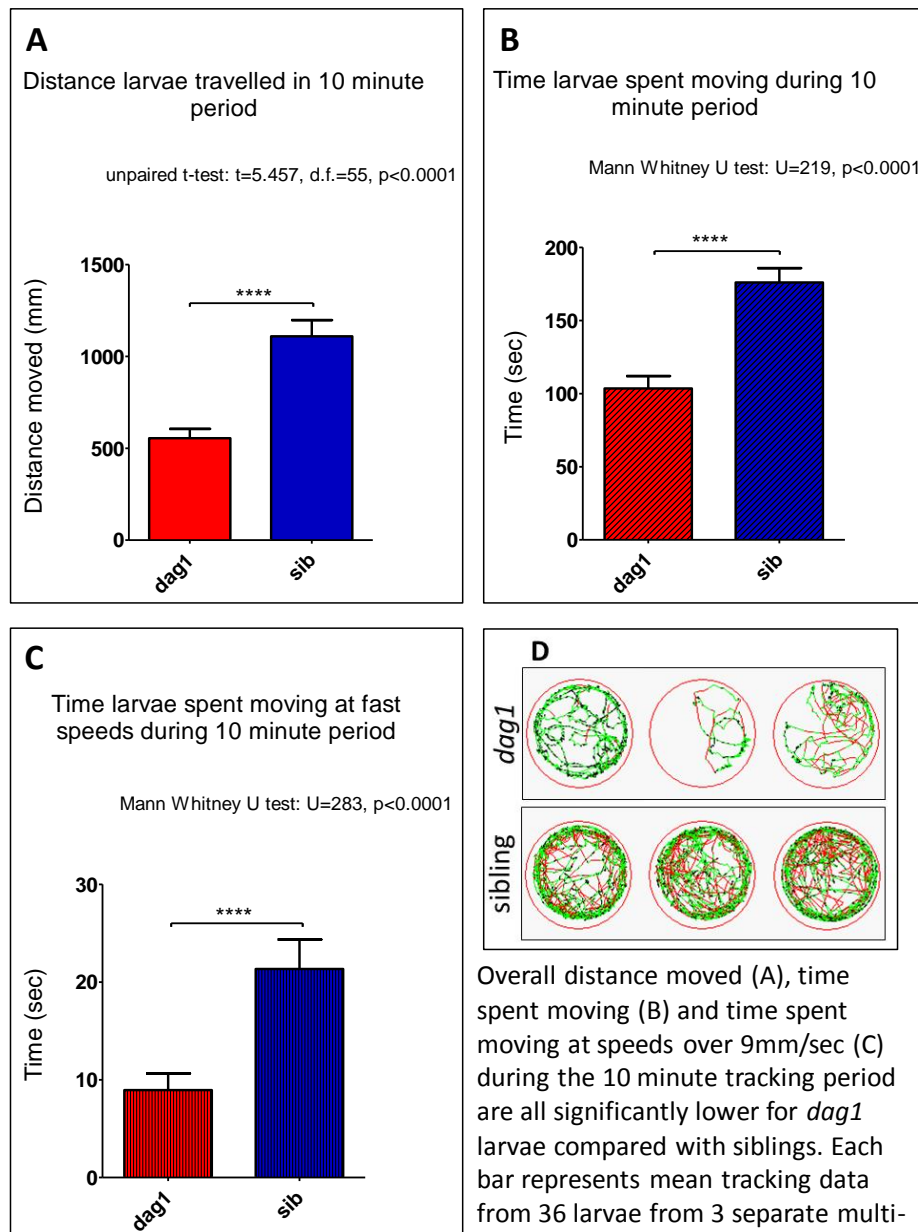
**Figure 3.9: Viewpoint Zebrabox movement analysis of 3, 4 and 5dpf larvae**



**Viewpoint tracking analysis of 3, 4 and 5dpf wildtype zebrafish.** (A) shows representative traces for 3dpf larvae. At this age, larvae do not swim spontaneously very often, and most did not move during the 10 minute tracking period. At 4dpf, responses are variable, with some larvae moving large distances, and others not moving at all during the tracking period. (B) shows representative traces of 4dpf larvae; (red lines = movement >10mm/sec, green lines = movement <10mm/sec) and (D) shows quantification of distance moved during the tracking period for 3 separate plates of larvae. At 5dpf, responses are more robust; (C) shows representative traces of 5dpf larvae, and (E) shows quantification of distance moved during the tracking period of 3 separate 24 well plates of larvae. Error bars represent  $\pm$ SEM.

In order to quantify the motility of *dag1* and sibling larvae, individuals were placed into wells of a 24-well plate at 5dpf, and the activity of each was tracked as described above. *dag1* larvae showed significant differences in the different parameters analysed (figure 3.10). Mutants moved shorter distances within the 10 minute period compared with siblings, spent less time moving, and less time moving at speeds greater than 10mm/sec.

**Figure 3.10: Viewpoint tracking analysis of *dag1*<sup>hu3072</sup> and sibling larvae**



### 3.5 Discussion

#### 3.5.1 Dystroglycan mutant zebrafish display a muscular dystrophy phenotype

The zebrafish provides a useful model for investigating the role of dystroglycan in muscle. This is difficult to study in mammals due to early embryonic lethality.

*dag1* mutant muscles can be properly specified and differentiated, but by 3dpf there is disruption in muscle integrity. The muscle damage appears to be randomly distributed throughout the trunk. This stochastic fibre damage is a hallmark of human muscular dystrophy and animal models, including the dystrophin-deficient zebrafish *sapje*. The muscle damage was shown to become more severe over time, suggesting the phenotype is progressive.

The muscle damage in *dag1* mutants appear more severe than in the other dystroglycan mutant *patchytail*, where muscle damage is initially restricted to posterior somites. It is unclear why there is an earlier onset of more severe muscle damage in *dag1* mutants compared with *patchytail*. The *patchytail* missense mutation may be a hypomorphic allele, but western blotting of embryo lysates did not detect  $\alpha$ - or  $\beta$ -dystroglycan. The different severities of these two mutants may reflect the broad variation in symptoms presented by dystroglycanopathy patients.

The zebrafish also provides useful models for examining the pathophysiological aspects of dystroglycanopathies. Dystroglycanopathies result from defective glycosylation of  $\alpha$ -dystroglycan, which reduces laminin-2 binding. Many genes encoding known or putative glycosyltransferases for dystroglycan have been reported,

including *LARGE*, *FKRP*, *FKTN*, *POMT1*, *POMT2* and *POMGNT1*. Orthologues of these glycosyltransferases are present in zebrafish (Moore et al., 2008). Excluding *POMGNT2*, morpholino knockdown analyses have confirmed that the orthologues function similarly in zebrafish, with morphants displaying muscle pathology (Thornhill et al., 2008, Avsar-Ban et al., 2010, Kawahara et al., 2010, Lin et al., 2011). This further validates the zebrafish as a model of muscular dystrophies.

When comparing the *dag1* mutant to mammalian models of muscular dystrophy, there are key differences in the timing of the onset of the dystrophic phenotype. The early onset may be due to an early developmental role of dystroglycan in basement membrane organisation. This may also be true in mammalian muscle, but cannot be investigated due to the peri-implantation lethality of *Dag1* knockout mice. Instead, the late onset in humans and mice may be due to regeneration that doesn't occur in the zebrafish. The mild phenotype of *mdx* mice, a model of Duchenne muscular dystrophy (DMD), is thought to result from, in part, a higher regenerative capacity of mouse muscle. Other zebrafish models of muscular dystrophy, such as the dystrophin mutant *sapje*, display an early onset of the dystrophic phenotype. This early phenotype in *dag1* and *sapje* may be a result of precocious locomotion. Zebrafish generate muscle load within the first 24 hours of development, and become free swimming larvae by 3dpf. Therefore weak muscle attachments resulting from mutations in DGC proteins may become damaged earlier in development.

### 3.5.2 Loss of dystrophin localisation in *dag1* mutants

Components of the DGC are important in maintaining the stability of other complex proteins. Dystroglycan is a key component of the DGC, providing the essential link between laminin in the ECM and the actin cytoskeleton, via the cytoskeletal linker dystrophin. There is a disruption in dystrophin localisation in the *dag1* mutants. Dystrophin expression is also reduced in *dag1* morphants (Parsons et al., 2002), *patchytail* embryos (Gupta et al., 2011) and in the dystroglycan deficient muscles of chimeric mice (Cote et al., 1999). Some muscles in MCK-DG null mice also showed decreased expression of dystrophin (Cohn et al., 2002). This highlights the importance of dystroglycan in the stabilisation of the DGC.

Conversely, dystroglycan localisation is perturbed in dystrophin deficient environments, as is the case in DMD. Loss of dystroglycan function at the sarcolemmal membrane is thought to be an important pathway in the aetiology of DMD. This idea will be explored further in subsequent chapters.

### 3.5.3 Zebrafish locomotion analysis

*dag1* mutants were found to exhibit impaired locomotion in the motility assays carried out. The automated tracking analysis of larval movement using the ZebraBox provides a simple method for quantifying movement. This could also be carried out in other models of muscular dystrophies and could be used as a read out of muscle function in drug screens for potential therapeutics, as a zebrafish equivalent of the 6 minute walk test in human trials (McDonald et al., 2010) and mobility tests used in mouse studies,

such as exercise resistance tests (Burdi et al., 2009, Tinsley et al., 2011, Kobayashi et al., 2012)

Further work investigating the motility of *dag1* mutants could include characterising the startle response. If muscle is weaker in *dag1* zebrafish, the latency of the response may be increased. This could be measured using a high speed camera, in conjunction with the Zebrabox system and Viewpoint tracking software.

### **3.6 Concluding remarks**

Dystroglycan is a core component of the DGC and is important for maintaining muscle integrity, and for stabilising dystrophin expression at the zebrafish myosepta.

Dystroglycan function is lost in a number of muscular dystrophies including the dystroglycanopathies and Duchenne muscular dystrophy. The loss of dystroglycan and the DGC is an important mechanism in the manifestation of DMD. Preventing the loss of dystroglycan from the sarcolemma may be able to stabilise muscle attachments and ameliorate dystrophy, and this hypothesis will be investigated in chapters 4 and 5.

**Chapter 4: Regulation of dystroglycan in a zebrafish model of Duchenne Muscular Dystrophy (*sapje*)**

---

## 4.1 Introduction

### 4.1.1 Loss of dystroglycan in Duchenne muscular dystrophy

Duchenne muscular dystrophy (DMD) is caused by mutations in the gene encoding dystrophin (Hoffman et al., 1987, Koenig et al., 1987), an important structural protein in muscle cells. Dystrophin was found to form part of a large complex at the sarcolemmal membrane (Ervasti et al., 1990). This complex, termed the dystrophin-associated glycoprotein complex (DGC), provides a link between the actin cytoskeleton and the extracellular matrix (Ervasti and Campbell, 1993). This link is thought to protect the sarcolemma from damage during continued cycles of contraction and relaxation.

The adhesion receptor dystroglycan is a major component of the DGC, forming the essential link between dystrophin and the rest of the DGC. Loss of dystroglycan function at the sarcolemma is common to many muscular dystrophies, including DMD.

There is a significant reduction in dystroglycan and other proteins in the DGC at the sarcolemma of skeletal muscles where dystrophin is lost, such as in *mdx* mice (Ohlendieck and Campbell, 1991) and DMD patients (Ohlendieck et al., 1993). In the absence of dystrophin, the DGC lacks stable connections to the actin cytoskeleton, which may destabilise complex components and render the proteins more vulnerable to degradation. This destabilisation and loss of the DGC is thought to weaken the sarcolemma, making it more susceptible to contraction-induced damage.

The molecular mechanisms by which dystroglycan and other complex components are lost from the sarcolemma in the absence of dystrophin are not completely understood. However, tyrosine phosphorylation of dystroglycan is thought to play an important role in controlling the integrity of the DGC (Moore and Winder, 2010, Miller et al., 2012).

#### **4.1.2 Dystroglycan phosphorylation**

Tyrosine phosphorylation of  $\beta$ -dystroglycan is an important mechanism for modulating the interaction between dystroglycan and its binding partners (James et al., 2000, IIsley et al., 2001, Sotgia et al., 2001, IIsley et al., 2002). The WW domain of dystrophin binds a PPXY motif at the C-terminal tail of  $\beta$ -dystroglycan. Phosphorylation of the tyrosine residue in this interaction site (Y892 in the human protein, Y890 in mouse) disrupts dystrophin binding (IIsley et al., 2001).

Phosphorylation of Y892 is proposed to be mediated by Src family kinases (Sotgia et al., 2001). Co-transfection of cells with c-src and  $\beta$ -dystroglycan induces the phosphorylation of  $\beta$ -dystroglycan, but co-transfection with other tyrosine kinases resulted in little or no phosphorylation.

Tyrosine phosphorylation is thought to promote  $\beta$ -dystroglycan internalisation. Y892 phosphorylated  $\beta$ -dystroglycan becomes localised to an intracellular compartment in Cos-7 cells co-expressing c-Src and an alkaline phosphatase tagged  $\beta$ -dystroglycan construct (Sotgia et al., 2003). Mouse muscle tissue probed with an antibody specific for phosphorylated dystroglycan shows intracellular punctate staining as opposed to

the sarcolemmal staining seen with non-phosphorylated dystroglycan (Sotgia et al., 2003). In addition, cell surface biotinylation assays in H2K mouse myoblasts provide further evidence for the internalisation of phosphorylated  $\beta$ -dystroglycan (Miller et al., 2012). Non-phosphorylated  $\beta$ -dystroglycan remains on the cell surface, whereas tyrosine phosphorylated  $\beta$ -dystroglycan can be detected on the cell surface and in the cytosol. Over time, levels of phosphorylated  $\beta$ -dystroglycan decreased at the cell surface and increased in the cytosol. These data support the hypothesis that phosphorylation of  $\beta$ -dystroglycan may be a signal for its internalisation.

One potential fate of internalised  $\beta$ -dystroglycan is degradation. Elevating the levels of phosphorylated  $\beta$ -dystroglycan, by transforming NIH 3TC cells with v-Src, results in a 3-4 fold reduction in the total levels of  $\beta$ -dystroglycan, suggesting phosphorylation may promote dystroglycan degradation (Sotgia et al., 2001).

#### **4.1.3 Degradation of dystroglycan in the absence of dystrophin**

The ubiquitin-dependent proteasomal pathway has been implicated in the degradation of DGC components in the absence of dystrophin. Proteasomes are strongly expressed in necrotic muscle fibres of DMD patients compared with control muscles (Kumamoto et al., 2000). Moreover, proteasomal inhibitor treatment of *mdx* mice and DMD muscle explants restores dystroglycan and other DGC components to the membrane and improves muscle pathophysiology (Bonuccelli et al., 2003, Assereto et al., 2006, Bonuccelli et al., 2007, Gazzero et al., 2010).

## 4.2 Aims and hypotheses

Dystrophin binding to dystroglycan obstructs the phosphorylation of the tyrosine in the PPxY motif, allowing the DGC to be maintained at the sarcolemma. It was hypothesised that in the absence of dystrophin in the mutant zebrafish *sapje*, the tyrosine in the PPxY motif of dystroglycan would be more exposed to tyrosine kinases and thus more readily phosphorylated. This in turn could lead to decreased stability of dystroglycan at the sarcolemma and an increase in the turnover of dystroglycan. In addition, there may be an increase in the degradation of dystroglycan. This would be an important pathway by which the integrity of the DGC is lost in the absence of dystrophin, and could potentially be manipulated in order to stabilise dystroglycan at the sarcolemma.

This chapter describes investigations in to the regulation of dystroglycan function in the zebrafish model of Duchenne muscular dystrophy. The potential of using pharmacological inhibitors to manipulate the phosphorylation and degradation of dystroglycan will also be assessed.

Hypotheses:

- Levels of dystroglycan will be lower in *sapje* compared with wildtype siblings due to an increase in phosphorylation and degradation.
- Inhibitors of Src kinase and the proteasome are able to increase levels of dystroglycan.

## 4.3 Results

### 4.3.1 *sapje* zebrafish have a dystrophic phenotype

#### 4.3.1.1 *sapje* show loss of birefringence

The *sapje* zebrafish was identified as a member of a group of dystrophic mutants in a large forward genetic screen (Granato et al., 1996). This class of zebrafish mutants showed disorganisation and detachment of normally differentiated skeletal muscle fibres. The muscle pathology can be detected by loss of birefringence of somitic muscle (figure 4.1), as with the *dag1* mutant zebrafish described in chapter 3.

#### 4.3.1.2 *sapje* show loss of dystrophin expression at somite borders

*sapje* results from a nonsense mutation within exon 4 of the zebrafish orthologue of the human DMD gene (Bassett et al., 2003). Dystrophin is localised at the peripheral ends of somitic myofibres, where they attach to the vertical myosepta (figure 4.1).

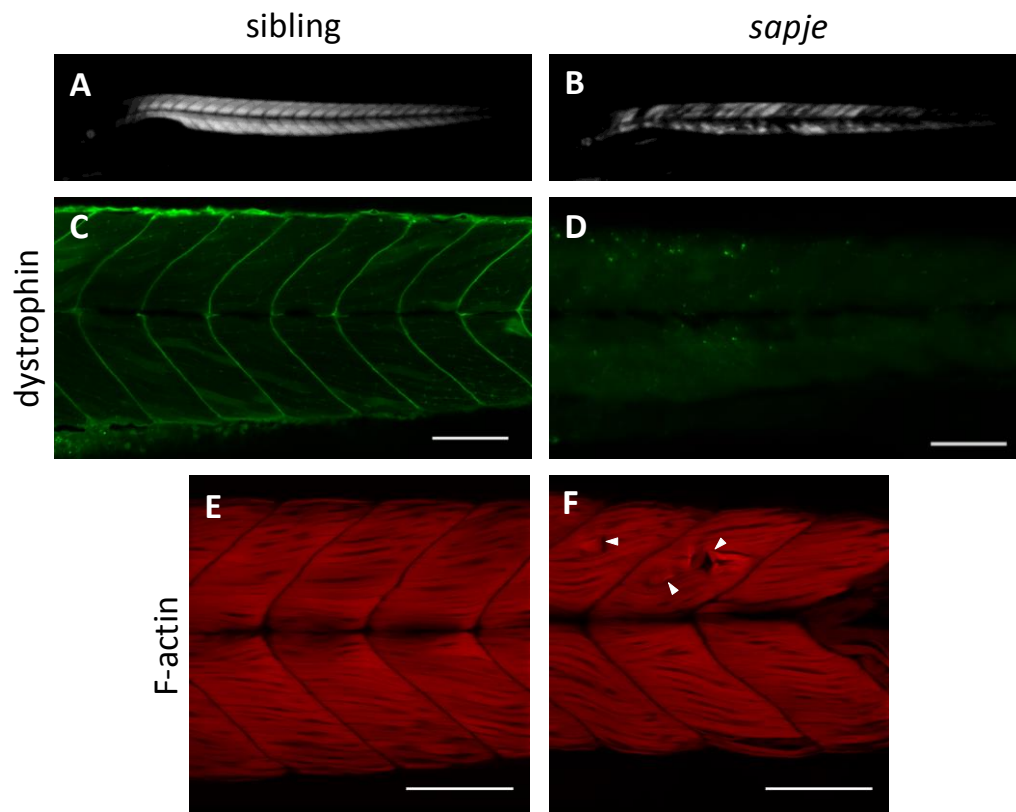
Immunohistochemistry with an antibody directed against a C-terminal epitope common to all isoforms of dystrophin, shows a loss of dystrophin at the somite borders in *sapje* (figure 4.1). Shorter isoforms of dystrophin are still expressed in *sapje* (Bassett et al., 2003).

Loss of dystrophin staining was to be expected in *sapje* embryos, since the nonsense mutation in dystrophin is upstream of the antibody epitope. If any truncated dystrophin was present, it would not be detected by this antibody, since it would not contain the recognition sequence.

#### 4.3.1.3 *sapje* show fibre detachment and disorganisation

The dystrophic phenotype of *sapje* mutants is caused by the mechanical failure of muscle attachments at the embryonic MTJ (myotendinous junction) (Bassett et al., 2003). Fibre detachment can be detected as early as 3dpf, demonstrating the importance of dystrophin in the maintenance of stable muscle attachments and integrity.

Muscle disorganisation and detachment can be observed in the zebrafish larvae by staining the F-actin in the muscle fibres with rhodamine phalloidin (figure 4.1). The myotome of sibling larvae is neatly organised, with muscle fibres spanning each somite block and attaching to the myosepta. However, the muscle architecture is disrupted in *sapje* mutants, and muscle fibres are detached from the myosepta.

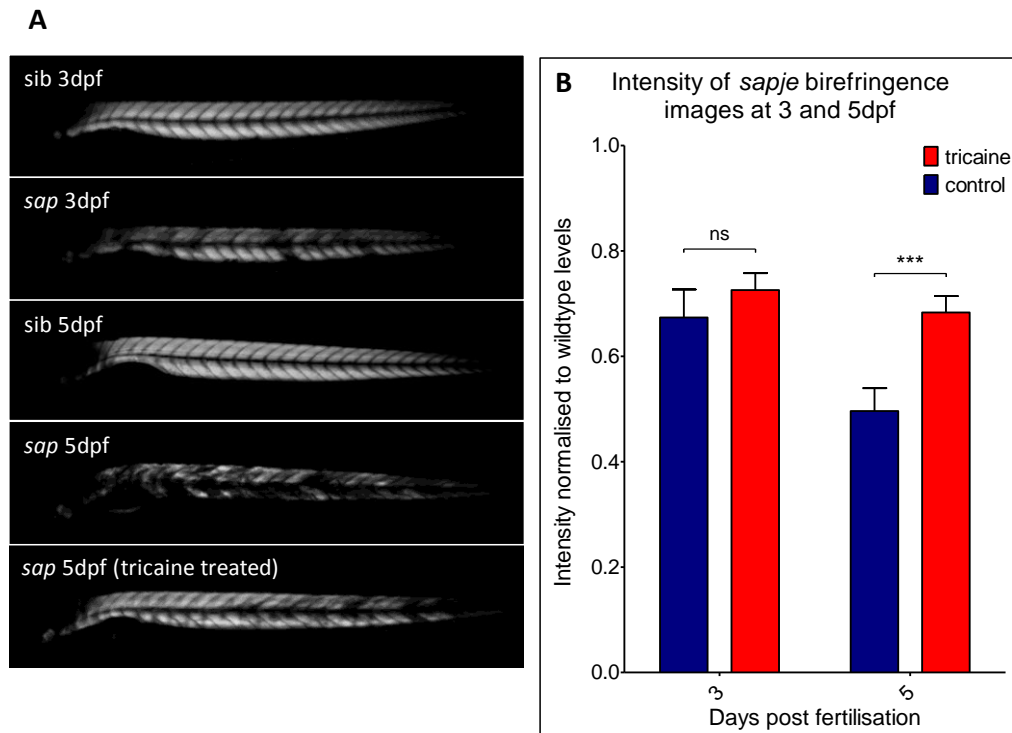
Figure 4.1: Characterisation of *sapje* zebrafish

(A) and (B): Birefringence images of sibling and *sapje* embryos at 4dpf. When viewed through a polarising filter, *sapje* display loss of muscle birefringence, as shown by dark patches on the trunk (B). Sibling larvae show no loss of birefringence (A). (C) and (D): confocal images of 4dpf larvae stained with an antibody against dystrophin. In sibling larvae dystrophin is localised to the vertical myosepta, at muscle fibres attachment sites (C). There is a loss of dystrophin staining at the somite borders in *sapje* (D). (E) and (F): confocal images of 4dpf larvae labelled with rhodamine phalloidin. *sapje* show disrupted muscle structure (F – white arrow heads) compared with sibling larvae (E). scale bars are 100 $\mu$ M

#### 4.3.1.4 The dystrophic phenotype worsens over time

Quantification of birefringence levels at 3 and 5dpf shows the progressive nature of the dystrophic phenotype. Birefringence intensity of sibling larvae was used as a benchmark to which all other values were normalised. Figure 4.2 shows the birefringence levels of *sapje* larvae decrease over time from 3dpf to 5dpf. At 3dpf the intensity of *sapje* birefringence is approximately 35% lower than sibling birefringence. This loss of birefringence progresses and at 5dpf the intensity is about 50% lower in *sapje*, compared with siblings.

Treatment from 2.5dpf to 5dpf with a 0.005% concentration of the anaesthetic tricaine (MS222) was able to reduce this decline in muscle integrity (figure 4.2). At 3dpf there is no significant difference between the birefringence intensity of MS222 and control treated *sapje*. However, at 5dpf, the birefringence intensity is significantly lower for control larvae. This suggests that inhibiting embryo movement prevents or slows down the rate of muscle damage and preserves muscle integrity to some extent.

**Figure 4.2: Loss of birefringence in *sapje* at 3 and 5dpf**

(A) Representative birefringence images at 3 and 5dpf. (B) Quantification of control and tricaine treated *sapje* birefringence images at 3 and 5dpf. Each plot represents mean birefringence of 15 larvae normalised against average sibling intensity and error bars represent SEM. There is a significant difference between the intensity of control and tricaine treated larvae at 5dpf (unpaired t-test,  $t=4.313$ ,  $df=28$ ,  $p=0.0002$ ), but not at 3dpf (unpaired t-test:  $t=0.9660$ ,  $df=28$ ,  $p=0.3423$ ).

#### 4.3.1.5 *sapje* show defects in motility

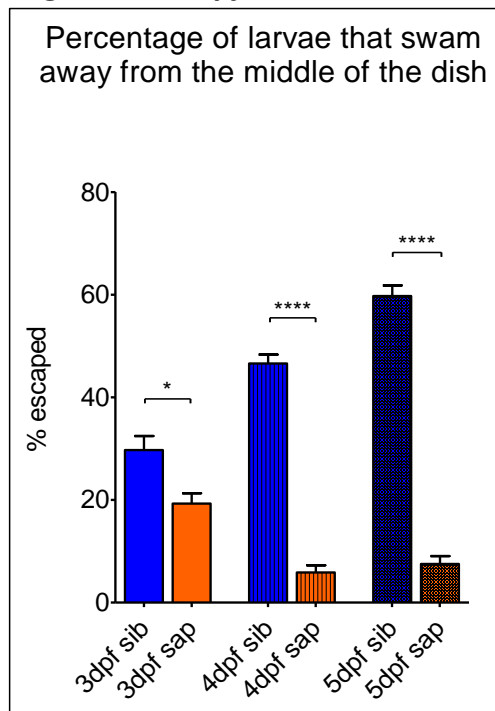
Unlike *dag1* embryos, hatching rate appears to be unaffected by the *sapje* mutation.

However, later in development, movement appears to be affected in the *sapje* mutants.

*sapje* show reduced motility in the swirl assay used in chapter 3 (Granato et al., 1996, Gupta et al., 2012). When a petri dish containing larvae is swirled around, larvae collect in the middle of the dish. Upon cessation of the swirling motion, larvae exhibit a

swimming response away from the centre. The percentage of *sapje* that escaped from the centre of the petri dish was significantly lower compared with siblings at 3, 4 and 5dpf (figure 4.3). This suggests the mutants have a defect in locomotion.

**Figure 4.3: *sapje* show defects in motility**

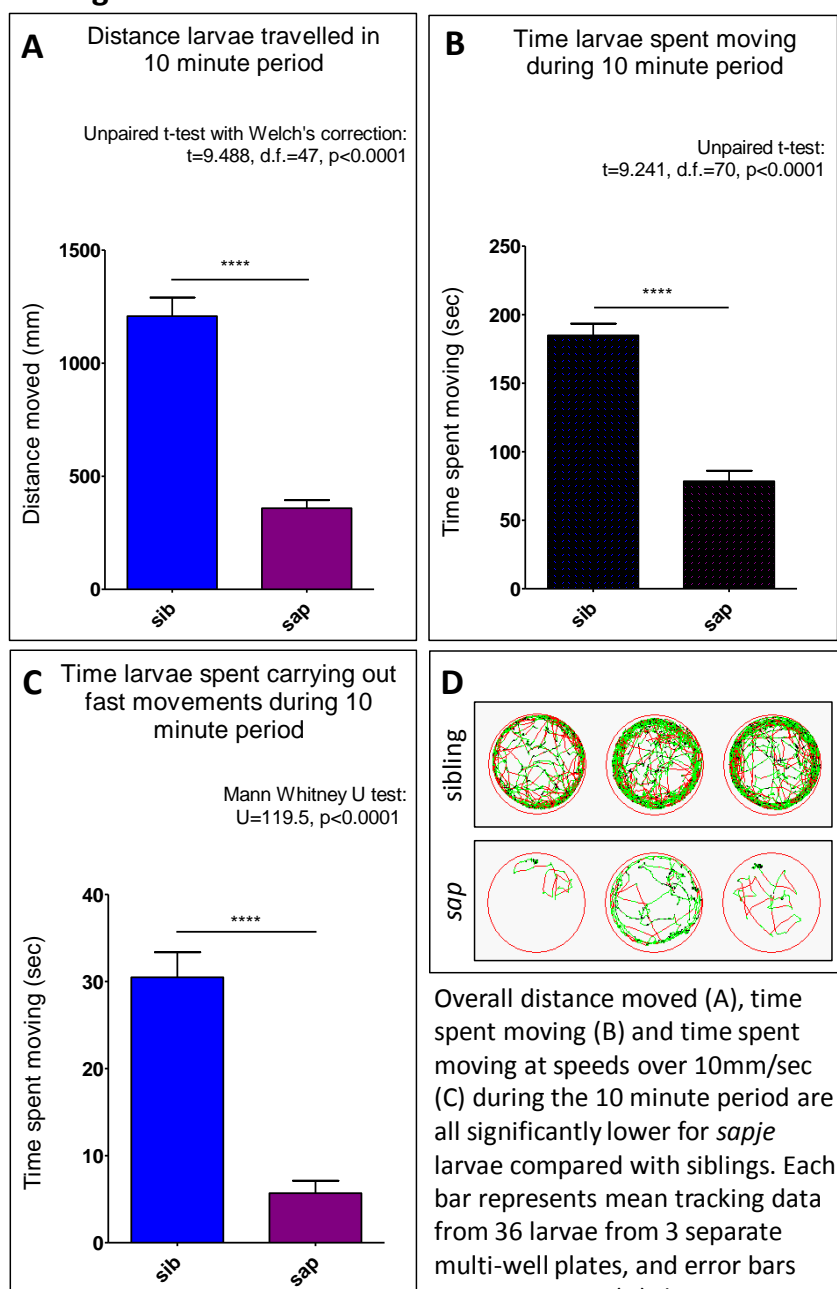


An embryo swirl assay was carried out on sibling (*sib*) and *sapje* (*sap*) larvae at 3, 4 and 5dpf. A petri dish containing 20 larvae from a heterozygous *sap/+* cross was swirled until larvae collected in the centre of the dish. The percentage of larvae that swam out of the centre (3cm diameter) of the petri dish upon cessation of the swirling motion was calculated. The bars represent the mean data of 3 independent repeats, and error bars represent SEM. Unpaired t-tests indicated significant differences between the percentage of sibling and *sap* embryos that swam away from the middle of the dish at 3dpf ( $t=3.068$ ,  $df=4$ ,  $p=0.0374$ ), 4dpf ( $t=18.24$ ,  $df=4$ ,  $p<0.0001$ ) and 5dpf ( $t=20.20$ ,  $df=4$ ,  $p<0.0001$ ).

The motility defect is further demonstrated by analysing the larval movement using the Viewpoint Zebrabox system and video tracking software used in chapter 3. 5dpf sibling and *sapje* larvae were placed into individual wells of a 24-well plate, and locomotion was tracked and quantified over a ten minute period. Alternating light and dark periods were used to stimulate larval movement.

Analysis of viewpoint tracking data revealed significant differences in the movement of *sapje* larvae, when compared with siblings (figure 4.4). *sapje* move significantly shorter distances than siblings over the ten minute period, with a mean distance travelled of  $359 \pm 35$ mm compared with  $1208 \pm 82$ mm. *sapje* larvae spend less time moving during the tracking period than siblings, with a mean time of  $78.4 \pm 7.7$  seconds compared with  $184.9 \pm 8.6$  seconds. Time moving at fast speeds (greater than 10mm/sec) was also significantly lower in *sapje* compared with siblings; *sapje* spent an average of  $6.7 \pm 2.1$  seconds swimming at high speeds, whilst siblings spent  $30.5 \pm 2.9$  seconds. Together, these results indicate the *sapje* mutation has effects on larval motility.

**Figure 4.4: Viewpoint tracking analysis of *sapje* and sibling larvae**



### 4.3.2 Loss of dystroglycan in *sapje* mutants

The DGC localises to the sarcolemmal membrane in zebrafish, existing as a membrane-associated complex (Guyon et al., 2003). In zebrafish embryos, DGC components are concentrated at the myosepta (Parsons et al., 2002, Chambers et al., 2003, Guyon et al., 2003).

Whole-mount immunohistochemistry shows dystroglycan localisation at the myosepta of sibling embryos, and also some punctate staining within the somites, which may represent NMJs (figure 4.5).

Since dystroglycan levels are reduced when dystrophin is absent in mammals, the levels of dystroglycan in sibling and *sapje* larvae were investigated. Compared with sibling larvae, there appears to be weaker dystroglycan staining in *sapje*. This is especially evident at 4 and 5dpf (figure 4.5).

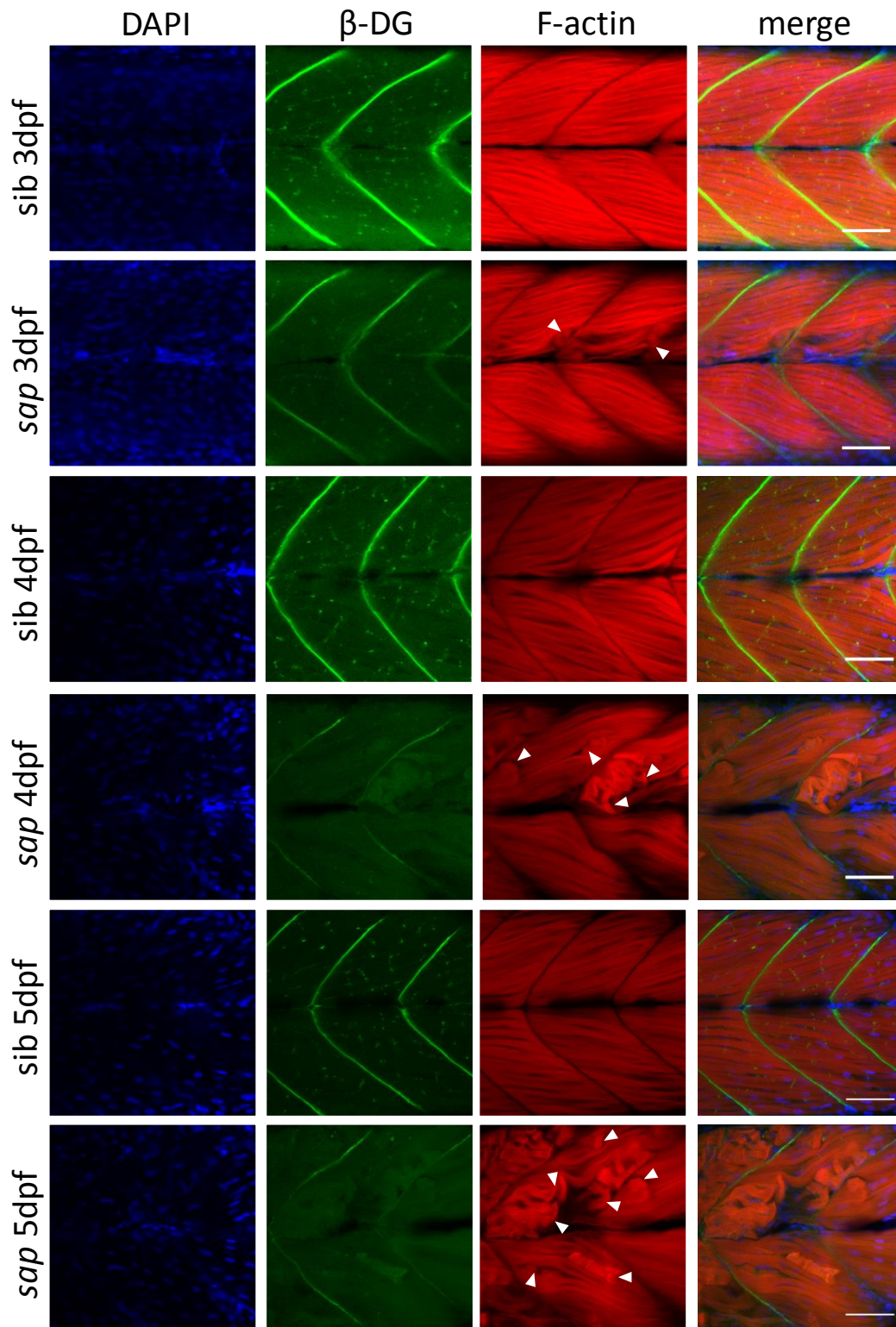
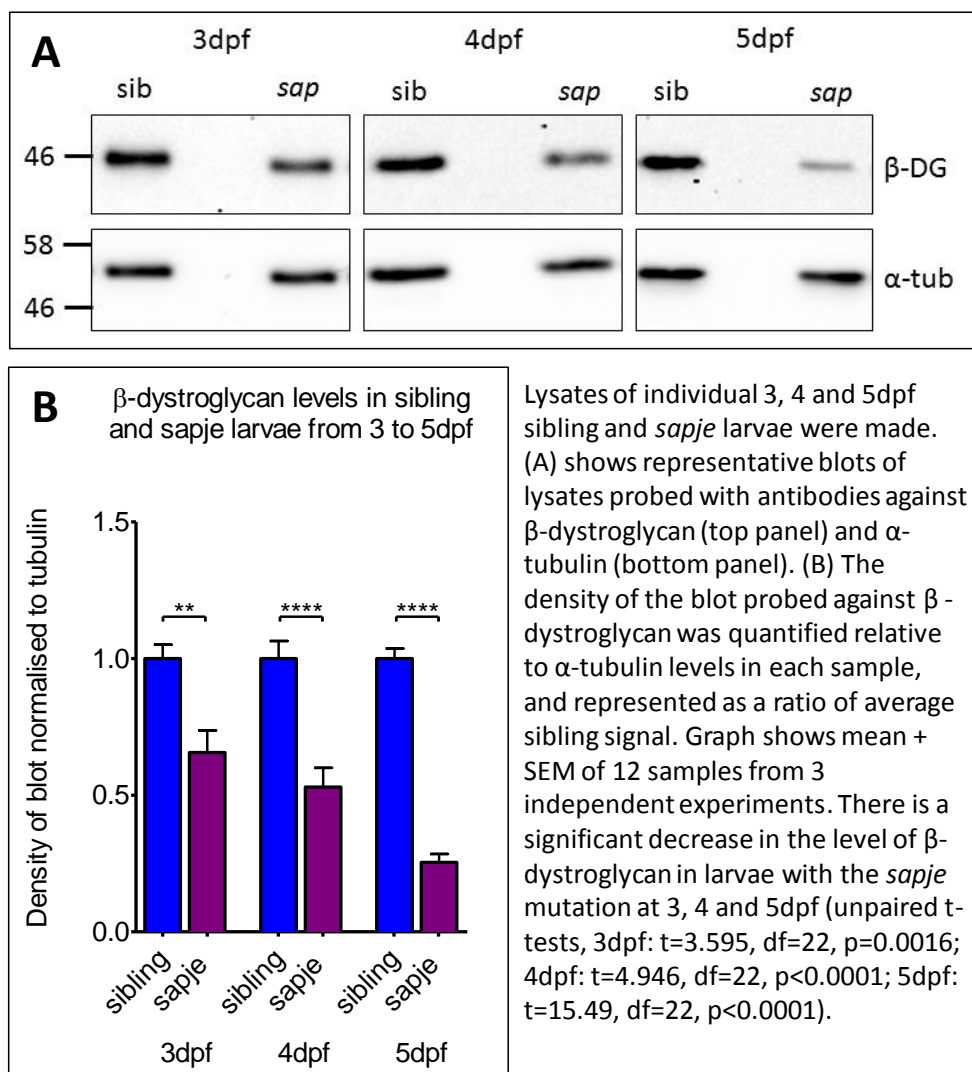


**Figure 4.5: Confocal images of 3,4 and 5dpf larvae stained with DAPI, MANDAG2 (antibody against  $\beta$ -DG) and rhodamine phalloidin**

Dystroglycan is localised to the vertical myosepta in sibling larvae and this staining appears to be weaker in *sapje*, especially at 4 and 5dpf. Rhodamine phalloidin staining shows the disrupted muscle structure in *sapje* somites (white arrow heads), compared with the neatly organised array of muscle fibres in sibling larvae (scale bars 50 $\mu$ m).

Western blotting of whole larvae lysates confirms lower dystroglycan protein levels in *sapje* compared with siblings (figure 4.6). Quantification of dystroglycan levels by densitometry showed a significant decrease in *sapje*, which became more pronounced from 3dpf to 5dpf. Compared with sibling larvae of the same age, the level of dystroglycan was reduced in *sapje* by approximately 34% at 3dpf, 47% at 4dpf and 75% at 5dpf.

**Figure 4.6:  $\beta$ -dystroglycan levels in sibling and *sapje* larvae**



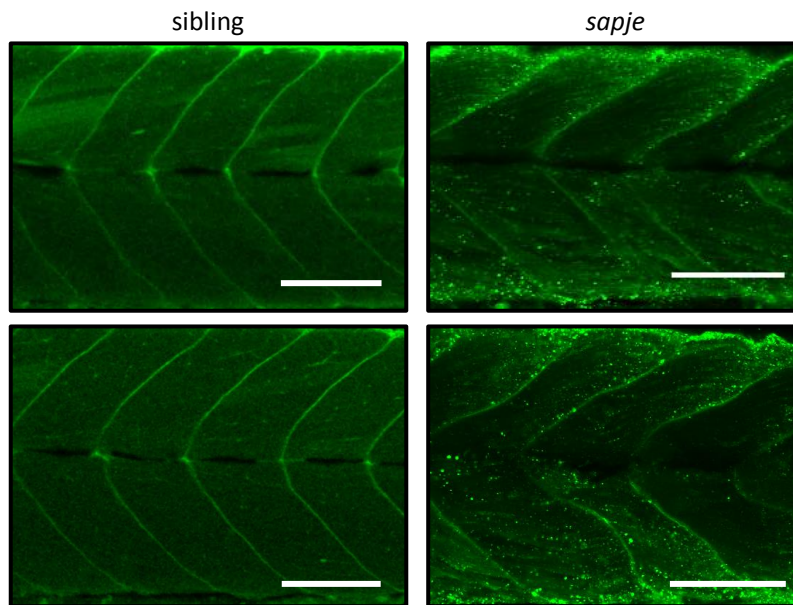
### 4.3.3 Levels of phosphorylated dystroglycan are elevated in *sapje*

It was hypothesised that in the absence of dystrophin binding, the C-terminal tail of  $\beta$ -dystroglycan may be more readily phosphorylated. Therefore, levels of phosphorylated  $\beta$ -dystroglycan in *sapje* and sibling larvae were examined.

Whereas MANDAG2 is sensitive to phosphorylation and does not recognise phosphorylated dystroglycan (Miller et al., 2012), the antibody 1709 specifically recognises dystroglycan with a phosphorylated tyrosine residue (Y892 in humans, Y863 in zebrafish).

Immunofluorescence staining for phosphorylated  $\beta$ -dystroglycan showed localisation at the myosepta (figure 4.7), but the staining did not appear as defined as that seen with non-phosphorylated  $\beta$ -dystroglycan (figure 4.5). Immunofluorescence staining of *sapje* larvae showed localisation to puncta within the somitic muscle blocks (figure 4.7). This can also be seen in some sibling larvae, but to a lesser extent.

**Figure 4.7: Confocal images of 3dpf larvae stained with 1709 (antibody against phosphorylated dystroglycan)**



Phosphorylated  $\beta$ -dystroglycan shows staining at the myosepta, with some staining within the somites. Scale bars are 100 $\mu$ m.

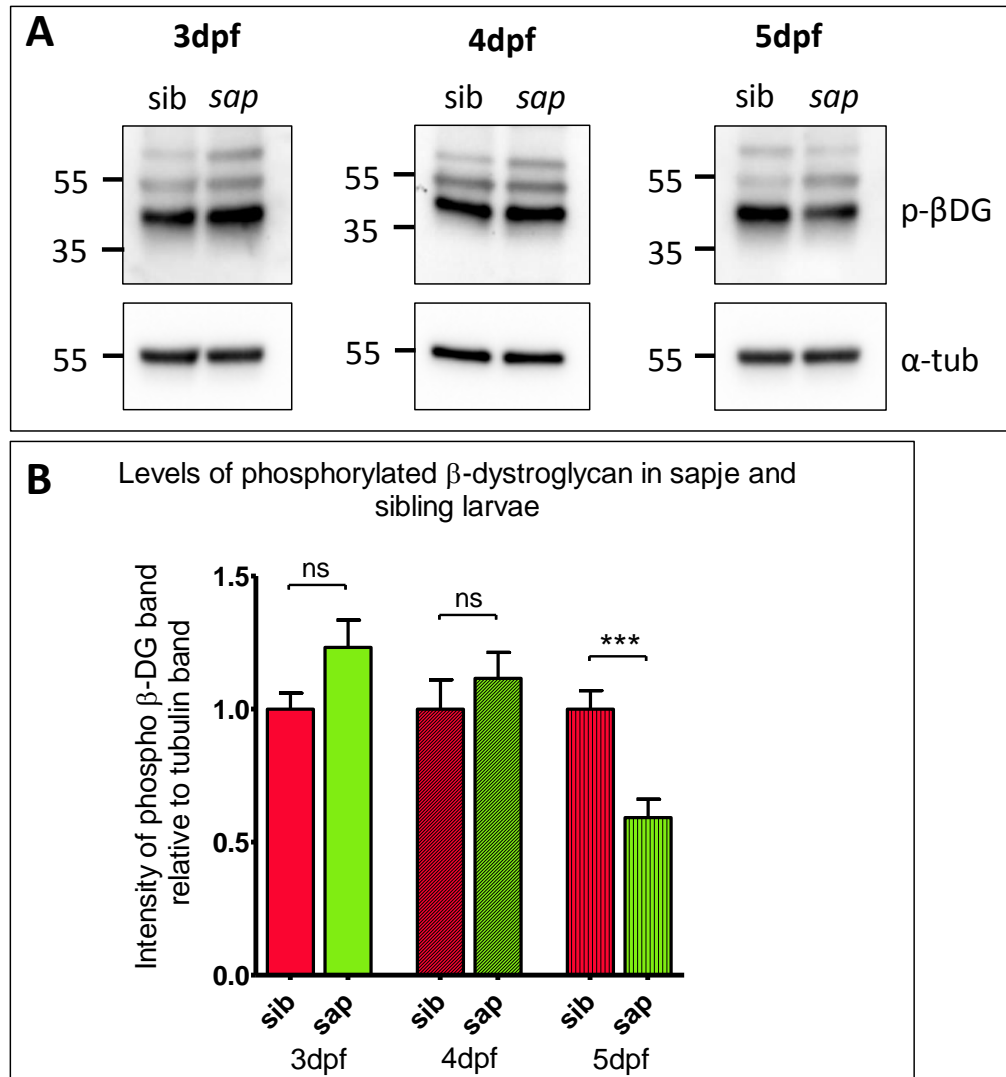
Western blotting with 1709 revealed a slight increase in phosphorylated  $\beta$ -dystroglycan levels in lysates of 3 and 4dpf *sapje* mutants, compared with siblings, but this was not statistically significant. Levels of phosphorylated  $\beta$ -dystroglycan are significantly lower in *sapje* at 5dpf (figure 4.8).

Levels of non-phosphorylated dystroglycan decrease over time in *sapje* (figure 4.6). Since the antibody MANDAG2 is sensitive to phosphorylation, and 1709 is specific for tyrosine phosphorylation (Miller et al., 2012), the ratio of phosphorylated to non-phosphorylated  $\beta$ -dystroglycan in *sapje* larvae can be assessed.

Quantification of MANDAG2 and 1709 western blots revealed a significant increase in the ratio of phosphorylated to non-phosphorylated dystroglycan at 3 and 4dpf in *sapje* compared with sibling larvae (figure 4.9). There was no significant difference between the ratios of phosphorylated to non-phosphorylated  $\beta$ -dystroglycan in 5dpf sibling and

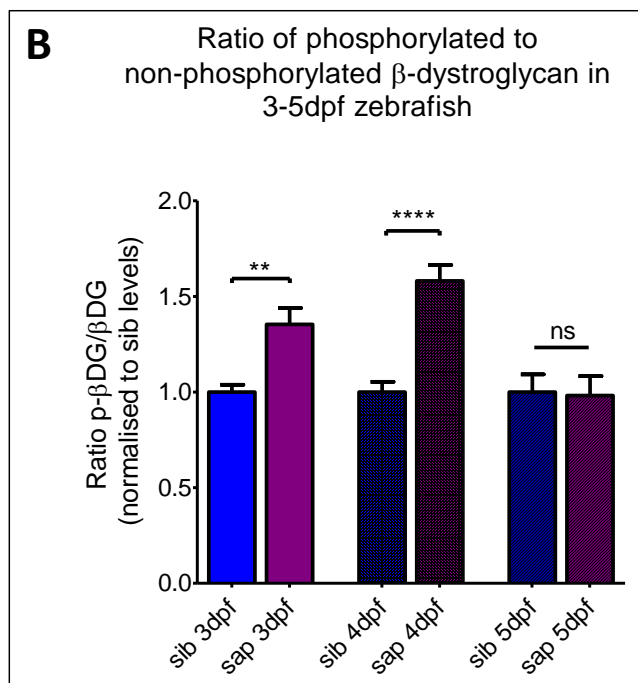
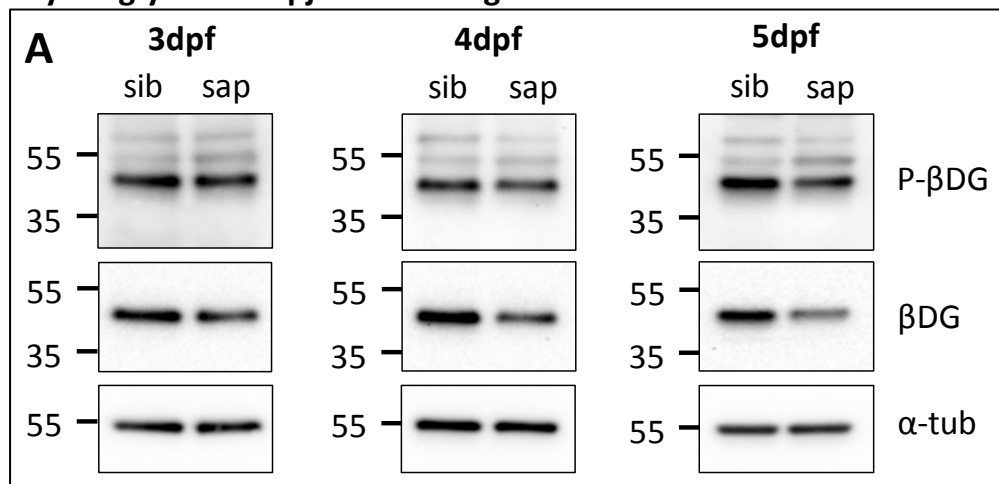
*sapje* samples. These results suggest the levels of phosphorylated  $\beta$ -dystroglycan are elevated relative to total dystroglycan in *sapje*, when compared with sibling larvae.

**Figure 4.8: Levels of phosphorylated  $\beta$ -dystroglycan in *sapje* and sibling larvae**



(A) Representative western blots of embryo lysates at 3,4 and 5dpf, probed with an antibody raised against phosphorylated  $\beta$ -dystroglycan (top panel) and anti- $\alpha$ -tubulin (bottom panel). (B) The density of the blot probed against phosphorylated dystroglycan was quantified relative to  $\alpha$ -tubulin levels in each sample, and represented as a ratio of average sibling signal. Graph shows mean + SEM of 9 samples from 3 independent experiments. Levels of phosphorylated dystroglycan are slightly increased in *sapje* at 3 and 4dpf, but this increase is not statistically significant (3dpf - Unpaired t-test:  $t=1.950$ , d.f.=16,  $p=0.0690$ ; 4dpf - Unpaired t-test:  $t=0.7851$ , d.f.=16,  $p=0.4439$ ). When compared with sibling lysates, levels of phosphorylated dystroglycan at 5dpf are significantly lower in *sapje* (Unpaired t-test:  $t=4.169$ , d.f.=16,  $p=0.0007$ ).

**Figure 4.9: Ratio of phosphorylated to non-phosphorylated dystroglycan in *sapje* and sibling zebrafish**



A) Western blots of 3, 4 and 5dpf sibling and *sapje* whole embryo lysates probed with antibodies for phosphorylated  $\beta$ DG (top panel),  $\beta$ DG (middle panel) and  $\alpha$ -tubulin (bottom panel).  $\alpha$ -tubulin signal indicates approximately equal loading of protein in each sample. B) The density of the blot probed against p- $\beta$ DG has been quantified relative to  $\beta$ DG levels in each sample and normalised to the average sibling signal. Graph shows mean + SEM of 8 samples from 3 independent experiments. There is a significant increase in the ratio of p- $\beta$ DG: $\beta$ DG in *sapje* compared with siblings at 3 and 4 dpf. (3dpf – Unpaired t-test with Welch’s correction:  $t=3.771$ ,  $d.f.=9$ ,  $p=0.0044$ ; 4dpf- Unpaired t-test:  $t=5.873$ ,  $d.f.=14$ ,  $p<0.0001$ ; 5dpf – Unpaired t-test:  $t=0.1324$ ,  $d.f.=14$ ,  $p=0.8966$ ).

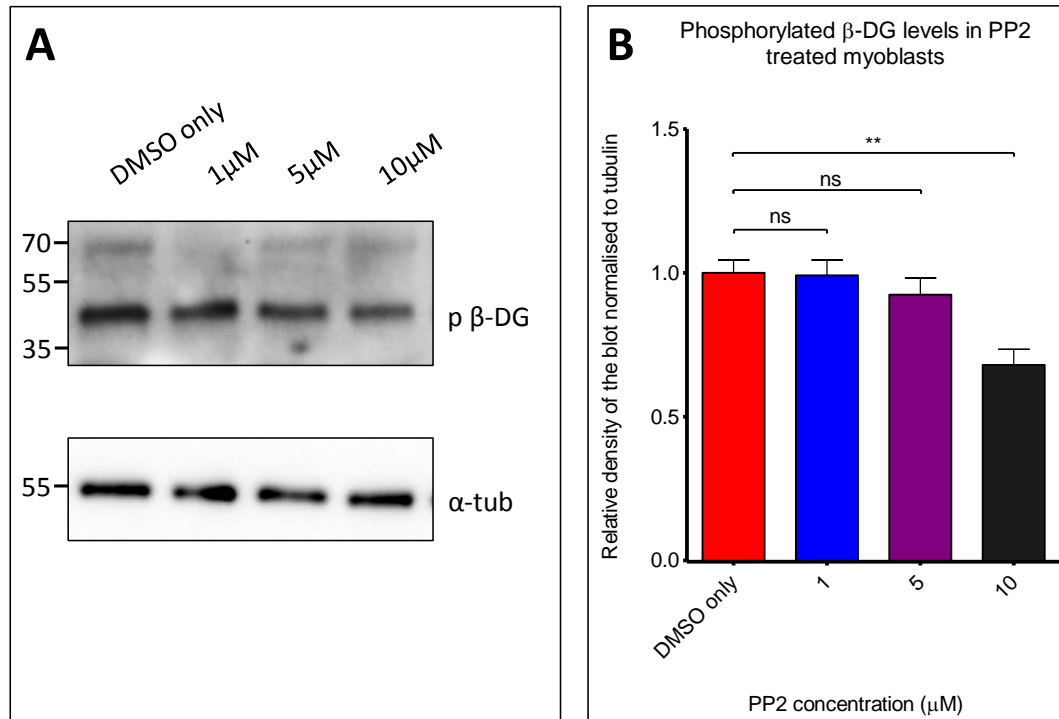
#### **4.3.4 Manipulation of dystroglycan phosphorylation**

Since earlier work has shown tyrosine residue 892 of dystroglycan to be a substrate for Src family kinases, the ability of Src inhibitors to alter the phosphorylation levels of dystroglycan was investigated.

##### **4.3.4.1 Src inhibitor treatment of H2k myoblasts**

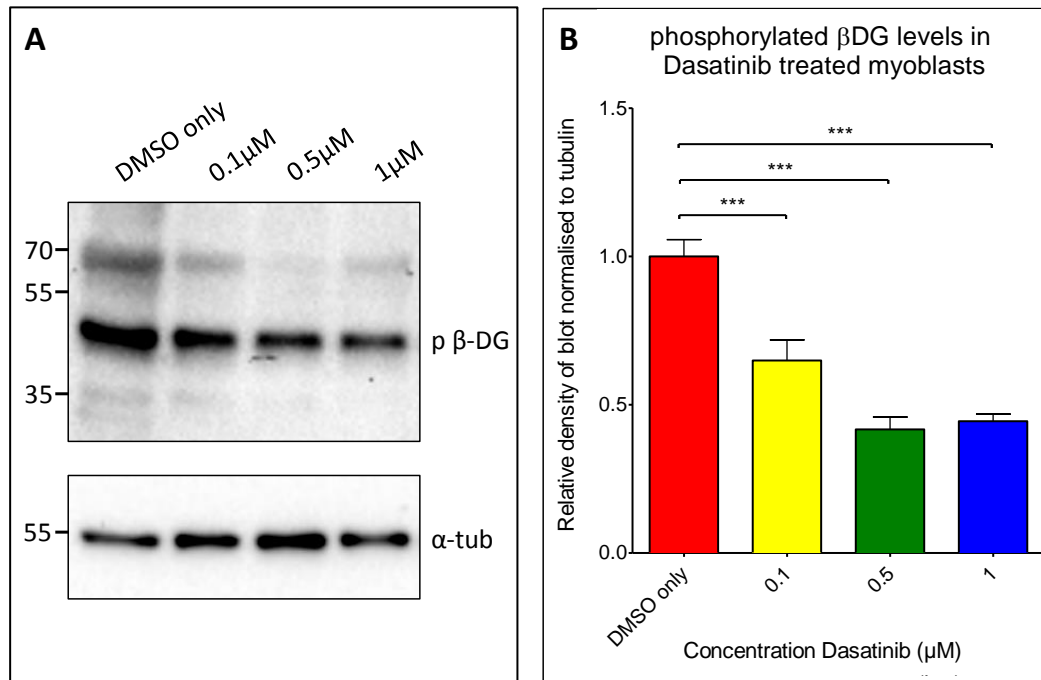
H2K myoblast cells were treated for 6 hours with either PP2 or Dasatinib, or with DMSO only. Western blot analysis of cell lysates was used to examine the effect of these inhibitors on the level of phosphorylated dystroglycan.

PP2, a well-established inhibitor of Src family tyrosine kinases, was able to significantly reduce levels of phosphorylated dystroglycan at a concentration of 10 $\mu$ M, compared with DMSO only treated cells (figure 4.10).

**Figure 4.10: Phosphorylated dystroglycan in PP2 treated myoblasts**

Myoblasts were treated with PP2 (or DMSO only) for 6 hours, before lysates were collected. (A) Representative western blot of myoblast lysates, probed with an antibody raised against phosphorylated  $\beta$ -dystroglycan (top panel) and anti- $\alpha$ -tubulin (bottom panel). (B) The density of the blot probed against phosphorylated dystroglycan was quantified relative to  $\alpha$ -tubulin levels in each sample, and represented as a ratio of average DMSO only control signal. Graph shows mean + SEM of 6 samples from 3 independent experiments. There is a significant effect of PP2 treatment on the levels of phosphorylated  $\beta$ -dystroglycan in myoblasts. The level of phosphorylated  $\beta$ -dystroglycan is significantly lower in myoblasts treated with 10 $\mu$ M PP2, compared with myoblasts treated with DMSO only. One way ANOVA was carried out ( $F=8.051$ ,  $d.f.=3,20$ ,  $p=0.0010$ ) followed by Dunnett's Multiple Comparison Test (ns=not significant,  $**p<0.005$ ).

Dasatinib (Luo et al., 2006) is a potent Abl and Src family inhibitor, used in the treatment of several types of leukaemia. It is able to decrease phosphorylated dystroglycan levels in H2K myoblasts at lower concentrations than PP2. Compared with DMSO only treated cells, there is a significant decrease in phosphorylated dystroglycan at concentrations of 0.1, 0.5 and 1 $\mu$ M (figure 4.11).

**Figure 4.11: Phosphorylated dystroglycan in Dasatinib treated myoblasts**

Myoblasts were treated with Dasatinib (or DMSO only) for 6 hours, before lysates were collected. (A) Representative western blot of myoblast lysates, probed with an antibody raised against phosphorylated  $\beta$ -dystroglycan (top panel) and anti- $\alpha$ -tubulin (bottom panel). (B) The density of the blot probed against phosphorylated dystroglycan was quantified relative to  $\alpha$ -tubulin levels in each sample, and represented as a ratio of average DMSO only control signal. Graph shows mean + SEM of 6 samples from 3 independent experiments. There is a significant decrease in the levels of phosphorylated  $\beta$ -dystroglycan in Dasatinib treated myoblasts, compared with DMSO treated controls. One way ANOVA was carried out ( $F=27.94$ ,  $d.f.=3,20$ ,  $p<0.0001$ ) followed by Dunnett's Multiple Comparison Test (\*\* $p<0.001$ ).

Src inhibitor treatment worked in the expected way in H2k myoblasts, reducing levels of phosphorylated dystroglycan. The ability of Src inhibitors to alter the phosphorylation of dystroglycan *in vivo* in zebrafish embryos was therefore assessed.

#### 4.3.4.2 Src inhibitor treatment of LWT embryos

Dechorionated London Wild Type (LWT) embryos were treated with PP2 or Dasatinib, or DMSO only from 24hpf. This time point was chosen in order to minimise levels of

developmentally related embryo death and to prevent interfering with early embryogenesis. Embryo lysates were made after 24 and 48 hours of drug treatment.

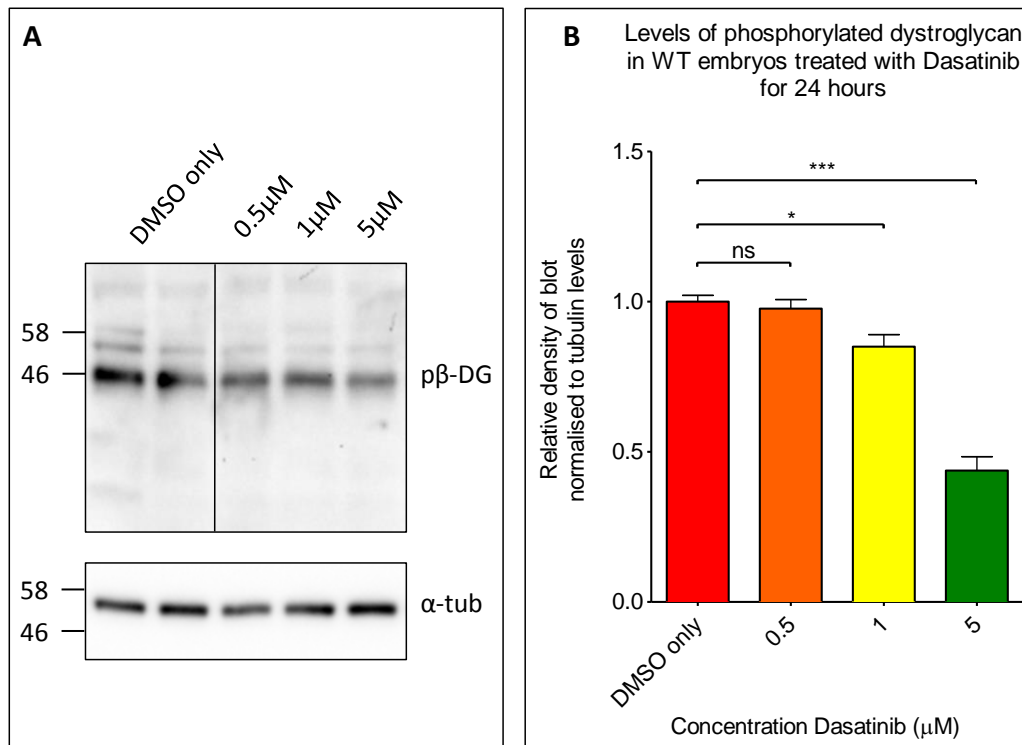
Dasatinib treatment of zebrafish embryos was able to decrease levels of phosphorylated dystroglycan in LWT embryos, and also decrease the ratio of phosphorylated to non-phosphorylated dystroglycan. PP2 treatment, however, was toxic at concentrations exceeding 1 $\mu$ M, with embryos displaying pericardial and yolk sac oedema.

Embryos that had been treated with 1 or 5 $\mu$ M Dasatinib for 24 hours, had significantly lower levels of phosphorylated dystroglycan than DMSO only treated controls (figure 4.12). Levels of phosphorylated dystroglycan were reduced by approximately 15% in embryos treated with 1 $\mu$ M Dasatinib, and by approximately 76% in embryos treated with 5 $\mu$ M Dasatinib.

Compared with treatment for 24 hours, treatment for 48 hours was found to be more effective in decreasing levels of phosphorylated dystroglycan. Western blots of embryo lysates and subsequent densitometric analysis indicated a significant decrease in the amount of phosphorylated dystroglycan in embryos treated with 1 or 5 $\mu$ M Dasatinib compared with DMSO only treated controls (figure 4.13). Phosphorylated dystroglycan levels were reduced by approximately 59 and 80% in embryos treated with 1 and 5 $\mu$ M Dasatinib respectively. In addition, there was a significant decrease in the ratio of phosphorylated to non-phosphorylated dystroglycan in embryos treated with Dasatinib (figure 4.13). The effect on the level of phosphorylated  $\beta$ -dystroglycan, compared with the level of the non-phosphorylated protein is more striking than the

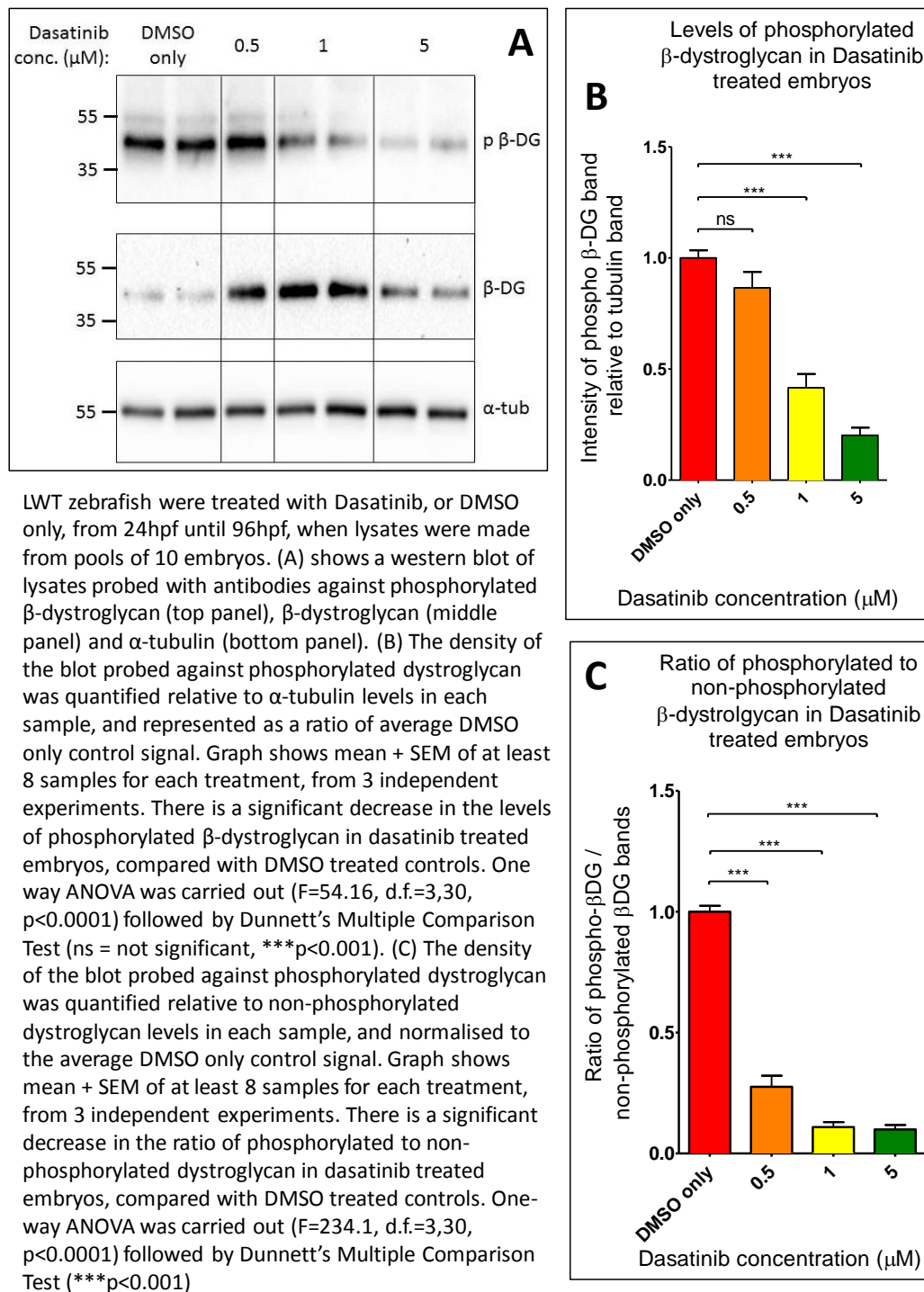
global decrease in phosphorylated  $\beta$ -dystroglycan, and can be observed in embryos treated with 0.5 $\mu$ M of Dasatinib.

**Figure 4.12: Phosphorylated dystroglycan in WT embryos treated with dasatinib for 24 hours**



Lysates were prepared from LWT embryos treated with Dasatinib (or DMSO only) for 24 hours from 24hpf. (A) Representative western blot of embryo lysates, probed with an antibody raised against phosphorylated  $\beta$ -dystroglycan (top panel) and anti- $\alpha$ -tubulin (bottom panel). (B) The density of the blot probed against phosphorylated dystroglycan was quantified relative to  $\alpha$ -tubulin levels in each sample, and represented as a ratio of average DMSO only control signal. Graph shows mean + SEM of at least 8 samples from 3 independent experiments. Dasatinib treatment significantly affects the level of phosphorylated  $\beta$ -dystroglycan in LWT embryos. One-way ANOVA was carried out ( $F=56.34$ ,  $d.f.=3,30$ ,  $p<0.0001$ ) followed by Dunnett's Multiple Comparison Test ( $ns$ = not significant,  $*p<0.05$ ,  $***p<0.001$ ).

**Figure 4.13: Phosphorylated dystroglycan in dasatinib treated wildtype embryos**

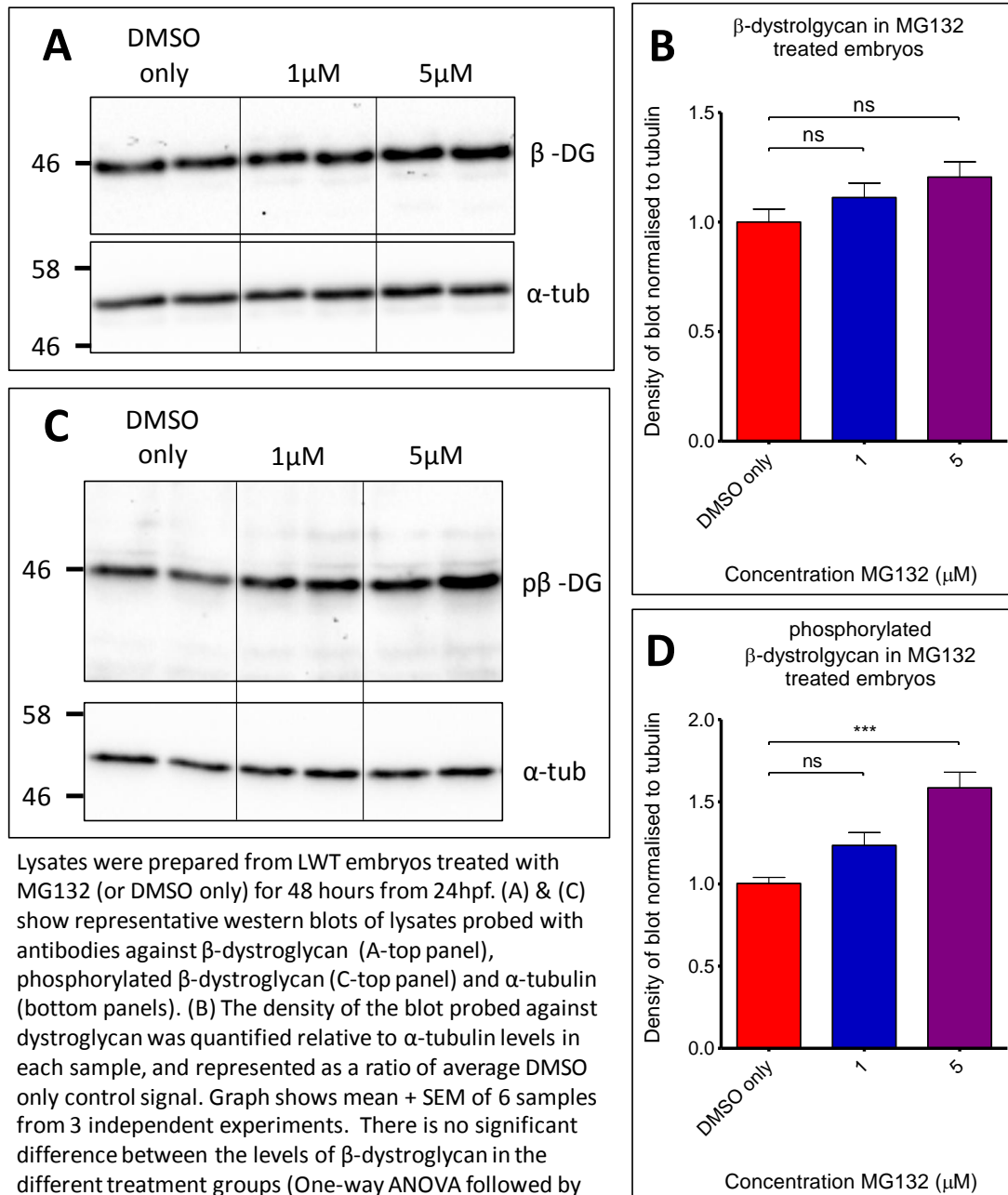


#### 4.3.5 Manipulation of proteasomal degradation

Data indicating a decrease in  $\beta$ -dystroglycan in *sapje*, when compared with sibling larvae is presented in section 4.3.2. This is also seen in DMD patients and mammalian models of the disease. It is thought that in the absence of dystrophin, dystroglycan and other DGC components are destabilised from the membrane and are subject to proteasome dependent degradation. Therefore, inhibitors of this pathway were used to investigate whether dystroglycan levels in zebrafish embryos could be manipulated.

Dechorionated LWT embryos were treated with the proteasome inhibitor MG132 or DMSO only from 24hpf. Embryo lysates were made after 48 hours of drug treatment and western blots carried out to analyse the levels of dystroglycan in the different treatment groups.

Western blots of embryo lysates and subsequent densitometric analysis indicated that the proteasome inhibitor MG132 had no significant effect on the levels of non-phosphorylated  $\beta$ -dystroglycan (figure 4.14). However, there was a significant increase in the levels of phosphorylated  $\beta$ -dystroglycan in embryos treated with 5 $\mu$ M MG132, compared with DMSO only treated controls (figure 4.14).

**Figure 4.14: Dystroglycan in MG132 treated LWT embryos**

Lysates were prepared from LWT embryos treated with MG132 (or DMSO only) for 48 hours from 24hpf. (A) & (C) show representative western blots of lysates probed with antibodies against  $\beta$ -dystroglycan (A-top panel), phosphorylated  $\beta$ -dystroglycan (C-top panel) and  $\alpha$ -tubulin (bottom panels). (B) The density of the blot probed against dystroglycan was quantified relative to  $\alpha$ -tubulin levels in each sample, and represented as a ratio of average DMSO only control signal. Graph shows mean + SEM of 6 samples from 3 independent experiments. There is no significant difference between the levels of  $\beta$ -dystroglycan in the different treatment groups (One-way ANOVA followed by Dunnett's Multiple Comparison test:  $F=2.500$ ,  $df=2,5$ ,  $p=0.1156$ ). (D) The density of the blot probed against phosphorylated  $\beta$ -dystroglycan was quantified relative to  $\alpha$ -tubulin levels in each sample, and represented as a ratio of average DMSO only control signal. Graph shows mean + SEM of 6 samples from 3 independent experiments. There is a significant difference between the levels of phosphorylated dystroglycan in the different treatment groups. One-way ANOVA was carried out ( $F=15.76$ ,  $df=2,15$ ,  $p=0.0002$ ) followed by Dunnett's Multiple comparison test (ns=not significant, \*\*\* $p<0.0005$ ).

## 4.4 Discussion

### 4.4.1 The muscular dystrophy phenotype of *sapje* progresses over time

*sapje* zebrafish are characterised by a dystrophic phenotype, observable by loss of birefringence of somitic muscle. Muscle damage and disorganisation can be seen more clearly by staining embryos with rhodamine phalloidin. Larval motility is also reduced in *sapje* mutants, as indicated by results from embryo swirl assays and the Viewpoint tracking data.

Quantifying the intensity of birefringence images revealed a progressive loss of muscle birefringency over time from 3 to 5dpf. Anesthetising embryos prevented this decline in muscle birefringence. This suggests that muscle damage may be related to motor activity. A similar effect is observed in *candyfloss* mutants, which result from mutations in the *laminin  $\alpha 2$*  gene; treating *candyfloss* embryos with tricaine resulted in a complete suppression of the dystrophic phenotype at 3dpf (Hall et al., 2007). Removal of tricaine was used to induce muscle contraction in *sapje* mutants, and using time lapse photomicroscopy, allowed the observation of myofibre detachment in real time (Berger et al., 2010). Together, these results provide evidence to suggest the generation of muscle force plays a key role in promoting the detachment of muscle fibres from the myosepta in zebrafish. As zebrafish motility increases with age, more myofibres become detached, resulting in a decrease in muscle integrity and worsening of the dystrophic phenotype.

#### 4.4.2 Age-dependent decrease in dystroglycan levels in *sapje*

The stability of the mammalian DGC is dependent on dystrophin expression and its localisation at the cell membrane. When dystrophin is absent, as in the *mdx* mouse and DMD patients, levels of dystroglycan and other DGC components are reduced (Ohlendieck and Campbell, 1991, Ohlendieck et al., 1993).

Loss of DGC components has previously been shown in dystrophin morphant zebrafish using western blot analysis (Guyon et al., 2003). However, whilst there was a clear reduction in levels of  $\beta$ -,  $\gamma$ - and  $\delta$ -sarcoglycan in morphant embryos, dystroglycan levels were variable; some experiments showed no change in  $\beta$ -dystroglycan expression, whilst others showed a clear decrease. Morphant embryos also displayed a spectrum of phenotypes, with some appearing normal. The authors estimated a 70% reduction in dystrophin expression in the anti-sense morpholino injected embryos. Residual dystrophin expression may account for the preservation of dystroglycan expression in some embryos. The morpholino was targeted against exon 1 of the muscle specific Dp427 isoform. Therefore other isoforms of dystrophin, which do not share this exon, could be present, and these may be able to bind and stabilise dystroglycan expression. In addition, blots were carried out at 4dpf when the effects of the morpholino may have worn off. The localisation of dystroglycan in morphant embryos was also not investigated; even though dystroglycan expression is not reduced in some embryos, it may not be localised to the membrane correctly.

Here, an age-dependent decrease in dystroglycan protein levels in dystrophin mutant zebrafish has been demonstrated. There is a marked reduction in  $\beta$ -dystroglycan levels in *sapje* compared with siblings of the same age. This can be observed using both

whole-mount immunohistochemistry and western blotting techniques. Quantification of western blot analysis clearly shows this loss becomes more pronounced over time. This suggests that, as in mammals, the stability of dystroglycan at the membrane is dependent on dystrophin expression.

As loss of dystroglycan expression is also seen in mammals with dystrophin mutations, these data provide further evidence that the biochemistry of the DGC is conserved between mammals and zebrafish. The downstream mechanism of dystroglycan loss as a consequence of dystrophin deficiency may be similar in mammals and zebrafish, and *sapje* provides a useful model for understanding this process in more detail.

The proposed mechanisms for the loss of dystroglycan at the membrane in dystrophin deficient environments are internalisation and degradation. Tyrosine phosphorylation is known to regulate the assembly and disassembly of many adhesion complexes (Burrige and Chrzanowska-Wodnicka, 1996). Phosphorylation of tyrosine residue 890 prevents dystroglycan from binding dystrophin and is thought to lead to its internalisation, thus promoting complex disassembly. It was hypothesised that loss of dystrophin would promote the phosphorylation and subsequent internalisation of dystroglycan.

#### **4.4.3 Increased phosphorylation of dystroglycan in *sapje***

It was hypothesised that the levels of phosphorylated dystroglycan would be increased in *sapje*. Using western blot analysis, the levels of phosphorylated dystroglycan in *sapje* larvae were examined, compared with siblings of the same age. Phosphorylated

dystroglycan levels are slightly increased in *sapje* at 3 and 4dpf, but these increases were not statistically significant. The fate of phosphorylated  $\beta$ -dystroglycan may be degradation, and this may explain why levels of phosphorylated species are not much higher in the *sapje* mutants at 3 and 4dpf. If the phosphorylated dystroglycan is being rapidly degraded, a large increase in dystroglycan phosphorylation may not be detectable without preventing degradation. At 5dpf, the level of phosphorylated dystroglycan is lower in *sapje* mutants. This may be due to elevated degradation.

Since the overall level of dystroglycan in the absence of dystrophin is lower, the amount of substrate to phosphorylate will also be lower. Therefore, the ratios of phosphorylated to non-phosphorylated dystroglycan in *sapje* and sibling larvae were investigated. Compared with the amount of non-phosphorylated  $\beta$ -dystroglycan, the level of phosphorylated  $\beta$ -dystroglycan was elevated in *sapje* at 3 and 4dpf. These data are in support of the hypothesis that the absence of dystrophin may lead to an elevation in the tyrosine phosphorylation of  $\beta$ -dystroglycan.

Since tyrosine phosphorylation is believed to lead to the internalisation of  $\beta$ -dystroglycan (Sotgia et al., 2003, Miller et al., 2012), there may be a shift in dystroglycan localisation from the sarcolemma to the cytosol. Non-phosphorylated dystroglycan shows strong staining at the myosepta, whereas phosphorylated dystroglycan staining is less defined. However, this could be due to high background staining of the 1709 antibody. Immunofluorescence staining of *sapje* larvae showed phosphorylated dystroglycan localised to punctate structures within the somitic muscle blocks. Although this may be non-specific binding of the antibody, it could represent internalised phosphorylated dystroglycan. However, the exact localisation of

this staining cannot be concluded. This could be further investigated by co-localisation experiments with markers of the endocytic, or other trafficking pathways. Sectioning of the zebrafish may provide better means for examining the cellular localisation of phosphorylated dystroglycan than whole-mount immunohistochemistry.

If the fate of phosphorylated dystroglycan is internalisation, the elevation of phosphorylation in *sapje* may be an important signalling pathway in the manifestation of the disease phenotype. Tyrosine phosphorylation of dystroglycan has previously been identified as an important mechanism for controlling the integrity of the DGC (Miller et al., 2012). Preventing this phosphorylation event may be able to promote the formation of stable dystroglycan complexes at the membrane and improve the dystrophic phenotype displayed in *sapje* zebrafish. Inhibitors of Src, the kinase thought to be involved in this process, were used to investigate whether the phosphorylation of dystroglycan could be manipulated.

#### **4.4.4 Manipulation of dystroglycan phosphorylation**

Src inhibitors were able to significantly lower the levels of phosphorylated dystroglycan in H2K myoblasts and LWT zebrafish embryos. Dasatinib was able to decrease phosphorylated dystroglycan levels in H2K myoblasts at lower concentrations than PP2. In contrast to PP2, Dasatinib was non-toxic to zebrafish embryos, where it was also able to reduce levels of phosphorylated dystroglycan.

Dasatinib and other Src inhibitors could be used in *sapje* to prevent the loss of dystroglycan and improve the muscular dystrophy phenotype. A similar approach has

been used in the *mdx* mouse; preventing the phosphorylation of dystroglycan Y890 by substituting the tyrosine for phenylalanine was able to restore expression of DGC proteins to the membrane and ameliorated the dystrophic phenotype (Miller et al., 2012).

Src phosphorylation provides a druggable target in the proposed pathway leading to the loss of dystroglycan in Duchenne muscular dystrophy. Many Src inhibitors, such as Dasatinib, have been developed in other therapeutic settings. Since Dasatinib is able to reduce the levels of phosphorylated dystroglycan in both myoblasts and zebrafish embryos, and is well-tolerated *in vivo*, it may be a promising candidate to improve the dystrophic phenotype in *sapje*. This idea will be explored further in chapter 5.

Although dystroglycan phosphorylation is thought to promote its internalisation, the fate of internalised dystroglycan is not fully understood. A cell surface biotinylation assay revealed a time-dependent decrease in the amount of phosphorylated dystroglycan at the cell surface and an increase in cytosolic phosphorylated dystroglycan. This suggests that tyrosine phosphorylation of dystroglycan may be a signal for its internalisation. However, the subsequent trafficking pathway is not known, as phosphorylated dystroglycan did not colocalise with transferrin receptors, EEA1 or lysotracker (Miller et al., 2012).

The phosphorylation of dystroglycan may be a signal for a subsequent downstream process, such as degradation. Phosphorylated  $\beta$ -dystroglycan has been shown to be ubiquitinated, whereas non-phosphorylated  $\beta$ -dystroglycan is not (Rob Piggott, unpublished results). There is evidence to support the hypothesis that phosphorylated

dystroglycan is degraded. Elevating the phosphorylation of  $\beta$ -dystroglycan, by transforming NIH 3TC cells with v-Src, resulted in a 3-4 fold reduction in the total levels of  $\beta$ -dystroglycan (Sotgia et al., 2001). Once internalised, phosphorylated dystroglycan may then be degraded in downstream pathways.

The decrease in dystroglycan levels over time in *sapje* suggests it may be being degraded. The proteasome-dependent degradation pathway is elevated in DMD (Kumamoto et al., 2000), and inhibiting this pathway has been shown to be beneficial to *mdx* mice (Bonuccelli et al., 2003, Bonuccelli et al., 2007). Therefore, the proteasome inhibitor MG132 was used to investigate whether the degradation of dystroglycan can be manipulated in zebrafish.

#### **4.4.5 Manipulation of proteasomal degradation**

Treatment of zebrafish embryos with MG132 slightly increased levels of  $\beta$ -dystroglycan, but this was not statistically significant. However, there was a significant increase in phosphorylated  $\beta$ -dystroglycan in treated embryos, compared with DMSO only treated controls. It is thought that phosphorylation of dystroglycan is a signal for its internalisation and possibly its degradation. If phosphorylated dystroglycan is indeed the species that is degraded, this may explain why there is a significant increase in phosphorylated dystroglycan in treated embryos, but not a significant increase in non-phosphorylated dystroglycan.

Proteasomal inhibitors may be able to increase dystroglycan levels more significantly in a system where the proteasomal degradation pathway is elevated. This may be the

case in *sapje*, where levels of dystroglycan are decreased. The *mdx* mouse also has decreased dystroglycan levels, which are thought to result from an elevation in protein degradation pathways. Proteasomal inhibitors may be able to ameliorate the dystrophic phenotype in *sapje*, as has been shown in *mdx* mice previously. If proteasomal inhibitors are beneficial to *sapje* muscle, this may provide evidence of the same pathophysiological pathway occurring in the dystrophin-deficient muscle of both fish and mammals, and would highlight the zebrafish as a useful tool in the DMD drug discovery pipeline.

#### 4.5 Concluding remarks

Loss of dystrophin in mammals and zebrafish leads to the loss of dystroglycan, and other DGC proteins. Phosphorylated dystroglycan is elevated in the zebrafish dystrophin mutant *sapje*. This change in the balance between phosphorylated and non-phosphorylated species may prevent dystroglycan from forming stable complexes at the membrane. Phosphorylation of dystroglycan has previously been identified as a possible signal for internalisation and is also important in controlling the integrity of the DGC. The fate of internalised dystroglycan is thought to be degradation.

Understanding the internalisation and degradation processes of dystroglycan may have therapeutic implications, as the loss of the DGC is a central part of the aetiology of Duchenne muscular dystrophy.

**Chapter 5: Chemical treatment of a zebrafish model of Duchenne  
Muscular Dystrophy (*sapje*)**

---

## 5.1 Introduction

### 5.1.1 Altered dystroglycan expression in *sapje*

As in mammals, dystroglycan stability in zebrafish appears to be dependent on dystrophin. The absence of dystrophin in the muscle of *sapje* mutants results in a time-dependent loss of dystroglycan expression. This could be explained by an elevation in dystroglycan degradation, as in the *mdx* mouse and DMD patients, where levels of dystroglycan and other DGC proteins are also reduced.

It is unknown what targets dystroglycan and other complex components for degradation in DMD. It has been suggested that in the absence of dystrophin, the DGC lacks stable connections to the actin cytoskeleton, and this loss of stability of the complex proteins may render them more susceptible to degradation.

As discussed in chapter 4, tyrosine phosphorylation of dystroglycan has been identified as a signal for internalisation, and this is believed to play an important role in controlling the integrity of the DGC.

In *sapje* mutants, there is a shift in the balance of phosphorylated and non-phosphorylated  $\beta$ -dystroglycan. The elevated phosphorylation levels may lead to an increased internalisation of dystroglycan and disassembly of the DGC. Once dystroglycan is internalised, it may then be degraded.

Inhibiting proteasomal degradation, the final step in the proposed pathway leading to the loss of dystroglycan in the absence of dystrophin, was able to restore dystroglycan

and other DGC proteins to the sarcolemma and improve muscle pathophysiology in *mdx* mice and explants from DMD patients (Bonuccelli et al., 2003, Assereto et al., 2006, Bonuccelli et al., 2007, Gazzero et al., 2010). Since dystroglycan levels are decreased in *sapje*, these inhibitors may also be beneficial in the zebrafish. Inhibitors of dystroglycan phosphorylation may also be able to improve dystrophy by preventing loss of dystroglycan function at the membrane. Preventing tyrosine phosphorylation of dystroglycan in the *mdx* mouse has also been shown to improve the dystrophic phenotype (Miller et al., 2012).

### 5.1.2 Usefulness of zebrafish in drug discovery

Zebrafish are rapidly emerging as a powerful tool in various stages of the drug discovery pipeline (Zon and Peterson, 2005). They are especially valuable in early stages of research, providing an *in vivo* system in which to demonstrate drug efficacy before more costly mammalian models are used.

Zebrafish are particularly amenable to muscular dystrophy drug discovery as disruption in muscle integrity and function can be readily observed in early stages of development. In addition, zebrafish express orthologues of most genes known to be mutated in human muscular dystrophies (Steffen et al., 2007). Mutations in these genes result in dystrophic phenotypes in zebrafish (Bassett et al., 2003, Guyon et al., 2005, Nixon et al., 2005, Hall et al., 2007).

Preventing dystroglycan phosphorylation, and its subsequent internalisation and degradation, has been identified as a potential target for DMD therapeutics. The

zebrafish provides a useful platform for assessing the effectiveness of preventing dystroglycan loss in ameliorating the dystrophic phenotype.

## 5.2 Aims and hypotheses

Increased phosphorylation of dystroglycan in *sapje* may be an important signalling pathway in the manifestation of the disease phenotype, resulting in increased internalisation and disassembly of the DGC. Once lost from the membrane, dystroglycan and other DGC proteins may then be degraded. The work described within this chapter aims to investigate whether inhibiting steps in the proposed pathway leading to the loss of dystroglycan in DMD is able to stabilise dystroglycan expression and ameliorate dystrophy in *sapje*.

Hypothesis:

- Inhibiting the phosphorylation and degradation of dystroglycan is able to ameliorate the dystrophic phenotype in *sapje*.

## 5.3 Results

### 5.3.1 Development of the assay

Muscle pathology can be readily observed in the zebrafish larva, by examining the birefringence under polarising light. Loss of birefringence can therefore be used as a simple visual readout of muscle damage.

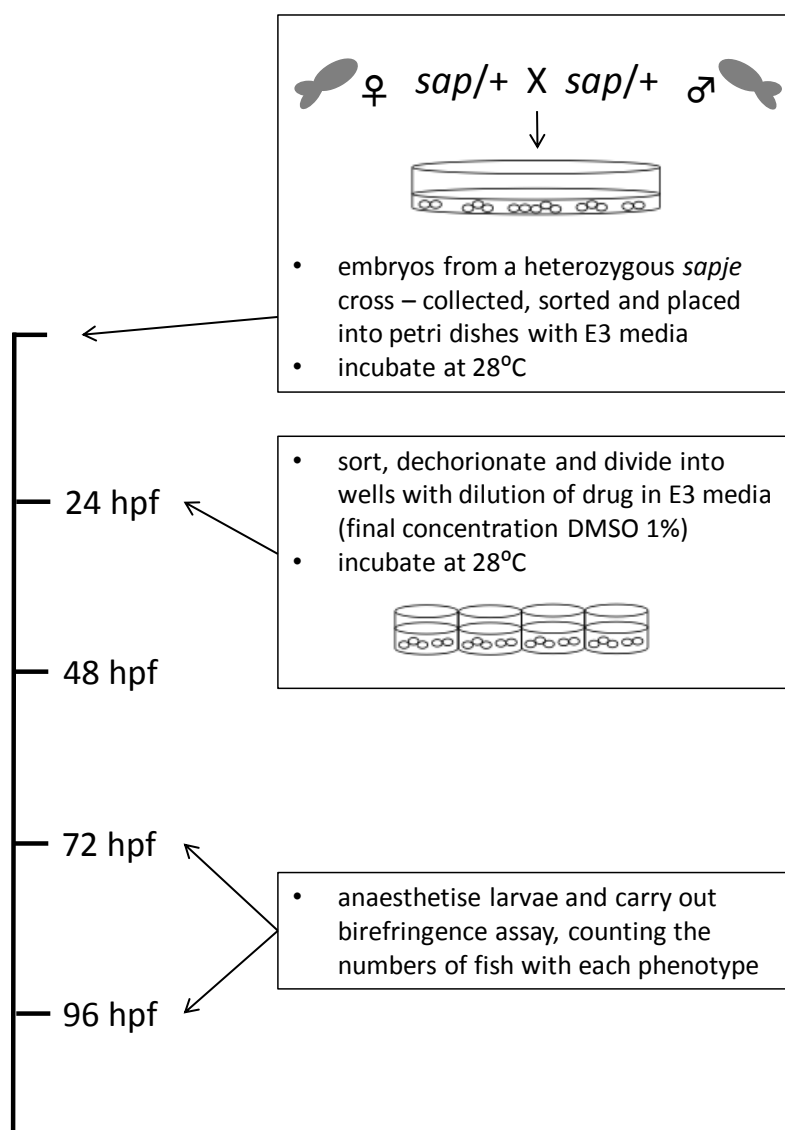
In order to identify drugs that may delay or prevent the onset of the dystrophic phenotype, compounds were added before mutants can be identified. Therefore, the assay was carried out on a mixed population of offspring from heterozygous *sapje* fish, comprising approximately 25% homozygous mutant embryos. If inhibitors of Src kinase or proteasomal degradation are able to prevent or slow the progression of dystrophy, they may be able to decrease the percentage of embryos displaying loss of birefringence.

Carrying out the assay on a mixed population meant large numbers of embryos were needed in each treatment group. This is to prevent false positive results, where low numbers of mutant fish are aliquotted into drug treatment groups by chance. 50 embryos were used per treatment group, so that sufficient numbers of homozygous mutants were treated with each concentration of drug. Assays were also repeated 5 times to improve the reliability of results.

Embryos were treated from 24hpf in order to prevent compounds affecting early development and to reduce the loss of embryos through developmentally related death. Treatment was carried out for at least 48 hours, when muscle birefringence can then be assessed. This duration of drug exposure was found to be effective in reducing levels of phosphorylated  $\beta$ -dystroglycan and increasing levels of non-phosphorylated  $\beta$ -dystroglycan when treating embryos with inhibitors of Src kinase and proteasomal degradation (chapter 4).

A schematic of the assay is shown in figure 5.1

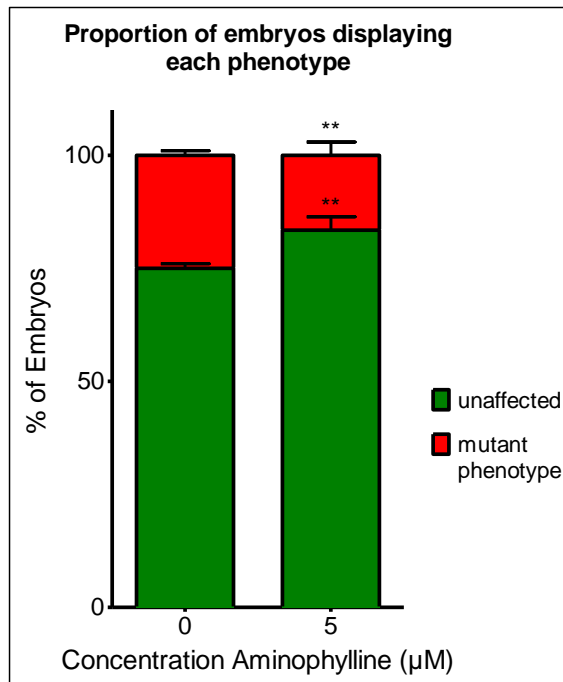
Figure 5.1: Schematic of assay



### 5.3.2 Positive control compound

A recent drug screen by the Kunkel group identified aminophylline, a non-selective phosphodiesterase (PDE) inhibitor, as effective in reducing the proportion of *sapje* and *sapje*-like fish displaying the muscle pathology detected by birefringence (Kawahara et al., 2011).

Aminophylline treatment of embryos from heterozygous *sapje* pairs resulted in a reduction of larvae displaying a dystrophic phenotype, compared with those treated with DMSO only (figure 5.2). There was a significant increase in the percentage of larvae showing an unaffected muscle phenotype in the groups treated with 5 $\mu$ M aminophylline compared with those treated with DMSO only. This validates the assay design in terms of its ability to detect compounds capable of correcting the dystrophic phenotype.

**Figure 5.2: Treatment of embryos with Aminophylline**

Embryos were treated with 5μM Aminophylline or DMSO only for 48 hours before a birefringence assay was carried out. The number of larvae showing normal or disrupted muscle birefringence were counted. There is a significant increase in the percentage of embryos showing an unaffected muscle birefringence phenotype in the treated group compared with DMSO only controls (Unpaired t-test:  $t=4.7$ ,  $df=4$ ,  $p=0.0093$ ). Data points represent mean values from 3 independent experiments, with a total of approximately 150 embryos per treatment group. Error bars represent SEM.

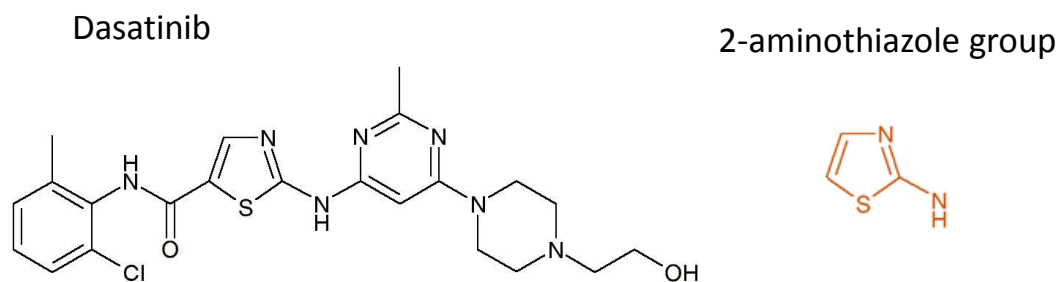
### 5.3.3 Src kinase inhibitors

#### 5.3.3.1 Dasatinib treatment is able to decrease the percentage of embryos showing a dystrophic phenotype

Dasatinib (figure 5.3), an inhibitor of Abl and Src family kinases, was shown to decrease levels of phosphorylated dystroglycan in H2K myoblasts and LWT embryos (chapter 4). *sapje* larvae have elevated levels of phosphorylated dystroglycan, and it is hypothesised that this may promote the disassembly of the DGC in the absence of

dystrophin. Embryos were therefore treated with Dasatinib to investigate whether inhibiting Src is beneficial to dystrophic muscle.

**Figure 5.3: Chemical structure of Dasatinib**



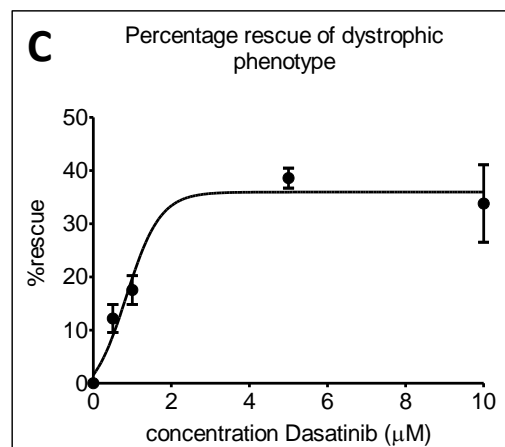
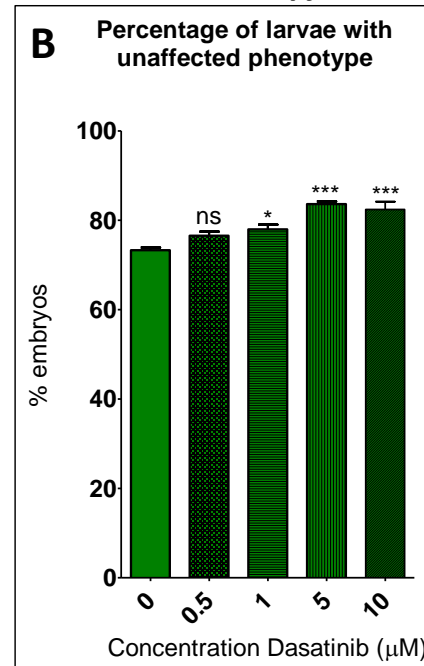
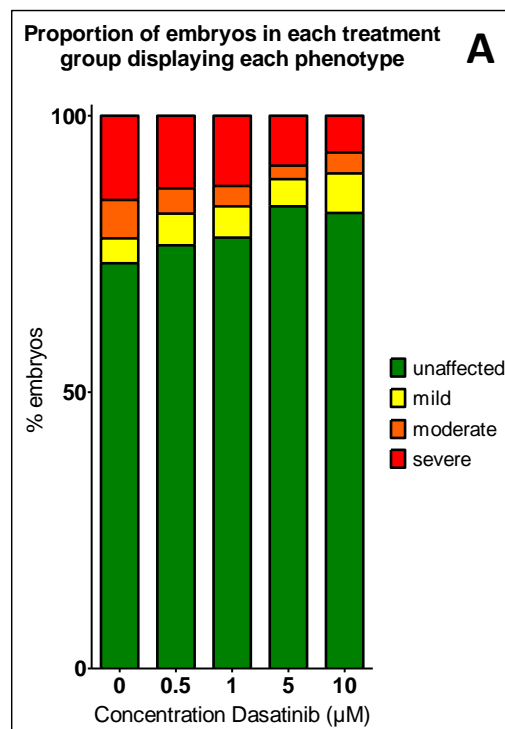
The chemical structure of Dasatinib is shown on the left. A screen of a compound collection identified 2-aminothiazole (right-hand panel) as a novel Src family kinase inhibitor template (Das et al., 2006). Dasatinib was developed through the optimisation of this template, using structure-activity relationship analysis. Dasatinib is a ATP-competitive kinase inhibitor; the aminothiazole moiety occupies the site normally bound by ATP. Aminothiazole derivatives generally have favourable in vivo properties and good bioavailability (Ghaemmaghami et al., 2010). Several kinase inhibitors with this scaffold have been described, including VEGF-2 kinase inhibitors (Borzilleri et al., 2006).

Treatment of *sapje* zebrafish with Dasatinib from 24 to 72hpf was able to reduce the proportion of embryos with a dystrophic phenotype (figure 5.4). For concentrations greater than 1 $\mu$ M Dasatinib, there is a significant increase in the percentage of embryos with an unaffected muscle birefringence phenotype (figure 5.4B).

There is a concentration-dependent restoration of muscle integrity (figure 5.4C).

Taking the proportion of dystrophic fish in DMSO only treated groups as 0% rescue, percentage rescue of the dystrophic phenotype was calculated. The effect of Dasatinib plateaued at about 2 $\mu$ M, with a maximum of approximately 35% of the dystrophic population displaying normal muscle birefringence.

**Figure 5.4: Effect of 48 hour Dasatinib treatment on *sapje* muscle phenotype**

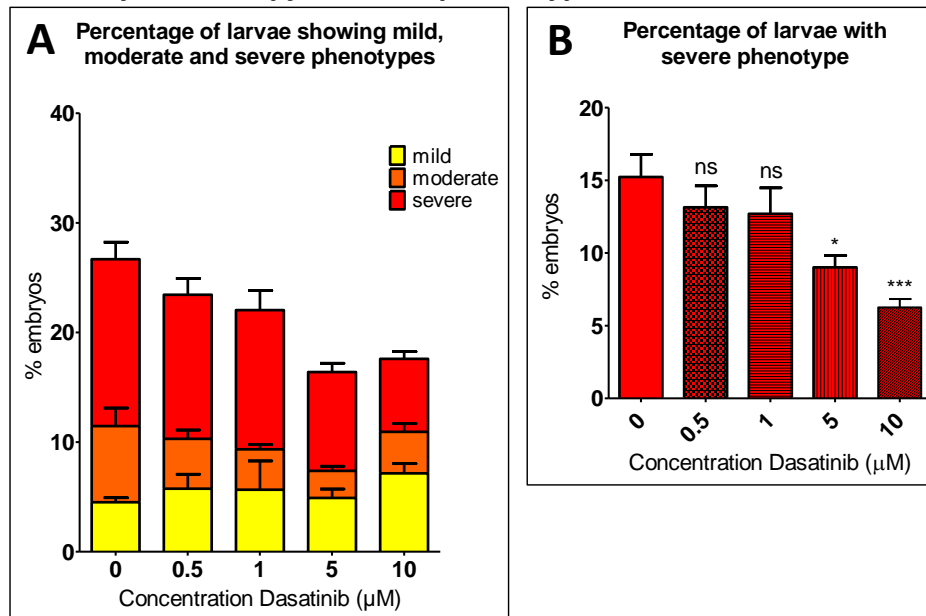


Embryos were treated with Dasatinib or DMSO only for 48 hours before a birefringence assay was carried out. The number of larvae showing normal or disrupted muscle birefringence were counted. Those showing disrupted birefringence were further subdivided into mild (disrupted birefringence affecting 1-5 somitic muscle blocks), moderate (6-10 somites) and severe (10+ somites) phenotypes. (A) shows the proportion of embryos displaying each phenotype. (B) shows there is a significant increase in the percentage of embryos showing an unaffected muscle birefringence phenotype in the groups treated with Dasatinib compared with the DMSO only control group (One-way ANOVA:  $F=15.66$ ,  $df=4,20$ ,  $p<0.0001$ , followed by Dunnett's Multiple Comparison Test: ns= not significant,  $*p<0.05$ ,  $***p<0.001$ ). (C) shows the percentage rescue of the dystrophic phenotype, taking the proportion of dystrophic fish in DMSO only treated groups as 0% rescue. Data points represent mean values of 5 independent experiments, with a total of approximately 250 embryos per treatment group. Error bars represent SEM.

The severity of the muscle damage was also examined (figure 5.5). Damage was classed as either mild (fewer than 5 somite blocks showing disrupted birefringence), moderate (5-10) or severe (10 or more). There is a significant decrease in the

percentage of larvae showing a severe phenotype in the groups treated with 5 and 10 $\mu$ M Dasatinib compared with DMSO alone.

**Figure 5.5: Effect of 48 hour Dasatinib treatment on the severity of the *sapje* muscle phenotype**

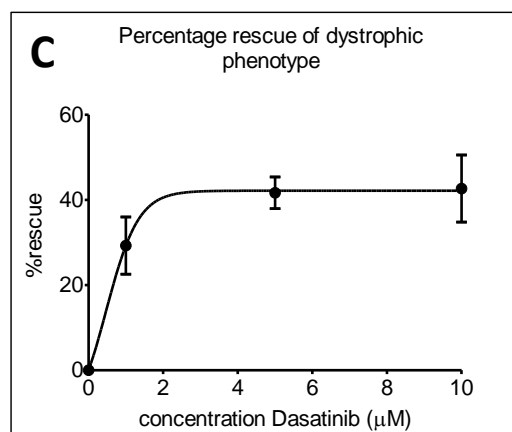
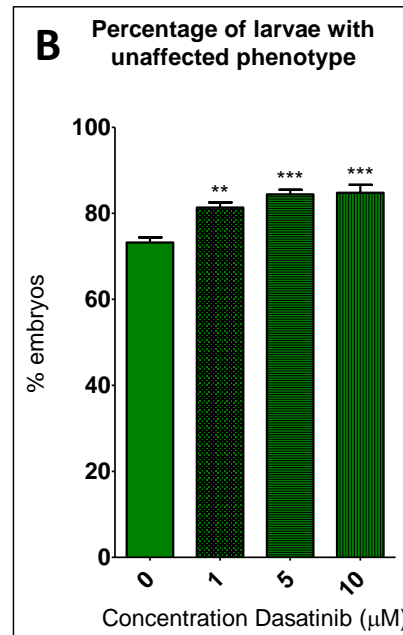
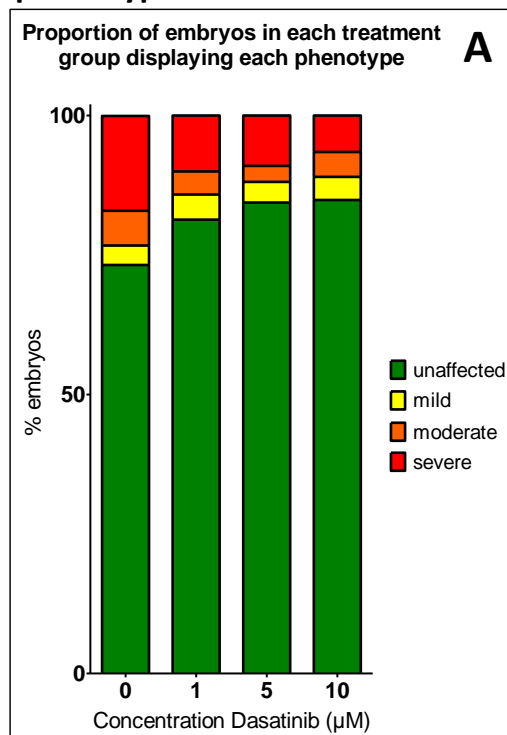


Embryos were treated with Dasatinib or DMSO only for 48 hours before a birefringence assay was carried out. The number of larvae showing normal or disrupted muscle birefringence were counted. Those showing disrupted birefringence were further subdivided into mild (disrupted birefringence affecting 1-5 somitic muscle blocks), moderate (6-10 somites) and severe (10+ somites) phenotypes. (A) shows the proportion of larvae showing mild, moderate and severe muscle damage. (B) shows there is a significant decrease in the percentage of larvae showing a severe phenotype in the groups treated with 5 and 10  $\mu$ M Dasatinib compared with DMSO alone (One-way ANOVA:  $F=7.332$ ,  $df=4,20$ ,  $p=0.0008$ , followed by Dunnett's Multiple Comparison Test:  $*p<0.05$ ,  $***p<0.001$ ). Data points represent mean values of 5 independent experiments, with a total of approximately 250 embryos per treatment group. Error bars represent SEM.

Similar results were obtained when embryos were treated with Dasatinib from 24 to 96hpf (figure 5.6 & 7), with treatment appearing slightly more effective in slowing or preventing the progression of the muscle pathology. There is a significant increase in the percentage of embryos with an unaffected muscle birefringence phenotype for all

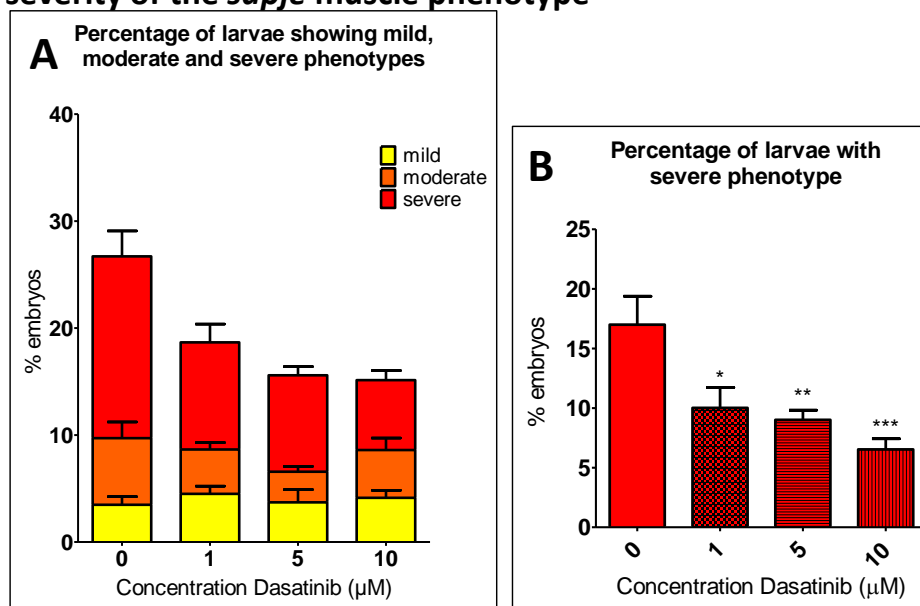
concentrations used, compared to embryos treated with DMSO only (figure 5.6B). 3 day Dasatinib treatment reduced the percentage of embryos showing disrupted muscle birefringence from ~25% to ~15%, a rescue of approximately 40% (figure 5.6C). There is also a significant decrease in the percentage of larvae showing a severe phenotype (figure 5.7).

**Figure 5.6: Effect of 72 hour Dasatinib treatment on *sapje* muscle phenotype**



Embryos were treated with Dasatinib or DMSO only for 72 hours before a birefringence assay was carried out. The number of larvae showing normal or disrupted muscle birefringence were counted. Those showing disrupted birefringence were further subdivided into mild (disrupted birefringence affecting 1-5 somitic muscle blocks), moderate (6-10 somites) and severe (10+ somites) phenotypes. (A) shows the proportion of embryos displaying each phenotype. (B) shows there is a significant increase in the percentage of embryos showing an unaffected muscle birefringence phenotype in the groups treated with Dasatinib compared with the DMSO only control group (One-way ANOVA:  $F=15.69$ ,  $df=3,16$ ,  $p<0.0001$ , followed by Dunnett's Multiple Comparison Test: \*\* $p<0.01$ , \*\*\* $p<0.001$ ). (C) shows the percentage rescue of the dystrophic phenotype, taking the proportion of dystrophic fish in DMSO only treated groups as 0% rescue. Data points represent mean values of 5 independent experiments, with a total of approximately 250 embryos per treatment group. Error bars represent SEM.

**Figure 5.7: Effect of 72 hour Dasatinib treatment on the severity of the *sapje* muscle phenotype**



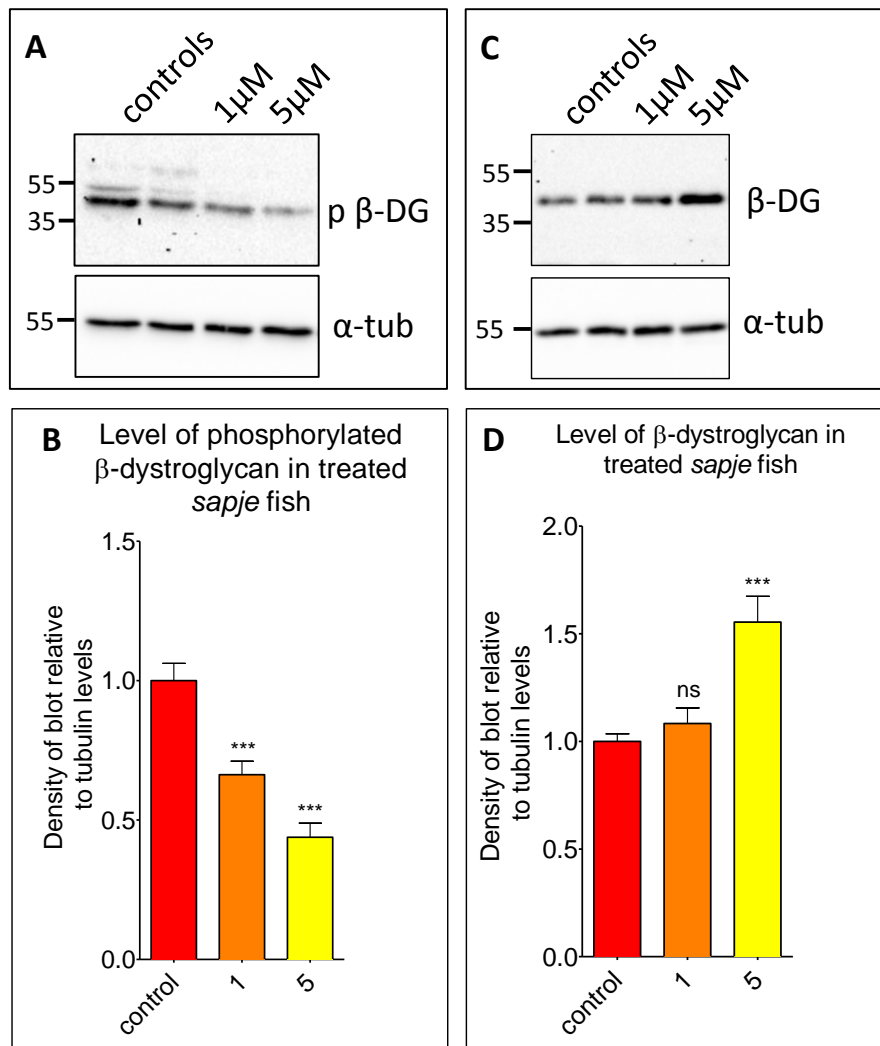
Embryos were treated with dasatinib or DMSO only for 72 hours before a birefringence assay was carried out. The number of larvae showing normal or disrupted muscle birefringence were counted. Those showing disrupted birefringence were further subdivided into mild (disrupted birefringence affecting 1-5 somitic muscle blocks), moderate (6-10 somites) and severe (10+ somites) phenotypes. (A) shows the proportion of larvae showing mild, moderate and severe muscle damage. (B) shows there is a significant decrease in the percentage of larvae showing a severe phenotype in the groups treated with dasatinib compared with DMSO alone (One-way ANOVA:  $F=8.016$ ,  $df=3,16$ ,  $p=0.0017$ , followed by Dunnett's Multiple Comparison Test:  $*p<0.05$ ,  $**p<0.01$ ,  $***p<0.001$ ). Data points represent mean values of 5 independent experiments, with a total of approximately 250 embryos per treatment group. Error bars represent SEM.

**5.3.3.2 Dasatinib is able to decrease levels of phosphorylated  $\beta$ -dystroglycan in *sapje***

It was hypothesised that Src kinase inhibitors may be able to improve the muscular dystrophy phenotype by preventing the phosphorylation, and subsequent loss of dystroglycan from the muscle membrane. Therefore, the levels of phosphorylated  $\beta$ -dystroglycan in treated *sapje* would be reduced compared to non-treated fish.

Western blot analysis of *sapje* larvae treated with Dasatinib indicated there were significantly lower levels of phosphorylated  $\beta$ -dystroglycan in these samples compared with *sapje* embryos treated with DMSO only (figure 5.8). Levels of non-phosphorylated dystroglycan were also examined, and these were found to be significantly higher in fish treated with 5 $\mu$ M Dasatinib, compared with DMSO treated controls.

**Figure 5.8: Effect of Dasatinib treatment on levels of phosphorylated and non-phosphorylated  $\beta$ -dystroglycan**



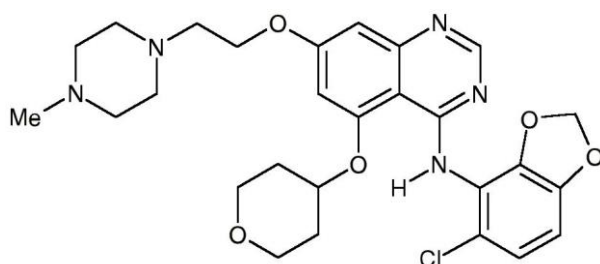
Lysates were made from embryos treated with Dasatinib or DMSO only. (A) shows western blots probed against antibodies for p  $\beta$ -DG (phosphorylated  $\beta$ -dystroglycan) and  $\alpha$ -tubulin. (B) The density of the blot probed against p  $\beta$ -DG was quantified relative to  $\alpha$ -tubulin levels in each sample, and normalised to average control signal. There is a significant decrease in the level of phosphorylated  $\beta$ -dystroglycan in larvae treated with Dasatinib, compared with controls (One-way ANOVA:  $F=27.23$ ,  $df=2,15$ ,  $p<0.0001$ , followed by Dunnett's Multiple Comparison test, \*\*\* $p<0.001$ ). (C) shows western blots probed against antibodies for  $\beta$ -DG ( $\beta$ -dystroglycan) and  $\alpha$ -tubulin. (D) The density of the blot probed against  $\beta$ -DG was quantified relative to  $\alpha$ -tubulin levels in each sample, and normalised to average control signal. There was a significant difference in the levels of  $\beta$ -DG in larvae between different treatment groups (One-way ANOVA:  $F=12.86$ ,  $df=2,15$ ,  $p=0.0006$ , followed by Dunnett's Multiple Comparison test, ns=not significant, \*\*\* $p<0.001$ ). Graphs represent the mean of 6 samples from 3 independent experiments, error bars are SEM.

### 5.3.3.3 Saracatinib treatment

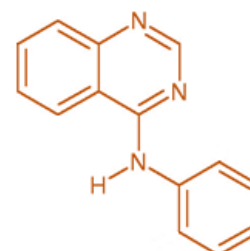
Saracatinib (figure 5.9) is another Abl and Src family kinase inhibitor used in the treatment of leukaemia. Treatment of *sapje* embryos with Saracatinib was able to reduce the proportion of embryos displaying a dystrophic phenotype (figure 5.10). However, it was not as effective as Dasatinib, and required higher concentrations to significantly increase the proportion of embryos showing unaffected muscle birefringence (figure 5.10B), and significantly decrease the proportion displaying a severe phenotype (figure 5.11). This may relate to the higher IC<sub>50</sub> of Saracatinib in comparison with Dasatinib.

**Figure 5.9 Chemical structure of Saracatinib**

Saracatinib

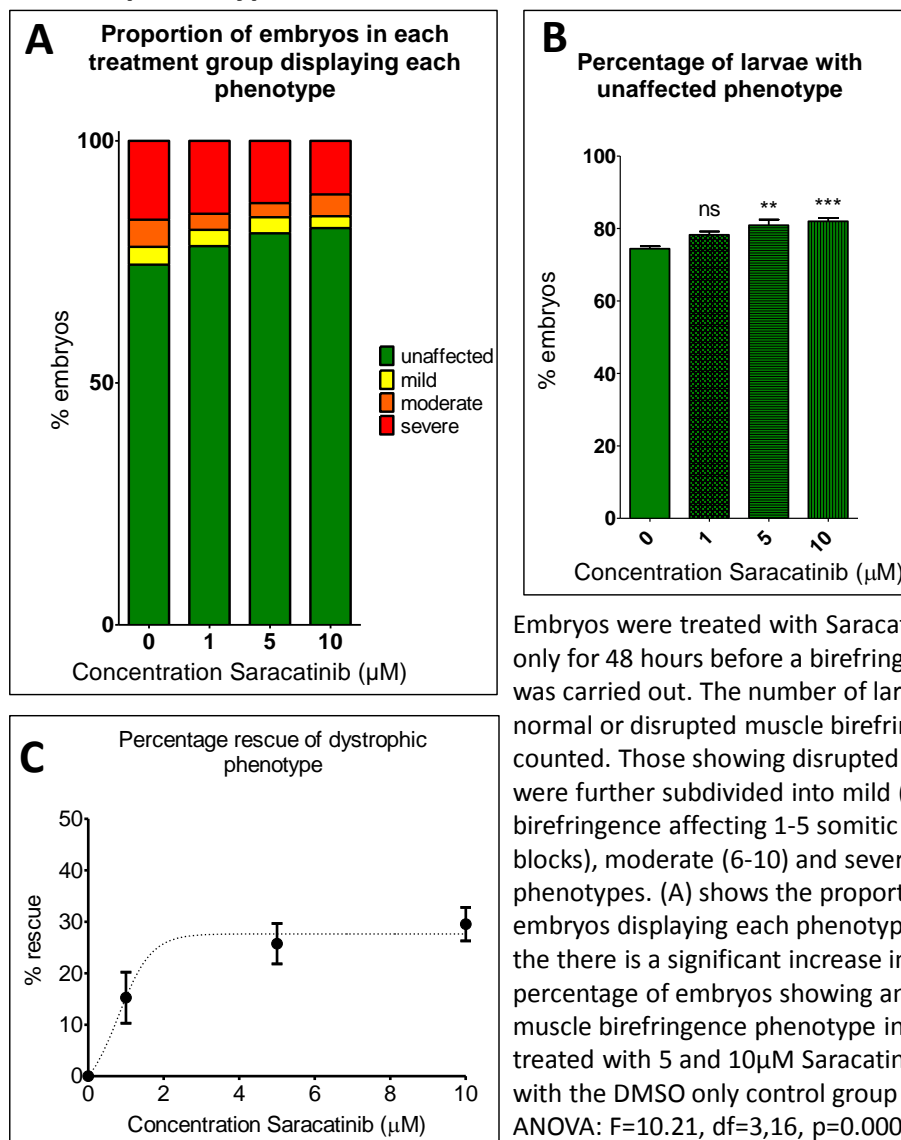


4-anilinoquinazoline



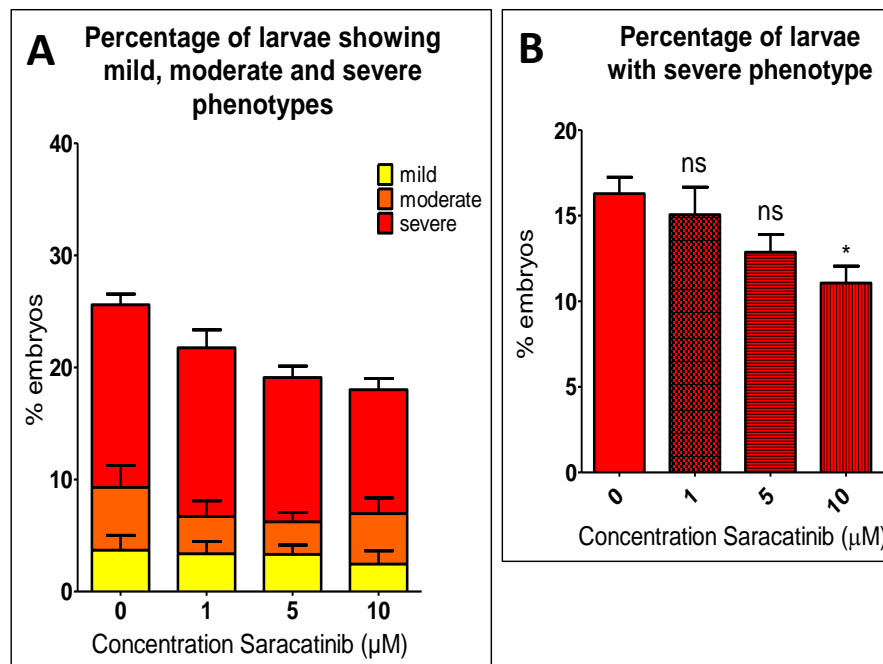
The chemical structure of Saracatinib is shown on the left. A 4-anilinoquinazoline scaffold (right-hand panel) forms the basis for several Src kinase inhibitors (Kluhs et al., 2007). The modification of this 4-anilinoquinazoline skeleton is important for kinase selectivity (Fang et al., 2013). Several structure-activity relationship analyses have demonstrated the significance of these modifications; the presence of nitrogen at position 1 and 3 of the anilinoquinazoline ring is important for the binding affinity of Saracatinib to the kinase domain of c-Src (Fang et al. 2013).

**Figure 5.10: Effect of 48 hour Saracatinib treatment on *sapje* muscle phenotype**



Embryos were treated with Saracatinib or DMSO only for 48 hours before a birefringence assay was carried out. The number of larvae showing normal or disrupted muscle birefringence were counted. Those showing disrupted birefringence were further subdivided into mild (disrupted birefringence affecting 1-5 somitic muscle blocks), moderate (6-10) and severe (10+) phenotypes. (A) shows the proportion of embryos displaying each phenotype. (B) shows there is a significant increase in the percentage of embryos showing an unaffected muscle birefringence phenotype in the groups treated with 5 and 10 μM Saracatinib compared with the DMSO only control group (One-way ANOVA:  $F=10.21$ ,  $df=3,16$ ,  $p=0.0005$ , followed by Dunnett's Multiple Comparison Test: ns= not significant,  $**p<0.01$ ,  $***p<0.001$ ). (C) shows the percentage rescue of the dystrophic phenotype, taking the proportion of dystrophic fish in DMSO only treated groups as 0% rescue. Data points represent mean values of 5 independent experiments, with a total of approximately 250 embryos per treatment group. Error bars represent SEM.

**Figure 5.11: Effect of 48 hour Saracatinib treatment on the severity of the *sapje* muscle phenotype**



Embryos were treated with Saracatinib or DMSO only for 48 hours before a birefringence assay was carried out. The number of larvae showing normal or disrupted muscle birefringence were counted. Those showing disrupted birefringence were further subdivided into mild (disrupted birefringence affecting 1-5 somitic muscle blocks), moderate (6-10) and severe (10+) phenotypes. (A) shows the proportion of larvae showing mild, moderate and severe muscle damage. (B) shows a significant decrease in the percentage of larvae showing a severe phenotype in the group treated with 10 $\mu\text{M}$  Saracatinib compared with DMSO alone (One-way ANOVA:  $F=3.893$ ,  $df=3,16$ ,  $p=0.0290$ , followed by Dunnett's Multiple Comparison Test: ns=not significant,  $*p<0.05$ ). Data points represent mean values of 5 independent experiments, with a total of approximately 250 embryos per treatment group. Error bars represent SEM.

### 5.3.4 Inhibiting ubiquitination and proteasomal degradation

It is thought that in the absence of dystrophin, there are increased levels of DGC protein degradation. One of the main degradation pathways in muscle is the ubiquitin-dependent proteasomal pathway. There are increased levels of proteasome expression in DMD patient muscle biopsies compared with control muscle and muscle biopsies from other neuromuscular diseases (Kumamoto et al., 2000). In addition, treatment

with proteasomal inhibitors has been shown to improve muscle pathophysiology in *mdx* mice and DMD muscle explants (Bonuccelli et al., 2003, Assereto et al., 2006, Bonuccelli et al., 2007, Gazzero et al., 2010).

Phosphorylation of  $\beta$ -dystroglycan has been identified as a signal for internalisation and possibly degradation (Sotgia et al., 2001, Sotgia et al., 2003, Miller et al., 2012). Evidence from our lab suggests phosphorylated  $\beta$ -dystroglycan, but not the non-phosphorylated protein, is ubiquitinated (Rob Piggott, unpublished results). Thus, it was hypothesised that phosphorylated  $\beta$ -dystroglycan is internalised, where it may be subject to ubiquitination and further downstream processes, such as degradation or translocation to the nucleus (Lara-Chacon et al., 2010).

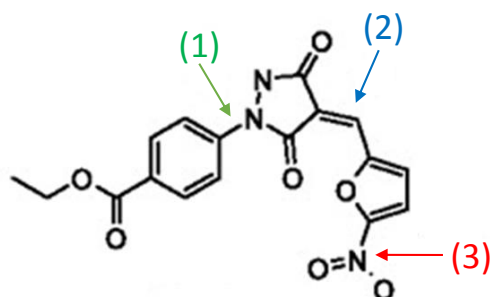
#### **5.3.4.1 PYR-41 is able to decrease the proportion of fish showing a dystrophic phenotype**

PYR-41 is an inhibitor of ubiquitin-activating enzyme (E1) (figure 5.12; Yang et al., 2007). Treatment of embryos from a heterozygous *sapje* cross, from 24 to 72hpf, was able to decrease the percentage of embryos with disrupted muscle birefringence (figure 5.13). When fish were treated with 0.5 or 1 $\mu$ M PYR-41, there was a significant increase in the percentage displaying a normal muscle birefringence pattern compared with control groups (figure 5.13B). An optimal concentration of 1 $\mu$ M PYR-41 was able to reduce the population of embryos with a dystrophic phenotype by approximately 45% (figure 5.13C). The effect of PYR-41 in preserving muscle integrity produced a bell-shaped dose-response curve; concentrations higher than 1 $\mu$ M were less effective at decreasing the proportion of embryos with a dystrophic phenotype (figure 5.13B & C).

When examining the severity of the muscle damage, there were significantly lower percentages of larvae displaying a severe phenotype in groups treated with PYR-41, compared with control groups (figure 5.14).

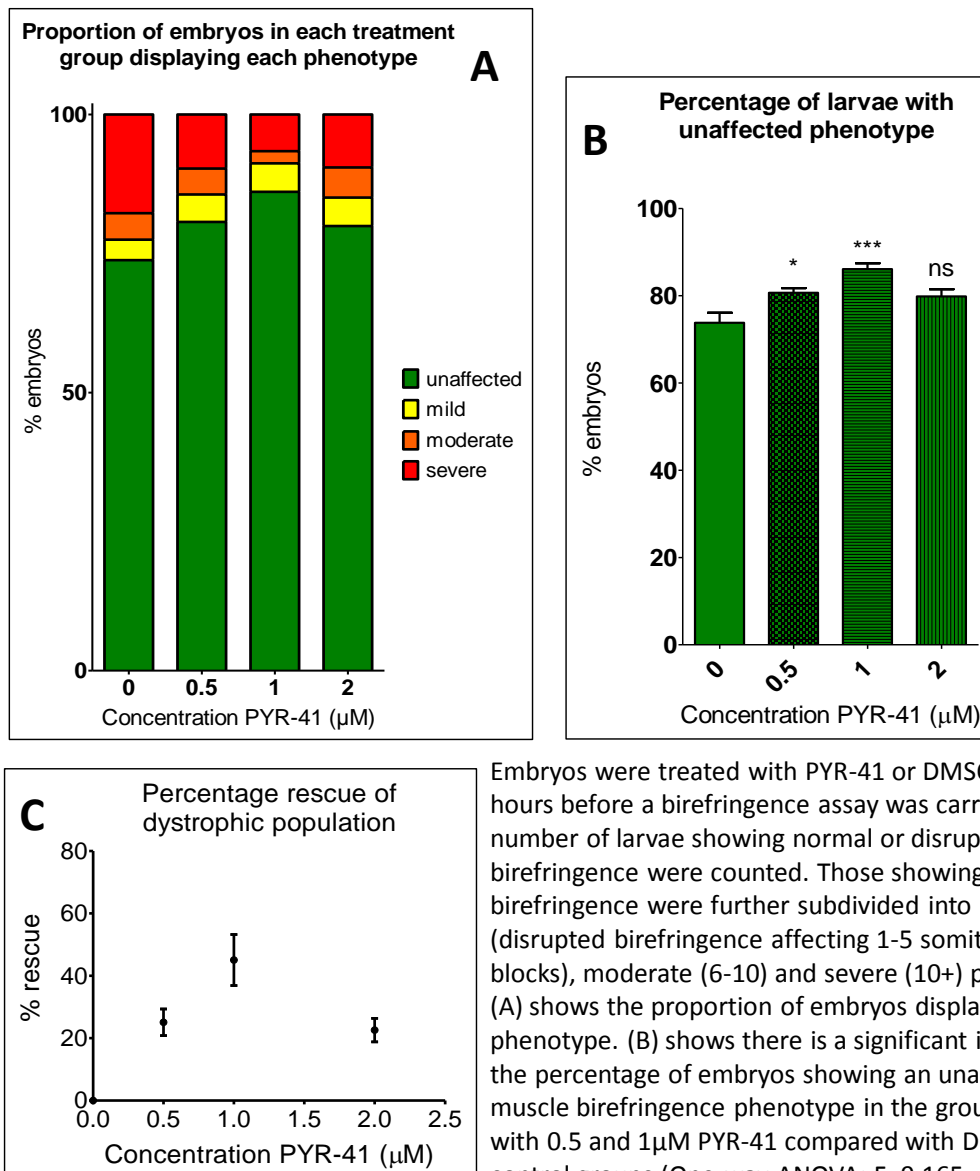
**Figure 5.12: Structure of PYR-41**

PYR-41



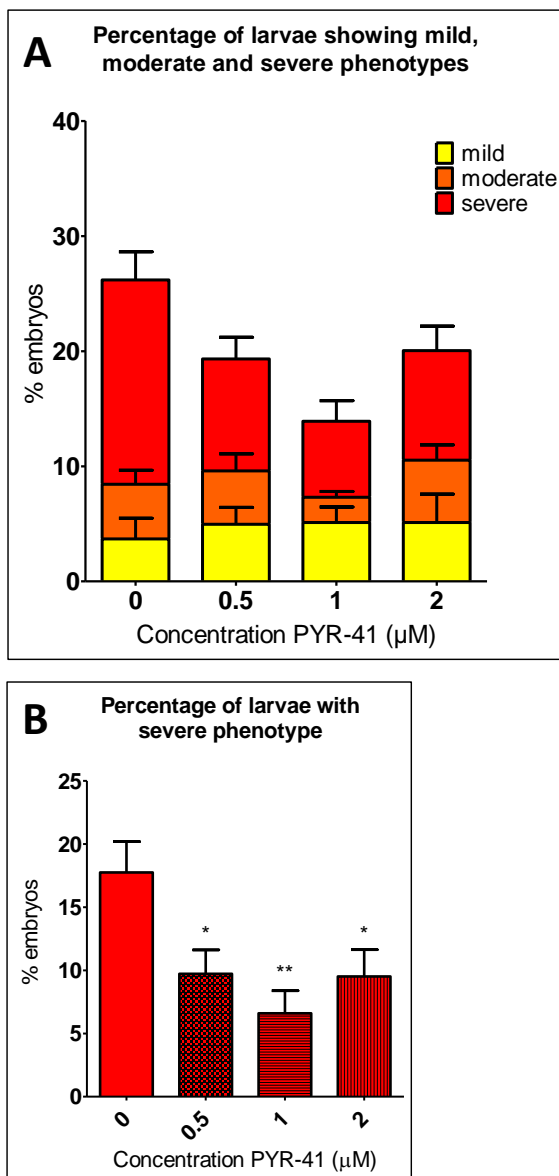
The chemical structure of PYR-41 is shown above. PYR-41 is a pyrazone derivative that identified from a high-throughput screen for inhibitors of ubiquitination (Yang et al. 2007). It is thought that this compound functions by covalently modifying the active site cysteine of ubiquitin-activating enzyme (E1) via either the N-aryl bond (1), or the exocyclic double bond (2). Related pyrazones were also evaluated for inhibitory activity against E1. Those compounds with the nitro substitute on the furan ring (3) inhibited E1, whereas those without did not, thus demonstrating the importance of this nitrogen for activity.

**Figure 5.13: Effect of 48 hour PYR-41 treatment on *sapje* muscle phenotype**



Embryos were treated with PYR-41 or DMSO only for 48 hours before a birefringence assay was carried out. The number of larvae showing normal or disrupted muscle birefringence were counted. Those showing disrupted birefringence were further subdivided into mild (disrupted birefringence affecting 1-5 somitic muscle blocks), moderate (6-10) and severe (10+) phenotypes. (A) shows the proportion of embryos displaying each phenotype. (B) shows there is a significant increase in the percentage of embryos showing an unaffected muscle birefringence phenotype in the groups treated with 0.5 and 1 μM PYR-41 compared with DMSO only control groups (One-way ANOVA:  $F=9.165$ ,  $df=3,16$ ,  $p=0.0009$ , followed by Dunnett's Multiple Comparison Test:  $*p<0.05$ ,  $***p<0.001$ ). (C) shows the percentage rescue of the dystrophic phenotype, taking the proportion of dystrophic fish in DMSO only treated groups as 0% rescue. Data points represent mean values of 5 independent experiments, with a total of approximately 300 embryos per treatment group. Error bars represent SEM.

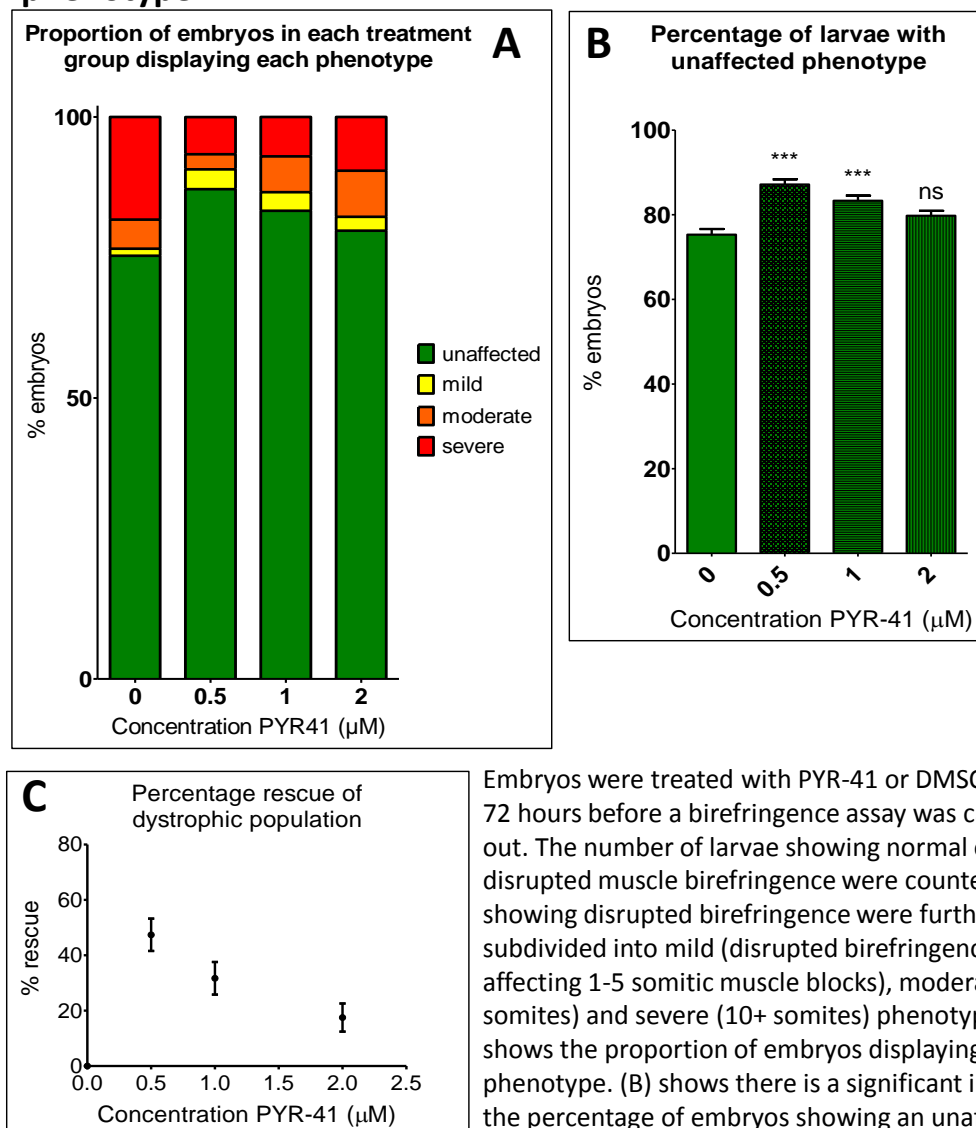
**Figure 5.14: Effect of 48 hour PYR-41 treatment on the severity of the *sapje* muscle phenotype**



Embryos were treated with PYR-41 or DMSO only for 48 hours before a birefringence assay was carried out. The number of larvae showing normal or disrupted muscle birefringence were counted. Those showing disrupted birefringence were further subdivided into mild (disrupted birefringence affecting 1-5 somitic muscle blocks), moderate (6-10) and severe (10+) phenotypes. (A) shows the proportion of larvae showing mild, moderate and severe muscle damage. (B) shows a significant decrease in the percentage of larvae showing a severe phenotype in the groups treated with PYR-41 compared with DMSO alone (One-way ANOVA:  $F=5.316$ ,  $df=3,16$ ,  $p=0.0098$ , followed by Dunnett's Multiple Comparison Test:  $*p<0.05$ ,  $**p<0.01$ ). Data points represent mean values of 5 independent experiments, with a total of approximately 300 embryos per treatment group. Error bars represent SEM.

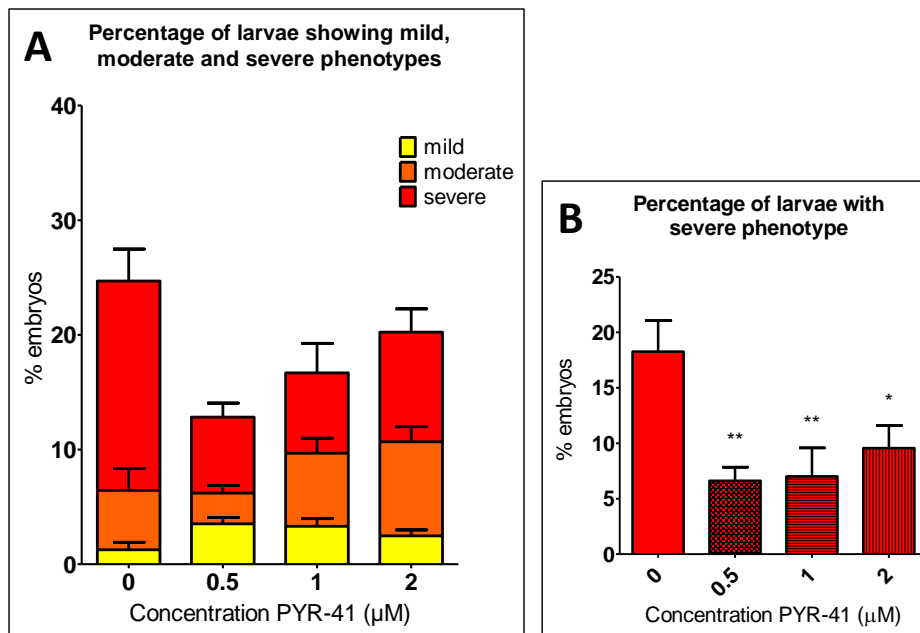
Similar results were obtained when fish were treated with PYR-41 from 24 to 96hpf (figure 5.15 & 16), with lower concentrations being most effective at reducing the percentage of larvae displaying a dystrophic phenotype. Here, a concentration of  $0.5\mu\text{M}$  PYR-41 showed the most significant increase in the proportion of larvae showing an unaffected muscle phenotype (figure 5.15B), and the largest decrease in larvae showing a severe dystrophic phenotype (figure 5.16).

**Figure 5.15: Effect of 72 hour PYR-41 treatment on *sapje* muscle phenotype**



Embryos were treated with PYR-41 or DMSO only for 72 hours before a birefringence assay was carried out. The number of larvae showing normal or disrupted muscle birefringence were counted. Those showing disrupted birefringence were further subdivided into mild (disrupted birefringence affecting 1-5 somitic muscle blocks), moderate (6-10 somites) and severe (10+ somites) phenotypes. (A) shows the proportion of embryos displaying each phenotype. (B) shows there is a significant increase in the percentage of embryos showing an unaffected muscle birefringence phenotype in the groups treated with PYR-41 compared with DMSO only control groups (One-way ANOVA:  $F=16.74$ ,  $df=3,16$ ,  $p<0.0001$ , followed by Dunnett's Multiple Comparison Test: ns = not significant, \*\*\* $p<0.001$ ). (C) shows the percentage rescue of the dystrophic phenotype, taking the proportion of dystrophic fish in DMSO only treated groups as 0% rescue. Data points represent mean values of 5 independent experiments, with a total of approximately 300 embryos per treatment group. Error bars represent SEM.

**Figure 5.16: Effect of 72 hour PYR-41 treatment on the severity of the *sapje* muscle phenotype**



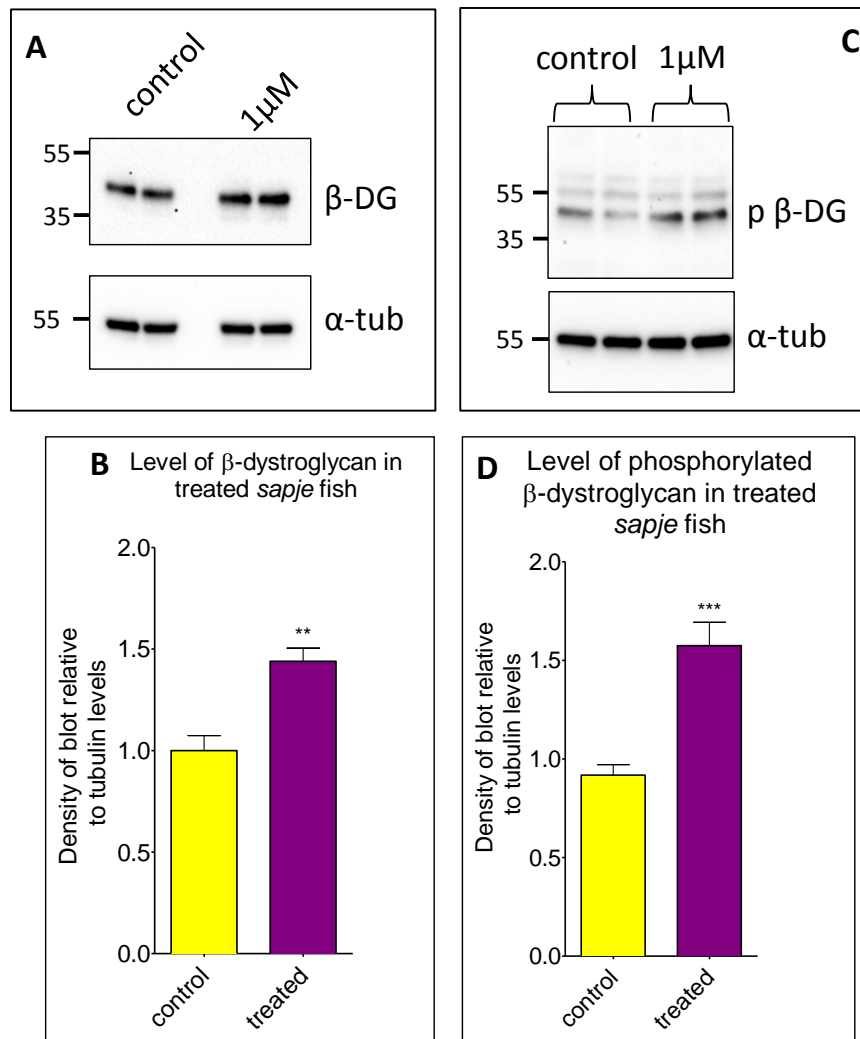
Embryos were treated with PYR-41 or DMSO only for 48 hours before a birefringence assay was carried out. The number of larvae showing normal or disrupted muscle birefringence were counted. Those showing disrupted birefringence were further subdivided into mild (disrupted birefringence affecting 1-5 somitic muscle blocks), moderate (6-10) and severe (10+) phenotypes. (A) shows the proportion of larvae showing mild, moderate and severe muscle damage. (B) shows a significant decrease in the percentage of larvae showing a severe phenotype in the groups treated with PYR-41 compared with DMSO alone (One-way ANOVA:  $F=5.875$ ,  $df=3,16$ ,  $p=0.0067$ , followed by Dunnett's Multiple Comparison Test:  $*p<0.05$ ,  $**p<0.01$ ). Data points represent mean values of 5 independent experiments, with a total of approximately 300 embryos per treatment group. Error bars represent SEM.

#### 5.3.4.2 PYR-41 is able to increase levels of dystroglycan in *sapje*

Western blotting was carried out to examine the levels of  $\beta$ -dystroglycan in treated and control fish, to investigate whether the effect of PYR-41 in maintaining muscle integrity in *sapje* fish is associated with an increase in dystroglycan protein levels.

Densitometric analysis of western blots indicated there were significantly higher levels of non-phosphorylated and phosphorylated  $\beta$ -dystroglycan in lysates from *sapje* larvae treated with PYR-41 compared with *sapje* larvae treated with DMSO only (figure 5.17).

**Figure 5.17: Effect of PYR41 treatment on levels of phosphorylated and non-phosphorylated  $\beta$ -dystroglycan**

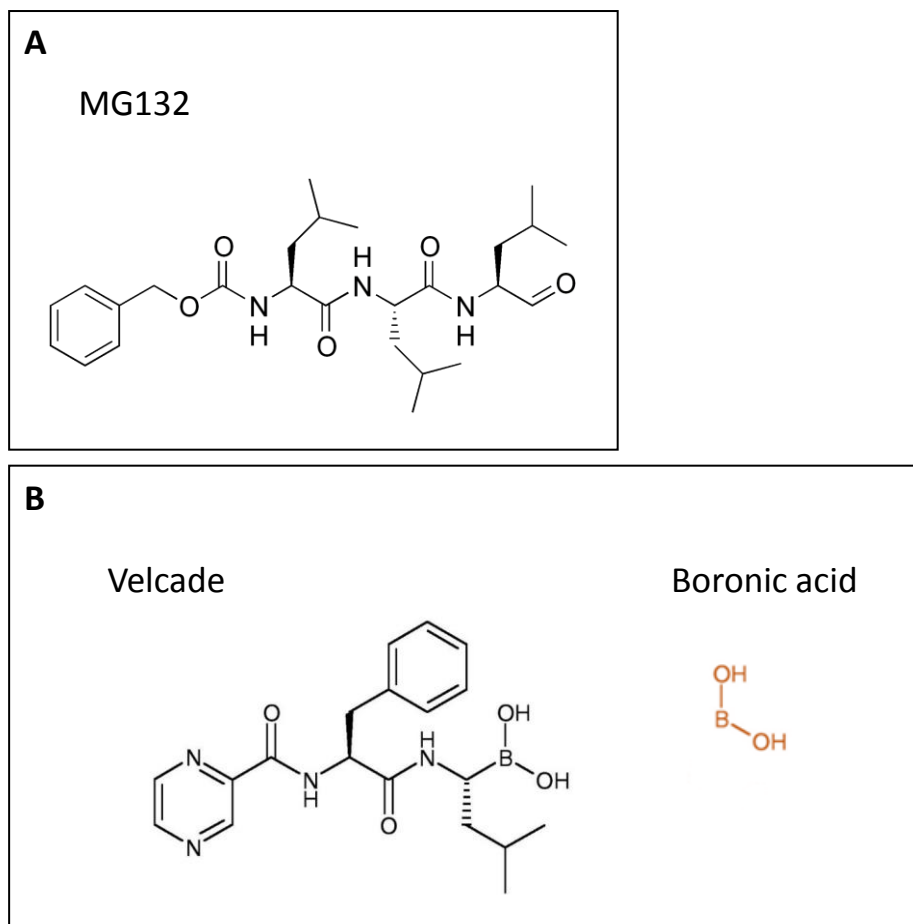


Lysates were made from embryos treated with 1 $\mu$ M PYR-41 or DMSO only. (A) shows western blots probed against antibodies for  $\beta$ -dystroglycan ( $\beta$ -DG) and  $\alpha$ -tubulin ( $\alpha$ -tub). (B) The density of the blot probed against  $\beta$ -DG was quantified relative to  $\alpha$ -tubulin levels in each sample, and normalised to average control signal. There was a significant increase in the level of  $\beta$ -dystroglycan in larvae treated with PYR-41, compared with controls (Unpaired t-test:  $t=4.479$ ,  $df=10$ ,  $p=0.0012$ ). (C) shows western blots probed against antibodies for phosphorylated  $\beta$ -dystroglycan (p $\beta$ -DG) and  $\alpha$ -tubulin ( $\alpha$ -tub). (D) The density of the blot probed against p  $\beta$ -DG was quantified relative to  $\alpha$ -tubulin levels in each sample, and normalised to average control signal. There was a significant increase in the levels of p $\beta$ -DG in larvae treated with PYR-41, compared with DMSO only treated controls (unpaired t-test:  $t=5.063$ ,  $df=12$ ,  $p=0.0003$ ). Graphs represent the mean of 6 samples from 3 independent experiments, error bars are SEM.

### 5.3.4.3 MG132 is able to reduce the percentage of *sapje* larvae with a dystrophic phenotype

MG132 (figure 5.18) is a proteasomal inhibitor, which was shown to increase levels of dystroglycan in zebrafish embryos (chapter 4).

**Figure 5.18: Chemical structure of 2 proteasomal inhibitors: MG132 and Velcade**

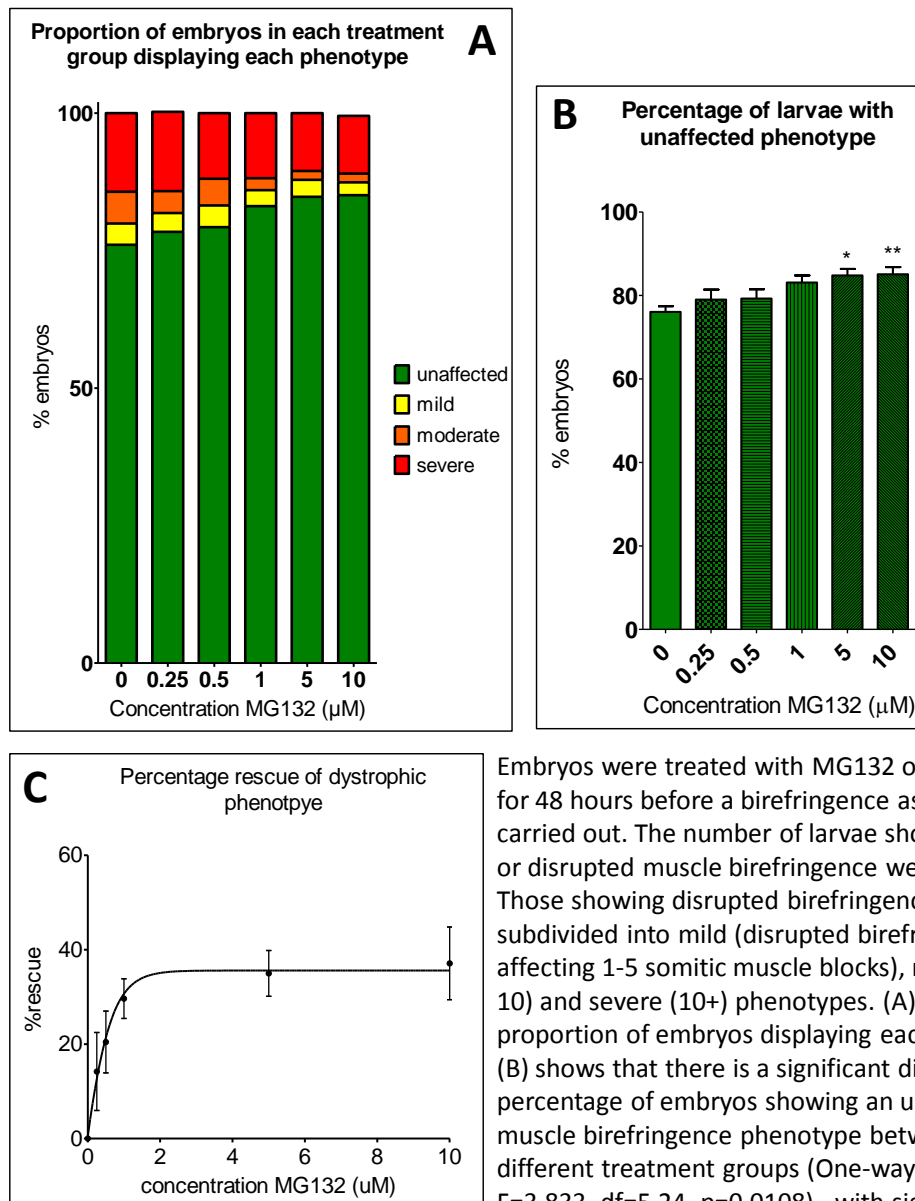


(A) Shows the chemical structure of MG132, one of the first proteasome inhibitors to be synthesised (Tsubuki et al., 1993). This compound inhibits the chymotrypsin-like activity of the proteasome. However, MG132 exhibits several properties that make it unsuitable as a drug molecule. These include lack of specificity and poor bioavailability (Adams et al., 1996). Replacing the aldehyde group of MG132 with boronic acid increased the potency of the compound 100-fold (Adams et al., 1998). This compound was modified further to create Velcade (shown in B). Compared with MG132, Velcade dissociates from the proteasome more slowly, conferring stable inhibition.

Treatment of embryos with MG132 from 24 to 72hpf was able to decrease the proportion of fish displaying a dystrophic phenotype (figure 5.19). There was a statistically significant increase in the percentage of embryos with an unaffected muscle phenotype in groups treated with 5 and 10 $\mu$ M MG132, compared to the DMSO only group (figure 5.19B).

The effect of MG132 in decreasing the ratio of affected fish was concentration dependent (figure 5.19C). The percentage rescue of the dystrophic population was calculated, taking the percentage of dystrophic fish in DMSO only control groups as 0% rescue. The effect of MG132 plateaus at a concentration of about 2 $\mu$ M, with a maximum of approximately 35% of the dystrophic population displaying normal muscle birefringence.

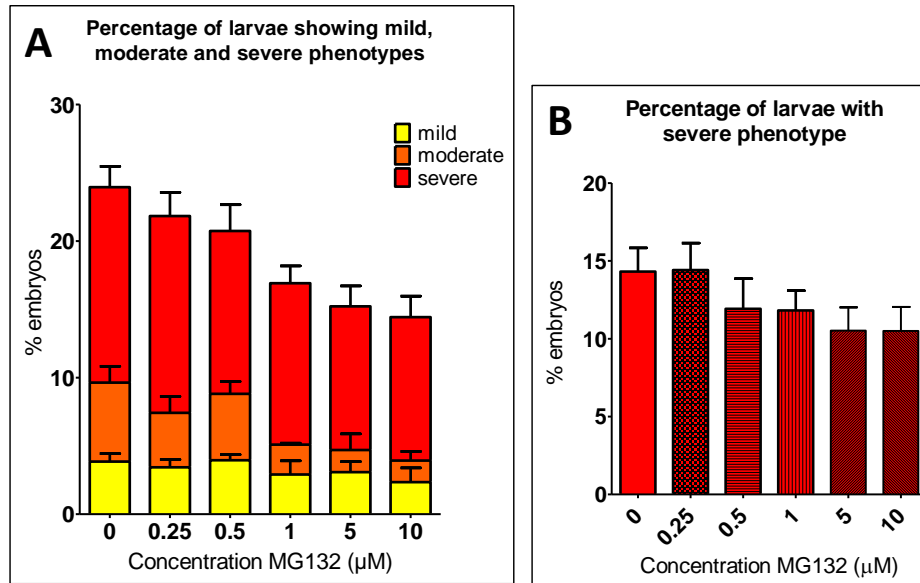
**Figure 5.19: Effect of 48 hour MG132 treatment on *sapje* muscle phenotype**



Embryos were treated with MG132 or DMSO only for 48 hours before a birefringence assay was carried out. The number of larvae showing normal or disrupted muscle birefringence were counted. Those showing disrupted birefringence were further subdivided into mild (disrupted birefringence affecting 1-5 somitic muscle blocks), moderate (6-10) and severe (10+) phenotypes. (A) shows the proportion of embryos displaying each phenotype. (B) shows that there is a significant difference in the percentage of embryos showing an unaffected muscle birefringence phenotype between the different treatment groups (One-way ANOVA:  $F=3.833$ ,  $df=5,24$ ,  $p=0.0108$ ), with significant increases between the DMSO only control group and those treated with 5 and 10  $\mu\text{M}$  MG132 (Dunnett's Multiple Comparison Test:  $*p<0.05$ ,  $**p<0.01$ ). (C) shows the percentage rescue of the dystrophic phenotype, taking the proportion of dystrophic fish in DMSO only treated groups as 0% rescue. Data points represent mean values of 5 independent experiments, with a total of approximately 250 embryos per treatment group. Error bars represent SEM.

When examining the severity of the muscle phenotypes in treated and non-treated groups, there was no significant difference between the percentages of embryos displaying a severe phenotype (figure 5.20).

**Figure 5.20: Effect of 48 hour MG132 treatment on the severity of the *sapje* muscle phenotype**



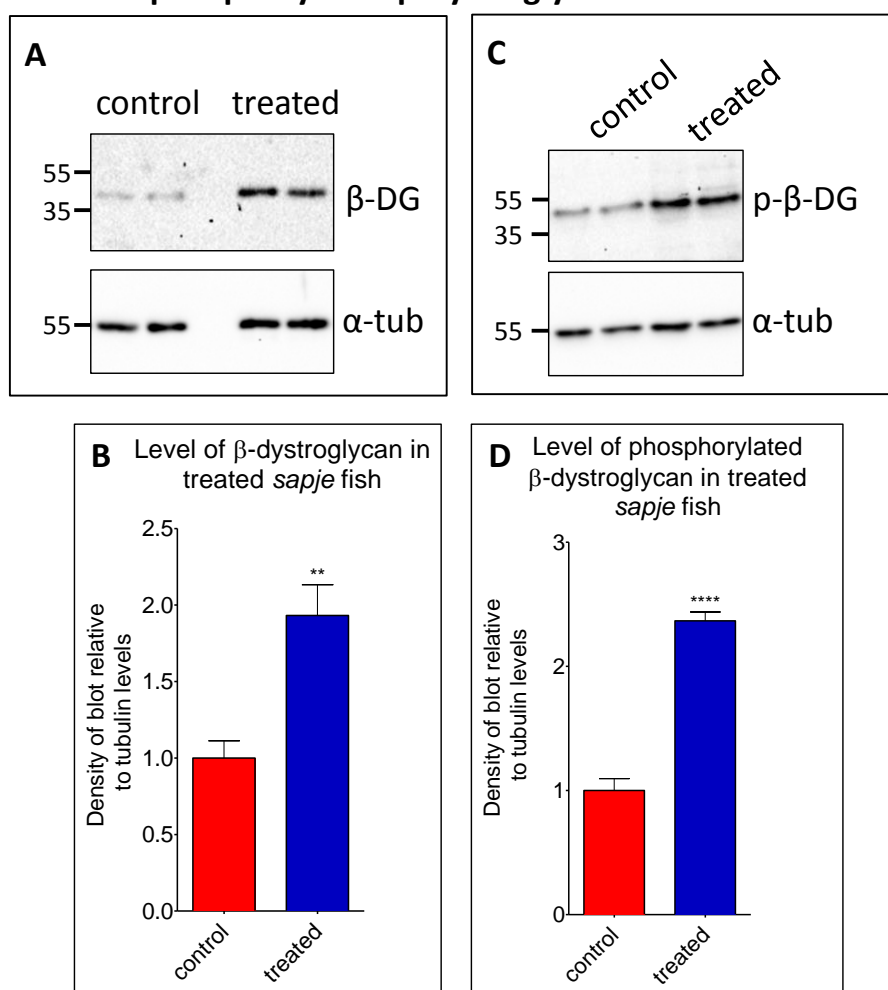
Embryos were treated with MG132 or DMSO only for 48 hours before a birefringence assay was carried out. The number of larvae showing normal or disrupted muscle birefringence were counted. Those showing disrupted birefringence were further subdivided into mild (disrupted birefringence affecting 1-5 somitic muscle blocks), moderate (6-10) and severe (10+) phenotypes. (A) shows the proportion of larvae showing mild, moderate and severe muscle damage. (B) shows there is no significant difference in the percentage of larvae showing a severe phenotype in the groups treated with MG132 compared with DMSO alone (One-way ANOVA followed by Dunnett's Multiple Comparison Test:  $F=1.197$ ,  $df=5,24$ ,  $p=0.3403$ ). Data points represent mean values of 5 independent experiments, with a total of approximately 250 embryos per treatment group. Error bars represent SEM.

#### 5.3.4.4 MG132 is able to increase levels of dystroglycan in *sapje*

If MG132 is able to delay the onset of the dystrophic phenotype and maintain muscle integrity, it may be acting by preventing the degradation of dystroglycan and other DGC proteins. Therefore, the levels of  $\beta$ -dystroglycan in treated and control fish were analysed using western blotting.

Densitometric analysis of western blotting data from treated and control treated fish indicated that there was significantly higher levels of  $\beta$ -dystroglycan in those exposed to MG132 (figure 5.21). In addition, the levels of phosphorylated  $\beta$ -dystroglycan were also higher.

**Figure 5.21: Effect of MG132 treatment on levels of phosphorylated and non-phosphorylated  $\beta$ -dystroglycan**

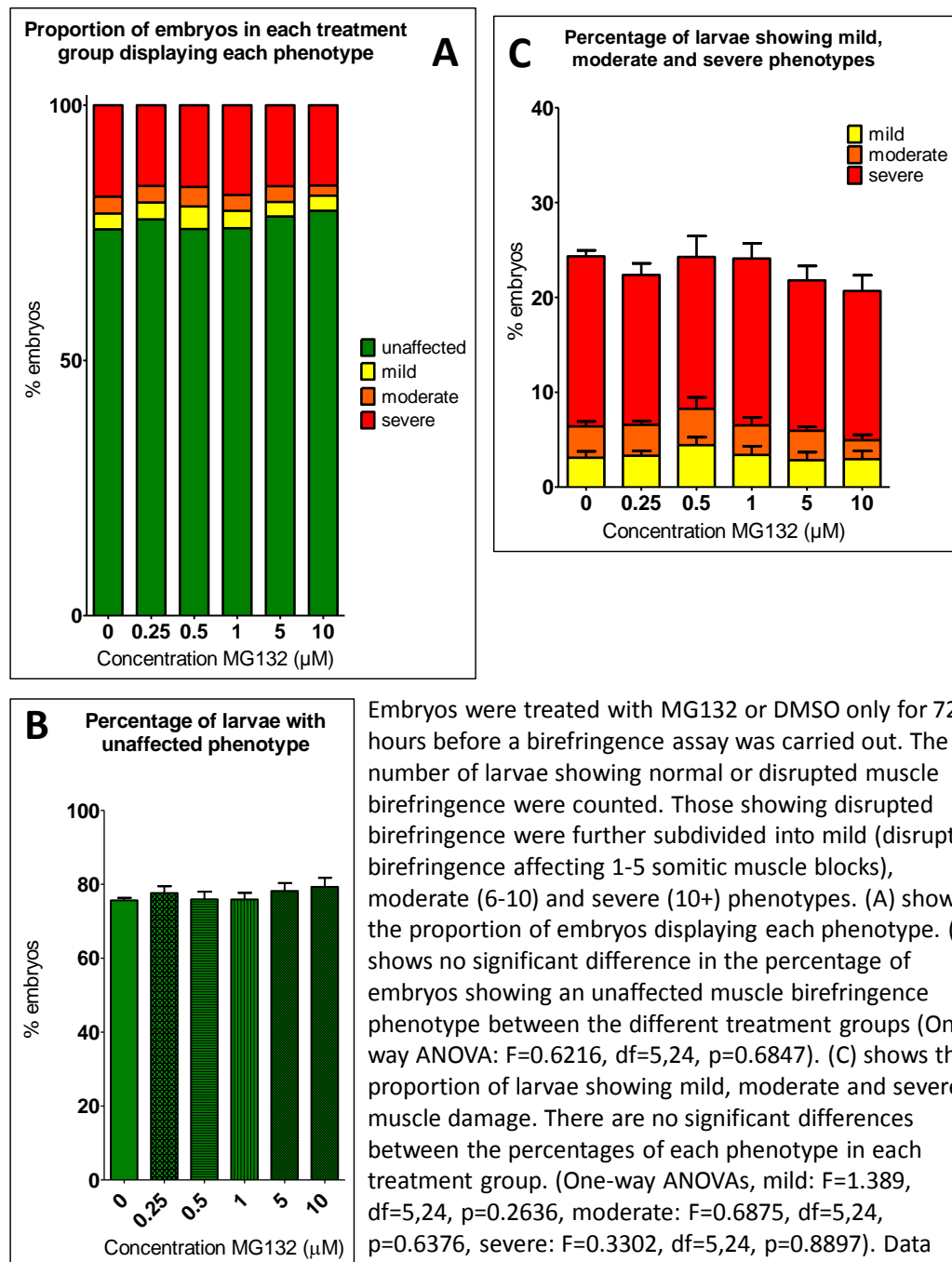


Lysates were made from embryos treated with 5 $\mu$ M MG132 or DMSO only. (A) shows western blots probed against antibodies for  $\beta$ -dystroglycan ( $\beta$ -DG) and  $\alpha$ -tubulin ( $\alpha$ -tub). (B) The density of the blot probed against  $\beta$ -DG was quantified relative to  $\alpha$ -tubulin levels in each sample, and normalised to average control signal. There is a significant increase in the level of  $\beta$ -dystroglycan in larvae treated with MG132, compared with controls (Unpaired t-test:  $t=4.048$ ,  $df=10$ ,  $p=0.0023$ ). (C) shows western blots probed against antibodies for phosphorylated  $\beta$ -dystroglycan (p  $\beta$ -DG) and  $\alpha$ -tubulin. (D) The density of the blot probed against p  $\beta$ -DG was quantified relative to  $\alpha$ -tubulin levels in each sample, and normalised to average control signal. There was a significant increase in the levels of  $\beta$ -DG in larvae between different treatment groups (Unpaired t-test:  $t=11.47$ ,  $df=10$ ,  $p<0.0001$ ). Graphs represent the mean of 6 samples from 3 independent experiments, error bars are SEM.

### 5.3.4.5 Longer treatment with MG132 is not beneficial to *sapje* fish

Longer treatment with MG132, from 24 to 96hpf, did not decrease the proportion of fish with affected muscle birefringence, or affect the severity of the muscle phenotype (figure 5.22).

**Figure 5.22: Effect of 72 hour MG132 treatment on *sapje* muscle phenotype**



Embryos were treated with MG132 or DMSO only for 72 hours before a birefringence assay was carried out. The number of larvae showing normal or disrupted muscle birefringence were counted. Those showing disrupted birefringence were further subdivided into mild (disrupted birefringence affecting 1-5 somitic muscle blocks), moderate (6-10) and severe (10+) phenotypes. (A) shows the proportion of embryos displaying each phenotype. (B) shows no significant difference in the percentage of embryos showing an unaffected muscle birefringence phenotype between the different treatment groups (One-way ANOVA:  $F=0.6216$ ,  $df=5,24$ ,  $p=0.6847$ ). (C) shows the proportion of larvae showing mild, moderate and severe muscle damage. There are no significant differences between the percentages of each phenotype in each treatment group. (One-way ANOVAs, mild:  $F=1.389$ ,  $df=5,24$ ,  $p=0.2636$ , moderate:  $F=0.6875$ ,  $df=5,24$ ,  $p=0.6376$ , severe:  $F=0.3302$ ,  $df=5,24$ ,  $p=0.8897$ ). Data points represent mean values of 5 independent experiments, with a total of approximately 250 embryos per treatment group. Error bars represent SEM.

#### **5.3.4.6 Velcade is able to decrease the proportion of larvae with a dystrophic phenotype**

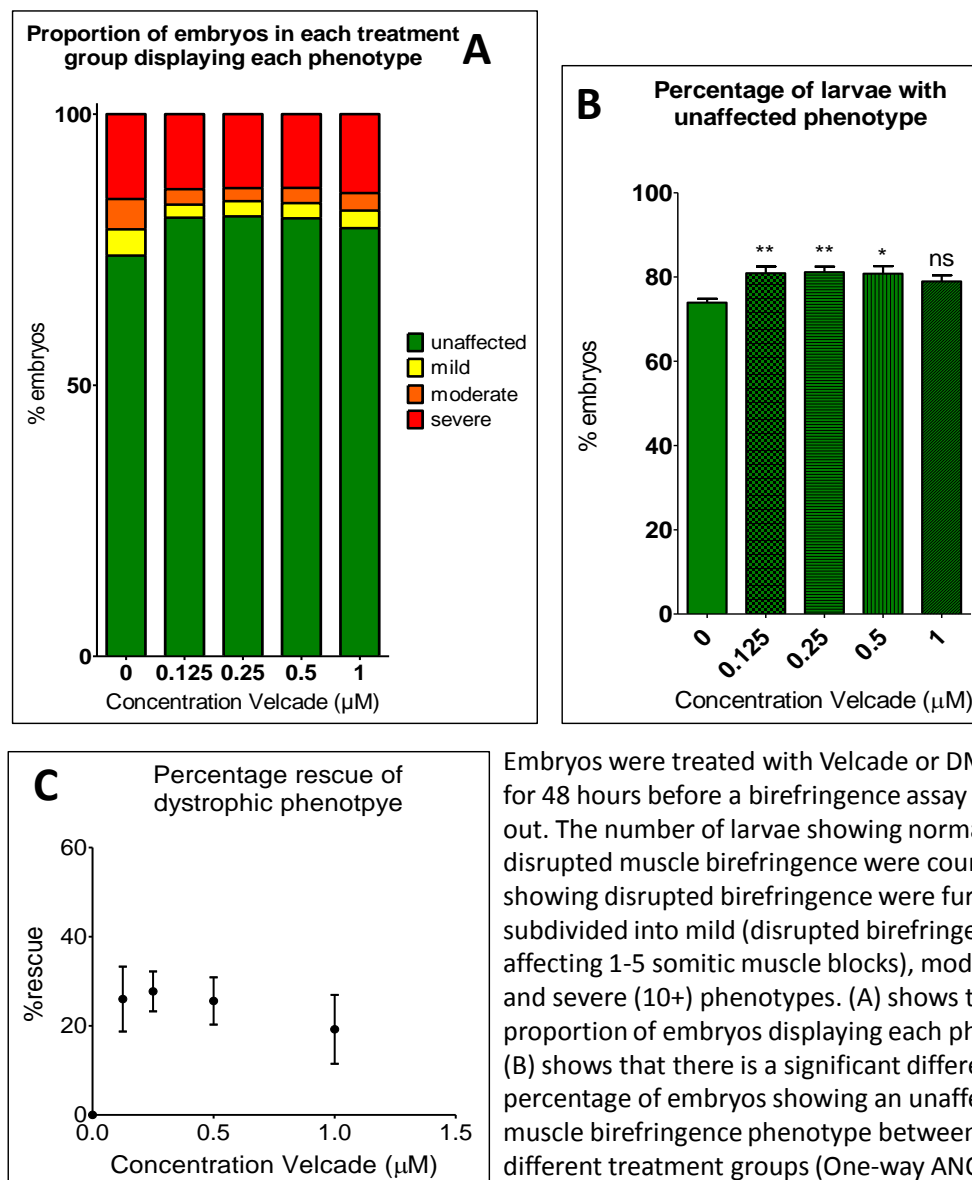
Velcade (figure 5.18) is a potent inhibitor of the proteasome, approved by the FDA for the treatment of multiple myeloma (Adams, 2004).

Treatment of embryos with Velcade was able to decrease the percentage of fish displaying aberrant muscle birefringence (figure 5.23). There was a statistically significant increase in the percentage of embryos with unaffected muscle birefringence in groups treated with 0.125, 0.25 and 0.5 $\mu$ M Velcade, compared to the DMSO only group (figure 5.23B). However, this was not significant at a concentration of 1 $\mu$ M.

At the concentrations used, there was not a concentration-dependent effect of Velcade on decreasing the percentage of dystrophic fish (figure 5.23C). However, this may have been observed if lower concentrations were used as the dose-response effect of Velcade may have plateaued.

As Velcade is a more potent proteasomal inhibitor than MG132, it was expected to elicit a greater effect in preserving muscle integrity. However, Velcade decreased the percentage of dystrophic fish to a lesser extent than MG132, with an optimal rescue of approximately 28% of the dystrophic population (figure 5.23C).

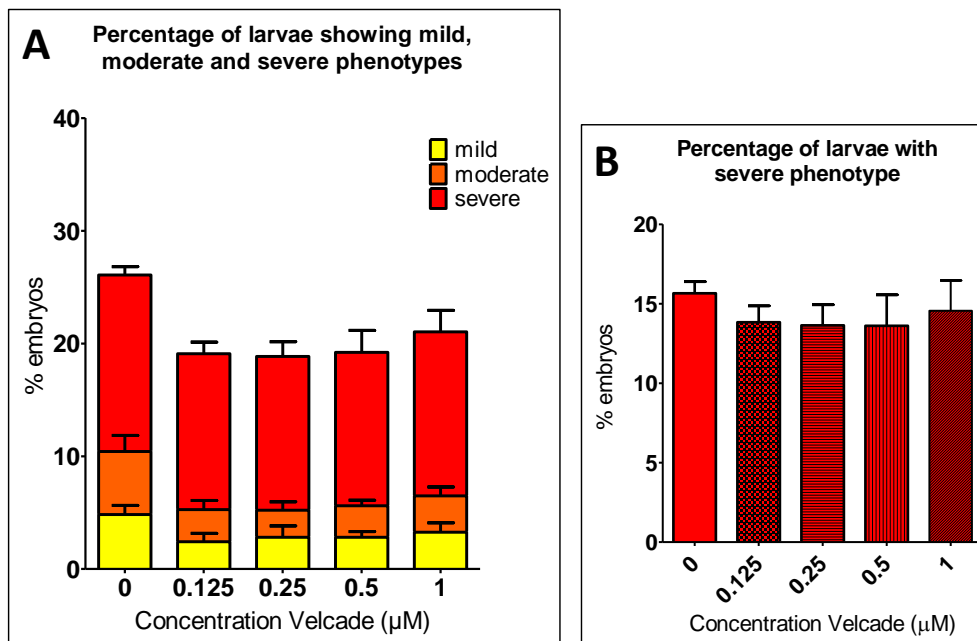
**Figure 5.23: Effect of 48 hour Velcade treatment on *sapje* muscle phenotype**



Embryos were treated with Velcade or DMSO only for 48 hours before a birefringence assay was carried out. The number of larvae showing normal or disrupted muscle birefringence were counted. Those showing disrupted birefringence were further subdivided into mild (disrupted birefringence affecting 1-5 somitic muscle blocks), moderate (6-10) and severe (10+) phenotypes. (A) shows the proportion of embryos displaying each phenotype. (B) shows that there is a significant difference in the percentage of embryos showing an unaffected muscle birefringence phenotype between the different treatment groups (One-way ANOVA:  $F=4.487$ ,  $df=4,20$ ,  $p=0.0095$ , followed by Dunnett's Multiple Comparison Test: ns= not significant,  $*p<0.05$ ,  $**p<0.005$ ). (C) shows the percentage rescue of the dystrophic phenotype, taking the proportion of dystrophic fish in DMSO only treated groups as 0% rescue. Data points represent mean values of 5 independent experiments, with a total of approximately 250 embryos per treatment group. Error bars represent SEM.

As with MG132, upon examining the severity of the muscle phenotypes in treated and control treated groups, there was no significant difference between the percentages of embryos displaying a severe phenotype (figure 5.24).

**Figure 5.24: Effect of 48 hour Velcade treatment on the severity of the *sapje* muscle phenotype**



Embryos were treated with Velcade or DMSO only for 48 hours before a birefringence assay was carried out. The number of larvae showing normal or disrupted muscle birefringence were counted. Those showing disrupted birefringence were further subdivided into mild (disrupted birefringence affecting 1-5 somitic muscle blocks), moderate (6-10 somites) and severe (10+ somites) phenotypes. (A) shows the proportion of larvae showing mild, moderate and severe muscle damage. (B) shows there is no significant difference in the percentage of larvae showing a severe phenotype in the groups treated with Velcade compared with DMSO alone (One-way ANOVA followed by Dunnett's Multiple Comparison Test:  $F=0.3547$ ,  $df=4,20$ ,  $p=0.8377$ ). Data points represent mean values of 5 independent experiments, with a total of approximately 250 embryos per treatment group. Error bars represent SEM.

### 5.3.5 Compound treatment of *dag1* embryos does not prevent development of the dystrophic phenotype

Although biochemical data suggest otherwise, it is possible that the drugs are improving muscle integrity in *sapje* fish through another mechanism, rather than by preventing  $\beta$ -dystroglycan phosphorylation and degradation. The ability of these inhibitors to delay or prevent the onset of the dystrophic phenotype in *dag1* fish was therefore investigated.

The pathophysiological mechanism leading to the dystrophic phenotype seen in *sapje* and *dag1* involves the loss of connection between the actin cytoskeleton and extracellular matrix, with both mutations causing defects in the DGC complex.

Therefore if these compounds are improving muscle integrity in *sapje* by a mechanism that is independent of dystroglycan and the DGC, treatment may also be beneficial to *dag1* fish.

Treatment of embryos from heterozygous *dag1* fish with Dasatinib, PYR-41 and MG132 was unable to decrease the proportion of embryos with a dystrophic phenotype, or alter the ratios of larvae displaying mild, moderate or severe phenotypes (figures 5.25, 5.26 and 5.27). This suggests that the effect of these drugs on the dystrophic phenotype may be dependent on dystroglycan expression.

**Figure 5.25: Effect of 48 hour Dasatinib treatment on *dag1* muscle phenotype**

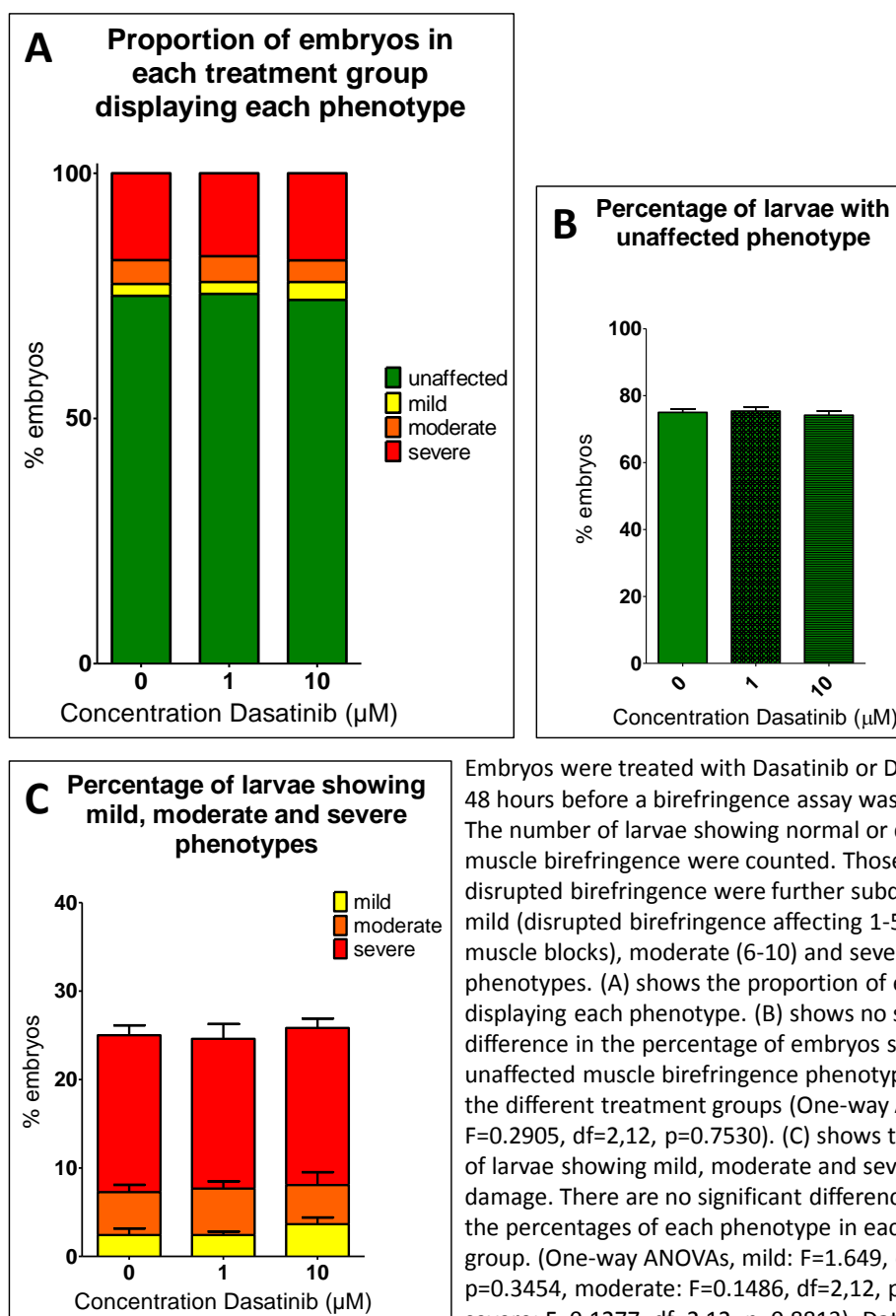


**Figure 5.26: Effect of 48 hour PYR-41 treatment on *dag1* muscle phenotype**

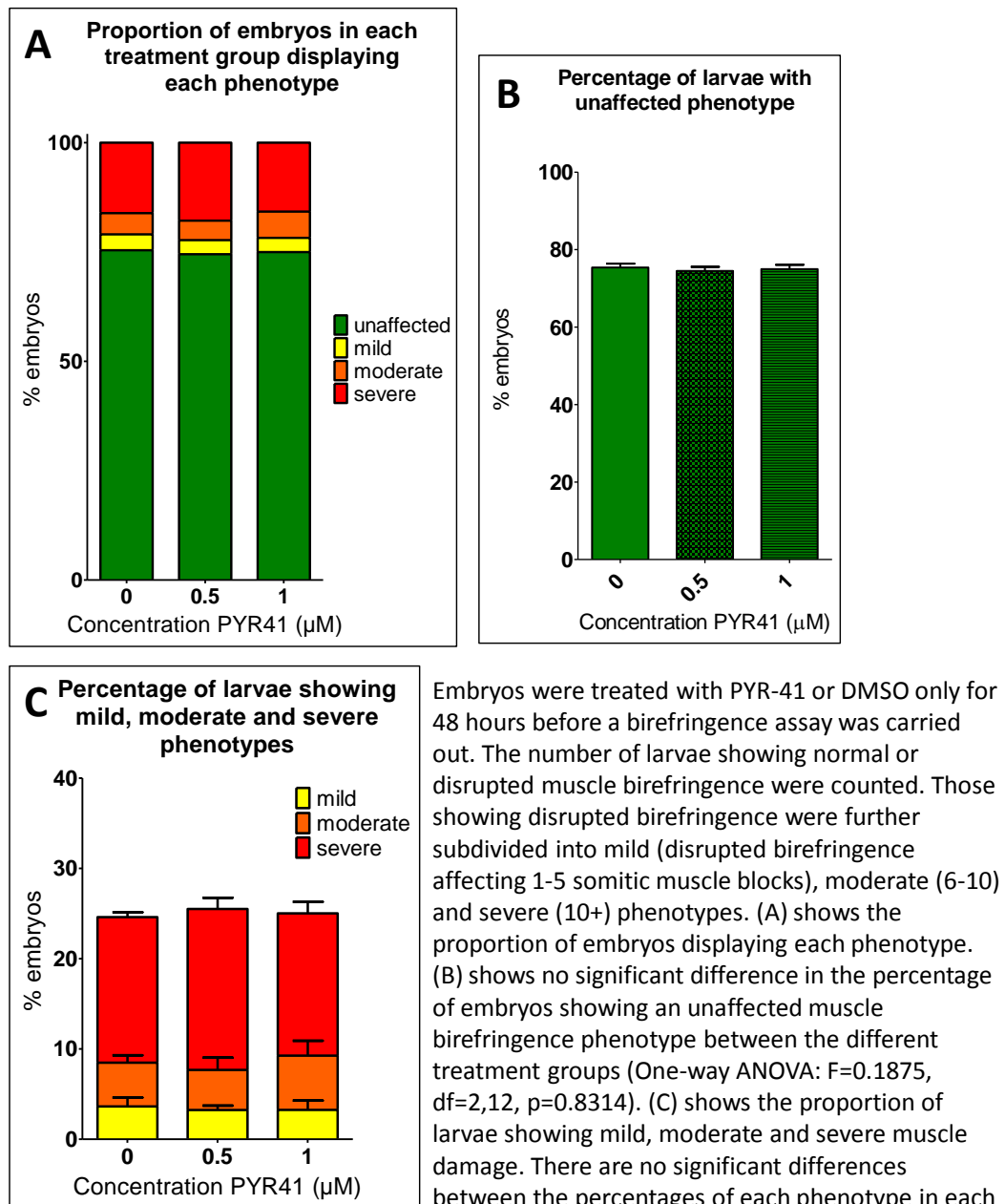
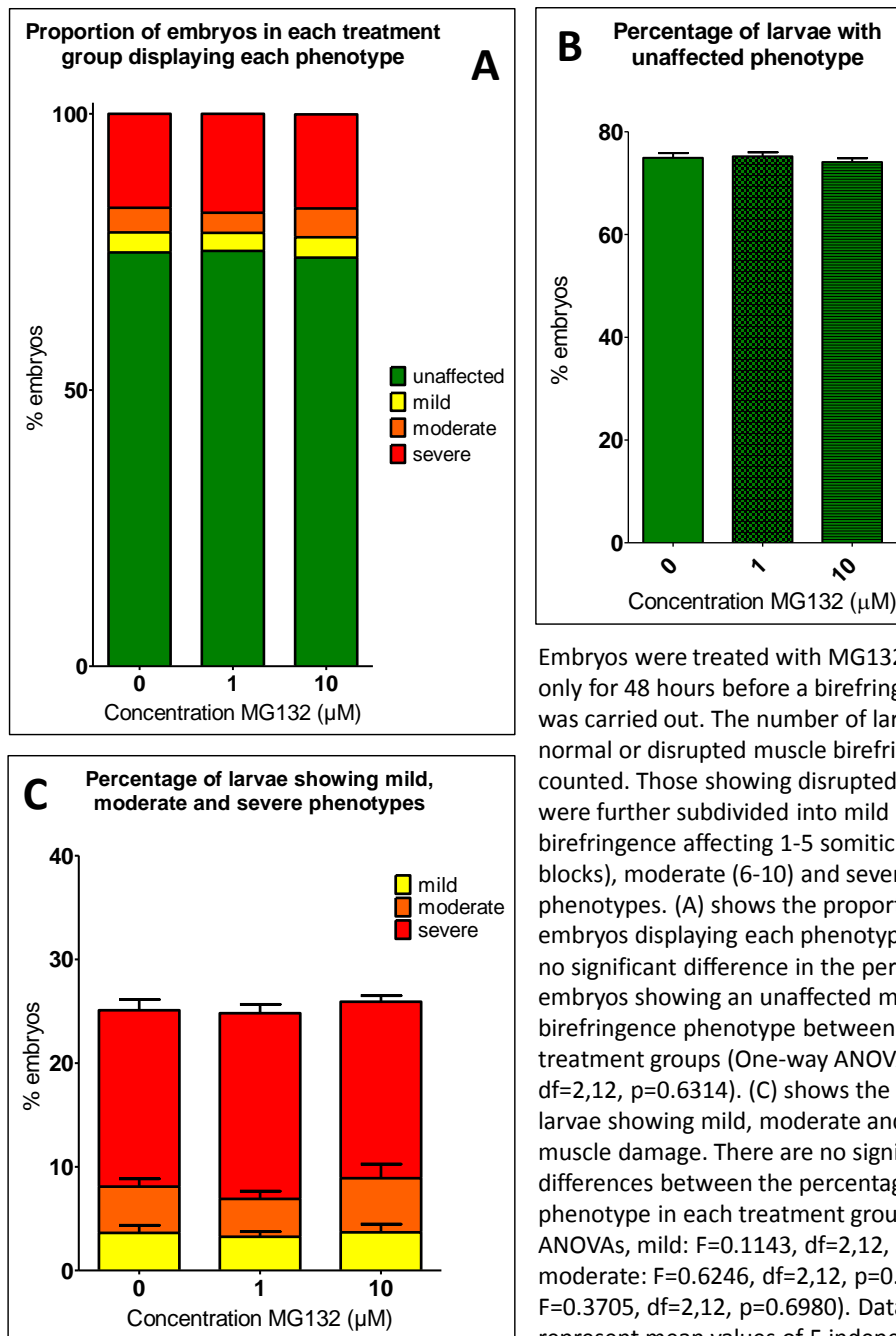


**Figure 5.27: Effect of 48 hour MG132 treatment on *dag1* muscle phenotype**



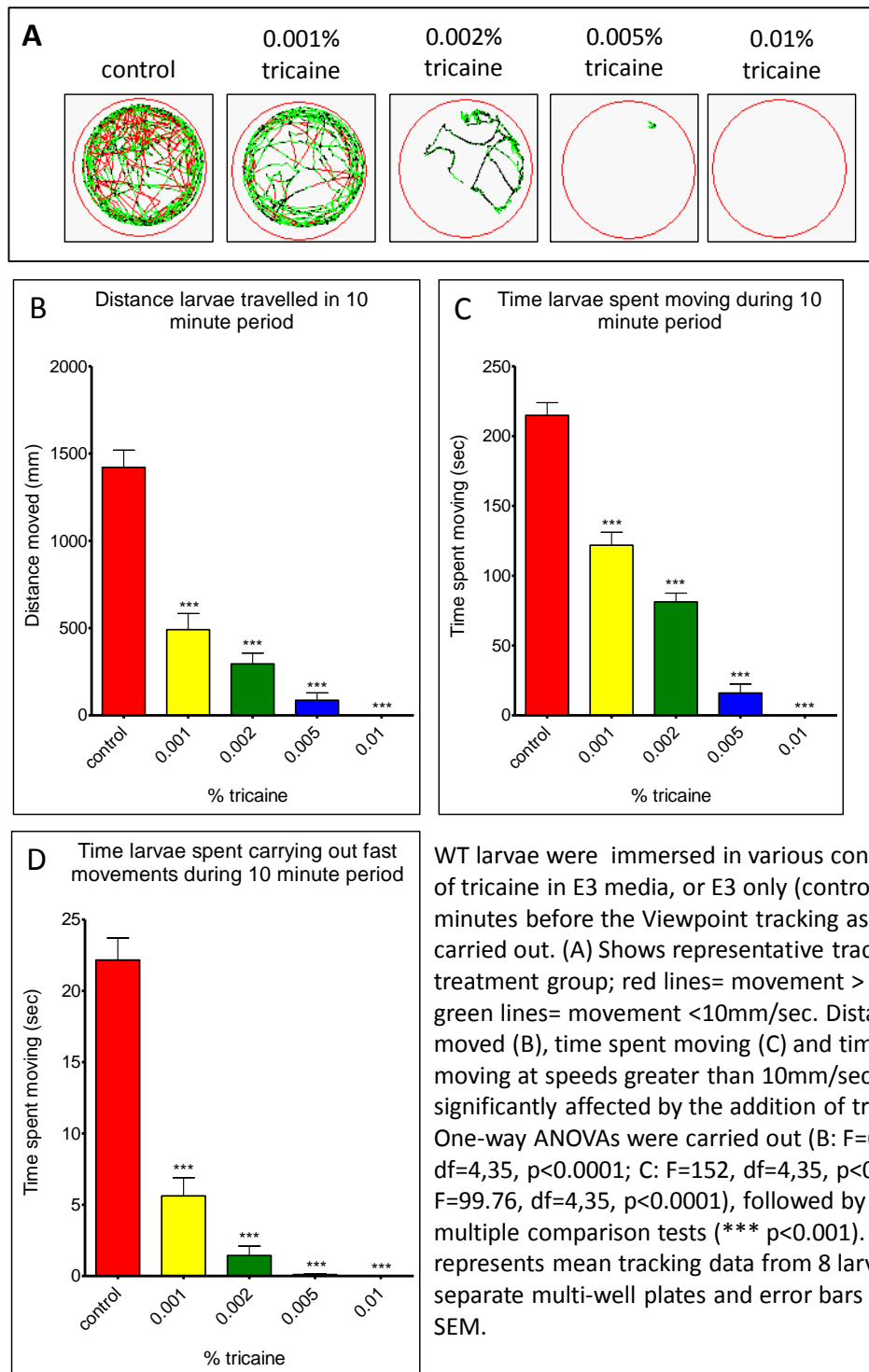
Embryos were treated with MG132 or DMSO only for 48 hours before a birefringence assay was carried out. The number of larvae showing normal or disrupted muscle birefringence were counted. Those showing disrupted birefringence were further subdivided into mild (disrupted birefringence affecting 1-5 somitic muscle blocks), moderate (6-10) and severe (10+) phenotypes. (A) shows the proportion of embryos displaying each phenotype. (B) shows no significant difference in the percentage of embryos showing an unaffected muscle birefringence phenotype between the different treatment groups (One-way ANOVA:  $F=0.4779$ ,  $df=2,12$ ,  $p=0.6314$ ). (C) shows the proportion of larvae showing mild, moderate and severe muscle damage. There are no significant differences between the percentages of each phenotype in each treatment group. (One-way ANOVAs, mild:  $F=0.1143$ ,  $df=2,12$ ,  $p=0.8929$ , moderate:  $F=0.6246$ ,  $df=2,12$ ,  $p=0.5520$ , severe:  $F=0.3705$ ,  $df=2,12$ ,  $p=0.6980$ ). Data points represent mean values of 5 independent experiments, with a total of approximately 250 embryos per treatment group. Error bars represent SEM.

### 5.3.6 Chemical treatment does not affect larval motility

As shown in chapter 4, it is possible to decrease the severity of the dystrophic phenotype by anaesthetising larvae. Tricaine (MS222) has also been shown to suppress

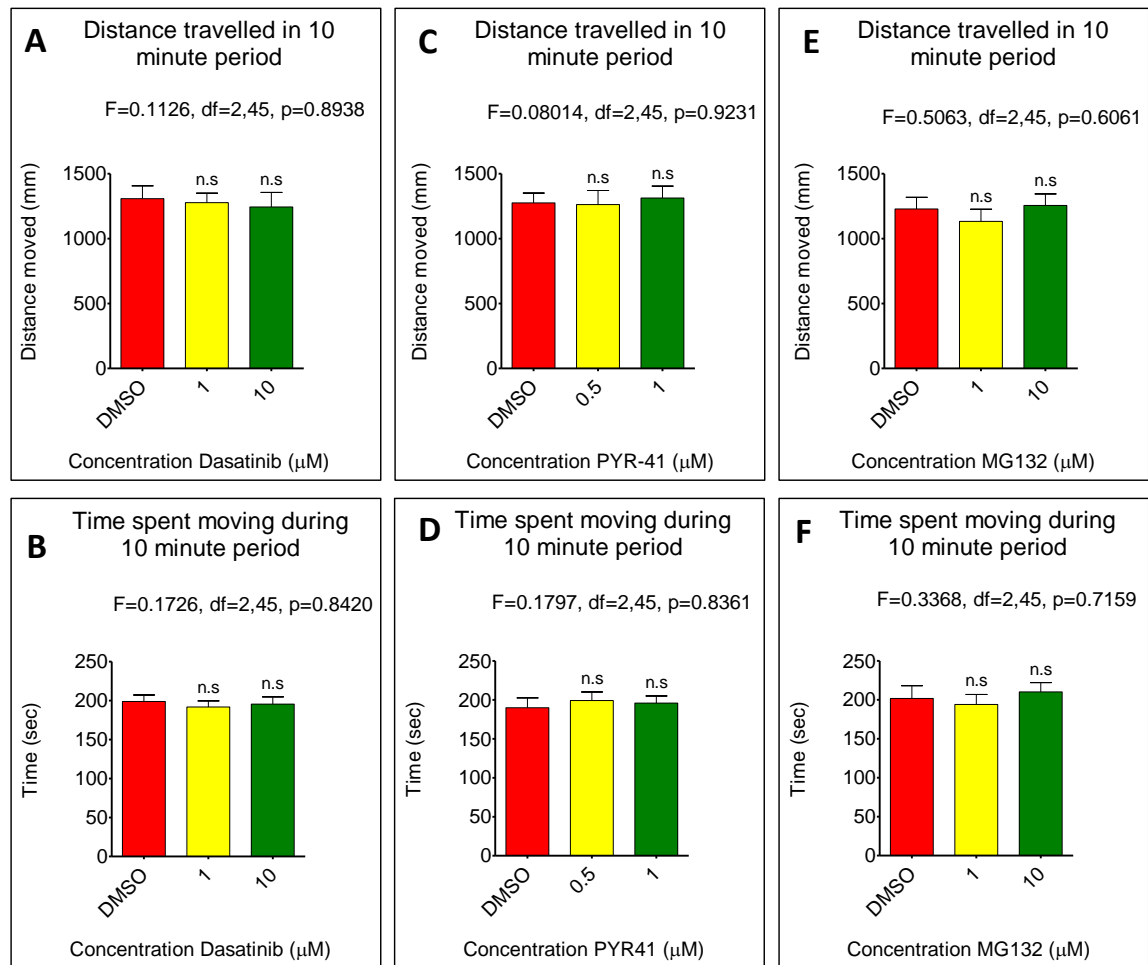
the phenotype of the *laminin  $\alpha$ 2* mutant *candyfloss* (Hall et al., 2007). To exclude the possibility that the drugs are acting to delay or prevent the onset of the dystrophic phenotype by paralysing the fish, or by decreasing the amount of movement, the motility of treated and control treated wildtype larvae was examined.

Treated larvae did not appear to show any visible motility defects, and exhibited a touch evoked escape response. However, to quantify the amount of movement carried out by treated and control treated fish more accurately, a Viewpoint tracking assay was performed. As a positive control for larval sedation, MS222 treated fish were also tested. At all concentrations of MS222 used, larvae travelled shorter distances, spent less time moving, and less time moving at fast speeds (figure 5.28). At low concentrations of MS222, larvae were still able to swim, but showed significantly lower levels of motility in the parameters analysed. This suggested that this tracking assay could be used to evaluate the effects of drugs on locomotor activity, and results from MS222 treated fish could be used as comparisons against compounds thought to have sedative effects.

**Figure 5.28: Effect of tricaine on WT zebrafish larvae motility**

Wildtype larvae were continually treated with Dasatinib, PYR-41, MG132, or DMSO only from 1 to 5dpf. Figure 5.29 indicates that these drugs had no effect on the total distance larvae travelled, or the time spent moving during the ten minute tracking period.

**Figure 5.29 Effect of drug treatment on motility of WT larvae**



LWT larvae were treated with indicated concentrations of drug, or DMSO only, from 1 to 5dpf. One-way ANOVA analysis of Viewpoint tracking data indicated no significant differences between drug treated and control groups for the distance moved (A,C & E), or time spent moving (B,D & F) in the ten minute tracking period. Bars represent mean tracking data of 16 larvae from 2 separate 24-well plates; SEM represents SEM.

### 5.3.7 Treatment of larvae after the onset of muscle damage

When patients are diagnosed with DMD, significant muscle damage has usually already occurred. Therefore, when evaluating the potential value of new therapeutic

interventions, it is crucial to elucidate whether the disease progression can be stopped, or slowed down, after the onset of muscle damage.

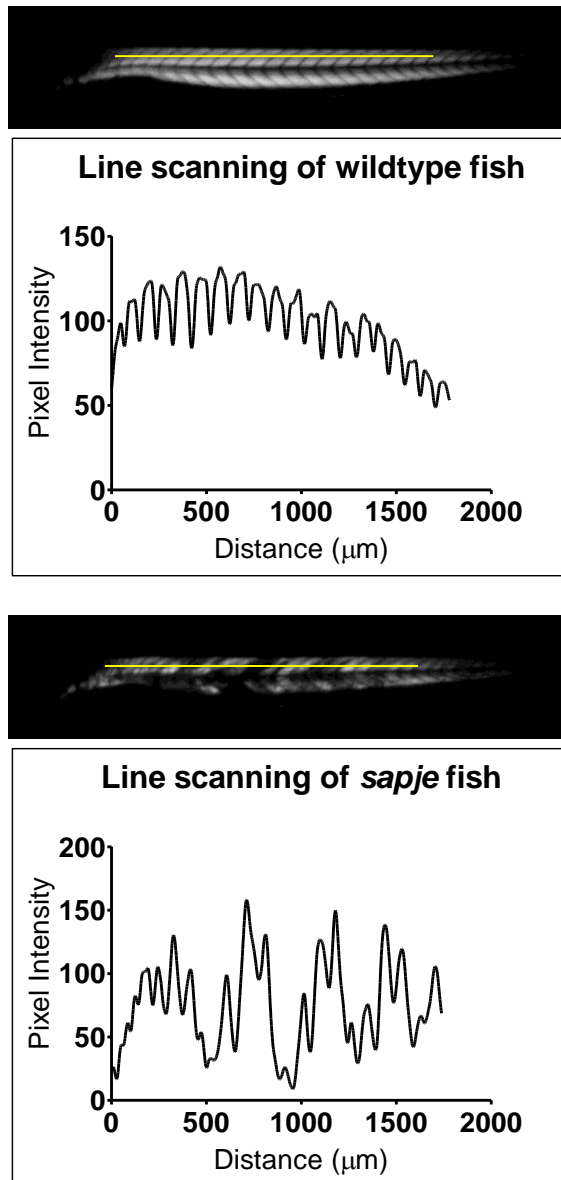
Muscle damage in *sapje* fish is progressive, with the phenotype worsening from 3 to 5dpf (chapter 4). The ability of drug treatment to alter the decline in muscle birefringence over time was examined.

Simple quantification of birefringence image intensity, as carried out in chapter 4, was found not to be a reliable method for quantifying muscle damage across different experiments. This was because the intensity of the image is sensitive to small changes in the orientation of the polarising lenses and the larva. When images are taken at the same time, these factors influencing the brightness of the birefringence can be easily controlled. However, this system is not robust enough to measure small changes in the level of muscle damage accurately over different experiments. An alternative method for quantifying muscle damage was therefore needed.

#### **5.3.7.1 A novel method of quantifying muscle damage**

Plotting a graph of birefringence image intensity along the length of a wildtype fish gives a regular and even pattern of peaks and troughs, representing bright somites and darker somite boundaries (figure 5.30). In contrast, *sapje* fish show a very irregular pattern of peaks and troughs due to the disruption of the birefringence pattern.

**Figure 5.30: Intensity profile plots of wildtype and *sapje* birefringence images at 3dpf**



(A) and (C) show birefringence images of wildtype and *sapje* larvae. Yellow lines shows the position used to generate the intensity profiles shown in (B) and (D) for wildtype and *sapje* fish respectively.

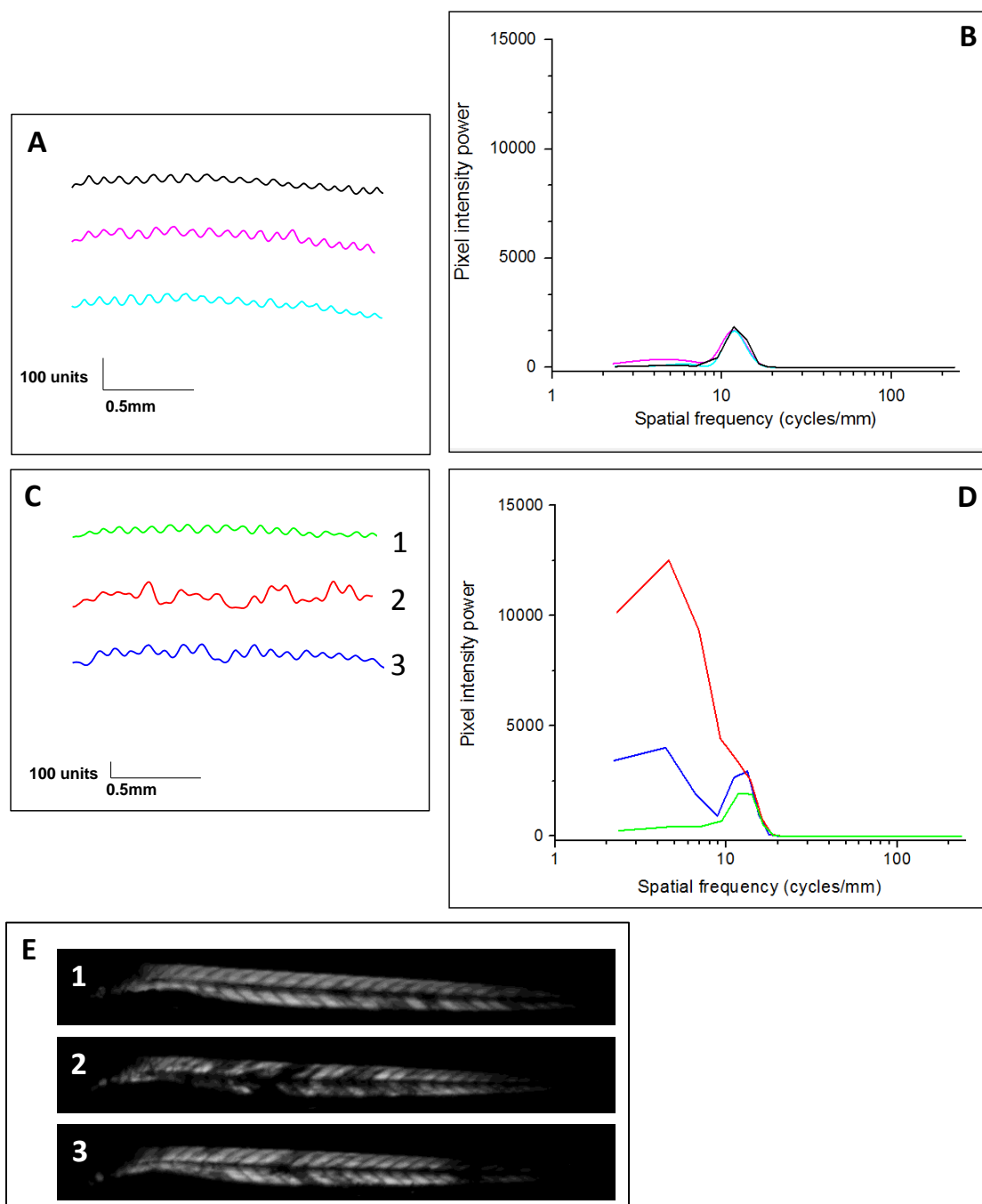
Carrying out Fourier transforms of the line scan data breaks down the graph into its individual frequencies. Wildtype fish show a single frequency of about 10 cycles per mm, corresponding to the number of peaks and troughs per mm. *sapje* fish show an underlying frequency of about 10 cycles per mm, but show a more disordered

frequency distribution due to the disruption in the periodicity of the line scan caused by loss of birefringence (figure 5.31). At a spatial frequency of 5 cycles/mm, the pixel intensity power of *sapje* is significantly higher than that of the wildtype at both 3 and 5dpf (figure 5.32).

Analysis of fish with greater levels of muscle birefringence disruption gives a higher value for pixel intensity power at 5 cycles per mm (red graph in figure 5.31 C & D). As the dystrophic phenotype worsens over time, the birefringence pattern becomes more disrupted, resulting in a quantitative difference using Fourier analysis (figure 5.32).

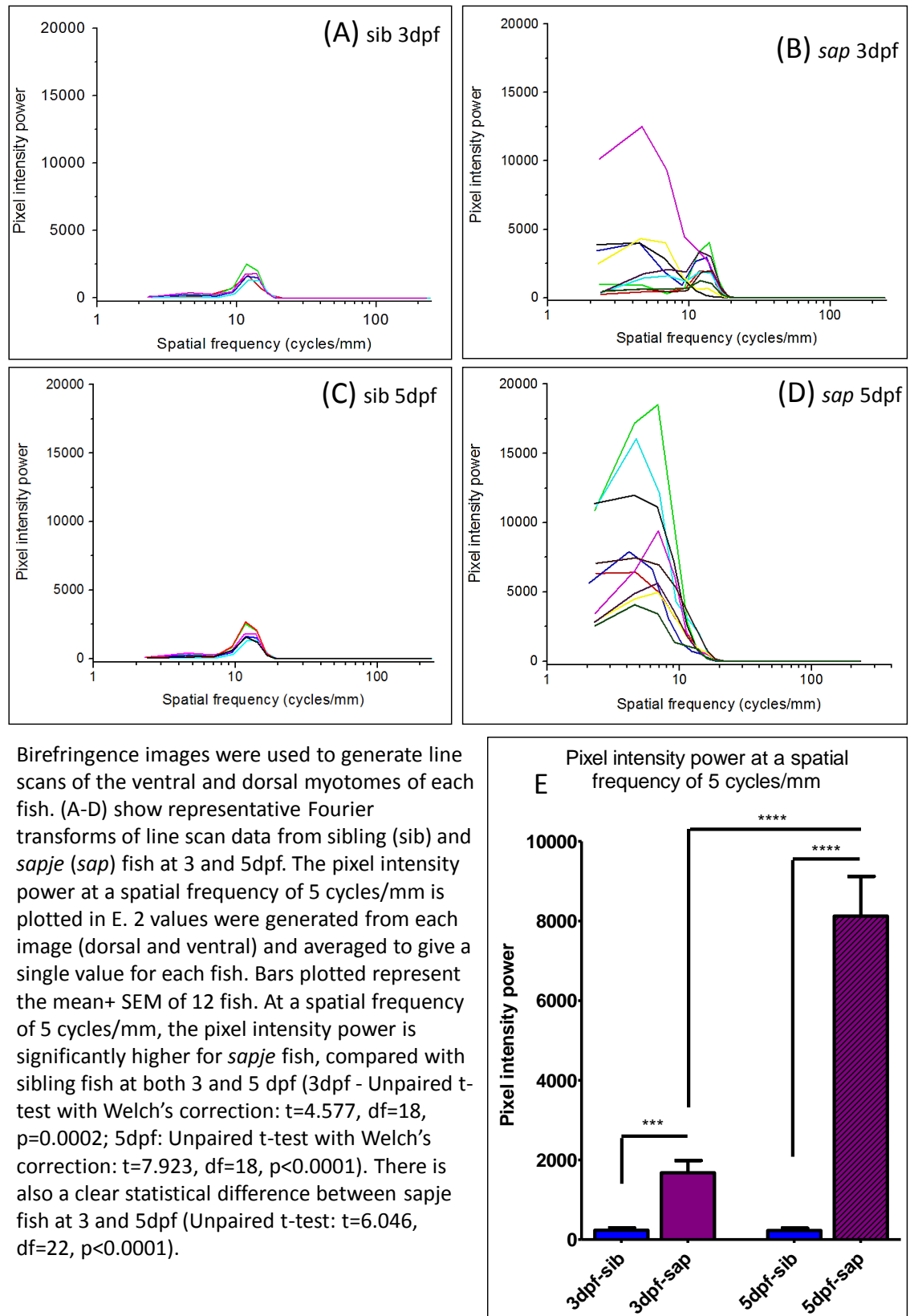
Between 3 and 5dpf, Fourier transforms of line scanning data show a significant increase in the pixel intensity power at 5 cycles per mm.

Figure 5.31: Line scans and Fourier transforms of 3dpf larvae



Left-hand panels show line scans of sibling (A) and *sapje* (C) muscle birefringence images. Right-hand graphs (B) and (D) show the Fourier transforms of the data. Fourier transforms of sibling fish (B) show a single frequency of just over 10 cycles/mm, representing the number of somites per mm. Fourier transforms of *sapje* fish line scans (D), show an underlying frequency at about 10 cycles/mm, but also exhibit other smaller frequency modes, due to the disruption in birefringence. (E) shows the images used to create the line scans in (C, D).

**Figure 5.32 Fourier analysis of 3 and 5dpf sibling and *sapje* fish**

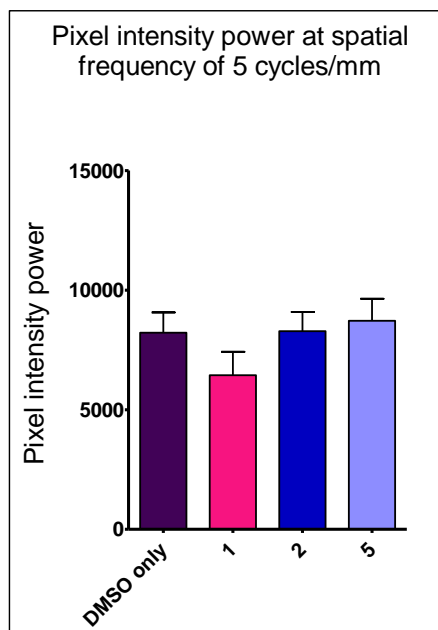


Birefringence images were used to generate line scans of the ventral and dorsal myotomes of each fish. (A-D) show representative Fourier transforms of line scan data from sibling (sib) and *sapje* (*sap*) fish at 3 and 5 dpf. The pixel intensity power at a spatial frequency of 5 cycles/mm is plotted in E. 2 values were generated from each image (dorsal and ventral) and averaged to give a single value for each fish. Bars plotted represent the mean+ SEM of 12 fish. At a spatial frequency of 5 cycles/mm, the pixel intensity power is significantly higher for *sapje* fish, compared with sibling fish at both 3 and 5 dpf (3dpf - Unpaired t-test with Welch's correction:  $t=4.577$ ,  $df=18$ ,  $p=0.0002$ ; 5dpf: Unpaired t-test with Welch's correction:  $t=7.923$ ,  $df=18$ ,  $p<0.0001$ ). There is also a clear statistical difference between *sapje* fish at 3 and 5 dpf (Unpaired t-test:  $t=6.046$ ,  $df=22$ ,  $p<0.0001$ ).

### 5.3.7.2 Effect of Dasatinib on muscle damage

The ability of Dasatinib to slow the progression of muscle damage was assessed, as this drug was most effective at reducing the percentage of fish with a dystrophic phenotype. Fourier transforms of line scanning data from *sapje* larvae treated with Dasatinib from 3 to 5dpf were carried out. At a concentration of 1 $\mu$ M, there is a slight decrease in the pixel intensity power at 5 cycles per mm, compared with DMSO only treated controls, but this was not statistically significant (figure 5.33). At higher concentrations of Dasatinib, there was also no significant difference in the values.

**Figure 5.33: Fourier analysis of Dasatinib treated embryos**



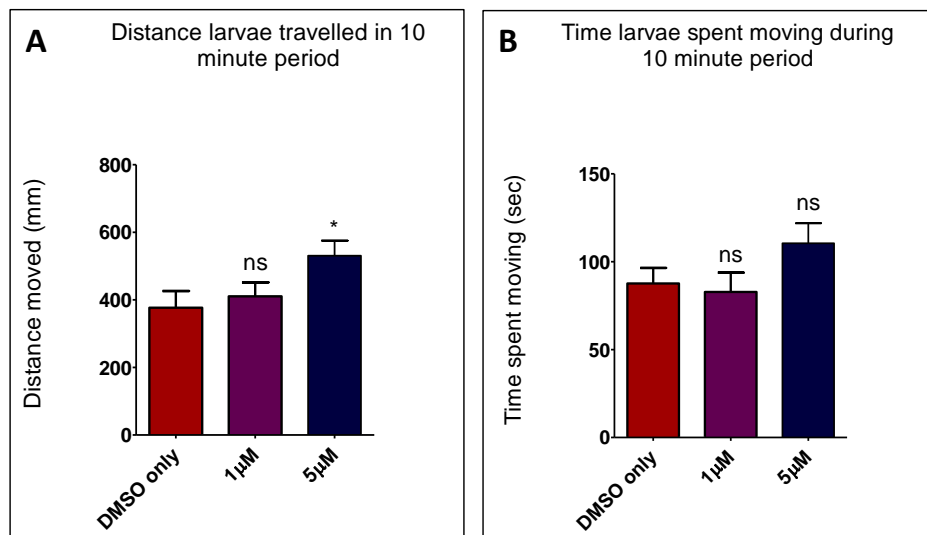
Birefringence images were used to generate line scans of the ventral and dorsal myotomes of each fish. Fourier transforms of line scan data from control treated and Dasatinib treated *sapje* fish were then carried out. The pixel intensity power at a spatial frequency of 5 cycles/mm was plotted in the adjacent graph. Bars represent the mean+ SEM of 30 fish for 3 independent experiments. At a spatial frequency of 5 cycles/mm, there is no statistical difference in the pixel intensity power between the different treatment groups (One-way ANOVA followed by Tukey's Multiple Comparison test:  $F=1.273$ ,  $df= 3,116$ ,  $p=0.2869$ )

### 5.3.7.3 Effect of Dasatinib on larval movement

Although the quantification of muscle damage indicated no detectable difference between treated and non-treated fish, there may be an improvement in muscle function. Therefore, the movement of larvae treated with Dasatinib between 3 and 5dpf was also analysed, using the Viewpoint tracking system.

There is a slight increase in the distance travelled by Dasatinib treated larvae within the tracking period, compared with DMSO treated controls (figure 5.34), and this increase is statistically significant at a concentration of 5 $\mu$ M. There was no significant difference between treated larvae and controls when comparing the time spent moving during the tracking period, although there is an upward trend.

**Figure 5.34: Viewpoint tracking analysis of Dasatinib treated embryos**



*sapje* larvae were treated with indicated concentrations of Dasatinib, or DMSO only, from 3 to 5dpf. One-way ANOVA analysis of Viewpoint tracking data indicated a significant increase between Dasatinib treated and control groups for the distance moved (A – One way ANOVA:  $F=3.188$ ,  $df=2,69$ ,  $p=0.0474$ , followed by Dunnett's multiple comparison test:  $*p<0.05$ , ns= not significant), but not time spent moving (B – One way ANOVA:  $F=1.995$ ,  $df=2,69$ ,  $p=0.1438$ , followed by Dunnett's multiple comparison test: ns= not significant)) in the ten minute tracking period. Bars represent mean data from 24 individual larvae from 3 separate 24-well plates; error bars are SEM.

## 5.4 Discussion

Inhibitors of Src kinase and the ubiquitin-dependent proteasomal pathway have been shown to be effective in reducing the proportion of larvae from a heterozygous *sapje* cross with a dystrophic phenotype. A summary of the results from the compound

treatment assay is shown in table 5.1. Inhibition of tyrosine kinase and E1 ubiquitin-ligase activity for 48 or 72 hours resulted in a decrease in the proportion of larvae with a dystrophic phenotype, and the proportion displaying a severe muscle phenotype. 48-hour proteasome inhibition was able to decrease the percentage of larvae with a dystrophic phenotype, but had no effect on percentage of embryos with a severe dystrophic phenotype. In addition, 72-hour treatment had no effect on the proportion of embryos with a dystrophic phenotype, or the severity of the phenotypes displayed.

The maximum rescue of the dystrophic population achieved in the compound treatment assay was approximately 30-45%, which is slightly lower than results from a recent screen by the Kunkel group (Kawahara et al., 2011). This could be explained by differences in the assay system used. The screen used fewer embryos per treatment, so would be more sensitive to fluctuations in the percentage of embryos with an affected muscle birefringence in each group. In addition, the screen was much higher throughput than the assay described in this study, which could mean numbers of affected fish were miscounted, especially if the phenotype was mild or the larvae was oriented incorrectly in relation to the polarising lenses. When aminophylline, a chemical pulled out from the screen carried out by Kawahara and colleagues, was used as a positive control, levels of rescue achieved were comparable to that achieved with the compounds used in this study.

Table 5.1: Summary table showing the effects of compound treatment on *sapje* phenotype

Compound	48 hour treatment		72 hour treatment	
	Effect on % larvae with dystrophic phenotype	Effect on % larvae with severe phenotype	Effect on % larvae with dystrophic phenotype	Effect on % larvae with severe phenotype
Tyrosine kinase inhibitors				
Dasatinib	↓	↓	↓	↓
Saracatinib	↓	↓	n/a	n/a
E1 ubiquitin-activating enzyme inhibitor				
PYR-41	↓	↓	↓	↓
Proteasomal inhibitors				
MG132	↓	↔	↔	↔
Velcade	↓	↔	n/a	n/a

Key:

↓ significant decrease in the proportion of larvae with dystrophic/severe phenotype, compared with control treated embryos

↔ no significant difference in the proportion of larvae with dystrophic/severe phenotype, compared with control treated embryos

#### 5.4.1 Inhibiting Src kinase

Src kinase inhibitors Dasatinib and Saracatinib were able to decrease the percentage of fish with a dystrophic phenotype. There was also a significant decrease in the percentage of embryos with a severe muscle phenotype. In addition, Dasatinib was able to significantly decrease the level of phosphorylated  $\beta$ -dystroglycan in *sapje* fish. This was associated with a concomitant increase in non-phosphorylated  $\beta$ -dystroglycan. This suggests that Dasatinib, by reducing levels of phosphorylated  $\beta$ -dystroglycan, is having an inhibitory effect on the phosphorylation of dystroglycan, and is able to delay or prevent the onset of dystrophy in some fish. These results are in

support of work carried out in the *mdx* mouse, where muscle histology and function were improved by preventing the phosphorylation of dystroglycan (Miller et al., 2012).

Dasatinib treatment of *dag1* embryos did not affect the percentage of fish with a dystrophic phenotype, suggesting that dystroglycan is required for the drug to affect muscle integrity. Furthermore, drug treatment of wildtype embryos did not affect larval movement, suggesting Dasatinib is not preventing the onset of dystrophy by paralysing the fish. These results, together with the biochemical data, are in support of Dasatinib affecting the muscle phenotype of *sapje* by a dystroglycan-dependent mechanism.

*sapje* larvae treated with Dasatinib after the onset of the dystrophic phenotype did not show a statistically significant improvement in the severity of muscle damage compared with non-treated controls. The vast variability in the amount of muscle damage in *sapje* larvae may have masked any beneficial effect of drug treatment, or the assay may not be sensitive enough to detect any effect. Alternatively, inhibiting Src kinase after the disease onset may not be able to slow the disease progression. There may have already been elevated phosphorylation and degradation of dystroglycan before 3dpf. Although there was no observable effect on muscle damage, there was a slight improvement in the motility of treated larvae. Longer treatment of larvae could be carried out to examine the effect of Dasatinib treatment on the life span of *sapje* mutants and their motility at later time points.

It would be important to carry out experiments with other kinase inhibitors, to show that the phenotypic rescue observed with Dasatinib and Saracatinib treatment is

specific to the activities of these drugs, and not a more general effect of kinase inhibition. Performing the assay with inhibitors of other kinases would also provide more evidence that the phosphorylation of dystroglycan is carried out by Src kinases; if these inhibitors are unable to reduce dystroglycan phosphorylation and improve muscle integrity in *sapje*, it would suggest that the Src family of kinases are responsible for this modification of dystroglycan.

#### **5.4.2 Inhibiting ubiquitination and proteasomal degradation**

PYR-41, an inhibitor of ubiquitin-activating enzyme (E1), was able to decrease the percentage of embryos with disrupted muscle birefringence and increase levels of  $\beta$ -dystroglycan protein. This suggests that PYR-41, by causing an increase in dystroglycan levels, is able to affect the cell biochemistry in the expected way. These data are in support of the hypothesised pathway by which dystroglycan is lost in the absence of dystrophin.

PYR-41 was more effective at lower concentrations (0.5 and 1 $\mu$ M) than at higher concentrations. This may be due to compensatory upregulation of other degradation pathways in response to an inhibition of the ubiquitin-dependent proteasomal pathway. PYR-41 has been shown to increase sumoylation in HEK293 cells (Yang et al., 2007). Therefore increased concentrations of PYR-41 may result in elevated degradation of DGC components, or other proteins that may have a protective effect on muscle integrity, by an alternative pathway.

Proteasomal inhibitors were able to increase dystroglycan levels, and slow the onset of the dystrophic phenotype in *sapje* zebrafish. These compounds have been previously shown to ameliorate muscle damage in *mdx* mice and the GRMD dog. These data further validate the zebrafish as a valuable tool for investigating new therapies for muscular dystrophy.

Both PYR-41 and MG132 increased levels of phosphorylated  $\beta$ -dystroglycan to a greater extent than non-phosphorylated  $\beta$ -dystroglycan. This may suggest it is the phosphorylated form of the protein which is primarily degraded in an ubiquitin- and proteasome-dependent manner. Combining these compounds with inhibitors of  $\beta$ -dystroglycan phosphorylation may be able to increase levels of non-phosphorylated dystroglycan even further. This may have greater effects on dystrophic muscle improvement, or enable lower doses of drugs to be used.

Several reports have highlighted the role of the ubiquitin-dependent proteasomal pathway in the pathogenesis of various muscle diseases. This pathway has been implicated in the atrophy of skeletal muscle in several conditions including sarcopenia and cachexia (Mitch and Goldberg, 1996, Altun et al., 2010), and proteasomal inhibitors are able to suppress the accelerated levels of protein breakdown and block atrophy in a number of animal models (Tawa et al., 1997, Fischer et al., 2000, Caron et al., 2011, Jamart et al., 2011, Zhang et al., 2013). In dystrophic muscle, proteasome activity is reported to be increased (Kumamoto et al., 2000, Selsby et al., 2010).

The data here further support the idea that the proteasomal pathway plays a role in protein degradation in dystrophin deficient muscle and suggests that increasing expression of dystroglycan is able to prevent muscle damage to some extent.

Results presented in chapters 4 and 5 suggest the decrease in dystroglycan expression observed in *sapje* fish could be mediated by the proteasome, either directly or indirectly. Since  $\beta$ -dystroglycan is a membrane protein, and the proteasome is primarily involved in the degradation of cytosolic proteins, the proteasomal pathway may be indirectly implicated in its degradation.

Ubiquitination and the activity of the proteasome is needed for the efficient translocation of the EGFR (endothelial growth factor receptor) to MVBs (multivesicular bodies), and MG132 is able to inhibit the degradation and promote the recycling of EGFR (Longva et al., 2002). The proteasome is also thought to play a role in the degradation of sodium channel  $\text{Na}_v1.5$ ; MG132 was able to restore the protein expression of  $\text{Na}_v1.5$  in the cardiac muscle of *mdx*<sup>5cv</sup> mice (Rougier et al., 2013).

Whether proteasomal degradation plays a direct or indirect role in the degradation of dystroglycan remains to be explored, but the fact that inhibitors of this pathway have been shown to be beneficial in several animal models of DMD suggests they may have potential in a therapeutic setting.

Although MG132 was effective in reducing the percentage of dystrophic fish when embryos were treated from 1 to 3dpf, it was not effective over longer incubations. Inhibition of the proteasome may be able to increase levels of  $\beta$ -dystroglycan to some extent, but over longer periods, it may be subject to internalisation, or increased

degradation by compensatory mechanisms. In addition, there was also no decrease in the percentage of larvae with a severe muscle phenotype in the treated groups, compared with the DMSO treated groups. This suggests MG132 may only be able to delay the onset of dystrophy in the mild phenotype group.

There has been conflicting evidence supporting a role for proteasomal inhibitors in rescuing the dystrophic phenotype in *mdx* mice. Continuous systemic treatment of *mdx* mice with MG-132 over 8 days resulted in the restoration of DGC proteins at the membrane and an improvement in muscle integrity (Bonuccelli et al., 2003). Similar improvement of the dystrophic phenotype has been observed using Velcade in *mdx* mice (Gazzerro et al., 2010) and the GRMD dog (Araujo et al., 2013). In another study, 8 day MG132 treatment increased the tetanic force of *mdx* muscles, but longer treatment appeared to be ineffective at improving muscle function (Selsby et al., 2012). In addition, muscles seemed to be more susceptible to contraction induced injury. Thus, inhibiting the proteasome may offer short term improvements to the pathophysiology of dystrophic muscle, but the continuous use of inhibitors may be ineffective, or even deleterious.

Velcade did not decrease the percentage of dystrophic fish as effectively as MG132, which was unexpected since it is a more potent inhibitor of the proteasome. As well as inhibiting the proteasome, MG132 has also been shown to inhibit calpains (Lee and Goldberg, 1998). As such, it is possible that the inhibitory effect of MG132 on calpains may also play a role in maintaining muscle integrity in treated *sapje* fish.

#### 5.4.2.1 Calpain

Calpain activity is thought to be increased in dystrophic muscle (Spencer et al., 1995).

Sarcolemmal damage allows increased calcium influx, which can lead to the overactivation of calpain (Alderton and Steinhardt, 2000).

Studies investigating the usefulness of calpain inhibition in improving the dystrophic phenotype are conflicting. Treatment of *mdx* mice with the calpain inhibitor leupeptin ameliorated the muscle pathology (Badalamente and Stracher, 2000). Treatment with BN82270, a combined calpain inhibitor and antioxidant, improved grip strength in the *mdx* mouse, but histological improvements were not observed (Burdi et al., 2006). The improvement in muscle function could be attributed to the antioxidant function of BN82270. Treatment of the *mdx* mouse with green tea extract was able to protect against oxidative stress and decrease muscle necrosis (Buetler et al., 2002). The antioxidant idebenone was also able to improve exercise performance and reduced the cardiac pathology in the *mdx* mouse (Buyse et al., 2009). Transgenic overexpression of calpastatin, an endogenous inhibitor of calpains, ameliorated muscle damage in *mdx* mice in one study (Spencer and Mellgren, 2002), but failed to do so in another (Briguet et al., 2008). In addition, recent studies using leupeptin and C101, a leupeptin-based compound, have also been unsuccessful in decreasing muscle damage or improving muscle function in *mdx* mice (Selsby et al., 2010) and the GRMD dog (Childers et al., 2011). Upon further investigation, m-calpain activation was increased in treated mice and dogs, suggesting there may be a compensatory mechanism to elevate calpain activity in response to exogenous inhibitors. In addition, there was also increased proteasomal activity. Thus, despite initial evidence to the contrary, calpain inhibitors do not appear to ameliorate the pathology of dystrophin-deficient muscle.

#### 5.4.2.2 NF- $\kappa$ B

Proteasomal inhibitors also modulate the nuclear factor-kappa B (NF- $\kappa$ B) pathway, which may also be important in the pathogenesis of DMD. NF- $\kappa$ B is involved in many cellular processes including the inflammatory response (Lawrence, 2009), and also in the muscle degeneration process in DMD (Acharyya et al., 2007, Peterson and Guttridge, 2008). In addition, PYR-41 has been shown to inhibit NF- $\kappa$ B activation (Yang et al., 2007).

Blocking activation of NF- $\kappa$ B has been shown to ameliorate muscle damage and improve muscle function in *mdx* mice (Messina et al., 2006, Delfin et al., 2011, Peterson et al., 2011). Thus, inhibitors of the proteasomal pathway may be working via a dual mechanism, preventing the degradation of dystroglycan and other DGC proteins, and also by suppressing elevated NF- $\kappa$ B activation. However, treatment of *dag1* embryos with MG132 and PYR-41 did not decrease the percentage of fish displaying a dystrophic phenotype, suggesting that the effect of proteasomal inhibitors on the NF- $\kappa$ B pathway alone may not be enough to improve muscle integrity.

#### 5.5 Concluding remarks

Inhibitors of Src kinase, ubiquitination and proteasomal degradation, are able to delay the onset of the dystrophic phenotype in the *sapje* zebrafish model of muscular dystrophy. It is hypothesised that these compounds are working to maintain muscle integrity by preventing the phosphorylation and degradation of  $\beta$ -dystroglycan. Preventing proteasomal degradation and phosphorylation of dystroglycan has also

been shown to improve muscle pathophysiology in *mdx* mice. Together, these results suggest that restoring dystroglycan expression may be beneficial to dystrophic muscle. The mechanism leading to loss of dystroglycan function in DMD may present new therapeutic targets for the treatment of this disease. Several inhibitors of Src kinase and the proteasome have already been developed, some of which are FDA approved, which may be able to speed up the drug development process.

## **Chapter 6: Discussion**

---

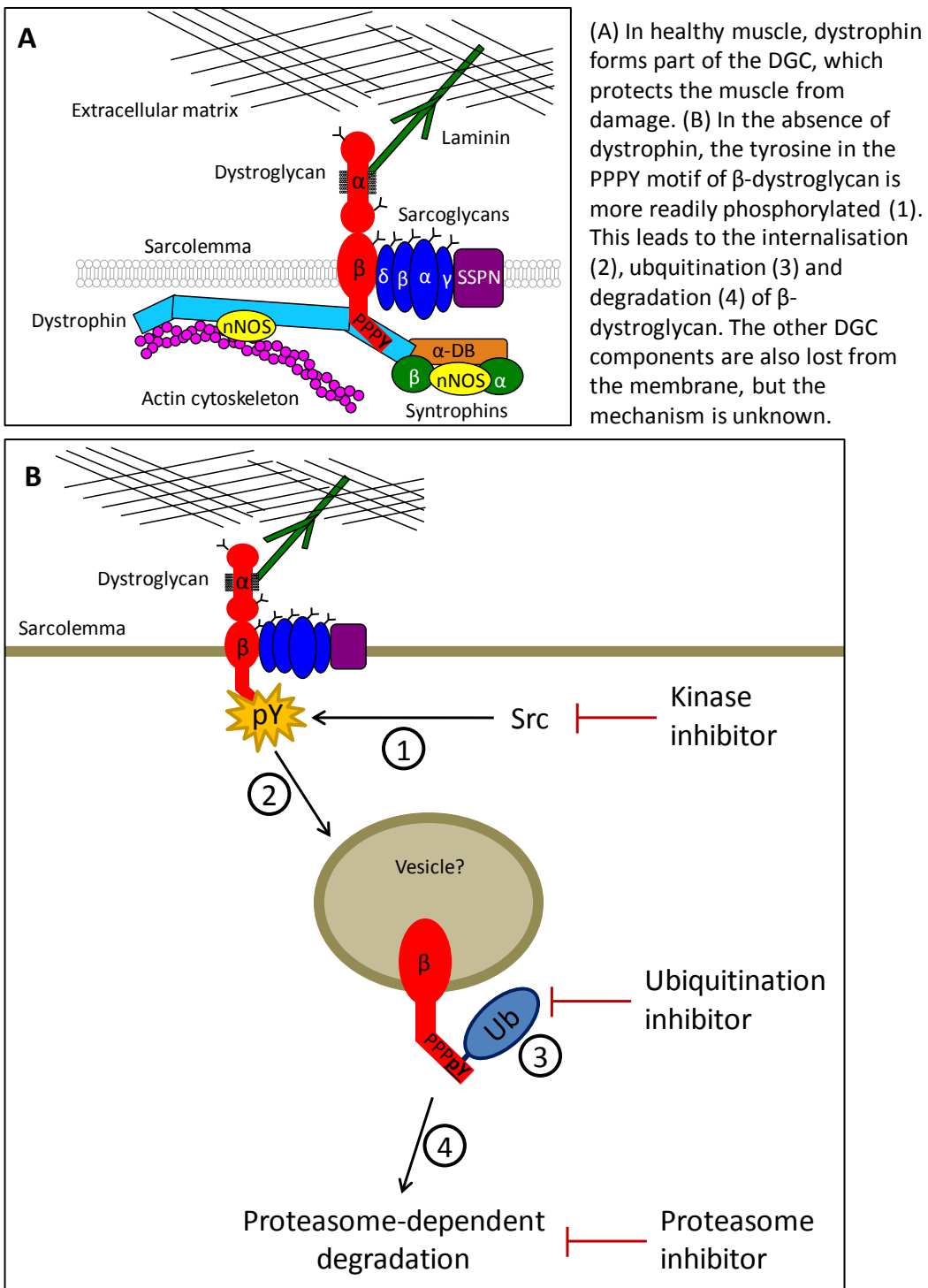
## 6.1 Summary

Dystroglycan is central to the DGC and plays important roles in muscle structure and function. This is exemplified in the dystroglycan mutant zebrafish (*dag1*), which displays loss of muscle integrity, and motility defects. Dystroglycan is also lost in the zebrafish model of DMD (*sapje*) and this occurs in an age-dependent manner. This is similar to what has been observed in dystrophin deficient muscle in mice and humans. Levels of phosphorylated dystroglycan are increased in *sapje*, compared with siblings. The loss of dystroglycan and the increase in phosphorylated dystroglycan in *sapje* is in support of the hypothesis that dystroglycan is more readily phosphorylated and degraded in the absence of dystrophin. This may be a key pathway in the pathogenesis of DMD, and preventing the loss of dystroglycan function may provide therapeutic potential.

## 6.2 Model of dystroglycan loss in dystrophic muscle

By contrast to approaches aiming to replace or repair genetic defect in DMD, the work presented in this thesis aimed to understand some of the downstream mechanisms that occur as a consequence of dystrophin deficiency in more detail. These findings can be added to the knowledge gained from other work to propose a model for the mechanism controlling the loss of sarcolemmal dystroglycan in dystrophin deficient muscle (figure 6.1).

**Figure 6.1 Model for loss of dystroglycan in DMD**



The phosphorylation of  $\beta$ -dystroglycan is associated with its internalisation from the plasma membrane (Sotgia et al., 2003, Miller et al., 2012). This is thought to be mediated by Src family kinases (Sotgia et al., 2001). In support of this hypothesis, inhibitors of Src were able to reduce levels of phosphorylated dystroglycan in H2K myoblasts and zebrafish embryos. Although Dasatinib is an inhibitor of multiple kinases including Src and Abl family kinases, it is a more potent inhibitor of Src (Lombardo et al., 2004). Dasatinib has greater efficacy against Src kinase activity than Saracatinib, and this may explain its ability to preserve muscle structure in *sapje* fish at lower concentrations than Saracatinib.

The endocytic route of phosphorylated dystroglycan has not been elucidated.

Phosphorylated  $\beta$ -dystroglycan was shown to co-localise with transferrin receptors in Cos-7 co-transfected with  $\beta$ -dystroglycan and c-Src, suggesting a clathrin-dependent mechanism (Sotgia et al., 2003). However, a later report showed a lack of co-localisation between phosphorylated  $\beta$ -dystroglycan and the transferrin receptor in H2K myoblasts (Miller et al., 2012). The absence of co-localisation with lysotracker also suggests phosphorylated dystroglycan is not trafficked to the lysosomal compartment.

It is also unknown whether  $\beta$ -dystroglycan is trafficked alone, or if it co-trafficks with  $\alpha$ -dystroglycan or any other components of the DGC. The DGC proteins are held together by various intermolecular contacts, and are all destabilised from the membrane in the absence of dystrophin. The mechanism by which each component is lost may be independent, but preventing the phosphorylation of  $\beta$ -dystroglycan in *mdx* mice led to the restoration of other components of the DGC including sarcoglycans and

sarcospan (Miller et al., 2012). This suggests that stabilising  $\beta$ -dystroglycan to the membrane is able to restore other complex components.

Once inside the cell, the fate of phosphorylated dystroglycan is unknown.

Phosphorylated dystroglycan has been shown to be ubiquitinated, whereas non-phosphorylated dystroglycan is not (Rob Piggott, unpublished results). This may drive the degradation of  $\beta$ -dystroglycan or target it for subsequent trafficking.

The proteasome has been implicated in the degradation of DGC components in the absence of dystrophin, and proteasomal inhibitors are able to restore DGC components and improve muscle pathophysiology in *mdx* mice and explants from DMD patients (Bonuccelli et al., 2003, Assereto et al., 2006, Bonuccelli et al., 2007, Gazzero et al., 2010). In addition, the proteasomal inhibitor Velcade was able to decrease inflammation and increase levels of DGC components in the GRMD dog (Araujo et al., 2013). The work presented here provides more evidence supporting a role for proteasomal inhibitors in DMD therapy. It also suggests that the pathway by which dystroglycan is lost in dystrophin deficient muscle is conserved in zebrafish, further highlighting *sapje* as a tool for DMD drug discovery.

The phosphorylation and degradation of dystroglycan has been identified as a key signalling pathway in the aetiology of DMD and this pathway provides druggable therapeutic targets. Inhibitors of this pathway were able to prevent or slow the progression of dystrophy in the zebrafish. This was associated with a concomitant increase in  $\beta$ -dystroglycan and a decrease in phosphorylated  $\beta$ -dystroglycan.

Several kinase and proteasome inhibitors have already been developed in different clinical settings. The repurposing of existing drugs holds great promise for rapidly advancing new therapeutic options to patient care. This would be an attractive strategy for reducing the time and cost of the drug development process.

### **6.3 Use of proteasomal inhibitors *in vivo***

Given the important role of the proteasome in normal cellular function, adverse side effects would be expected from inhibiting its activity. The clinical approval of Velcade for the treatment of multiple myeloma has validated the proteasomal pathway as a viable therapeutic target. However, although Velcade is reasonably well-tolerated in animal models (LeBlanc et al., 2002) and clinical trials, significant side effects are seen in some patients. These include peripheral neuropathy, gastrointestinal problems and thrombocytopenia (Richardson et al., 2005). More recently, cardiac problems have been identified (Takamatsu et al., 2010). DMD patients often have underlying cardiac defects (Finsterer and Stollberger, 2003), which could potentially be exacerbated by proteasomal inhibitor treatment. Inhibiting this pathway may also lead to the accumulation of damaged proteins, which may be toxic to the muscle cell.

Accumulations of damaged proteins are seen in many neurodegenerative diseases, in which proteasome function is impaired (Keller et al., 2000, McNaught et al., 2001, Zhou et al., 2003, Kabashi et al., 2004). In addition, there may be a compensatory upregulation of other degradation pathways. Thus, long term treatment with proteasomal inhibitors may not be effective, or may even be deleterious. This could be mitigated by intermittent dosing of the drug. It would also be important to ensure the

dose was high enough to gain a therapeutic effect, whilst keeping unwanted side effects to a minimum.

A more specific approach could be used to reduce off-target effects. An inhibitor of the E3 ubiquitin ligase for  $\beta$ -dystroglycan could be used to prevent its ubiquitination.

Although the identity of this enzyme is not yet known, WW domains within the Nedd4 family of ubiquitin ligases have been shown to bind the C-terminal domain of  $\beta$ -dystroglycan *in vitro* (Pirozzi et al., 1997). This approach has been suggested as a therapy for other muscle wasting disorders in which the ubiquitin-dependent proteasomal degradation pathway has been implicated. The E3 ligase MuRF1 is upregulated in atrophic muscle, and has been implicated in the degradation of muscle components including myosin and creatine kinase (Witt et al., 2005, Clarke et al., 2007, Cohen et al., 2009). A specific inhibitor of MuRF1 has been identified (Eddins et al., 2011), but these have not yet been used in models of muscle atrophy.

#### **6.4 Src kinase inhibitors *in vivo***

Given their important role in the regulation of many cellular processes, such as growth, proliferation, migration and survival, toxic effects would be expected from inhibitors of Src family kinases. As with Velcade, Dasatinib has some significant side effects, including cytopenia and fluid retention, but these can often be managed by reducing doses or intermittent treatment (Breccia and Alimena, 2013).

Despite initial concerns over toxicity, many kinase inhibitors have been developed, and 13 are currently approved for clinical use (Levitzki, 2013). These drugs are used in the

treatment of various cancers, but an increasing number of compounds are being tested in clinical trials for other diseases such as rheumatoid arthritis, psoriasis, asthma and inflammatory bowel disease (Kontzias et al., 2012).

Although both proteasome and Src kinase inhibition are associated with side effects, combining both drugs may provide a synergistic effect. Using lower doses of both drugs may provide the same clinical benefit to dystrophic muscle with fewer side effects. Combining doses of proteasome and Src inhibitors could be explored in *sapje* initially, and then refined in the *mdx* mouse.

In addition, a medicinal chemistry approach could be utilised to refine the properties of the inhibitor compounds used in the assay, in order to increase potency and reduce side effects. Modification of the efficacy and toxicity profiles drugs can be achieved by making small changes to their chemical structure. The zebrafish provides an ideal platform on which to test the biological effects of large numbers of modified compounds *in vivo*. Zebrafish are also good model in which to investigate the toxicity of each of the compounds. Thus, optimisation of the kinase and proteasome inhibitors could be carried out using the zebrafish as a screening tool, with the refined compounds taken forward to mammalian models.

## 6.5 Towards new therapies for DMD

### 6.5.1 Therapies tested in clinical trials

Each potential therapy for DMD has limitations. Therapies that aim to replace or repair the genetic defect in DMD, by delivery of dystrophin mini genes or anti-sense oligonucleotides, are limited by the risk of immune rejection and the route of delivery. Intramuscular injections prohibit the treatment of inaccessible muscle groups, and delivery is limited to fibres near the site of injection. Systemic delivery may be possible, but is limited by poor cellular uptake and rapid clearance from the circulation.

Upregulation of utrophin circumvents immunological problems and may be achieved by oral delivery of compounds. However, utrophin may not fully restore all the binding partners of dystrophin. Specifically, utrophin does not contain the nNOS binding site found in the rod domain of dystrophin.

Stop codon read through may also be achieved via an orally bioavailable compound. However, both utrophin upregulation and stop codon read through have, so far, not translated well in patient trials and may require a lot of refinement to improve efficacy.

Therapies that have been taken forward to clinical trials have shown variable results between different patients. This, in part, may be due to the heterogeneity of the disease.

In DMD, different muscle groups are affected to varying degrees, and patients lose the ability to walk at different ages. Similarly, the severity of BMD is very variable. The functionality and stability of the truncated protein product is somewhat related to the variation in clinical phenotype (Bushby et al., 1993, Angelini et al., 1996). However, patients with the same genetic lesion also show varying degrees of severity (Anthony et al., 2011). This suggests that other factors may modulate the disease course.

Various factors are thought to play a role in the modification of the dystrophic pathology. For example, genetic modifiers that affect the translation efficiency or expression levels of dystrophin have been identified (Cacchiarelli et al., 2010, Cacchiarelli et al., 2011, Bello et al., 2012). Utrophin expression has also been correlated with disease severity (Kleopa et al., 2006). Additional unknown factors may also play a role. It is possible that levels of proteasome and kinase activity may also modulate disease severity; lower levels of degradation and phosphorylation may preserve complex components at the sarcolemma, promoting muscle integrity and the slowing of disease progression. It may be of interest to investigate this further, given the importance of understanding the processes involved in the dystrophic pathology.

### **6.5.2 Alternative therapies for DMD**

Many therapies have not translated well in humans. This may be due to the heterogeneity of the disease and factors downstream of dystrophin loss, which are currently not well understood.

Certain therapies such as stop codon read through and exon skipping would only be applicable to patients with particular genetic changes. In addition, these therapies are aimed at converting DMD to a milder, BMD-like phenotype. Therefore, there is scope for alternative therapies that may further slow disease progression.

Knowledge of the downstream pathways resulting from loss of dystrophin, such as the mechanism by which dystroglycan is lost from the sarcolemma, could be utilised to develop new therapies. These therapies may be less expensive and would not be mutation-specific. They could also be used as adjuncts to other therapies that do not elicit a complete cure.

Preventing dystroglycan phosphorylation and degradation has shown promise in ameliorating the dystrophic phenotype. Proteasome inhibitors are able to restore dystroglycan and other DGC components to the membrane, and improve muscle pathophysiology in the *mdx* mouse. Preventing dystroglycan phosphorylation in this mouse model was also able to improve the dystrophic phenotype. The work presented in this thesis also suggests that inhibitors of Src kinase and the proteasome are beneficial to dystrophic muscle in the *sapje* zebrafish.

Although this approach offers no correction of the underlying cause of the disease (i.e. dystrophin is not being repaired or replaced), other cytoskeletal linkers, such as utrophin or plectin, may be able to compensate for the loss of dystrophin. Both utrophin and plectin are naturally upregulated in dystrophin-deficient muscle, and this is thought to have a protective role (Karpati et al., 1993b, Rezniczek et al., 2007).

Plectin expression at the sarcolemma is further increased in  $Y890F^{+/+}:$ *mdx* mice (Miller

et al., 2012). Thus, stabilising dystroglycan expression at the membrane, by preventing its phosphorylation and internalisation, may allow the formation of alternative adhesion complexes.

All potential DMD therapies have caveats, but could be used in combination to provide better treatment of patients. Given the heterogeneity of the disease, different combinations may be beneficial for different patients. Stabilising dystroglycan at the sarcolemma may be able to enhance the effectiveness of other approaches such as utrophin upregulation or exon skipping, and inhibitors of Src kinase and the proteasome may be powerful adjuncts to these other therapies that are being developed.

## References

---

- AARTSMA-RUS, A., FOKKEMA, I., VERSCHUUREN, J., GINJAAR, I., VAN DEUTEKOM, J., VAN OMMEN, G. J. & DEN DUNNEN, J. T. 2009. Theoretic applicability of antisense-mediated exon skipping for Duchenne muscular dystrophy mutations. *Hum Mutat*, 30, 293-9.
- ACHARYYA, S., VILLALTA, S. A., BAKKAR, N., BUPHA-INTR, T., JANSSEN, P. M., CARATHERS, M., LI, Z. W., BEG, A. A., GHOSH, S., SAHENK, Z., WEINSTEIN, M., GARDNER, K. L., RAFAEL-FORTNEY, J. A., KARIN, M., TIDBALL, J. G., BALDWIN, A. S. & GUTTRIDGE, D. C. 2007. Interplay of IKK/NF-kappaB signaling in macrophages and myofibers promotes muscle degeneration in Duchenne muscular dystrophy. *J Clin Invest*, 117, 889-901.
- ADAMO, C. M., DAI, D. F., PERCIVAL, J. M., MINAMI, E., WILLIS, M. S., PATRUCCO, E., FROEHNER, S. C. & BEAVO, J. A. 2010. Sildenafil reverses cardiac dysfunction in the mdx mouse model of Duchenne muscular dystrophy. *Proc Natl Acad Sci U S A*, 107, 19079-83.
- ADAMS, J., & STEIN, R. 1996. Novel inhibitors of the proteasome and their therapeutic use in inflammation. *Annu Rep Med Chem*, 31, 279-288.
- ADAMS, J., BEHNKE, M., CHEN, S., CRUICKSHANK, A. A., DICK, L. R., GRENIER, L., KLUNDER, J. M., MA, Y. T., PLAMONDON, L. & STEIN, R.L. 1998. Potent and selective inhibitors of the proteasome: dipeptidyl boronic acids. *Bioorg Med Chem Lett*, 8, 333-8.
- ADAMS, J. 2004. The development of proteasome inhibitors as anticancer drugs. *Cancer Cell*, 5, 417-21.
- ALBRECHT, D. E. & FROEHNER, S. C. 2002. Syntrophins and dystrobrevins: defining the dystrophin scaffold at synapses. *Neurosignals*, 11, 123-9.
- ALDERTON, J. M. & STEINHARDT, R. A. 2000. Calcium influx through calcium leak channels is responsible for the elevated levels of calcium-dependent proteolysis in dystrophic myotubes. *J Biol Chem*, 275, 9452-60.
- ALI, S., CHAMPAGNE, D. L. & RICHARDSON, M. K. 2012. Behavioral profiling of zebrafish embryos exposed to a panel of 60 water-soluble compounds. *Behav Brain Res*, 228, 272-83.
- ALTER, J., LOU, F., RABINOWITZ, A., YIN, H., ROSENFELD, J., WILTON, S. D., PARTRIDGE, T. A. & LU, Q. L. 2006. Systemic delivery of morpholino oligonucleotide restores dystrophin expression bodywide and improves dystrophic pathology. *Nat Med*, 12, 175-7.
- ALTUN, M., BESCHE, H. C., OVERKLEEF, H. S., PICCIRILLO, R., EDELMANN, M. J., KESSLER, B. M., GOLDBERG, A. L. & ULFHAKE, B. 2010. Muscle wasting in aged, sarcopenic rats is associated with enhanced activity of the ubiquitin proteasome pathway. *J Biol Chem*, 285, 39597-608.
- AMANN, K. J., RENLEY, B. A. & ERVASTI, J. M. 1998. A cluster of basic repeats in the dystrophin rod domain binds F-actin through an electrostatic interaction. *J Biol Chem*, 273, 28419-23.
- ANDERSON, J. E., WEBER, M. & VARGAS, C. 2000. Deflazacort increases laminin expression and myogenic repair, and induces early persistent functional gain in mdx mouse muscular dystrophy. *Cell Transplant*, 9, 551-64.

- ANGELINI, C., FANIN, M., FREDA, M. P., MARTINELLO, F., MIORIN, M., MELACINI, P., SICILIANO, G., PEGORARO, E., ROSA, M. & DANIELI, G. A. 1996. Prognostic factors in mild dystrophinopathies. *J Neurol Sci*, 142, 70-8.
- ANTHONY, K., CIRAK, S., TORELLI, S., TASCA, G., FENG, L., ARECHAVALA-GOMEZA, V., ARMAROLI, A., GUGLIERI, M., STRAATHOF, C. S., VERSCHUUREN, J. J., AARTSMA-RUS, A., HELDERMAN-VAN DEN ENDEN, P., BUSHBY, K., STRAUB, V., SEWRY, C., FERLINI, A., RICCI, E., MORGAN, J. E. & MUNTONI, F. 2011. Dystrophin quantification and clinical correlations in Becker muscular dystrophy: implications for clinical trials. *Brain*, 134, 3547-59.
- ARAUJO, K. P., BONUCCELLI, G., DUARTE, C. N., GAIAD, T. P., MOREIRA, D. F., FEDER, D., BELIZARIO, J. E., MIGLINO, M. A., LISANTI, M. P. & AMBROSIO, C. E. 2013. Bortezomib (PS-341) treatment decreases inflammation and partially rescues the expression of the dystrophin-glycoprotein complex in GRMD dogs. *PLoS One*, 8, e61367.
- ASSERETO, S., STRINGARA, S., SOTGIA, F., BONUCCELLI, G., BROCCOLINI, A., PEDEMONTE, M., TRAVERSO, M., BIANCHERI, R., ZARA, F., BRUNO, C., LISANTI, M. P. & MINETTI, C. 2006. Pharmacological rescue of the dystrophin-glycoprotein complex in Duchenne and Becker skeletal muscle explants by proteasome inhibitor treatment. *Am J Physiol Cell Physiol*, 290, C577-82.
- AVSAR-BAN, E., ISHIKAWA, H., MANYA, H., WATANABE, M., AKIYAMA, S., MIYAKE, H., ENDO, T. & TAMARU, Y. 2010. Protein O-mannosylation is necessary for normal embryonic development in zebrafish. *Glycobiology*, 20, 1089-102.
- BADALAMENTE, M. A. & STRACHER, A. 2000. Delay of muscle degeneration and necrosis in mdx mice by calpain inhibition. *Muscle Nerve*, 23, 106-11.
- BAR, S., BARNEA, E., LEVY, Z., NEUMAN, S., YAFFE, D. & NUDEL, U. 1990. A novel product of the Duchenne muscular dystrophy gene which greatly differs from the known isoforms in its structure and tissue distribution. *Biochem J*, 272, 557-60.
- BARTON-DAVIS, E. R., CORDIER, L., SHOTURMA, D. I., LELAND, S. E. & SWEENEY, H. L. 1999. Aminoglycoside antibiotics restore dystrophin function to skeletal muscles of mdx mice. *J Clin Invest*, 104, 375-81.
- BARTON, E. R. 2006. Impact of sarcoglycan complex on mechanical signal transduction in murine skeletal muscle. *Am J Physiol Cell Physiol*, 290, C411-9.
- BASSETT, D. I., BRYSON-RICHARDSON, R. J., DAGGETT, D. F., GAUTIER, P., KEENAN, D. G. & CURRIE, P. D. 2003. Dystrophin is required for the formation of stable muscle attachments in the zebrafish embryo. *Development*, 130, 5851-60.
- BELLO, L., PIVA, L., BARP, A., TAGLIA, A., PICILLO, E., VASCO, G., PANE, M., PREVITALI, S. C., TORRENTE, Y., GAZZERRO, E., MOTTA, M. C., GRIECO, G. S., NAPOLITANO, S., MAGRI, F., D'AMICO, A., ASTREA, G., MESSINA, S., SFRAMELI, M., VITA, G. L., BOFFI, P., MONGINI, T., FERLINI, A., GUALANDI, F., SORARU, G., ERMANI, M., VITA, G., BATTINI, R., BERTINI, E., COMI, G. P., BERARDINELLI, A., MINETTI, C., BRUNO, C., MERCURI, E., POLITANO, L., ANGELINI, C., HOFFMAN, E. P. & PEGORARO, E. 2012. Importance of SPP1 genotype as a covariate in clinical trials in Duchenne muscular dystrophy. *Neurology*, 79, 159-62.
- BERGER, J., BERGER, S., HALL, T. E., LIESCHKE, G. J. & CURRIE, P. D. 2010. Dystrophin-deficient zebrafish feature aspects of the Duchenne muscular dystrophy pathology. *Neuromuscul Disord*, 20, 826-32.

- BERGER, J., SZTAL, T. & CURRIE, P. D. 2012. Quantification of birefringence readily measures the level of muscle damage in zebrafish. *Biochem Biophys Res Commun*, 423, 785-8.
- BERRY, S. E., LIU, J., CHANEY, E. J. & KAUFMAN, S. J. 2007. Multipotential mesoangioblast stem cell therapy in the mdx/utrn<sup>-/-</sup> mouse model for Duchenne muscular dystrophy. *Regen Med*, 2, 275-88.
- BETTS, C., SALEH, A. F., ARZUMANOV, A. A., HAMMOND, S. M., GODFREY, C., COURSIINDEL, T., GAIT, M. J. & WOOD, M. J. 2012. Pip6-PMO, a new generation of peptide-oligonucleotide conjugates with improved cardiac exon skipping activity for DMD treatment. *Mol Ther Nucleic Acids*, 1, e38.
- BONUCCELLI, G., SOTGIA, F., CAPOZZA, F., GAZZERRO, E., MINETTI, C. & LISANTI, M. P. 2007. Localized treatment with a novel FDA-approved proteasome inhibitor blocks the degradation of dystrophin and dystrophin-associated proteins in mdx mice. *Cell Cycle*, 6, 1242-8.
- BONUCCELLI, G., SOTGIA, F., SCHUBERT, W., PARK, D. S., FRANK, P. G., WOODMAN, S. E., INSABATO, L., CAMMER, M., MINETTI, C. & LISANTI, M. P. 2003. Proteasome inhibitor (MG-132) treatment of mdx mice rescues the expression and membrane localization of dystrophin and dystrophin-associated proteins. *Am J Pathol*, 163, 1663-75.
- BORK, P. & SUDOL, M. 1994. The WW domain: a signalling site in dystrophin? *Trends Biochem Sci*, 19, 531-3.
- BORZILLERI, R. M., BHIHDE, R. S., BARRISH, J. C., D'ARIENZO, C. J., DERBIN, G. M., FARGNOLI, J., HUNT, J.T., JEYASEELAN, R. S. R., KAMATH, A., KUKRAL, D. W., MARATHE, P., MORTILLO, S., QIAN, L., TOKARSKI, J. S., WAUTLET, B. S., ZHENG, X. & LOMBARDO L. J. 2006. Discovery and evaluation of N-cyclopropyl-2,4-difluoro-5-((2-(pyridin-2-ylamino)thiazol-5-ylmethyl)amino)benzamide (BMS-605541), a selective and orally efficacious inhibitor of vascular endothelial growth factor receptor-2. *J Med Chem*, 49, 3766-9.
- BRANCACCIO, A., SCHULTHESS, T., GESEMANN, M. & ENGEL, J. 1995. Electron microscopic evidence for a mucin-like region in chick muscle alpha-dystroglycan. *FEBS Lett*, 368, 139-42.
- BRECCIA, M. & ALIMENA, G. 2013. Occurrence and current management of side effects in chronic myeloid leukemia patients treated frontline with tyrosine kinase inhibitors. *Leuk Res*, 37, 713-20.
- BRENNAN, J. E., CHAO, D. S., GEE, S. H., MCGEE, A. W., CRAVEN, S. E., SANTILLANO, D. R., WU, Z., HUANG, F., XIA, H., PETERS, M. F., FROEHNER, S. C. & BREDDT, D. S. 1996. Interaction of nitric oxide synthase with the postsynaptic density protein PSD-95 and alpha1-syntrophin mediated by PDZ domains. *Cell*, 84, 757-67.
- BRENNAN, J. E., CHAO, D. S., XIA, H., ALDAPE, K. & BREDDT, D. S. 1995. Nitric oxide synthase complexed with dystrophin and absent from skeletal muscle sarcolemma in Duchenne muscular dystrophy. *Cell*, 82, 743-52.
- BRIGUET, A., ERB, M., COURDIER-FRUH, I., BARZAGHI, P., SANTOS, G., HERZNER, H., LESCOP, C., SIENDT, H., HENNEBOEHLE, M., WEYERMANN, P., MAGYAR, J. P., DUBACH-POWELL, J., METZ, G. & MEIER, T. 2008. Effect of calpain and proteasome inhibition on Ca<sup>2+</sup>-dependent proteolysis and muscle histopathology in the mdx mouse. *FASEB J*, 22, 4190-200.

- BUETLER, T. M., RENARD, M., OFFORD, E. A., SCHNEIDER, H. & RUEGG, U. T. 2002. Green tea extract decreases muscle necrosis in mdx mice and protects against reactive oxygen species. *Am J Clin Nutr*, 75, 749-53.
- BULFIELD, G., SILLER, W. G., WIGHT, P. A. & MOORE, K. J. 1984. X chromosome-linked muscular dystrophy (mdx) in the mouse. *Proc Natl Acad Sci U S A*, 81, 1189-92.
- BURDI, R., DIDONNA, M. P., PIGNOL, B., NICO, B., MANGIERI, D., ROLLAND, J. F., CAMERINO, C., ZALLONE, A., FERRO, P., ANDREETTA, F., CONFALONIERI, P. & DE LUCA, A. 2006. First evaluation of the potential effectiveness in muscular dystrophy of a novel chimeric compound, BN 82270, acting as calpain-inhibitor and anti-oxidant. *Neuromuscul Disord*, 16, 237-48.
- BURDI, R., ROLLAND, J. F., FRAYSSE, B., LITVINOVA, K., COZZOLI, A., GIANNUZZI, V., LIANTONIO, A., CAMERINO, G. M., SBLENDORIO, V., CAPOGROSSO, R. F., PALMIERI, B., ANDREETTA, F., CONFALONIERI, P., DE BENEDICTIS, L., MONTAGNANI, M. & DE LUCA, A. 2009. Multiple pathological events in exercised dystrophic mdx mice are targeted by pentoxifylline: outcome of a large array of in vivo and ex vivo tests. *J Appl Physiol*, 106, 1311-24.
- BURGESS, H. & GRANATO, M. 2007. Modulation of locomotor activity in larval zebrafish during light adaptation. *J Exp Biol*, 210, 2526-2539.
- BURGESS, H. & GRANATO, M. 2008. The neurogenetic frontier—lessons from misbehaving zebrafish. *Brief Funct Genomic Proteomic*, 7, 474-482.
- BURKIN, D. J., WALLACE, G. Q., NICOL, K. J., KAUFMAN, D. J. & KAUFMAN, S. J. 2001. Enhanced expression of the alpha 7 beta 1 integrin reduces muscular dystrophy and restores viability in dystrophic mice. *J Cell Biol*, 152, 1207-18.
- BURRIDGE, K. & CHRZANOWSKA-WODNICKA, M. 1996. Focal adhesions, contractility, and signaling. *Annu Rev Cell Dev Biol*, 12, 463-518.
- BUSHBY, K. M., GARDNER-MEDWIN, D., NICHOLSON, L. V., JOHNSON, M. A., HAGGERTY, I. D., CLEGHORN, N. J., HARRIS, J. B. & BHATTACHARYA, S. S. 1993. The clinical, genetic and dystrophin characteristics of Becker muscular dystrophy. II. Correlation of phenotype with genetic and protein abnormalities. *J Neurol*, 240, 105-12.
- BUYSE, G. M., VAN DER MIEREN, G., ERB, M., D'HOOGHE, J., HERIJGERS, P., VERBEKEN, E., JARA, A., VAN DEN BERGH, A., MERTENS, L., COURDIER-FRUH, I., BARZAGHI, P. & MEIER, T. 2009. Long-term blinded placebo-controlled study of SNT-MC17/idebenone in the dystrophin deficient mdx mouse: cardiac protection and improved exercise performance. *Eur Heart J*, 30, 116-24.
- BYERS, T. J., LIDOV, H. G. & KUNKEL, L. M. 1993. An alternative dystrophin transcript specific to peripheral nerve. *Nat Genet*, 4, 77-81.
- CACCHIARELLI, D., INCITTI, T., MARTONE, J., CESANA, M., CAZZELLA, V., SANTINI, T., STHANDIER, O. & BOZZONI, I. 2011. miR-31 modulates dystrophin expression: new implications for Duchenne muscular dystrophy therapy. *EMBO Rep*, 12, 136-41.
- CACCHIARELLI, D., MARTONE, J., GIRARDI, E., CESANA, M., INCITTI, T., MORLANDO, M., NICOLETTI, C., SANTINI, T., STHANDIER, O., BARBERI, L., AURICCHIO, A., MUSARO, A. & BOZZONI, I. 2010. MicroRNAs involved in molecular circuitries relevant for the Duchenne muscular dystrophy pathogenesis are controlled by the dystrophin/nNOS pathway. *Cell Metab*, 12, 341-51.
- CARON, A. Z., HAROUN, S., LEBLANC, E., TRENSZ, F., GUINDI, C., AMRANI, A. & GRENIER, G. 2011. The proteasome inhibitor MG132 reduces immobilization-induced skeletal muscle atrophy in mice. *BMC Musculoskelet Disord*, 12, 185.

- CHAMBERLAIN, J. S., METZGER, J., REYES, M., TOWNSEND, D. & FAULKNER, J. A. 2007. Dystrophin-deficient mdx mice display a reduced life span and are susceptible to spontaneous rhabdomyosarcoma. *FASEB J*, 21, 2195-204.
- CHAMBERLAIN, J. S., PEARLMAN, J. A., MUZNY, D. M., GIBBS, R. A., RANIER, J. E., CASKEY, C. T. & REEVES, A. A. 1988. Expression of the murine Duchenne muscular dystrophy gene in muscle and brain. *Science*, 239, 1416-8.
- CHAMBERS, S. P., ANDERSON, L. V., MAGUIRE, G. M., DODD, A. & LOVE, D. R. 2003. Sarcoglycans of the zebrafish: orthology and localization to the sarcolemma and myosepta of muscle. *Biochem Biophys Res Commun*, 303, 488-95.
- CHAN, Y. M., BONNEMANN, C. G., LIDOV, H. G. & KUNKEL, L. M. 1998. Molecular organization of sarcoglycan complex in mouse myotubes in culture. *J Cell Biol*, 143, 2033-44.
- CHARVET, B., MALBOUYRES, M., PAGNON-MINOT, A., RUGGIERO, F. & LE GUELLEC, D. 2011. Development of the zebrafish myoseptum with emphasis on the myotendinous junction. *Cell Tissue Res*, 346, 439-49.
- CHILDERS, M. K., BOGAN, J. R., BOGAN, D. J., GREINER, H., HOLDER, M., GRANGE, R. W. & KORNEGAY, J. N. 2011. Chronic administration of a leupeptin-derived calpain inhibitor fails to ameliorate severe muscle pathology in a canine model of duchenne muscular dystrophy. *Front Pharmacol*, 2, 89.
- CHUNG, W. & CAMPANELLI, J. T. 1999. WW and EF hand domains of dystrophin-family proteins mediate dystroglycan binding. *Mol Cell Biol Res Commun*, 2, 162-71.
- CLARKE, B. A., DRUJAN, D., WILLIS, M. S., MURPHY, L. O., CORPINA, R. A., BUROVA, E., RAKHILIN, S. V., STITT, T. N., PATTERSON, C., LATRES, E. & GLASS, D. J. 2007. The E3 Ligase MuRF1 degrades myosin heavy chain protein in dexamethasone-treated skeletal muscle. *Cell Metab*, 6, 376-85.
- COFFEY, A. J., ROBERTS, R. G., GREEN, E. D., COLE, C. G., BUTLER, R., ANAND, R., GIANNELLI, F. & BENTLEY, D. R. 1992. Construction of a 2.6-Mb contig in yeast artificial chromosomes spanning the human dystrophin gene using an STS-based approach. *Genomics*, 12, 474-84.
- COHEN, S., BRAULT, J. J., GYGI, S. P., GLASS, D. J., VALENZUELA, D. M., GARTNER, C., LATRES, E. & GOLDBERG, A. L. 2009. During muscle atrophy, thick, but not thin, filament components are degraded by MuRF1-dependent ubiquitylation. *J Cell Biol*, 185, 1083-95.
- COHN, R. D., HENRY, M. D., MICHELE, D. E., BARRESI, R., SAITO, F., MOORE, S. A., FLANAGAN, J. D., SKWARCHUK, M. W., ROBBINS, M. E., MENDELL, J. R., WILLIAMSON, R. A. & CAMPBELL, K. P. 2002. Disruption of DAG1 in differentiated skeletal muscle reveals a role for dystroglycan in muscle regeneration. *Cell*, 110, 639-48.
- COOPER, B. J., WINAND, N. J., STEDMAN, H., VALENTINE, B. A., HOFFMAN, E. P., KUNKEL, L. M., SCOTT, M. O., FISCHBECK, K. H., KORNEGAY, J. N., AVERY, R. J. & ET AL. 1988. The homologue of the Duchenne locus is defective in X-linked muscular dystrophy of dogs. *Nature*, 334, 154-6.
- COTE, P. D., MOUKHLES, H., LINDENBAUM, M. & CARBONETTO, S. 1999. Chimaeric mice deficient in dystroglycans develop muscular dystrophy and have disrupted myoneural synapses. *Nat Genet*, 23, 338-42.
- CROSBIE, R. H., HEIGHWAY, J., VENZKE, D. P., LEE, J. C. & CAMPBELL, K. P. 1997. Sarcospan, the 25-kDa transmembrane component of the dystrophin-glycoprotein complex. *J Biol Chem*, 272, 31221-4.

- CROSBIE, R. H., LEBAKKEN, C. S., HOLT, K. H., VENZKE, D. P., STRAUB, V., LEE, J. C., GRADY, R. M., CHAMBERLAIN, J. S., SANES, J. R. & CAMPBELL, K. P. 1999. Membrane targeting and stabilization of sarcospan is mediated by the sarcoglycan subcomplex. *J Cell Biol*, 145, 153-65.
- CROSBIE, R. H., LIM, L. E., MOORE, S. A., HIRANO, M., HAYS, A. P., MAYBAUM, S. W., COLLIN, H., DOVICO, S. A., STOLLE, C. A., FARDEAU, M., TOME, F. M. & CAMPBELL, K. P. 2000. Molecular and genetic characterization of sarcospan: insights into sarcoglycan-sarcospan interactions. *Hum Mol Genet*, 9, 2019-27.
- D'SOUZA, V. N., NGUYEN, T. M., MORRIS, G. E., KARGES, W., PILLERS, D. A. & RAY, P. N. 1995. A novel dystrophin isoform is required for normal retinal electrophysiology. *Hum Mol Genet*, 4, 837-42.
- DANGAIN, J. & VRBOVA, G. 1984. Muscle development in mdx mutant mice. *Muscle Nerve*, 7, 700-4.
- DAS, J., CHEN, P., NORRIS, D., PADMANABHA, R., LIN, J., MOQUIN, R. V., SHEN, Z., COOK, L. S., DOWEYKO, A. M., PITT, S., PANG, S., SHEN, D. R., FANG, Q., DE FEX, H. F., MCINTYRE, K. W., SHUSTER, D. J., GILLOOLY, K. M., BEHNIA, K., SCHIEVEN, G. L., WITYAK, J. & BARRISH, J. C. 2006. 2-aminothiazole as a novel kinase inhibitor template. Structure-activity relationship studies toward the discovery of N-(2-chloro-6-methylphenyl)-2-[[6-[4-(2-hydroxyethyl)-1-piperazinyl]]-2-methyl-4-pyrimidinyl]amino]-1,3-thiazole-5-carboxamide (dasatinib, BMS-354825) as a potent pan-Src kinase inhibitor. *J Med Chem*, 49, 6819-32.
- DAVIES, J., GILBERT, W. & GORINI, L. 1964. Streptomycin, Suppression, and the Code. *Proc Natl Acad Sci U S A*, 51, 883-90.
- DAVIES, K. E., PEARSON, P. L., HARPER, P. S., MURRAY, J. M., O'BRIEN, T., SARFARAZI, M. & WILLIAMSON, R. 1983. Linkage analysis of two cloned DNA sequences flanking the Duchenne muscular dystrophy locus on the short arm of the human X chromosome. *Nucleic Acids Res*, 11, 2303-12.
- DE LUCA, A., PIERNO, S., LIANTONIO, A., CETRONE, M., CAMERINO, C., FRAYSSE, B., MIRABELLA, M., SERVIDEI, S., RUEGG, U. T. & CONTE CAMERINO, D. 2003. Enhanced dystrophic progression in mdx mice by exercise and beneficial effects of taurine and insulin-like growth factor-1. *J Pharmacol Exp Ther*, 304, 453-63.
- DECONINCK, A. E., RAFAEL, J. A., SKINNER, J. A., BROWN, S. C., POTTER, A. C., METZINGER, L., WATT, D. J., DICKSON, J. G., TINSLEY, J. M. & DAVIES, K. E. 1997. Utrophin-dystrophin-deficient mice as a model for Duchenne muscular dystrophy. *Cell*, 90, 717-27.
- DELFIN, D. A., XU, Y., PETERSON, J. M., GUTTRIDGE, D. C., RAFAEL-FORTNEY, J. A. & JANSSEN, P. M. 2011. Improvement of cardiac contractile function by peptide-based inhibition of NF-kappaB in the utrophin/dystrophin-deficient murine model of muscular dystrophy. *J Transl Med*, 9, 68.
- DELLORUSSO, C., CRAWFORD, R. W., CHAMBERLAIN, J. S. & BROOKS, S. V. 2001. Tibialis anterior muscles in mdx mice are highly susceptible to contraction-induced injury. *J Muscle Res Cell Motil*, 22, 467-75.
- DEVOTO, S. H., MELANCON, E., EISEN, J. S. & WESTERFIELD, M. 1996. Identification of separate slow and fast muscle precursor cells in vivo, prior to somite formation. *Development*, 122, 3371-80.
- DI STASIO, E., SCIANDRA, F., MARAS, B., DI TOMMASO, F., PETRUCCI, T. C., GIARDINA, B. & BRANCACCIO, A. 1999. Structural and functional analysis of the N-terminal

- extracellular region of beta-dystroglycan. *Biochem Biophys Res Commun*, 266, 274-8.
- EDDINS, M. J., MARBLESTONE, J. G., SURESH KUMAR, K. G., LEACH, C. A., STERNER, D. E., MATTERN, M. R. & NICHOLSON, B. 2011. Targeting the ubiquitin E3 ligase MuRF1 to inhibit muscle atrophy. *Cell Biochem Biophys*, 60, 113-8.
- EMERY, A. E. H. 1993. *Duchenne Muscular Dystrophy*, Oxford University Press.
- EMRAN, F., RIHEL, J. & DOWLING, J. E. 2008. A behavioral assay to measure responsiveness of zebrafish to changes in light intensities. *J Vis Exp*.
- ERVASTI, J. M. & CAMPBELL, K. P. 1991. Membrane organization of the dystrophin-glycoprotein complex. *Cell*, 66, 1121-31.
- ERVASTI, J. M. & CAMPBELL, K. P. 1993. A role for the dystrophin-glycoprotein complex as a transmembrane linker between laminin and actin. *J Cell Biol*, 122, 809-23.
- ERVASTI, J. M., OHLENDIECK, K., KAHL, S. D., GAVER, M. G. & CAMPBELL, K. P. 1990. Deficiency of a glycoprotein component of the dystrophin complex in dystrophic muscle. *Nature*, 345, 315-9.
- FANG, F, LI, D-D., LI, J-R., SUN, J., DU, Q-R., GONG, H-B. & ZHU H-L. 2013. Design, synthesis, and evaluation of substituted 6-amide-4-anilinoquinazoline derivatives as c-src inhibitors. *RSC Adv*, 3, 26230-40.
- FENICHEL, G. M., FLORENCE, J. M., PESTRONK, A., MENDELL, J. R., MOXLEY, R. T., 3RD, GRIGGS, R. C., BROOKE, M. H., MILLER, J. P., ROBISON, J., KING, W. & ET AL. 1991. Long-term benefit from prednisone therapy in Duchenne muscular dystrophy. *Neurology*, 41, 1874-7.
- FINKEL, R. S. 2010. Read-through strategies for suppression of nonsense mutations in Duchenne/Becker muscular dystrophy: aminoglycosides and ataluren (PTC124). *J Child Neurol*, 25, 1158-64.
- FINSTERER, J. & STOLLBERGER, C. 2003. The heart in human dystrophinopathies. *Cardiology*, 99, 1-19.
- FISCHER, D., GANG, G., PRITTS, T. & HASSELGREN, P. O. 2000. Sepsis-induced muscle proteolysis is prevented by a proteasome inhibitor in vivo. *Biochem Biophys Res Commun*, 270, 215-21.
- GAZZERRO, E., ASSERETO, S., BONETTO, A., SOTGIA, F., SCARFI, S., PISTORIO, A., BONUCCELLI, G., CILLI, M., BRUNO, C., ZARA, F., LISANTI, M. P. & MINETTI, C. 2010. Therapeutic potential of proteasome inhibition in Duchenne and Becker muscular dystrophies. *Am J Pathol*, 176, 1863-77.
- GEE, S. H., MADHAVAN, R., LEVINSON, S. R., CALDWELL, J. H., SEALOCK, R. & FROEHNER, S. C. 1998. Interaction of muscle and brain sodium channels with multiple members of the syntrophin family of dystrophin-associated proteins. *J Neurosci*, 18, 128-37.
- GHAEMMAGHAMI, S., MAY, B. C., RENSLO, A. R. & PRUSINER, S. B. Discovery of 2-aminothiazoles as potent antiprion compounds. *J Virol*, 84, 3408-12.
- GODFREY, C., CLEMENT, E., MEIN, R., BROCKINGTON, M., SMITH, J., TALIM, B., STRAUB, V., ROBB, S., QUINLIVAN, R., FENG, L., JIMENEZ-MALLEBRERA, C., MERCURI, E., MANZUR, A. Y., KINALI, M., TORELLI, S., BROWN, S. C., SEWRY, C. A., BUSHBY, K., TOPALOGLU, H., NORTH, K., ABBS, S. & MUNTONI, F. 2007a. Refining genotype phenotype correlations in muscular dystrophies with defective glycosylation of dystroglycan. *Brain*, 130, 2725-35.
- GODFREY, C., CLEMENT, E., MEIN, R., BROCKINGTON, M., SMITH, J., TALIM, B., STRAUB, V., ROBB, S., QUINLIVIAN, R., FENG, L., JIMENEZ-MALLEBRERA, C., MERCURI, E., MANZUR, A., KINALI, M., TORELLI, S., BROWN, S., SEWRY, C.,

- BUSHBY, K., TOPALOGU, H., NORTH, K., ABBS, S. & MUNTONI, F. 2007b. Refining genotype phenotype correlations in muscular dystrophies with defective glycosylation of dystroglycan. *Brain*, 130, 2725-2735.
- GORECKI, D. C., MONACO, A. P., DERRY, J. M., WALKER, A. P., BARNARD, E. A. & BARNARD, P. J. 1992. Expression of four alternative dystrophin transcripts in brain regions regulated by different promoters. *Hum Mol Genet*, 1, 505-10.
- GOYENVALLE, A., BABBS, A., POWELL, D., KOLE, R., FLETCHER, S., WILTON, S. D. & DAVIES, K. E. 2010. Prevention of dystrophic pathology in severely affected dystrophin/utrophin-deficient mice by morpholino-oligomer-mediated exon-skipping. *Mol Ther*, 18, 198-205.
- GRADY, R. M., GRANGE, R. W., LAU, K. S., MAIMONE, M. M., NICHOL, M. C., STULL, J. T. & SANES, J. R. 1999. Role for alpha-dystrobrevin in the pathogenesis of dystrophin-dependent muscular dystrophies. *Nat Cell Biol*, 1, 215-20.
- GRANATO, M., EEDEN, F. V., SCHACH, U., TROWE, T., BRAND, M., FURUTANI-SEIKI, M., HAFFTER, P., HAMMERSCHMIDT, M., HEISENBERG, C., JIANG, Y., KANE, D., KELSH, R., MULLINS, M., ODENTHAL, J. & NÜSSLEIN-VOLHARD, C. 1996. Genes controlling and mediating locomotion behaviour of the zebrafish embryo and larva. *Development*, 123, 399-413.
- GUPTA, V., KAWAHARA, G., GUNDRY, S. R., CHEN, A. T., LENCER, W. I., ZHOU, Y., ZON, L. I., KUNKEL, L. M. & BEGGS, A. H. 2011. The zebrafish dag1 mutant: a novel genetic model for dystroglycanopathies. *Hum Mol Genet*, 20, 1712-25.
- GUPTA, V. A., KAWAHARA, G., MYERS, J. A., CHEN, A. T., HALL, T. E., MANZINI, M. C., CURRIE, P. D., ZHOU, Y., ZON, L. I., KUNKEL, L. M. & BEGGS, A. H. 2012. A splice site mutation in laminin-alpha2 results in a severe muscular dystrophy and growth abnormalities in zebrafish. *PLoS One*, 7, e43794.
- GUYON, J. R., MOSLEY, A. N., JUN, S. J., MONTANARO, F., STEFFEN, L. S., ZHOU, Y., NIGRO, V., ZON, L. I. & KUNKEL, L. M. 2005. Delta-sarcoglycan is required for early zebrafish muscle organization. *Exp Cell Res*, 304, 105-15.
- GUYON, J. R., MOSLEY, A. N., ZHOU, Y., O'BRIEN, K. F., SHENG, X., CHIANG, K., DAVIDSON, A. J., VOLINSKI, J. M., ZON, L. I. & KUNKEL, L. M. 2003. The dystrophin associated protein complex in zebrafish. *Hum Mol Genet*, 12, 601-15.
- HALL, T. E., BRYSON-RICHARDSON, R. J., BERGER, S., JACOBY, A. S., COLE, N. J., HOLLWAY, G. E., BERGER, J. & CURRIE, P. D. 2007. The zebrafish candyfloss mutant implicates extracellular matrix adhesion failure in laminin alpha2-deficient congenital muscular dystrophy. *Proc Natl Acad Sci U S A*, 104, 7092-7.
- HARA, Y., BALCI-HAYTA, B., YOSHIDA-MORIGUCHI, T., KANAGAWA, M., BELTRAN-VALERO DE BERNABE, D., GUNDESLI, H., WILLER, T., SATZ, J. S., CRAWFORD, R. W., BURDEN, S. J., KUNZ, S., OLDSTONE, M. B., ACCARDI, A., TALIM, B., MUNTONI, F., TOPALOGU, H., DINCER, P. & CAMPBELL, K. P. 2011. A dystroglycan mutation associated with limb-girdle muscular dystrophy. *N Engl J Med*, 364, 939-46.
- HASEGAWA, M., CUENDA, A., SPILLANTINI, M. G., THOMAS, G. M., BUEE-SCHERRER, V., COHEN, P. & GOEDERT, M. 1999. Stress-activated protein kinase-3 interacts with the PDZ domain of alpha1-syntrophin. A mechanism for specific substrate recognition. *J Biol Chem*, 274, 12626-31.
- HELLIWELL, T. R., MAN, N. T., MORRIS, G. E. & DAVIES, K. E. 1992. The dystrophin-related protein, utrophin, is expressed on the sarcolemma of regenerating

- human skeletal muscle fibres in dystrophies and inflammatory myopathies. *Neuromuscul Disord*, 2, 177-84.
- HEMLER, M. E. 2001. Specific tetraspanin functions. *J Cell Biol*, 155, 1103-7.
- HENRY, C. A. & AMACHER, S. L. 2004. Zebrafish slow muscle cell migration induces a wave of fast muscle morphogenesis. *Dev Cell*, 7, 917-23.
- HOFFMAN, E. P., BROWN, R. H., JR. & KUNKEL, L. M. 1987. Dystrophin: the protein product of the Duchenne muscular dystrophy locus. *Cell*, 51, 919-28.
- HOFFMAN, E. P., REEVES, E., DAMSKER, J., NAGARAJU, K., MCCALL, J. M., CONNOR, E. M. & BUSHBY, K. 2012. Novel approaches to corticosteroid treatment in Duchenne muscular dystrophy. *Phys Med Rehabil Clin N Am*, 23, 821-8.
- HOLT, K. H. & CAMPBELL, K. P. 1998. Assembly of the sarcoglycan complex. Insights for muscular dystrophy. *J Biol Chem*, 273, 34667-70.
- HOLT, K. H., CROSBIE, R. H., VENZKE, D. P. & CAMPBELL, K. P. 2000. Biosynthesis of dystroglycan: processing of a precursor propeptide. *FEBS Lett*, 468, 79-83.
- HOYTE, K., JAYASINHA, V., XIA, B. & MARTIN, P. T. 2004. Transgenic overexpression of dystroglycan does not inhibit muscular dystrophy in mdx mice. *Am J Pathol*, 164, 711-8.
- HUANG, X., POY, F., ZHANG, R., JOACHIMIAK, A., SUDOL, M. & ECK, M. J. 2000. Structure of a WW domain containing fragment of dystrophin in complex with beta-dystroglycan. *Nat Struct Biol*, 7, 634-8.
- IBRAGHIMOV-BESKROVNAYA, O., ERVASTI, J., LEVEILLE, C., SLAUGHTER, C., SERNETT, S. & CAMPBELL, K. 1992. Primary structure of dystrophin-associated glycoproteins linking dystrophin to the extracellular matrix. *Nature*, 355, 696-702.
- ILSLEY, J. L., SUDOL, M. & WINDER, S. J. 2001. The interaction of dystrophin with beta-dystroglycan is regulated by tyrosine phosphorylation. *Cell Signal*, 13, 625-32.
- ILSLEY, J. L., SUDOL, M. & WINDER, S. J. 2002. The WW domain: linking cell signalling to the membrane cytoskeleton. *Cell Signal*, 14, 183-9.
- ISHIKAWA-SAKURAI, M., YOSHIDA, M., IMAMURA, M., DAVIES, K. E. & OZAWA, E. 2004. ZZ domain is essentially required for the physiological binding of dystrophin and utrophin to beta-dystroglycan. *Hum Mol Genet*, 13, 693-702.
- JACOBS, S. C., BOOTSMA, A. L., WILLEMS, P. W., BAR, P. R. & WOKKE, J. H. 1996. Prednisone can protect against exercise-induced muscle damage. *J Neurol*, 243, 410-6.
- JAMART, C., RAYMACKERS, J. M., LI AN, G., DELDICQUE, L. & FRANCAUX, M. 2011. Prevention of muscle disuse atrophy by MG132 proteasome inhibitor. *Muscle Nerve*, 43, 708-16.
- JAMES, M., NGUYEN, T. M., WISE, C. J., JONES, G. E. & MORRIS, G. E. 1996. Utrophin-dystroglycan complex in membranes of adherent cultured cells. *Cell Motil Cytoskeleton*, 33, 163-74.
- JAMES, M., NUTTALL, A., ILSLEY, J. L., OTTERSBAACH, K., TINSLEY, J. M., SUDOL, M. & WINDER, S. J. 2000. Adhesion-dependent tyrosine phosphorylation of (beta)-dystroglycan regulates its interaction with utrophin. *J Cell Sci*, 113 ( Pt 10), 1717-26.
- KABASHI, E., AGAR, J. N., TAYLOR, D. M., MINOTTI, S. & DURHAM, H. D. 2004. Focal dysfunction of the proteasome: a pathogenic factor in a mouse model of amyotrophic lateral sclerosis. *J Neurochem*, 89, 1325-35.
- KANAGAWA, M., SAITO, F., KUNZ, S., YOSHIDA-MORIGUCHI, T., BARRESI, R., KOBAYASHI, Y. M., MUSCHLER, J., DUMANSKI, J. P., MICHELE, D. E., OLDSTONE,

- M. B. & CAMPBELL, K. P. 2004. Molecular recognition by LARGE is essential for expression of functional dystroglycan. *Cell*, 117, 953-64.
- KARPATI, G., AJDUKOVIC, D., ARNOLD, D., GLEDHILL, R. B., GUTTMANN, R., HOLLAND, P., KOCH, P. A., SHOUBRIDGE, E., SPENCE, D., VANASSE, M. & ET AL. 1993a. Myoblast transfer in Duchenne muscular dystrophy. *Ann Neurol*, 34, 8-17.
- KARPATI, G., CARPENTER, S., MORRIS, G. E., DAVIES, K. E., GUERIN, C. & HOLLAND, P. 1993b. Localization and quantitation of the chromosome 6-encoded dystrophin-related protein in normal and pathological human muscle. *J Neuropathol Exp Neurol*, 52, 119-28.
- KAWAHARA, G., GUYON, J. R., NAKAMURA, Y. & KUNKEL, L. M. 2010. Zebrafish models for human FKRP muscular dystrophies. *Hum Mol Genet*, 19, 623-33.
- KAWAHARA, G., KARPFF, J. A., MYERS, J. A., ALEXANDER, M. S., GUYON, J. R. & KUNKEL, L. M. 2011. Drug screening in a zebrafish model of Duchenne muscular dystrophy. *Proc Natl Acad Sci U S A*, 108, 5331-6.
- KELLER, J. N., HANNI, K. B. & MARKESBERY, W. R. 2000. Impaired proteasome function in Alzheimer's disease. *J Neurochem*, 75, 436-9.
- KHURANA, T. S., WATKINS, S. C., CHAFEY, P., CHELLY, J., TOME, F. M., FARDEAU, M., KAPLAN, J. C. & KUNKEL, L. M. 1991. Immunolocalization and developmental expression of dystrophin related protein in skeletal muscle. *Neuromuscul Disord*, 1, 185-94.
- KIMMEL, C. B., BALLARD, W. W., KIMMEL, S. R., ULLMANN, B. & SCHILLING, T. F. 1995. Stages of embryonic development of the zebrafish. *Dev Dyn*, 203, 253-310.
- KIMMEL, C. B., PATTERSON, J. & KIMMEL, R. O. 1974. The development and behavioral characteristics of the startle response in the zebra fish. *Dev Psychobiol*, 7, 47-60.
- KINALI, M., ARECHAVALA-GOMEZA, V., FENG, L., CIRAK, S., HUNT, D., ADKIN, C., GUGLIERI, M., ASHTON, E., ABBS, S., NIHOYANNOPOULOS, P., GARRALDA, M. E., RUTHERFORD, M., MCCULLEY, C., POPPLEWELL, L., GRAHAM, I. R., DICKSON, G., WOOD, M. J., WELLS, D. J., WILTON, S. D., KOLE, R., STRAUB, V., BUSHBY, K., SEWRY, C., MORGAN, J. E. & MUNTONI, F. 2009. Local restoration of dystrophin expression with the morpholino oligomer AVI-4658 in Duchenne muscular dystrophy: a single-blind, placebo-controlled, dose-escalation, proof-of-concept study. *Lancet Neurol*, 8, 918-28.
- KISSEL, J. T., BURROW, K. L., RAMMOHAN, K. W. & MENDELL, J. R. 1991. Mononuclear cell analysis of muscle biopsies in prednisone-treated and untreated Duchenne muscular dystrophy. CIDD Study Group. *Neurology*, 41, 667-72.
- KLAMUT, H. J., GANGOPADHYAY, S. B., WORTON, R. G. & RAY, P. N. 1990. Molecular and functional analysis of the muscle-specific promoter region of the Duchenne muscular dystrophy gene. *Mol Cell Biol*, 10, 193-205.
- KLEOPA, K. A., DROUSIOTOU, A., MAVRIKIOU, E., ORMISTON, A. & KYRIAKIDES, T. 2006. Naturally occurring utrophin correlates with disease severity in Duchenne muscular dystrophy. *Hum Mol Genet*, 15, 1623-8.
- KLOHS, W. D., FRY, D. W. & KRAKER, A. J. 2007. Inhibitors of tyrosine kinase. *Curr Opin Oncol*, 9, 562-8.
- KOBAYASHI, Y. M., RADER, E. P., CRAWFORD, R. W. & CAMPBELL, K. P. 2012. Endpoint measures in the mdx mouse relevant for muscular dystrophy pre-clinical studies. *Neuromuscul Disord*, 22, 34-42.
- KOENIG, M., BEGGS, A. H., MOYER, M., SCHERPF, S., HEINDRICH, K., BETTECKEN, T., MENG, G., MULLER, C. R., LINDLOF, M., KAARIAINEN, H. & ET AL. 1989. The

- molecular basis for Duchenne versus Becker muscular dystrophy: correlation of severity with type of deletion. *Am J Hum Genet*, 45, 498-506.
- KOENIG, M., HOFFMAN, E. P., BERTELSON, C. J., MONACO, A. P., FEENER, C. & KUNKEL, L. M. 1987. Complete cloning of the Duchenne muscular dystrophy (DMD) cDNA and preliminary genomic organization of the DMD gene in normal and affected individuals. *Cell*, 50, 509-17.
- KOENIG, M. & KUNKEL, L. M. 1990. Detailed analysis of the repeat domain of dystrophin reveals four potential hinge segments that may confer flexibility. *J Biol Chem*, 265, 4560-6.
- KOENIG, M., MONACO, A. P. & KUNKEL, L. M. 1988. The complete sequence of dystrophin predicts a rod-shaped cytoskeletal protein. *Cell*, 53, 219-28.
- KOMINAMI, E., KUNIO, I. & KATUNUMA, N. 1987. Activation of the intramyofibrillar autophagic-lysosomal system in muscular dystrophy. *Am J Pathol*, 127, 461-6.
- KONTZIAS, A., LAURENCE, A., GADINA, M. & O'SHEA, J. J. 2012. Kinase inhibitors in the treatment of immune-mediated disease. *F1000 Med Rep*, 4, 5.
- KORNEGAY, J. N., TULER, S. M., MILLER, D. M. & LEVESQUE, D. C. 1988. Muscular dystrophy in a litter of golden retriever dogs. *Muscle Nerve*, 11, 1056-64.
- KUMAMOTO, T., FUJIMOTO, S., ITO, T., HORINOUCHE, H., UEYAMA, H. & TSUDA, T. 2000. Proteasome expression in the skeletal muscles of patients with muscular dystrophy. *Acta Neuropathol*, 100, 595-602.
- LAI, Y., ZHAO, J., YUE, Y. & DUAN, D. 2013. alpha2 and alpha3 helices of dystrophin R16 and R17 form a microdomain in the alpha1 helix of dystrophin R17 for neuronal NOS binding. *Proc Natl Acad Sci U S A*, 110, 525-30.
- LARA-CHACON, B., DE LEON, M. B., LEOCADIO, D., GOMEZ, P., FUENTES-MERA, L., MARTINEZ-VIEYRA, I., ORTEGA, A., JANS, D. A. & CISNEROS, B. 2010. Characterization of an Importin alpha/beta-recognized nuclear localization signal in beta-dystroglycan. *J Cell Biochem*, 110, 706-17.
- LAVAL, S. H. & BUSHBY, K. M. 2004. Limb-girdle muscular dystrophies--from genetics to molecular pathology. *Neuropathol Appl Neurobiol*, 30, 91-105.
- LAWRENCE, T. 2009. The nuclear factor NF-kappaB pathway in inflammation. *Cold Spring Harb Perspect Biol*, 1, a001651.
- LEBAKKEN, C. S., VENZKE, D. P., HRSTKA, R. F., CONSOLINO, C. M., FAULKNER, J. A., WILLIAMSON, R. A. & CAMPBELL, K. P. 2000. Sarcospan-deficient mice maintain normal muscle function. *Mol Cell Biol*, 20, 1669-77.
- LEBLANC, R., CATLEY, L. P., HIDESHIMA, T., LENTZSCH, S., MITSIADES, C. S., MITSIADES, N., NEUBERG, D., GOLOUBEVA, O., PIEN, C. S., ADAMS, J., GUPTA, D., RICHARDSON, P. G., MUNSHI, N. C. & ANDERSON, K. C. 2002. Proteasome inhibitor PS-341 inhibits human myeloma cell growth in vivo and prolongs survival in a murine model. *Cancer Res*, 62, 4996-5000.
- LEE, D. H. & GOLDBERG, A. L. 1998. Proteasome inhibitors: valuable new tools for cell biologists. *Trends Cell Biol*, 8, 397-403.
- LEVITZKI, A. 2013. Tyrosine kinase inhibitors: views of selectivity, sensitivity, and clinical performance. *Annu Rev Pharmacol Toxicol*, 53, 161-85.
- LIDOV, H. G., SELIG, S. & KUNKEL, L. M. 1995. Dp140: a novel 140 kDa CNS transcript from the dystrophin locus. *Hum Mol Genet*, 4, 329-35.
- LIESCHKE, G. J. & CURRIE, P. D. 2007. Animal models of human disease: zebrafish swim into view. *Nat Rev Genet*, 8, 353-67.
- LIN, Y. Y. 2012. Muscle diseases in the zebrafish. *Neuromuscul Disord*, 22, 673-84.

- LIN, Y. Y., WHITE, R. J., TORELLI, S., CIRAK, S., MUNTONI, F. & STEMPLE, D. L. 2011. Zebrafish Fukutin family proteins link the unfolded protein response with dystroglycanopathies. *Hum Mol Genet*, 20, 1763-75.
- LOMBARDO, L. J., LEE, F. Y., CHEN, P., NORRIS, D., BARRISH, J. C., BEHNIA, K., CASTANEDA, S., CORNELIUS, L. A., DAS, J., DOWEYKO, A. M., FAIRCHILD, C., HUNT, J. T., INIGO, I., JOHNSTON, K., KAMATH, A., KAN, D., KLEI, H., MARATHE, P., PANG, S., PETERSON, R., PITT, S., SCHIEVEN, G. L., SCHMIDT, R. J., TOKARSKI, J., WEN, M. L., WITYAK, J. & BORZILLERI, R. M. 2004. Discovery of N-(2-chloro-6-methyl-phenyl)-2-(6-(4-(2-hydroxyethyl)-piperazin-1-yl)-2-methylpyrimidin-4-ylamino)thiazole-5-carboxamide (BMS-354825), a dual Src/Abl kinase inhibitor with potent antitumor activity in preclinical assays. *J Med Chem*, 47, 6658-61.
- LONGVA, K. E., BLYSTAD, F. D., STANG, E., LARSEN, A. M., JOHANNESSEN, L. E. & MADSHUS, I. H. 2002. Ubiquitination and proteasomal activity is required for transport of the EGF receptor to inner membranes of multivesicular bodies. *J Cell Biol*, 156, 843-54.
- LOVE, D. R., HILL, D. F., DICKSON, G., SPURR, N. K., BYTH, B. C., MARSDEN, R. F., WALSH, F. S., EDWARDS, Y. H. & DAVIES, K. E. 1989. An autosomal transcript in skeletal muscle with homology to dystrophin. *Nature*, 339, 55-8.
- LUO, F. R., YANG, Z., CAMUSO, A., SMYKLA, R., MCGLINCHEY, K., FAGER, K., FLEFLEH, C., CASTANEDA, S., INIGO, I., KAN, D., WEN, M. L., KRAMER, R., BLACKWOOD-CHIRCHIR, A. & LEE, F. Y. 2006. Dasatinib (BMS-354825) pharmacokinetics and pharmacodynamic biomarkers in animal models predict optimal clinical exposure. *Clin Cancer Res*, 12, 7180-6.
- MACPHAIL, R. C., BROOKS, J., HUNTER, D. L., PADNOS, B., IRONS, T. D. & PADILLA, S. 2009. Locomotion in larval zebrafish: Influence of time of day, lighting and ethanol. *Neurotoxicology*, 30, 52-8.
- MARSHALL, J. L., CHOU, E., OH, J., KWOK, A., BURKIN, D. J. & CROSBIE-WATSON, R. H. 2012. Dystrophin and utrophin expression require sarcospan: loss of alpha7 integrin exacerbates a newly discovered muscle phenotype in sarcospan-null mice. *Hum Mol Genet*, 21, 4378-93.
- MATSUMURA, K., ERVASTI, J. M., OHLENDIECK, K., KAHL, S. D. & CAMPBELL, K. P. 1992. Association of dystrophin-related protein with dystrophin-associated proteins in mdx mouse muscle. *Nature*, 360, 588-91.
- MCDONALD, C. M., HENRICSON, E. K., HAN, J. J., ABRESCH, R. T., NICORICI, A., ELFRING, G. L., ATKINSON, L., REHA, A., HIRAWAT, S. & MILLER, L. L. 2010. The 6-minute walk test as a new outcome measure in Duchenne muscular dystrophy. *Muscle Nerve*, 41, 500-510.
- MCNAUGHT, K. S., OLANOW, C. W., HALLIWELL, B., ISACSON, O. & JENNER, P. 2001. Failure of the ubiquitin-proteasome system in Parkinson's disease. *Nat Rev Neurosci*, 2, 589-94.
- MENDELL, J. R., CAMPBELL, K., RODINO-KLAPAC, L., SAHENK, Z., SHILLING, C., LEWIS, S., BOWLES, D., GRAY, S., LI, C., GALLOWAY, G., MALIK, V., COLEY, B., CLARK, K. R., LI, J., XIAO, X., SAMULSKI, J., MCPHEE, S. W., SAMULSKI, R. J. & WALKER, C. M. 2010. Dystrophin immunity in Duchenne's muscular dystrophy. *N Engl J Med*, 363, 1429-37.
- MENDELL, J. R., KISSEL, J. T., AMATO, A. A., KING, W., SIGNORE, L., PRIOR, T. W., SAHENK, Z., BENSON, S., MCANDREW, P. E., RICE, R. & ET AL. 1995. Myoblast transfer in the treatment of Duchenne's muscular dystrophy. *N Engl J Med*, 333, 832-8.

- MESSINA, S., BITTO, A., AGUENNOUZ, M., MINUTOLI, L., MONICI, M. C., ALTAVILLA, D., SQUADRITO, F. & VITA, G. 2006. Nuclear factor kappa-B blockade reduces skeletal muscle degeneration and enhances muscle function in Mdx mice. *Exp Neurol*, 198, 234-41.
- MICHELE, D., BARRESI, R., KANAGAWA, M., SAITO, F., COHN, R., SATZ, J., DOLLAR, J., NISHINO, I., KELLEY, R., SOMER, H., STRAUB, V., MATHEWS, K., MOORE, S. & CAMPBELL, K. 2002a. Post-translational disruption of dystroglycan-ligand interactions in congenital muscular dystrophies. *Nature*, 418, 417-422.
- MICHELE, D. E., BARRESI, R., KANAGAWA, M., SAITO, F., COHN, R. D., SATZ, J. S., DOLLAR, J., NISHINO, I., KELLEY, R. I., SOMER, H., STRAUB, V., MATHEWS, K. D., MOORE, S. A. & CAMPBELL, K. P. 2002b. Post-translational disruption of dystroglycan-ligand interactions in congenital muscular dystrophies. *Nature*, 418, 417-22.
- MILLER, G., MOORE, C. J., TERRY, R., LA RIVIERE, T., MITCHELL, A., PIGGOTT, R., DEAR, T. N., WELLS, D. J. & WINDER, S. J. 2012. Preventing phosphorylation of dystroglycan ameliorates the dystrophic phenotype in mdx mouse. *Hum Mol Genet*, 21, 4508-20.
- MITCH, W. E. & GOLDBERG, A. L. 1996. Mechanisms of muscle wasting. The role of the ubiquitin-proteasome pathway. *N Engl J Med*, 335, 1897-905.
- MONACO, A. P., BERTELSON, C. J., LIECHTI-GALLATI, S., MOSER, H. & KUNKEL, L. M. 1988. An explanation for the phenotypic differences between patients bearing partial deletions of the DMD locus. *Genomics*, 2, 90-5.
- MONACO, A. P., WALKER, A. P., MILLWOOD, I., LARIN, Z. & LEHRACH, H. 1992. A yeast artificial chromosome contig containing the complete Duchenne muscular dystrophy gene. *Genomics*, 12, 465-73.
- MOORE, C. J., GOH, H. T. & HEWITT, J. E. 2008. Genes required for functional glycosylation of dystroglycan are conserved in zebrafish. *Genomics*, 92, 159-67.
- MOORE, C. J. & HEWITT, J. E. 2009. Dystroglycan glycosylation and muscular dystrophy. *Glycoconj J*, 26, 349-57.
- MOORE, C. J. & WINDER, S. J. 2010. Dystroglycan versatility in cell adhesion: a tale of multiple motifs. *Cell Commun Signal*, 8, 3.
- MORGAN, J. E., BEAUCHAMP, J. R., PAGEL, C. N., PECKHAM, M., ATALIOTIS, P., JAT, P. S., NOBLE, M. D., FARMER, K. & PARTRIDGE, T. A. 1994. Myogenic cell lines derived from transgenic mice carrying a thermolabile T antigen: a model system for the derivation of tissue-specific and mutation-specific cell lines. *Dev Biol*, 162, 486-98.
- MORRIS, G. E., SEDGWICK, S. G., ELLIS, J. M., PEREBOEV, A., CHAMBERLAIN, J. S. & NGUYEN THI, M. 1998. An epitope structure for the C-terminal domain of dystrophin and utrophin. *Biochemistry*, 37, 11117-27.
- MUNTONI, F., BROCKINGTON, M., TORELLI, S. & BROWN, S. C. 2004. Defective glycosylation in congenital muscular dystrophies. *Curr Opin Neurol*, 17, 205-9.
- MUNTONI, F., TORELLI, S., WELLS, D. J. & BROWN, S. C. 2011. Muscular dystrophies due to glycosylation defects: diagnosis and therapeutic strategies. *Curr Opin Neurol*, 24, 437-42.
- NADARAJAH, V. D., VAN PUTTEN, M., CHAOUCH, A., GARROOD, P., STRAUB, V., LOCHMULLER, H., GINJAAR, H. B., AARTSMA-RUS, A. M., VAN OMMEN, G. J., DEN DUNNEN, J. T. & T HOEN, P. A. 2011. Serum matrix metalloproteinase-9 (MMP-9) as a biomarker for monitoring disease progression in Duchenne muscular dystrophy (DMD). *Neuromuscul Disord*, 21, 569-78.

- NEELY, J. D., AMIRY-MOGHADDAM, M., OTTERSEN, O. P., FROEHNER, S. C., AGRE, P. & ADAMS, M. E. 2001. Syntrophin-dependent expression and localization of Aquaporin-4 water channel protein. *Proc Natl Acad Sci U S A*, 98, 14108-13.
- NEWBY, S. E., BENSON, M. A., PONTING, C. P., DAVIES, K. E. & BLAKE, D. J. 2000. Alternative splicing of dystrobrevin regulates the stoichiometry of syntrophin binding to the dystrophin protein complex. *Curr Biol*, 10, 1295-8.
- NGUYEN, H. H., JAYASINHA, V., XIA, B., HOYTE, K. & MARTIN, P. T. 2002. Overexpression of the cytotoxic T cell GalNAc transferase in skeletal muscle inhibits muscular dystrophy in mdx mice. *Proc Natl Acad Sci U S A*, 99, 5616-21.
- NGUYEN, T. M., ELLIS, J. M., LOVE, D. R., DAVIES, K. E., GATTER, K. C., DICKSON, G. & MORRIS, G. E. 1991. Localization of the DMDL gene-encoded dystrophin-related protein using a panel of nineteen monoclonal antibodies: presence at neuromuscular junctions, in the sarcolemma of dystrophic skeletal muscle, in vascular and other smooth muscles, and in proliferating brain cell lines. *J Cell Biol*, 115, 1695-700.
- NGUYEN, T. M., GINJAAR, I. B., VAN OMMEN, G. J. & MORRIS, G. E. 1992. Monoclonal antibodies for dystrophin analysis. Epitope mapping and improved binding to SDS-treated muscle sections. *Biochem J*, 288 ( Pt 2), 663-8.
- NIXON, S. J., WEGNER, J., FERGUSON, C., MERY, P. F., HANCOCK, J. F., CURRIE, P. D., KEY, B., WESTERFIELD, M. & PARTON, R. G. 2005. Zebrafish as a model for caveolin-associated muscle disease; caveolin-3 is required for myofibril organization and muscle cell patterning. *Hum Mol Genet*, 14, 1727-43.
- NUDEL, U., ROBZYK, K. & YAFFE, D. 1988. Expression of the putative Duchenne muscular dystrophy gene in differentiated myogenic cell cultures and in the brain. *Nature*, 331, 635-8.
- NUDEL, U., ZUK, D., EINAT, P., ZEELON, E., LEVY, Z., NEUMAN, S. & YAFFE, D. 1989. Duchenne muscular dystrophy gene product is not identical in muscle and brain. *Nature*, 337, 76-8.
- NÜSSLEIN-VOLHARD, C. & DAHM, R. 2002. *Zebrafish: A Practical Approach*, Oxford University Press.
- OAK, S. A., RUSSO, K., PETRUCCI, T. C. & JARRETT, H. W. 2001. Mouse alpha1-syntrophin binding to Grb2: further evidence of a role for syntrophin in cell signaling. *Biochemistry*, 40, 11270-8.
- OHLENDIECK, K. & CAMPBELL, K. P. 1991. Dystrophin-associated proteins are greatly reduced in skeletal muscle from mdx mice. *J Cell Biol*, 115, 1685-94.
- OHLENDIECK, K., MATSUMURA, K., IONASESCU, V. V., TOWBIN, J. A., BOSCH, E. P., WEINSTEIN, S. L., SERNETT, S. W. & CAMPBELL, K. P. 1993. Duchenne muscular dystrophy: deficiency of dystrophin-associated proteins in the sarcolemma. *Neurology*, 43, 795-800.
- OZAWA, E., MIZUNO, Y., HAGIWARA, Y., SASAOKA, T. & YOSHIDA, M. 2005. Molecular and cell biology of the sarcoglycan complex. *Muscle Nerve*, 32, 563-76.
- PADILLA, S., HUNTER, D., PADNOS, B., FRADY, S. & MACPHAIL, R. 2011. Assessing locomotor activity in larval zebrafish: Influence of extrinsic and intrinsic variables. *Neurotoxicol Teratol*, 33, 624-630.
- PARSONS, M. J., CAMPOS, I., HIRST, E. M. & STEMPEL, D. L. 2002. Removal of dystroglycan causes severe muscular dystrophy in zebrafish embryos. *Development*, 129, 3505-12.

- PARTRIDGE, T. A., MORGAN, J. E., COULTON, G. R., HOFFMAN, E. P. & KUNKEL, L. M. 1989. Conversion of mdx myofibres from dystrophin-negative to -positive by injection of normal myoblasts. *Nature*, 337, 176-9.
- PERCIVAL, J. M., WHITEHEAD, N. P., ADAMS, M. E., ADAMO, C. M., BEAVO, J. A. & FROEHLER, S. C. 2012. Sildenafil reduces respiratory muscle weakness and fibrosis in the mdx mouse model of Duchenne muscular dystrophy. *J Pathol*, 228, 77-87.
- PEREBOEV, A. V., AHMED, N., THI MAN, N. & MORRIS, G. E. 2001. Epitopes in the interacting regions of beta-dystroglycan (PPxY motif) and dystrophin (WW domain). *Biochim Biophys Acta*, 1527, 54-60.
- PETERSON, J. M. & GUTTRIDGE, D. C. 2008. Skeletal muscle diseases, inflammation, and NF-kappaB signaling: insights and opportunities for therapeutic intervention. *Int Rev Immunol*, 27, 375-87.
- PETERSON, J. M., KLINE, W., CANAN, B. D., RICCA, D. J., KASPAR, B., DELFIN, D. A., DIRIENZO, K., CLEMENS, P. R., ROBBINS, P. D., BALDWIN, A. S., FLOOD, P., KAUMAYA, P., FREITAS, M., KORNEGAY, J. N., MENDELL, J. R., RAFAEL-FORTNEY, J. A., GUTTRIDGE, D. C. & JANSSEN, P. M. 2011. Peptide-based inhibition of NF-kappaB rescues diaphragm muscle contractile dysfunction in a murine model of Duchenne muscular dystrophy. *Mol Med*, 17, 508-15.
- PIROZZI, G., MCCONNELL, S. J., UVEGES, A. J., CARTER, J. M., SPARKS, A. B., KAY, B. K. & FOWLKES, D. M. 1997. Identification of novel human WW domain-containing proteins by cloning of ligand targets. *J Biol Chem*, 272, 14611-6.
- PONTING, C. P., BLAKE, D. J., DAVIES, K. E., KENDRICK-JONES, J. & WINDER, S. J. 1996. ZZ and TAZ: new putative zinc fingers in dystrophin and other proteins. *Trends Biochem Sci*, 21, 11-13.
- PROBER, D. A., RIHEL, J., ONAH, A. A., SUNG, R. J. & SCHIER, A. F. 2006. Hypocretin/orexin overexpression induces an insomnia-like phenotype in zebrafish. *J Neurosci*, 26, 13400-10.
- RENTSCHLER, S., LINN, H., DEININGER, K., BEDFORD, M. T., ESPANEL, X. & SUDOL, M. 1999. The WW domain of dystrophin requires EF-hands region to interact with beta-dystroglycan. *Biol Chem*, 380, 431-42.
- REZNICZEK, G. A., KONIECZNY, P., NIKOLIC, B., REIPERT, S., SCHNELLER, D., ABRAHAMSBURG, C., DAVIES, K. E., WINDER, S. J. & WICHE, G. 2007. Plectin 1f scaffolding at the sarcolemma of dystrophic (mdx) muscle fibers through multiple interactions with beta-dystroglycan. *J Cell Biol*, 176, 965-77.
- RHEN, T. & CIDLOWSKI, J. A. 2005. Antiinflammatory action of glucocorticoids--new mechanisms for old drugs. *N Engl J Med*, 353, 1711-23.
- RICHARDSON, P. G., SONNEVELD, P., SCHUSTER, M. W., IRWIN, D., STADTMAUER, E. A., FACON, T., HAROUSSEAU, J. L., BEN-YEHUDA, D., LONIAL, S., GOLDSCHMIDT, H., REECE, D., SAN-MIGUEL, J. F., BLADE, J., BOCCADORO, M., CAVENAGH, J., DALTON, W. S., BORAL, A. L., ESSELTINE, D. L., PORTER, J. B., SCHENKEIN, D., ANDERSON, K. C. & ASSESSMENT OF PROTEASOME INHIBITION FOR EXTENDING REMISSIONS, I. 2005. Bortezomib or high-dose dexamethasone for relapsed multiple myeloma. *N Engl J Med*, 352, 2487-98.
- ROBERTS, R. G., COFFEY, A. J., BOBROW, M. & BENTLEY, D. R. 1993. Exon structure of the human dystrophin gene. *Genomics*, 16, 536-8.
- ROUGIER, J. S., GAVILLET, B. & ABRIEL, H. 2013. Proteasome inhibitor (MG132) rescues Nav1.5 protein content and the cardiac sodium current in dystrophin-deficient mdx (5cv) mice. *Front Physiol*, 4, 51.

- RYBAKOVA, I. N., AMANN, K. J. & ERVASTI, J. M. 1996. A new model for the interaction of dystrophin with F-actin. *J Cell Biol*, 135, 661-72.
- RYBAKOVA, I. N. & ERVASTI, J. M. 1997. Dystrophin-glycoprotein complex is monomeric and stabilizes actin filaments in vitro through a lateral association. *J Biol Chem*, 272, 28771-8.
- SAINT-AMANT, L. & DRAPEAU, P. 1998. Time course of the development of motor behaviors in the zebrafish embryo. *J Neurobiol*, 37, 622-32.
- SAMPAOLESI, M., BLOT, S., D'ANTONA, G., GRANGER, N., TONLORENZI, R., INNOCENZI, A., MOGNOL, P., THIBAUD, J. L., GALVEZ, B. G., BARTHELEMY, I., PERANI, L., MANTERO, S., GUTTINGER, M., PANSARASA, O., RINALDI, C., CUSELLA DE ANGELIS, M. G., TORRENTE, Y., BORDIGNON, C., BOTTINELLI, R. & COSSU, G. 2006. Mesoangioblast stem cells ameliorate muscle function in dystrophic dogs. *Nature*, 444, 574-9.
- SANDER, M., CHAVOSHAN, B., HARRIS, S. A., IANNACCONE, S. T., STULL, J. T., THOMAS, G. D. & VICTOR, R. G. 2000. Functional muscle ischemia in neuronal nitric oxide synthase-deficient skeletal muscle of children with Duchenne muscular dystrophy. *Proc Natl Acad Sci U S A*, 97, 13818-23.
- SATZ, J. S., BARRESI, R., DURBEEJ, M., WILLER, T., TURNER, A., MOORE, S. A. & CAMPBELL, K. P. 2008. Brain and eye malformations resembling Walker-Warburg syndrome are recapitulated in mice by dystroglycan deletion in the epiblast. *J Neurosci*, 28, 10567-75.
- SCHULTZ, J., HOFFMULLER, U., KRAUSE, G., ASHURST, J., MACIAS, M. J., SCHMIEDER, P., SCHNEIDER-MERGENER, J. & OSCHKINAT, H. 1998. Specific interactions between the syntrophin PDZ domain and voltage-gated sodium channels. *Nat Struct Biol*, 5, 19-24.
- SELSBY, J., MORRIS, C., MORRIS, L. & SWEENEY, L. 2012. A proteasome inhibitor fails to attenuate dystrophic pathology in mdx mice. *PLoS Curr*, 4, e4f84a944d8930.
- SELSBY, J., PENDRAK, K., ZADEL, M., TIAN, Z., PHAM, J., CARVER, T., ACOSTA, P., BARTON, E. & SWEENEY, H. L. 2010. Leupeptin-based inhibitors do not improve the mdx phenotype. *Am J Physiol Regul Integr Comp Physiol*, 299, R1192-201.
- SICINSKI, P., GENG, Y., RYDER-COOK, A. S., BARNARD, E. A., DARLISON, M. G. & BARNARD, P. J. 1989. The molecular basis of muscular dystrophy in the mdx mouse: a point mutation. *Science*, 244, 1578-80.
- SOTGIA, F., BONUCCELLI, G., BEDFORD, M., BRANCACCIO, A., MAYER, U., WILSON, M. T., CAMPOS-GONZALEZ, R., BROOKS, J. W., SUDOL, M. & LISANTI, M. P. 2003. Localization of phospho-beta-dystroglycan (pY892) to an intracellular vesicular compartment in cultured cells and skeletal muscle fibers in vivo. *Biochemistry*, 42, 7110-23.
- SOTGIA, F., LEE, H., BEDFORD, M. T., PETRUCCI, T., SUDOL, M. & LISANTI, M. P. 2001. Tyrosine phosphorylation of beta-dystroglycan at its WW domain binding motif, PPxY, recruits SH2 domain containing proteins. *Biochemistry*, 40, 14585-92.
- SOTGIA, F., LEE, J. K., DAS, K., BEDFORD, M., PETRUCCI, T. C., MACIOCE, P., SARGIACOMO, M., BRICARELLI, F. D., MINETTI, C., SUDOL, M. & LISANTI, M. P. 2000. Caveolin-3 directly interacts with the C-terminal tail of beta - dystroglycan. Identification of a central WW-like domain within caveolin family members. *J Biol Chem*, 275, 38048-58.
- SPENCE, H. J., DHILLON, A. S., JAMES, M. & WINDER, S. J. 2004. Dystroglycan, a scaffold for the ERK-MAP kinase cascade. *EMBO Rep*, 5, 484-9.

- SPENCER, M. J., CROALL, D. E. & TIDBALL, J. G. 1995. Calpains are activated in necrotic fibers from mdx dystrophic mice. *J Biol Chem*, 270, 10909-14.
- SPENCER, M. J. & MELLGREN, R. L. 2002. Overexpression of a calpastatin transgene in mdx muscle reduces dystrophic pathology. *Hum Mol Genet*, 11, 2645-55.
- STEDMAN, H. H., SWEENEY, H. L., SHRAGER, J. B., MAGUIRE, H. C., PANETTIERI, R. A., PETROF, B., NARUSAWA, M., LEFEROVICH, J. M., SLADKY, J. T. & KELLY, A. M. 1991. The mdx mouse diaphragm reproduces the degenerative changes of Duchenne muscular dystrophy. *Nature*, 352, 536-9.
- STEFFEN, L. S., GUYON, J. R., VOGEL, E. D., BELTRE, R., PUSACK, T. J., ZHOU, Y., ZON, L. I. & KUNKEL, L. M. 2007. Zebrafish orthologs of human muscular dystrophy genes. *BMC Genomics*, 8, 79.
- STEMPLE, D. L. 2004. TILLING--a high-throughput harvest for functional genomics. *Nat Rev Genet*, 5, 145-50.
- TAKAMATSU, H., YAMASHITA, T., KOTANI, T., SAWAZAKI, A., OKUMURA, H. & NAKAO, S. 2010. Ischemic heart disease associated with bortezomib treatment combined with dexamethasone in a patient with multiple myeloma. *Int J Hematol*, 91, 903-6.
- TAKEDA, S., KONDO, M., SASAKI, J., KURAHASHI, H., KANO, H., ARAI, K., MISAKI, K., FUKUI, T., KOBAYASHI, K., TACHIKAWA, M., IMAMURA, M., NAKAMURA, Y., SHIMIZU, T., MURAKAMI, T., SUNADA, Y., FUJIKADO, T., MATSUMURA, K., TERASHIMA, T. & TODA, T. 2003. Fukutin is required for maintenance of muscle integrity, cortical histiogenesis and normal eye development. *Hum Mol Genet*, 12, 1449-59.
- TANABE, Y., ESAKI, K. & NOMURA, T. 1986. Skeletal muscle pathology in X chromosome-linked muscular dystrophy (mdx) mouse. *Acta Neuropathol*, 69, 91-5.
- TAWA, N. E., JR., ODESSEY, R. & GOLDBERG, A. L. 1997. Inhibitors of the proteasome reduce the accelerated proteolysis in atrophying rat skeletal muscles. *J Clin Invest*, 100, 197-203.
- THOMAS, G. D., SANDER, M., LAU, K. S., HUANG, P. L., STULL, J. T. & VICTOR, R. G. 1998. Impaired metabolic modulation of alpha-adrenergic vasoconstriction in dystrophin-deficient skeletal muscle. *Proc Natl Acad Sci U S A*, 95, 15090-5.
- THORNHILL, P., BASSETT, D., LOCHMULLER, H., BUSHBY, K. & STRAUB, V. 2008. Developmental defects in a zebrafish model for muscular dystrophies associated with the loss of fukutin-related protein (FKRP). *Brain*, 131, 1551-61.
- TINSLEY, J. M., BLAKE, D. J. & DAVIES, K. E. 1993. Apo-dystrophin-3: a 2.2kb transcript from the DMD locus encoding the dystrophin glycoprotein binding site. *Hum Mol Genet*, 2, 521-4.
- TINSLEY, J. M., FAIRCLOUGH, R. J., STORER, R., WILKES, F. J., POTTER, A. C., SQUIRE, S. E., POWELL, D. S., COZZOLI, A., CAPOGROSSO, R. F., LAMBERT, A., WILSON, F. X., WREN, S. P., DE LUCA, A. & DAVIES, K. E. 2011. Daily treatment with SMTc1100, a novel small molecule utrophin upregulator, dramatically reduces the dystrophic symptoms in the mdx mouse. *PLoS One*, 6, e19189.
- TINSLEY, J. M., POTTER, A. C., PHELPS, S. R., FISHER, R., TRICKETT, J. I. & DAVIES, K. E. 1996. Amelioration of the dystrophic phenotype of mdx mice using a truncated utrophin transgene. *Nature*, 384, 349-53.
- TRIKIC, M. Z., MONK, P., ROEHL, H. & PARTRIDGE, L. J. 2011. Regulation of zebrafish hatching by tetraspanin cd63. *PLoS One*, 6, e19683.

- TSUBUKI, S., KAWASAKI, H., SAITO, Y., MIYASHITA, N., INOMATA, M. & KAWASHIMA, S. 1993. Purification and characterization of a Z-Leu-Leu-Leu-MCA degrading protease expected to regulate neurite formation: a novel catalytic activity in proteasome. *Biochem Biophys Res*, 196, 1195-201.
- VAINZOF, M., PASSOS-BUENO, M. R., CANOVAS, M., MOREIRA, E. S., PAVANELLO, R. C., MARIE, S. K., ANDERSON, L. V., BONNEMANN, C. G., MCNALLY, E. M., NIGRO, V., KUNKEL, L. M. & ZATZ, M. 1996. The sarcoglycan complex in the six autosomal recessive limb-girdle muscular dystrophies. *Hum Mol Genet*, 5, 1963-9.
- VALENTINE, B. A., COOPER, B. J., DE LAHUNTA, A., O'QUINN, R. & BLUE, J. T. 1988. Canine X-linked muscular dystrophy. An animal model of Duchenne muscular dystrophy: clinical studies. *J Neurol Sci*, 88, 69-81.
- VAN DEUTEKOM, J. C., JANSON, A. A., GINJAAR, I. B., FRANKHUIZEN, W. S., AARTSMARUS, A., BREMMER-BOUT, M., DEN DUNNEN, J. T., KOOP, K., VAN DER KOOI, A. J., GOEMANS, N. M., DE KIMPE, S. J., EKHART, P. F., VENNEKER, E. H., PLATENBURG, G. J., VERSCHUUREN, J. J. & VAN OMMEN, G. J. 2007. Local dystrophin restoration with antisense oligonucleotide PRO051. *N Engl J Med*, 357, 2677-86.
- VAN RAAMSDONK, W., POOL, C. W. & TE KRONNIE, G. 1978. Differentiation of muscle fiber types in the teleost *Brachydanio rerio*. *Anat Embryol (Berl)*, 153, 137-55.
- WANG, B., LI, J. & XIAO, X. 2000. Adeno-associated virus vector carrying human minidystrophin genes effectively ameliorates muscular dystrophy in mdx mouse model. *Proc Natl Acad Sci U S A*, 97, 13714-9.
- WANG, Z., ALLEN, J. M., RIDDELL, S. R., GREGOREVIC, P., STORB, R., TAPSCOTT, S. J., CHAMBERLAIN, J. S. & KUHR, C. S. 2007. Immunity to adeno-associated virus-mediated gene transfer in a random-bred canine model of Duchenne muscular dystrophy. *Hum Gene Ther*, 18, 18-26.
- WEHLING-HENRICKS, M., LEE, J. J. & TIDBALL, J. G. 2004. Prednisolone decreases cellular adhesion molecules required for inflammatory cell infiltration in dystrophin-deficient skeletal muscle. *Neuromuscul Disord*, 14, 483-90.
- WEHLING, M., SPENCER, M. J. & TIDBALL, J. G. 2001. A nitric oxide synthase transgene ameliorates muscular dystrophy in mdx mice. *J Cell Biol*, 155, 123-31.
- WELCH, E. M., BARTON, E. R., ZHUO, J., TOMIZAWA, Y., FRIESEN, W. J., TRIFILLIS, P., PAUSHKIN, S., PATEL, M., TROTTA, C. R., HWANG, S., WILDE, R. G., KARP, G., TAKASUGI, J., CHEN, G., JONES, S., REN, H., MOON, Y. C., CORSON, D., TURPOFF, A. A., CAMPBELL, J. A., CONN, M. M., KHAN, A., ALMSTEAD, N. G., HEDRICK, J., MOLLIN, A., RISHER, N., WEETALL, M., YEH, S., BRANSTROM, A. A., COLACINO, J. M., BABIAK, J., JU, W. D., HIRAWAT, S., NORTH CUTT, V. J., MILLER, L. L., SPATRICK, P., HE, F., KAWANA, M., FENG, H., JACOBSON, A., PELTZ, S. W. & SWEENEY, H. L. 2007. PTC124 targets genetic disorders caused by nonsense mutations. *Nature*, 447, 87-91.
- WESTERFIELD, M. 2000. *The zebrafish book. A guide for the laboratory use of zebrafish (Danio rerio)*, University of Oregon Press, Eugene.
- WIENHOLDS, E., VAN EEDEN, F., KOSTERS, M., MUDDE, J., PLASTERK, R. H. & CUPPEN, E. 2003. Efficient target-selected mutagenesis in zebrafish. *Genome Res*, 13, 2700-7.
- WILLER, T., PRADOS, B., FALCON-PEREZ, J. M., RENNER-MULLER, I., PRZEMECK, G. K., LOMMEL, M., COLOMA, A., VALERO, M. C., DE ANGELIS, M. H., TANNER, W., WOLF, E., STRAHL, S. & CRUCES, J. 2004. Targeted disruption of the Walker-

- Warburg syndrome gene *Pomt1* in mouse results in embryonic lethality. *Proc Natl Acad Sci U S A*, 101, 14126-31.
- WILLIAMSON, R., HENRY, M., DANIELS, K., HRSTKA, R., LEE, J., SUNADA, Y., IBRAGHIMOV-BESKROVNAYA, O. & CAMPBELL, K. 1997. Dystroglycan is essential for early embryonic development: disruption of Reichert's membrane in *Dag1*-null mice. *Hum Mol Genet*, 6, 831-841.
- WITT, S. H., GRANZIER, H., WITT, C. C. & LABELIT, S. 2005. MURF-1 and MURF-2 target a specific subset of myofibrillar proteins redundantly: towards understanding MURF-dependent muscle ubiquitination. *J Mol Biol*, 350, 713-22.
- YAMAMOTO, M., IUCHI, I. & YAMAGAMI, K. 1979. Ultrastructural changes of the teleostean hatching gland cell during natural and electrically induced precocious secretion. *Dev Biol*, 68, 162-74.
- YANG, B., JUNG, D., MOTTO, D., MEYER, J., KORETZKY, G. & CAMPBELL, K. P. 1995. SH3 domain-mediated interaction of dystroglycan and *Grb2*. *J Biol Chem*, 270, 11711-4.
- YANG, Y., KITAGAKI, J., DAI, R. M., TSAI, Y. C., LORICK, K. L., LUDWIG, R. L., PIERRE, S. A., JENSEN, J. P., DAVYDOV, I. V., OBEROI, P., LI, C. C., KENTEN, J. H., BEUTLER, J. A., VOUSDEN, K. H. & WEISSMAN, A. M. 2007. Inhibitors of ubiquitin-activating enzyme (E1), a new class of potential cancer therapeutics. *Cancer Res*, 67, 9472-81.
- YOKOTA, T., NAKAMURA, A., NAGATA, T., SAITO, T., KOBAYASHI, M., AOKI, Y., ECHIGOYA, Y., PARTRIDGE, T., HOFFMAN, E. P. & TAKEDA, S. 2012. Extensive and prolonged restoration of dystrophin expression with *vivo*-morpholino-mediated multiple exon skipping in dystrophic dogs. *Nucleic Acid Ther*, 22, 306-15.
- YOSHIDA, M., SUZUKI, A., YAMAMOTO, H., NOGUCHI, S., MIZUNO, Y. & OZAWA, E. 1994. Dissociation of the complex of dystrophin and its associated proteins into several unique groups by *n*-octyl beta-D-glucoside. *Eur J Biochem*, 222, 1055-61.
- ZELLNER, D., PADNOS, B., HUNTER, D. L., MACPHAIL, R. C. & PADILLA, S. 2011. Rearing conditions differentially affect the locomotor behavior of larval zebrafish, but not their response to valproate-induced developmental neurotoxicity. *Neurotoxicol Teratol*, 33, 674-9.
- ZHANG, L., TANG, H., KOU, Y., LI, R., ZHENG, Y., WANG, Q., ZHOU, X. & JIN, L. 2013. MG132-mediated inhibition of the ubiquitin-proteasome pathway ameliorates cancer cachexia. *J Cancer Res Clin Oncol*, 139, 1105-15.
- ZHOU, H., CAO, F., WANG, Z., YU, Z. X., NGUYEN, H. P., EVANS, J., LI, S. H. & LI, X. J. 2003. Huntingtin forms toxic NH2-terminal fragment complexes that are promoted by the age-dependent decrease in proteasome activity. *J Cell Biol*, 163, 109-18.
- ZON, L. I. & PETERSON, R. T. 2005. *In vivo* drug discovery in the zebrafish. *Nat Rev Drug Discov*, 4, 35-44.